



UNIVERSITAT DE  
BARCELONA

## The transcriptional regulator HDAC7 role in B cell development and associated malignancies

Ainara Meler Marquina

**ADVERTIMENT.** La consulta d'aquesta tesi queda condicionada a l'acceptació de les següents condicions d'ús: La difusió d'aquesta tesi per mitjà del servei TDX ([www.tdx.cat](http://www.tdx.cat)) i a través del Dipòsit Digital de la UB ([diposit.ub.edu](http://diposit.ub.edu)) ha estat autoritzada pels titulars dels drets de propietat intel·lectual únicament per a usos privats emmarcats en activitats d'investigació i docència. No s'autoritza la seva reproducció amb finalitats de lucre ni la seva difusió i posada a disposició des d'un lloc aliè al servei TDX ni al Dipòsit Digital de la UB. No s'autoritza la presentació del seu contingut en una finestra o marc aliè a TDX o al Dipòsit Digital de la UB (framing). Aquesta reserva de drets afecta tant al resum de presentació de la tesi com als seus continguts. En la utilització o cita de parts de la tesi és obligat indicar el nom de la persona autora.

**ADVERTENCIA.** La consulta de esta tesis queda condicionada a la aceptación de las siguientes condiciones de uso: La difusión de esta tesis por medio del servicio TDR ([www.tdx.cat](http://www.tdx.cat)) y a través del Repositorio Digital de la UB ([diposit.ub.edu](http://diposit.ub.edu)) ha sido autorizada por los titulares de los derechos de propiedad intelectual únicamente para usos privados enmarcados en actividades de investigación y docencia. No se autoriza su reproducción con finalidades de lucro ni su difusión y puesta a disposición desde un sitio ajeno al servicio TDR o al Repositorio Digital de la UB. No se autoriza la presentación de su contenido en una ventana o marco ajeno a TDR o al Repositorio Digital de la UB (framing). Esta reserva de derechos afecta tanto al resumen de presentación de la tesis como a sus contenidos. En la utilización o cita de partes de la tesis es obligado indicar el nombre de la persona autora.


**WARNING.** On having consulted this thesis you're accepting the following use conditions: Spreading this thesis by the TDX ([www.tdx.cat](http://www.tdx.cat)) service and by the UB Digital Repository ([diposit.ub.edu](http://diposit.ub.edu)) has been authorized by the titular of the intellectual property rights only for private uses placed in investigation and teaching activities. Reproduction with lucrative aims is not authorized nor its spreading and availability from a site foreign to the TDX service or to the UB Digital Repository. Introducing its content in a window or frame foreign to the TDX service or to the UB Digital Repository is not authorized (framing). Those rights affect to the presentation summary of the thesis as well as to its contents. In the using or citation of parts of the thesis it's obliged to indicate the name of the author.





UNIVERSITAT DE  
BARCELONA



**Josep Carreras**   
LEUKAEMIA  
Research Institute

Facultat de Farmàcia i Ciències de l'Alimentació  
Programa de doctorat en Biomedicina

# The transcriptional regulator HDAC7 role in B cell development and associated malignancies

Memòria presentada per **Ainara Meler Marquina** per optar al grau de  
Doctora per la Universitat de Barcelona

Aquesta tesi s'ha realitzat al Grup "Lymphocyte development and disease" a  
l'Institut de Recerca Contra la Leucèmia Josep Carreras, sota la direcció de la  
Dra. Maribel Parra.

**Albert  
Tauler i  
Girona**

Firmado  
digitalmente por  
Albert Tauler i  
Girona  
Fecha: 2023.04.12  
12:46:16 +02'00'

Directora:

**Dra. Maribel Parra Bola**

Doctoranda:

**Ainara Meler Marquina**

Tutor:

**Dr. Albert Tauler Girona**

Abril del 2023



# **THESIS ABSTRACT**



## THESIS ABSTRACT

Proper B cell identity demands a tight controlled genomic and epigenomic landscape at each stage of cellular differentiation during B lymphocyte development. It has been previously identified in our group that HDAC7 is an essential regulator of early B cell development, and its absence leads to a dramatic block at the pro-B to pre-B cell transition. In this work, we have depicted, the molecular mechanisms by which HDAC7 modulates early B cell development. Specifically, HDAC7 loss induces TET2 expression, which promotes DNA 5-hydroxymethylation and chromatin de-condensation. These findings shed light on the mechanisms by which HDAC7 loss or misregulation may lead to pro-B hematological malignancies. Actually, within this work we demonstrate that HDAC7 loss in infant acute lymphoblastic leukemia of pro-B (pro-B-ALL) cells correlates with a worse prognosis. The ectopic expression of HDAC7 in pro-B-ALL cell lines leads to a transcriptional phenotype closely related to healthy B cell progenitors, highlighting its importance in the guidance of B cell identity.

However, HDAC7 role in mature B cell biology and associated malignancies is unknown. We demonstrate that HDAC7 is essential for the entry and initiation of the germinal center (GC) reaction. Upon HDAC7 loss, there is a blockade of B cell development at the pre-GC stage, which leads to the generation of aberrant GC B cells, diminished class switch recombination and plasma cell formation. We observe that HDAC7 is generally underexpressed in diffuse large B cell lymphoma (DLBCL) tumors, and its low expression is associated with a poor prognosis of the patients. HDAC7 exogenous expression in DLBCL cell lines reduces its tumorigenicity.

In summary, this thesis project aims to describe first, the mechanistical regulation of HDAC7 in early B cell development, and second, HDAC7 implication in terminal B cell development. Concomitantly, we intended to decipher the potential contribution of HDAC7 deregulation in pro-B-ALL and DLBCL, which are B cell derived malignancies in the pro-B and GC B cell developmental stages, respectively.





# **CONTENTS**



# CONTENTS

<b>LIST OF FIGURES AND TABLES.....</b>	<b>13</b>
<b>ABBREVIATIONS.....</b>	<b>17</b>
<b>INTRODUCTION.....</b>	<b>23</b>
<b>1. B lymphocyte development</b>	
1.1. Early B cell development.....	25
1.1.1. Transcriptional regulation during early B cell development.....	26
1.2. Terminal B cell development.....	28
1.2.1. The Germinal Center reaction.....	29
1.2.2. Germinal Center dynamics.....	30
1.2.3. SHM and CSR.....	31
1.2.4. pre-GC: early events before the GC reaction.....	33
1.2.5. Transcriptional control during terminal B cell development.....	34
<b>2. Haematologic B cell malignancies</b>	
2.1. pro-B Acute Lymphoblastic Leukemia.....	38
2.2. Diffuse Large B Cell lymphoma.....	41
<b>3. Epigenetic mechanisms</b>	
3.1. DNA methylation.....	46
3.2. DNA demethylation.....	47
3.3. TET proteins.....	48
3.4. Histone modifications.....	49
<b>4. Histone or protein deacetylases</b>	
4.1. Class IIa HDACs.....	53
4.1.1. HDAC7.....	53
<b>OBJECTIVES.....</b>	<b>57</b>
<b>RESULTS.....</b>	<b>61</b>
<b>Director's report.....</b>	<b>63</b>

<b>Summary of results</b> .....	<b>65</b>
<b>Article 1</b> .....	<b>71</b>
<i>“The HDAC7-TET2 epigenetic axis is essential during early B lymphocyte development”</i>	
<b>Article 2</b> .....	<b>105</b>
<i>“HDAC7 is a major contributor in the pathogenesis of infant t(4;11) proB acute lymphoblastic leukemia ”</i>	
<b>Article 3</b> .....	<b>135</b>
<i>“HDAC7 is essential in early pre-germinal center formation and its deregulation is associated with DLBCL”</i>	
<b>DISCUSSION</b> .....	<b>179</b>
<b>CONCLUSIONS</b> .....	<b>195</b>
<b>BIBLIOGRAPHY</b> .....	<b>199</b>
<b>ANNEX</b> .....	<b>232</b>
Review: <i>“MYC's Fine Line Between B Cell Development and Malignancy”</i>	

## **LIST OF FIGURES AND TABLES**



## LIST OF FIGURES AND TABLES

<b>Figure 1.</b> The hematopoietic system.....	<b>26</b>
<b>Figure 2.</b> Transcription factors expressed during early B cell development....	<b>27</b>
<b>Figure 3.</b> Secondary lymphoid organs' structure.....	<b>29</b>
<b>Figure 4.</b> Schematic representation of the germinal center reaction.....	<b>30</b>
<b>Figure 5.</b> Schematic representation of the antibody structure.....	<b>32</b>
<b>Figure 6.</b> Schematic representation of the TFs driving the GC reaction	<b>34</b>
<b>Figure 7.</b> <i>De novo</i> methylation and passive/active demethylation schema....	<b>48</b>
<b>Figure 8.</b> Schematic representation of the chromatin status depending on HDAC or HAT enzymatic activity.....	<b>51</b>
<b>Figure 9.</b> HDACs family classification.....	<b>52</b>
<b>Figure 10.</b> Schematic representation of HDAC7 silencing hypothesis in the GC entrance.....	<b>189</b>
<b>Figure 11.</b> Graphical summary of HDAC7 role in early and late B cell development, and in derived malignancies.....	<b>193</b>
<b>Table 1.</b> DLBCL classification based on genetic alterations.....	<b>42</b>





## **ABBREVIATIONS**



## ABBREVIATIONS

5-caC: 5-carboxylcytosine

5-fC: 5-formylcytosine

5-hmC: 5-hydroxymethylcytosine

5-mC: 5-methylcytosine

ABC-DLBCL: Activated B cell like - diffuse large B cell lymphoma

ADP: Adenosine diphosphate

AID/*Aicda*: Activation induced cytidine deaminase

ALL: Acute lymphoblastic leukemia

APC: Antigen presenting cell

APE1: Apurinic-apyrimidinic endonuclease 1

BACH2: BTB domain and CNC homolog 2

B-ALL: Acute lymphoblastic leukemia of B cells

BATF: Basic leucine zipper ATF-like transcription factor

BCL2: B cell lymphoma 2

BCL6: B cell lymphoma 6

BCR: B cell receptor

BER: Base excision repair

BLIMP1/*Prdm1*: Positive regulatory domain I

CAR-T: T cell with a chimeric antigen receptor

*Ccnd3*: Cyclin D 3

CD19/22/38/40/80/83/86: Cluster of differentiation 19/22/38/40/80/83/86

*Cdkn1a*: Cyclin dependent kinase inhibitor 1A

CLP: Common lymphoid progenitors

CMP: Common myeloid progenitor

c-MYC: variant c of MYC proto-oncogene, bHLH transcription factor

CREBBP: cAMP-response element binding protein

CSR: Class-switch recombination

CTL: Cytotoxic T cell

CXCL12/13: Chemokine ligand 12/13

CXCR4/5: Chemokine receptor 4/5

DEL: Double-expressor lymphoma

DLBCL: Diffuse large B cell lymphoma

DNMT: DNA methyltransferase  
DZ: Dark zone  
EBF1: Early B cell factor  
EBI2/GPR183: Epstein-Barr virus-induced gene 2  
EP300: E1A binding protein p300  
Eph-B1: Ephrin B1  
EZH2: Enhancer of zeste 2 polycomb repressive complex 2 subunit  
FAS: Fas cell surface death receptor  
FDC: Follicular dendritic cell  
FOXO1: Forkhead box O1  
GC: Germinal center  
GCB-DLBCL: Germinal center like-diffuse large B cell lymphoma  
GL-7: Glycoprotein 7  
H2A/2B/3/4: Histone 2A/2B/3/4  
H3K14ac: acetylation of the 14<sup>th</sup> lysine residue of histone 3  
H3K27: 27<sup>th</sup> lysine residue of histone 3  
H3K4: 4<sup>th</sup> lysine residue of histone 3  
H3K79: 79<sup>th</sup> lysine residue of histone 3  
H3K9: 9<sup>th</sup> lysine residue of histone 3  
H4K16ac: acetylation of the 16<sup>th</sup> lysine residue of histone 4  
HAT: Histone acetyl transferase  
*Hda1*: Histone deacetylase-A1  
HDAC: Histone deacetylase  
HDMT: Histone demethylase  
HMT: Histone methyltransferase  
HOXA: Homeobox A  
HSC: Hematopoietic stem cell  
IgA/D/IgE/G/G2a/G2b/G3/M: Immunoglobulin A/D/E/G/G2a/G2b/G3/M  
IgH: Immunoglobulin heavy chain  
IgL: Immunoglobulin light chain  
IgV: Immunoglobulin variable region  
IKZF: IKAROS family zinc finger 1  
IL7r: Interleukin 7 receptor  
iPSC: Induced pluripotent stem cell

IRF4: Interferon regulatory factor 4  
IRF8: Interferon regulatory factor 8  
KMT2A/D: Lysine methyltransferase 2A/D  
LMPP: Lymphoid-primed multipotent progenitor  
LZ: Light zone  
*Mac-1*: Macrophage-1 antigen  
MAPK: Mitogen-activated protein kinase 1  
MBC: Memory B cell  
MBP: Methyl binding protein  
MEF2B/C/D: Myocyte enhancer 2B/C/D  
MEIS1: Meis homeobox 1  
MEN1: Menin 1  
MEP: Megakaryocyte/erythrocyte progenitors  
MHC: Major histocompatibility complex  
MLL: Mixed lineage leukemia  
MME: Membrane metalloendopeptidase  
MMP10: Metalloproteinase 10  
mTORC1: Mechanistic target of rapamycin kinase 1  
NAD: Nicotinamide-adenine dinucleotide  
NCOR1/2: Nuclear receptor corepressor 1/2  
NK: Natural killer  
p53/TP53: tumor protein 53  
PAX5: Paired box protein 5  
PC: Plasma cell  
PD-1: Programmed death-1  
PDL-1: Programmed death-ligand 1  
PI3K: Phosphatidylinositol-4,5-bisphosphate 3-kinase  
PKD-1: Polycystic kidney disease 1  
PNA: Peanut agglutinin  
PP2A: Protein phosphatase 2  
PRC2: Polycomb repressive complex 2  
Pre-B: Precursor B  
Pre-GC: precursor-germinal center  
Pre-pro-B: Precursor-progenitor B

Pro-B: Progenitor B  
PU.1: Spi1 proto-oncogene  
R-CHOP: cyclophosphamide, doxorubicin, prednisone, rituximab and vincristine  
*Rpd3*: Reduced potassium dependency 3  
rrDLBCL: relapsed or refractory DLBCL  
RUNX2: Runt-related factor 1  
S1P2: Sphingosine-1-phosphatase receptor 2  
SAM: S-adenosyl-L-methionine  
SGK1: Serum/glucocorticoid regulate kinase 1  
SHM: Somatic hypermutation  
*Sir2*: Silent information regulator 2  
SIRT: Sirtuin  
TCR: T cell receptor  
TDG: the thymidine DNA glycosylase  
TET: Ten-eleven translocation  
TF: Transcription factor  
 $T_{fh}$ : T follicular helper  
THL: Triple-hit lymphomas  
UHRF1: Ubiquitin like with PHD and ring finger domains 1  
UNG: Uracil-DNA glycosylase  
Vpreb: V-Set pre-B cell surrogate light chain 1  
XBP1: X-box binding protein 1

## **INTRODUCTION**





# INTRODUCTION

## 1. B lymphocyte development

### 1.1. Early B cell development

The hematopoietic system generates all blood cell types that are required throughout life. This process involves several cellular transitions to achieve functional differentiated cells (Figure 1). In the bone marrow, hematopoietic stem cells (HSC) have the potential to continuously replenish all types of blood cells through processes of lineage-restricted cell commitment. At very initial stages, HSC differentiate into lymphoid-primed multipotent progenitors (LMPP), which have the capacity to direct cell fate to both lymphoid and myeloid lineages. These LMPPs may differentiate into common lymphoid progenitors (CLP), which will generate B cells, T cells and Natural Killer cells (NK). However, LMPPs also have the potential to give rise to common myeloid progenitors (CMP), that will further differentiate into either megakaryocyte/erythrocyte progenitors (MEP) or granulocyte/macrophage progenitors (GMP).

During early B cell development in the bone marrow, CLPs give rise to B cell progenitors (pro-B cells), which in turn will later differentiate into B cell precursors (pre-B cells) and immature B cells. To deal with pathogens or foreign molecules, B cells need to modify their immunoglobulin (Ig) gene loci, a process named primary Ig diversification, that starts in pre-B cells. These cells have the capacity to assemble a complete IgM antigen receptor and expose it on the B cell surface by a specific recombination process named V(D)J recombination, thus generating the pre-BCR. Signals from the pre-BCR orchestrate cell proliferation and consequent differentiation into immature B cells (Herzog, Reth, and Jumaa 2009). Later, immature B cells leave the bone marrow and migrate to secondary lymphoid organs such as the spleen and lymph nodes, to finally differentiate into memory B cells (MBC) and long-lived plasma cells (PC).

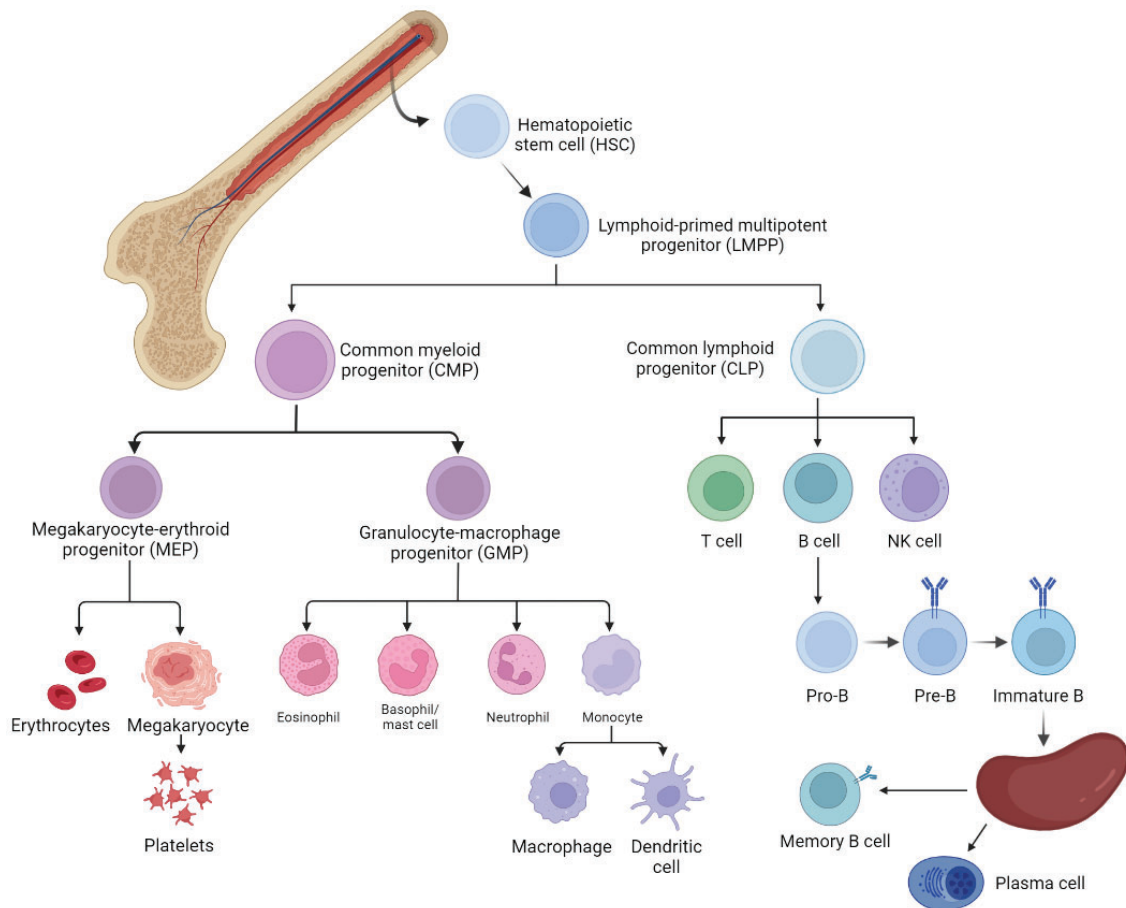


**Figure 1. The hematopoietic system.** Schematic representation of the cell differentiation process of both lymphoid and myeloid branches. In the bone marrow, Hematopoietic Stem Cells (HSC) differentiate into Lymphoid-primed Multipotent Progenitors (LMPP), which can differentiate into Common Lymphoid Progenitors (CLP) and Common Myeloid Progenitors (CMP). CLPs will generate T cells, Natural Killer cells (NK) or B cells. The latter differentiate into pro-B, pre-B and immature B cells. Immature B cells migrate to secondary lymphoid organs and differentiate to Plasma cells or Memory B cells. CMPs differentiate into either megakaryocyte/erythrocyte progenitors (MEP) or granulocyte/macrophage progenitors (GMP). MEPs develop into either erythrocytes or platelets. Finally, GMPs differentiate into eosinophil, basophil, neutrophil or monocyte.

### 1.1.1. Transcriptional regulation during early B cell development

Early B cell commitment and differentiation is a complex developmental process that requires a tight regulation and orchestration of transcriptional and epigenetic events. Progenitor cells in the bone marrow need to coordinate different transcriptional programs that are lineage-characteristic, in order to achieve a differentiated cell state. During early B cell development, a

considerable number of transcription factors (TF) have been reported to play a crucial role at various cell commitment, lineage choices and differentiation steps (Figure 2).

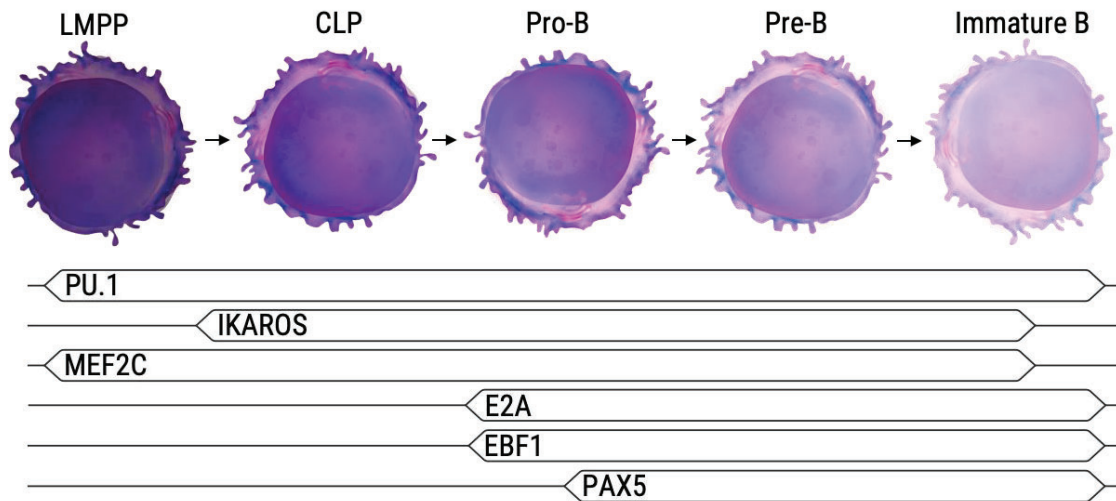


**Figure 2. Transcription factors expressed during early B cell development.** Representation of early B cell developmental stages and TFs' expression patterns, which are displayed in the bars below. LMPP (lymphoid-primed multipotent progenitor), CLP (common lymphoid progenitor), pro-B (progenitor B), pre-B (precursor B). Figure modified from (Ramírez, Lukin, and Hagman 2010).

At LMPP stage, the TF IKAROS, encoded by the *Ikzf1* gene, is involved in the generation of both CMPs and CLPs and, as demonstrated in mice models, its deficiency prevents the generation of erythrocytes and B and T lymphocytes (Heizmann, Kastner, and Chan 2013; Yoshida et al. 2009). Simultaneously, the TF PU.1, encoded by the *Sfpi1* gene, dictates the switch choice towards the lymphoid or myeloid lineages, in a dose-dependent manner. In fact, high levels of PU.1 promote myeloid differentiation, whereas lower concentrations favor the commitment into the lymphoid lineage (Ramírez, Lukin, and Hagman 2011; E. W. Scott et al. 1994). PU.1 controls the expression of MEF2C TF, which is involved in the silencing of myeloid-lineage genes and activation of lymphoid-lineage genes (Herglotz et al. 2016; Kong et al. 2016; Stehling-Sun et al. 2009). The differentiation of CLP into pro-B cells depends on IL7r signaling and the coordinated action of the TFs PAX5, EBF1 and E2A (Nutt and Kee 2007). PAX5 is considered the “guardian of B cell identity” and is continuously expressed from pro-B cells to terminally differentiated B cells. Indeed, PAX5 activates specific

genes of the B cell lineage but, at the same time, represses inappropriate genes from alternative lineages (Cobaleda et al. 2007). On top of that, E2A is required for the initiation and maintenance of *Pax5* and *Ebf1* expression, at the initial steps of B cell differentiation in the bone marrow (Kwon et al. 2008). Loss of expression of EBF1 or E2A in mouse models leads to a complete pre-pro-B cell stage blockade and a failure in proliferation (H. Lin and Grosschedl 1995). In addition, PAX5, EBF1 and E2A regulate the expression of many essential genes, such as *Cd19*, *Ii7r*, *mb-1* or *Vpreb*, among many others, therefore being crucial for correct B cell development.

## **1.2. Terminal B cell development**

Humoral immunity is an antibody-mediated response that occurs upon foreign antigen detection and is primarily driven by B lymphocytes.

The establishment of the humoral response occurs after migration of immature B cells from the bone marrow to the secondary lymphoid organs, which are the spleen and the lymph nodes. Anatomically, secondary lymphoid organs are composed of spherical follicles, the structure of which can be observed in Figure 3. Within the follicles, mature resting or naïve B cells are located between the T cell zone and the marginal zone in the spleen or between the T cell zone and the capsule in the lymph nodes. Additionally, a specific subset of stromal cells called follicular dendritic cells (FDC) is held together in these follicles (C. D. C. Allen and Cyster 2008; Heesters, Myers, and Carroll 2014). Here, within the follicles, is where naïve B cells undergo the germinal center (GC) reaction and gain antigen affinity through class switch recombination (CSR) and somatic hypermutation (SHM) processes, to finally generate MBC and PC.

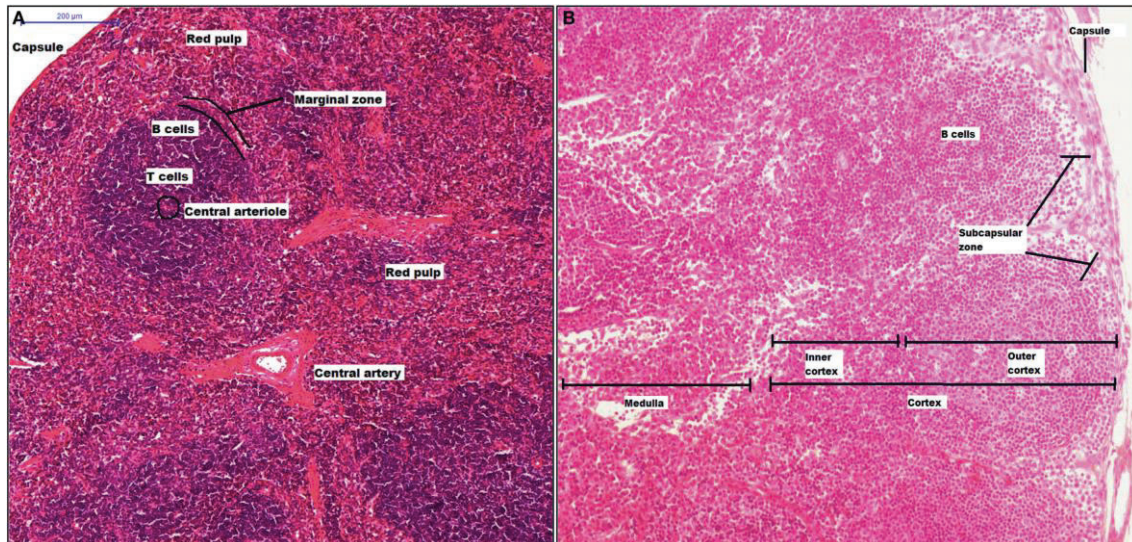


**Figure 3. Secondary lymphoid organs' structure.** The spleen (left panel) has two mayor components, white pulp that includes a central arteriole, T and B cells, and red pulp. A lymph Node (right panel) is surrounded by a capsule, and the parenchyma is divided into cortex and medulla. The cortex has two zones: outer and inner zone. Adapted from (Chávez-Galán et al. 2015).

### 1.2.1 The Germinal Center reaction

Upon antigen encounter, naïve B cells migrate to the border of the follicle, where they interact with T follicular helper cells ( $T_{fh}$ ) that have been previously primed by antigen presenting cells (APC) (Garside et al. 1998).  $T_{fh}$  cells trigger proliferation and expansion of naïve B lymphocytes into clones, which then will differentiate into short-lived PC,  $IgM^+$  MBCs, or migrate to the focus of FDC network and initiate the GC reaction (Inamine et al. 2005; Kaji et al. 2012; Okada et al. 2005) (Figure 4).

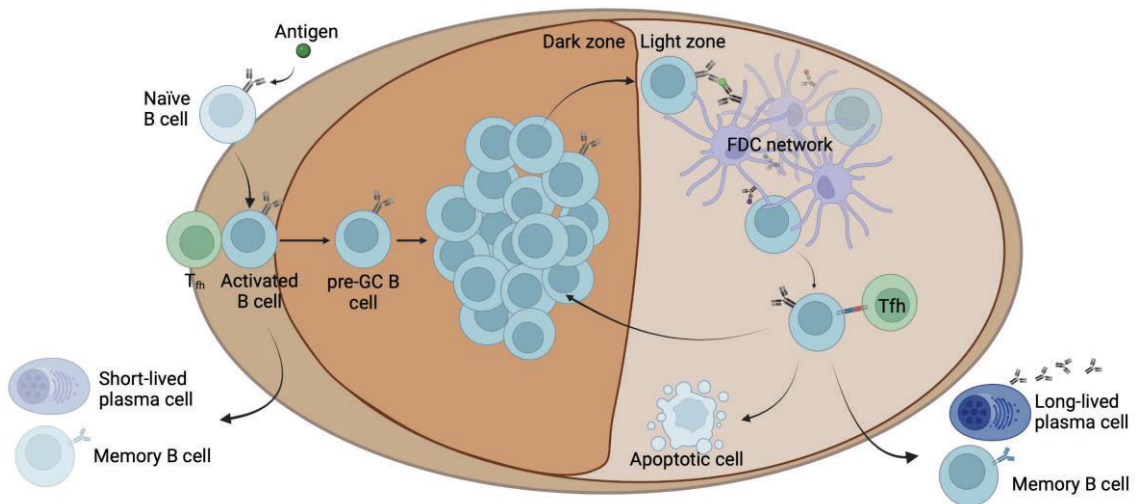


**Figure 4. Schematic representation of the germinal center reaction.** Naïve B cells become activated by the antigen presented T follicular helper cells ( $T_{fh}$ ) and i) differentiate into short-lived plasma cells or  $IgM^+$  MBCs, or ii) enter the germinal center reaction where the activated B cell undergoes further rounds of affinity maturation to become a long-lived plasma cell or a memory B cell. FDC (Follicular dendritic cell).

### 1.2.2. Germinal Center dynamics

The GC reaction begins when B cells clonally expand after being primed by T cells. Mature GC are generated approximately one week after the initial B cell activation. At this time, the cluster of hyperproliferative GC B cells becomes polarized into two distinct zones, the dark zone (DZ) and the light zone (LZ), which form the mature GC (C. D. Allen, Okada, and Cyster 2008; De Silva and Klein 2015). Anatomically, both zones are histologically distinguishable, as the LZ appears lighter than the DZ due to the abundance of stromal cells and the sparser distribution of lymphocytes, resulting in a lower nuclei density in the staining (C. D. Allen, Okada, and Cyster 2008).

It must be noted that GC B cells dynamics are not arbitrary. In fact, they are promoted by changes in gene expression and in the expression of cell surface proteins that are routinely used to distinguish naïve B cells from GC B cells and DZ and LZ subpopulations. The downregulation of the orphan G protein-coupled receptor EBI2/GPR183 and the upregulation of S1P2 (in humans P2RY8) in

activated B cells, allow their mobility to the center of the follicle and to the FDC cluster, respectively, promoting niche confinement (Gatto et al. 2009; Green et al. 2011; Lu et al. 2019; Muppidi, Lu, and Cyster 2015; Pereira et al. 2009). Migration of the activated B cells to the center of the follicle is also driven by the upregulation of n-glycolylneuraminic acid that is recognized by the antibody GL-7; Gal- $\beta$ (1-3)-GalNAc, a ligand for peanut agglutinin (PNA) (Rose et al. 1980); the proapoptotic receptor Fas (Yoshino et al. 1994); and the Ephrin-related tyrosine kinase ligand Eph-B1, also upregulated in GC memory precursor cells (Laidlaw et al. 2017). Additionally GC B cells are characterized by the downregulation of IgD (Mccluskey and Schlossman 1981). The cyclic ADP ribose hydrolase CD38 is also downregulated in mouse but upregulated in human GC B cells (Oliver, Martin, and Kearney 1997). Deeping into the GC polarization, CXCR4 expression indicates GC B cell localization in the DZ, whereas CD83 and CD86 cell surface markers are indicative of GC B cells in the LZ (Nie et al. 2004; Victora et al. 2010).

As described before, complex events determine the anatomical structure of the GC which, at the same time, is closely related to its function. Classically, it was proposed that B cells in the GC undergo iterative cycles of selection between the DZ and the LZ, in a process called cyclic re-entry (Kepler and Perelson 1993; Oprea and Perelson 1997). Throughout years, research studies have added more layers of information into the GC compartments, identifying the DZ as an hyperproliferative zone where GC B cells or “centroblasts” diversify the Ig variable region (IgV), and a LZ, where GC B cells become quiescent B cells or “centrocytes” and are tested for affinity by FDCs and T<sub>fh</sub> cells (Victora and Nussenzweig 2022).

### **1.2.3 SHM and CSR**

For a proper humoral response, GC B cells need to generate a hugely diverse repertoire of antibodies. Antibodies are composed of two pairs of identical chains, the immunoglobulin light chain (IgL) and the immunoglobulin heavy chain (IgH), that are joined to form a secreted “Y”-shaped molecule (Figure 5). The

aminoacid sequence within the extremes of the “Y” structure varies among different antibodies and is named as variable region. The variable region includes the terminal regions of the light and heavy chains and gives the antibody the specificity to recognize any antigen. For this purpose, the variable region undergoes antibody diversification through V(D)J recombination reaction. Germline DNA possesses hundreds of different V, D and J segments that randomly assemble into the IgV, expressed as the BCR.

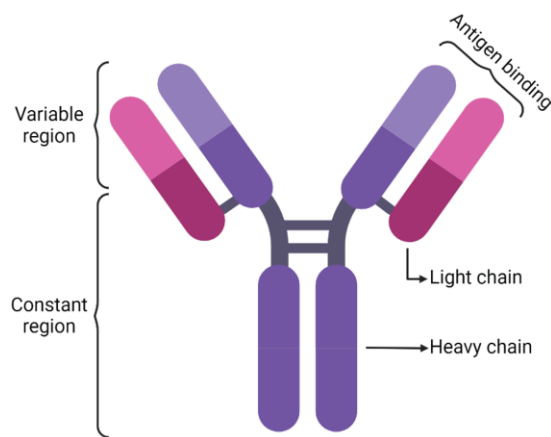


**Figure 5. Schematic representation of the antibody structure.** The antibody consists of two identical heavy chains (purple) and two light chains (pink), divided into constant and variable regions, as detailed in the figure. Disulfide bridges link the four chains.

Within the GC, B cells' IgV diversification occurs through the previously mentioned CSR and SHM processes, both controlled by activation-induced cytidine deaminase (AID). On one hand, SHM engages the introduction of point mutations by AID in the IgV, arising subtle changes that may allow to gain specificity against the antigen (Muramatsu et al. 2000; Neuberger and Milstein 1995; Di Noia and Neuberger 2007). On the other, CSR is a recombination process of the IgH chain that allows the IgM<sup>+</sup>/IgD<sup>+</sup> mature B cell to express other isotype antibodies for a better protection against the antigen (Stavnezer, Guikema, and Schrader 2008). CSR mainly relies on the action of AID, APE1 and UNG to target intronic areas called switch regions, introduce DNA breaks and lead to the recombination of V(D)J segments with different IgH chains (Guikema et al. 2007; Muramatsu et al. 2000; Rada et al. 2002; Stavnezer, Guikema, and Schrader 2008). In contrast to the classical view that describe these antibodies diversification processes in the DZ, it has recently been demonstrated that CSR



can be already initiated upon T cell priming, before the GC formation and therefore prior to SHM (Roco et al. 2019).

At the same time, GC B cells cycle between the DZ and the LZ undergoing rounds of affinity maturation. In the DZ, SHM mostly generates non-functional BCR, leading to apoptotic cell death (Lau and Brink 2020). However, B cells from the DZ to whom SHM confers a functional mutated BCR, migrate to the LZ to test the affinity of these newly generated BCRs. Then, within the LZ, GC B cells that have acquired enough affinity for a specific antigen receive recirculating signals to migrate back to the DZ for further rounds of SHM, or exit the GC to differentiate into MBC or PC (Mayer et al. 2017; Victora et al. 2010).

#### **1.2.4 pre-GC: early events before the GC reaction**

The classical view of the GC reaction described in previous sections has been recently challenged by several works demonstrating that B cells can differentiate into MBC and PC before entering the GC. To secrete antibodies into the bloodstream, B cells must exit the GC reaction and migrate into the PC compartment. This can happen through the classical path, consisting of the differentiation of GC B cells into plasmablasts and later PCs, or through a distinct pathway where MBC that have exited (or never entered) the GC, differentiate into PCs upon a secondary antigen encounter.

Single-cell transfer experiments unveiled the formation of GC-independent MBC derived from activated B cells, at the time that GC are just beginning to coalesce (Taylor, Pape, and Jenkins 2012; Zuccarino-Catania et al. 2014). Several studies have added complexity to this MBC population generated in the pre-GC, highlighting that MBCs can be segregated into different subsets upon recall. After immunization, IgM<sup>+</sup> and IgG1<sup>+</sup> MBCs are generated and, after a second antigen encounter, IgG1<sup>+</sup> MBCs differentiate into antibody producing PCs in a GC-independent manner, whereas IgM<sup>+</sup> MBC initiate the GC reaction. These studies reinforce the thoughts on IgM<sup>+</sup> as long-lasting MBC and IgG1<sup>+</sup> as GC-independent PC generators (Dogan et al. 2009; He et al. 2017; Viant et al. 2021;

Zuccarino-Catania et al. 2014). Another recent twist to the classical model is that long-lived MBCs originate in the pre-GC region or early GC stages, whereas long-lived PCs tend to arise from the later phase of the GC reaction (Weisel et al. 2016).

### 1.2.5 Transcriptional control during terminal B cell development

Likewise early B cell development, terminal B cell differentiation is tightly regulated at the transcriptional level. Specific TF networks are required during the differentiation processes of naïve B cells into PC and MBC (Figure 6).

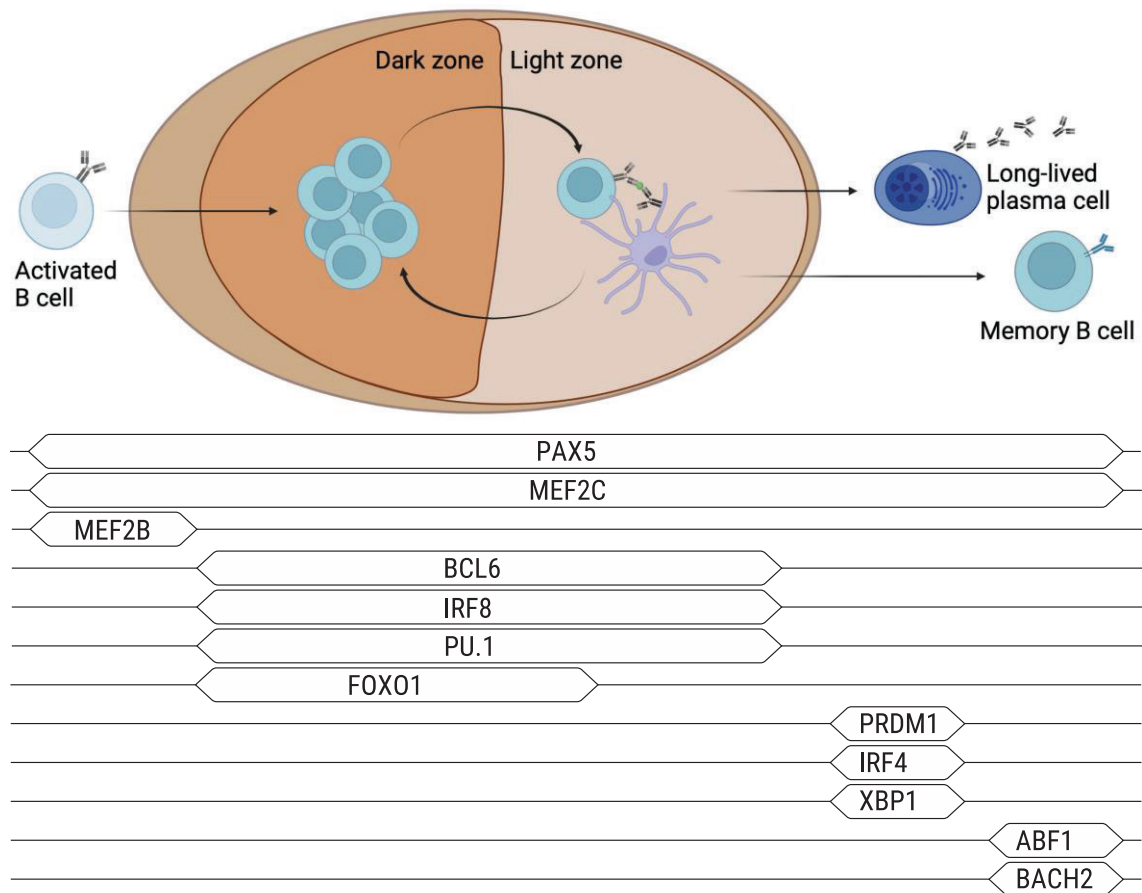


**Figure 6. Schematic representation of the TFs driving the GC reaction.** Boxes in the lower panel represent the expression of the different TFs, being thinner when not expressed and thicker when expressed, in relation with the biological stage of the upper panel.

The TF BCL6 is considered one of the main regulators of the GC reaction. In fact, *Bcl6* knock out mice lack GC formation and do not possess the ability to produce high-affinity antibodies (Dent et al. 1997; Bihui H. Ye et al. 1997). BCL6 recruits corepressors such as NCOR1 and NCOR2 among others to maintain the GC B cell signature and repress PC gene program. BCL6 mediates cellular clonal expansion and allows SHM to produce DNA damage by repressing the cell cycle checkpoint *Cdkn1a* (p21) and the DNA damage repair associated gene *Tp53* (Phan et al. 2005; Phan and Dalla-Favera 2004). The anti-apoptotic gene *Bcl2* is also repressed by BCL6, leading to cell apoptosis in clonal deletion (Saito et al. 2009). In addition, BCL6 represses the expression of the B cell surface marker *Cd80*, and the Programmed Death-ligand 1 (*PD-L1*) (Niu, Cattoretti, and Dalla-Favera 2003). *PD-L1* is expressed by APCs and binds to CD80. At the same time PD-L1 regulates the balance of the T cell response by interacting with PD-1, in terms of activation and tolerance (Borriello et al. 1997; Keir et al. 2008). Reducing the expression of *CD80* and *PD-L1* diminishes the interaction between B and T cells, allowing the proliferation and expansion of B cells. During the progression of B cells into the post-GC stage, *Bcl6* is silenced.

Focusing on GC B cells, PAX5 regulates the expression of critical genes for B cell identity, such as BCR, IRF4 and IRF8, as it occurs in early B cell development within bone marrow. PAX5 knock out cells exhibit a decrease of IgM expression and completely lose BCR signaling (Nera et al. 2006). At the same time, PAX5 represses lineage-inappropriate genes, known to be essential for other cell types (Delogu et al. 2006). For this reason, PAX5 downregulation is required for the commitment of PC, as detailed below.

The TF MEF2B directly binds to the *Bcl6* gene leading to the activation of its expression, in mice. Remarkably, MEF2B expression is induced even before BCL6, immediately after T-cell dependent antigen activation (Ryan et al. 2015; Wilker et al. 2008; Ying et al. 2013). In mice, GC B cells that lack *Mef2b* expression, present a reduced number of GC and an altered DZ:LZ ratio (Brescia et al. 2018). MEF2C has also been reported to regulate the proliferation of GC B cells, since it is a direct target of the p38 MAPK pathway, which in turn functions downstream the BCR. In parallel, loss of MEF2C in murine models also results

in a defective GC formation, a blockade in B-cell proliferation and reduced immune response to antigens (Khiem et al. 2008). Different from MEF2B, MEF2C is present at all stages of mature B cell differentiation (Khiem et al. 2008; Wilker et al. 2008).

Several works have reported that the TF FOXO1 is the main regulator of the DZ (Dominguez-Sola et al. 2015; Sander et al. 2015). FOXO1 is highly expressed in the DZ and represses the LZ transcriptional program, where its activity is repressed by PI3K expression and signaling. In *Foxo1*-deficient mice, GC lose their architectural distribution, resulting in LZ-only GCs and impaired affinity maturation, partially due to the direct downregulation of CXCR4 and the indirect upregulation of BATF, a TF highly expressed in the LZ (Dominguez-Sola et al. 2015; Inoue et al. 2017; Sander et al. 2015)

The TF BLIMP1, encoded by the gene *Prdm1*, is the main regulator of the PC differentiation program (Turner, Mack, and Davis 1994). BLIMP1 is well known to repress key B cell identity genes such as *Pax5*, *Ciita* and *c-Myc*, and to activate genes required for PC identity acquisition, such as *IgH* (K.-I. Lin et al. 2002a; Y. Lin, Wong, and Calame 1997; Minnich et al. 2016a; Piskurich et al. 2000). A sustained expression of the TF IRF4 is required for the proper PC differentiation (Klein et al. 2006; Ochiai et al. 2013). *Irf4*-deficient B cells in mice present an impaired expression of AID, lack CSR and completely abrogate CD138<sup>+</sup> PC generation (Klein et al. 2006). *Prdm1* is a downstream target of IRF4, and its expression increases IRF4 protein levels, in a feed forward loop (Minnich et al. 2016b). Consequently, BLIMP1 together with IRF4 are key TFs for the generation of PC, and their expression is suppressed by BCL6 (Cattoretti et al. 2006; Tunyaplin et al. 2004).

IRF4 and BLIMP1 act upstream of XBP1, a TF required to coordinate cellular structural changes for the antibody production in PC (Reimold et al. 2001; Shaffer et al. 2004). Before late GC stages, XBP1 is repressed by PAX5, preventing PC differentiation. Therefore, BLIMP1-mediated repression of *Pax5* is necessary for the expression of XBP1, but not sufficient. In this context, BLIMP1 requires IRF4 reinforcement to achieve PC differentiation (K.-I. Lin et al. 2002b;

Reimold et al. 2001). Another IRF family member, IRF8, has also been reported to play a role during terminal B cells differentiation. The coordinated action of IRF8 and PU.1 inhibits GC B cells differentiation towards PC (Carotta et al. 2014), suggesting that a balance between all the TFs involved in this network is essential.

Finally, during MBC differentiation, the TF ABF1 blocks the PC differentiation program. Transgenic overexpression of ABF1 in murine B cells results in an increase of GC and MBC, whereas the PC response is dampened (Chiu et al. 2014). BACH2 also contributes to the MBC commitment. It has been observed that LZ cells with a low affinity BCR have a higher expression of *Bach2* than its high affinity BCR counterparts, and cells with high BACH2 levels are prone to enter the MBC pool. Therefore, *Bach2*-deficient mice present a reduced generation of MBC (Shinnakasu et al. 2016).

## 2. Haematologic B cell malignancies

Despite the existence of several types of B cell malignancies depending on the developmental stage altered, in this section I will focus on two of them: pro-B cell acute lymphoblastic leukemia (pro-B-ALL) and diffuse large B cell lymphoma (DLBCL), that arise from pro-B and GC B cells, respectively. It is commonly known that the characteristics of each malignancy rely on the cell-of-origin. Therefore, the deregulation of the transcriptional programs underlying early and terminal B cell generation may lead to the development of hematological malignancies with distinct features and malignant capacity.

### 2.1. pro-B-Acute Lymphoblastic Leukemia

ALL is the most common pediatric malignancy, accounting for 25% of cancers in children. Among those, 85% derive from B cells, characterized by an uncontrolled expansion of progenitors and precursors within the bone marrow (Bhojwani, Yang, and Pui 2015; Pui and Evans 2013). Despite current cure rates are around 90% (Inaba, Greaves, and Mullighan 2013) in pediatric B-ALL, statistics in infant patients (<1 year of age) remain unfavorable. Low-response to chemotherapy and an aggressive early clinical presentation, set infant pro-B-ALL survival rate below 35% (van der Linden et al. 2009).

Infant pro-B-ALL harboring rearrangements of the mixed-lineage leukemia gene (*MLL*, also known as *KMT2A*), which leads to the expression of aberrant fusion proteins, constitute a subgroup with a very aggressive presentation. (C. Meyer et al. 2018). Particularly, *MLL* is a histone methyltransferase that methylates lysine 4 histone 3 (H3K4) residue. This epigenetic mark acts as a transcriptional activator and positively regulates gene expression, including that of *Hox* genes. *MLL* can assemble large nuclear complexes, and its interacting partners are, among others, MEN1, PP2A, PRC1/2 group complex and CREBBP. The N-terminal region of *MLL* protein can bind to the DNA and read chromatin signatures, whereas the C-terminal domain harbors its enzymatic activity (Dou et al. 2005; Xia et al. 2003; Yokoyama et al. 2004). Therefore, the *MLL* complex can bind several genes by recognizing specific epigenetic marks.

MLL rearranged acute leukemias are the result of the translocation of the *MLL* gene to other genomic regions, leading to the formation of aberrant fusion proteins. Up to date, more than fifty protein partners have been identified as MLL fusion proteins due to translocations in leukemia; however, a subset accounts for most cases. The most frequent fusion proteins derived from MLL rearrangements are MLL-AF4, MLL-AF9, MLL-AF10, MLL-ENL and MLL-ELL, which comprise about 85% of all fusions described in pro-B-ALL (Wang et al. 2011). Among pro-B-ALL chromosomal alterations, it must be noted that MLL-AF4, which is originated by t(4;11) translocation, represents the most prevalent fusion protein in infants, accounting for the poorest prognosis, given its strong leukemogenic potential (C. Meyer et al. 2009). MLL-AF4 is expressed in mesenchymal stem cells of patients' bone marrow, indicating that cells containing this alteration may arise in early pre-hematopoietic precursors (Menendez et al. 2009).

From an etiologic point of view, t(4;11) pro-B-ALL is ruled by a two-hit cancer model. MLL-AF4 is the first and driver oncogenic event, but the very short latency of this leukemia indicates there must be a secondary hit arising very early after birth (Sanjuan-Pla et al. 2015). Indeed, it has been described that the leukemic transformation by MLL fusion proteins requires the participation of H3K79 methyltransferase DOT1L (Chen and Armstrong 2015). This epigenetic modulator induces the expression of homeobox genes such as *HOXA* cluster and *MEIS1*, widely described as leukemic hits in hematopoietic progenitors. Importantly, genome-wide studies of infant pro-B-ALL patients, highlight that very few mutations or "second hits" are required to cooperate with MLL-AF4 to develop leukemia (Doblas et al. 2019). Therefore, MLL-AF4 arises in the embryonic state as a pre-leukemic clone or first hit, followed by a second hit that might come from the expression of *HOXA* or *MEIS1* genes (Sanjuan-Pla et al. 2015). Nowadays, current murine and humanized models of t(4;11) pro-B-ALL do not recapitulate the pathogenesis of this disease (C. Bueno et al. 2011; Clara Bueno et al. 2013), suggesting again that it is insufficient to initiate leukemogenesis but enough to create a pre-leukemic clone.

Importantly, DOT1L suppression inhibits the expression of MLL-AF4 target genes, demonstrating H3K79me is a distinguishable feature of MLL-AF4

leukemia and that it is dependent on DOT1L enzymatic activity (Chen and Armstrong 2015; Sanjuan-Pla et al. 2015). However, the transcriptional machinery associated to MLL-AF4 fusion protein involves several additional epigenetic modulators, such as MEN1 or class I HDACs (HDAC1/2). Some of these cofactors represent interesting entry points for the novel therapies that are being developed in this type of leukemia.

The standard treatment of infant t(4;11) pro-B-ALL includes intensive chemotherapy to induce remission or, in case of unfavorable prognosis, an allogenic hematopoietic stem cell transplantation (Pieters et al. 2007; Van der Velden et al. 2009). In fact, this type of leukemia shows chemoresistance to current treatment and high relapse rate, converting acute leukemia in the main cause of pediatric associated death. However, the use of T cells genetically modified to express a chimeric antigen receptor (CAR-T cells) has emerged as a hot topic in the therapeutic field over the last decade (Holstein and Lunning 2020). This treatment consists on a harnessing process of the own patients' immune T cells to provide them with the appropriate machinery (CARs), to specifically destroy cancer cells (Srivastava and Riddell 2015). For instance, dual CAR-T cells against CD19 and CD22 markers have demonstrated to be a promising therapeutic strategy in B-ALL patients who have previously failed conventional therapy regimens (Cordoba et al. 2021). The use of standard CD19 CAR-T therapy in infants is not yet implemented, despite promising results in small cohorts of infants have been published (Ghorashian et al. 2022).

Despite this success, some B-ALL subtypes undergo immune escape mechanisms, leading to the failure of CAR-T cells therapy. The use of such therapies in children <1 year of age renders novel obstacles, such as apheresis feasibility due to size, catheter placement, T cell fitness or the onset of neurotoxicity as a severe adverse effect (Shalabi and Shah 2022). The difficulty of finding a precise therapy against MLL-AF4 leukemic patients (and others) has driven to the research of new treatments against the many cofactors of this fusion protein, and to the investigation of novel biomarkers to improve the patients' outcome.



## 2.2. Diffuse Large B Cell Lymphoma

DLBCL represents 30% of all non-Hodgkin lymphoma cases, being the most common B lymphoid malignancy in adults. The age of diagnosis is in the mid-60s, and it can arise from a hidden low-grade B cell lymphoma (Ferlay et al. 2018; Sant, Allemani, and Tereanu 2011). DLBCL patients present rapid lymphadenopathy and demand therapy. R-CHOP is the first-line therapy, a combination of anti-CD20 monoclonal antibody named rituximab (R), plus cyclophosphamide (C), doxorubicin (H), vincristine (O) and prednisone (P) (Fisher et al. 1993; Roschewski, Staudt, and Wilson 2014). Around 60% of the patients have a good response to R-CHOP therapy; however, 40% of cases relapse after treatment or have refractory disease (Friedberg 2011). The prognosis for these patients is poor, as almost 80% of this population dies from the disease (Crump et al. 2017).

DLBCL is characterized by a striking degree of genetic heterogeneity. Many mutations in TF and epigenetic regulators place a barrier in the response to current standard immunotherapy. For this reason, a full comprehension of the different DLBCL subtypes at the molecular level is key to achieve new targeted therapies and develop new personalized treatments. Early studies of gene expression profiling have categorized almost 85% of DLBCLs in two subgroups, based on the cell-of-origin (COO): one of them resembles germinal center B cells (GCB-DLBCL), while the other one is similar to activated B cells (ABC-DLBCL), with a worse prognosis (Alizadeh et al. 2000; D. W. Scott et al. 2015). The remaining 15% of the cases are categorized as “unclassified”. More recently, with the advent of next-generation sequencing technology, Schmitz and colleagues devised a new classification named after the main features of each group (Schmitz et al. 2018; Wright et al. 2020), (Table 1). This classification further subdivided GCB and ABC subgroups and shed light into the variability between patients.

**Table 1. DLBCL classification based on genetic alterations.** Column on the left comprises the different groups name determined by the characteristics from the column on the middle. Right column reflects the expression subgroup of from original classification.

<b>Name</b>	<b>Genetic feature</b>	<b>Gene expression subgroup</b>
<i>MCD-DLBCL</i>	MYD88 and CD79B mutations	ABC
<i>EZB-DLBCL</i>	EZH2 mutation BCL2 translocation	GCB and ABC
<i>BN2-DLBCL</i>	BCL6 structural alteration NOTCH2 mutation	GCB and ABC
<i>N1-DLBCL</i>	NOTCH1 mutations	ABC
<i>ST2-DLBCL</i>	Mutations in SGK1 and TET2	GCB and ABC
<i>A53-DLBCL</i>	Aneuploid TP53 inactivation	GCB and ABC

Among the above classification, further research has unveiled other epigenetic regulators and TFs that are involved in DLBCL pathogenesis, corroborating its high heterogeneity. In fact, the accumulation of mutations in these regulators is thought to occur during SHM at the GC reaction. Point mutations in crucial genes may drive cells to gain immune privilege and proliferation.

As one of these crucial genes, *MEF2B* is mutated in almost 11% of DLBCL cases. Physiologically, *MEF2B* directly induces the expression of *BCL6* in GC B cells but, when mutated, the lymphomagenic activity of *MEF2B* is enhanced. Consequently, *BCL6* activity is also deregulated and partially confers GC B cells an increased proliferative capacity, leading to lymphomagenesis (Ying et al. 2013).

In terms of own genetic alterations, *BCL6* is mutated in ~40% of DLBCL cases (Lo Coco et al. 1994; B H Ye et al. 1993). In healthy GC B cells, *BCL6* autoregulates its expression through binding to its own promoter and negatively

regulating its own transcription (Pasqualucci et al. 2003). However, genetic lesions that take place in DLBCL patients, abrogate this autoregulatory circuit, leading to an uncontrolled expression levels of BCL6 (Hatzi et al. 2013; Hatzi and Melnick 2014). Oppositely to BCL6 expression pattern, we can find FOXP1, suggesting that this TF regulates the transition from resting follicular B cells to activated GC B cells. Therefore, FOXP1 needs to be downregulated, for an optimal GC formation. In fact, in transgenic mice, the constitutive expression of *Foxp1* impairs GC reaction, thus contributing to B cell lymphomagenesis (Sagardoy et al. 2013).

Mutations impairing the enzymatic activity of *KMT2D*, that encodes MLL2/4 proteins, are also recurrent in DLBCL (~30%) (Alizadeh et al. 2000). *KMT2D* preserves the epigenetic landscape of GC B cells and, in mice, its abrogation results in a global diminishment of H3K4 methylation. In this sense, *Kmt2d* deletion before the initiation of the GC reaction strengthens B cell proliferation in mice, contributing to lymphomagenesis (Zhang, Nat medicine 2015).

In line, DNA methylation in DLBCL can be affected by mutations in *TET2*, which occur in ~10% of cases. *TET2* deficiency in mice leads to DNA hypermethylation of regulatory regions and to the silencing of affected genes. This hypermethylation impedes the binding of TFs crucial for the GC reaction, causing a pre-neoplastic phenotype (Dominguez et al. 2018; Rosikiewicz et al. 2020). Additionally, *TET2* mediates DNA hydroxymethylation, which is the initial step of DNA demethylation, of genes that mediate the GC exit, such as *PRDM1*, crucial to achieve PC differentiation (Dominguez et al. 2018). Therefore, *TET2* loss disrupts the GC exit, a common event also observed in *CREBBP*-mutant DLBCLs.

Importantly, inactivating mutations in *CREBBP* are also common in DLBCL (~10% of cases). *CREBBP* is a histone acetyltransferase that regulates enhancer networks involved on the main GC and post-GC decisions. Mechanistically, *CREBBP* mediates H3K27 acetylation in enhancer regions essential for B cell cycle exit. Concomitantly, the BCL6-SMRT/NCOR-HDAC3 complex binds to these same enhancer regions, resulting in a poised H3K27 deacetylated

configuration and its consequent gene repression. Before the GC exit, the complex is removed, unveiling H3K27ac epigenetic marks to boost the enhancers in post-GC decisions. In contrast, CREBBP loss-of-function in mice promotes the repression of enhancers that need to be deactivated in GCs, therefore impairing GC B cells exit and maintaining the GC phenotype, thus contributing to lymphomagenesis. The loss-of-function mutations in CREBBP are insufficient to induce malignant transformation, but have a role in lymphoma initiation (Jiang et al. 2017; Zhang et al. 2017).

CREBBP functional paralogue EP300 is also mutated in DLBCL but less frequently (~5% of cases). Its deletion in mice impairs the fitness of the GC reaction but, differently from CREBBP mutations, it mainly affects DNA repair, replication and cell cycle, alterations that also contribute to lymphomagenesis (S. N. Meyer et al. 2019).

Another essential epigenetic regulator in GC B cells is EZH2, a component of the PRC2 complex that catalyzes the methylation of H3K27, a mark associated to transcriptional repression. The epigenetic silencing of EZH2 in GC B cells promotes proliferation and prevents differentiation, common features in lymphomas (Su et al. 2003; Velichutina et al. 2010).

All this transcriptional and epigenetic heterogeneity is linked to resistance to therapy and poor clinical outcome. In parallel to classifications based on transcriptional patterns or epigenetic alterations, subtypes of DLBCL have also been pathologically defined. For instance, DLBCL simultaneously overexpressing the oncogenes BCL2 and MYC, named double-expressor lymphomas (DEL), end up to 50% of relapsed or refractory DLBCL (rrDLBCL) (Herrera et al. 2017). It is also known that the so-called tripe-hit lymphomas (THL) carrying genetic rearrangements in *MYC*, *BCL2* and *BCL6*, have a poor response to standard treatments (Ennishi et al. 2017).

For all these reasons, treatment resistance remains as a major challenge in DLBCL patients. Conventional R-CHOP treatment requires the supplementation of novel agents specifically targeting the molecular pathways altered, but also the

epigenetic mechanisms that allow DLBCL cells escaping from conventional therapies. For instance, EZH2 inhibitors such as GSK126 and tazemetostat have anti-apoptotic and anti-proliferative effects in DLBCL models, and have also demonstrated efficacy in clinical trials (Brach et al. 2017). The use of immunotherapy has also been tested in DLBCL. Similarly to leukemia treatment, CD19-engineered CAR-T cell therapy has provided a complete recovery in almost 50% of rrDLBCL patients (Kochenderfer et al. 2017). These therapies are promising strategies for treating rrDLBCL and improve the outcome of patients but, unfortunately, only a small proportion of the patients respond with complete remission due to occurrence of resistance.

### 3. Epigenetic mechanisms

DNA is wrapped around nucleosomes, which are composed by eight globular histone proteins, two of each of the following proteins: H2A, H2B, H3 and H4. H1 protein links histones between them to wrap neighboring nucleosomes (Khorasanizadeh 2004; Koyama and Kurumizaka 2018). This layer of DNA binding with histone proteins and histone modifiers has settled the base of epigenetics. Epigenetics can be defined as the changes in gene expression that occur without alterations in the DNA sequence itself. Epigenetic modifications are the base for these transcriptional changes and include, among others, DNA methylation and histone modifications.

#### 3.1. DNA methylation

DNA methylation is one of the most extensively studied epigenetic mechanisms, and it consists on the covalent attachment of a methyl group (-CH<sub>3</sub>) by DNA methyltransferase enzymes (DNMTs) to the fifth carbon of the pyrimidine ring of a cytosine, resulting in a 5-methylcytosine (5-mC) residue (Zeng and Chen 2019).

Three main DNMTs catalyze DNA methylation in mammals: DNMT1, DNMT3A and DNMT3B, and use the cofactor S-adenosyl-L-methionine (SAM) as the methyl group donor (Figure 6). DNMT3A and DNMT3B are responsible for *de novo* DNA methylation, and both of them are essential during embryonic development (Okano et al. 1999). In parallel, DNMT1 maintains DNA methylation patterns across cell divisions. This enzyme binds to hemi-methylated DNA double strands after replication and, guided by UHRF1 protein, adds a new methyl group parallel to the previously existing one (Song et al. 2011, 2012).

The distribution of DNA methylation is mainly restricted to CG dinucleotides, located in regions called “CpG islands”, which are regions GC-rich of approximately 200bp and around 70% of them are located in promoter regions (Deaton and Bird 2011). Functionally, CG methylation is linked to transcriptional repression, and occurs through two distinct mechanisms. On one hand, DNA

methylation results in steric impediment exerted by the methyl group that interferes with the recruitment of TFs to their DNA-binding sites. On the other hand, DNA methylation results in the recruitment of methyl-CpG-binding proteins (MBPs), which repress transcription by interacting with co-repressors, such as HDACs or members of the Polycomb complex (Jin, Li, and Robertson 2011; Weber and Schübeler 2007; Zeng and Chen 2019).

### **3.2. DNA demethylation**

DNA demethylation can occur either by passive or active mechanisms (Figure 7). Passive DNA demethylation erasure of methyl group takes place upon a DNMT loss-of-function, that can be caused by mutations driving to loss of expression or inhibition of its activity. Consequently, DNA methylation is lost after successive cell divisions. Oppositely, active demethylation involves the catalytic removal of the methyl group by the ten-eleven translocation (TET) family of enzymes. TET family is composed by TET1, TET2 and TET3, which catalyze, in a multistep process, the oxidation of 5-mC to 5-hydroxymethylcytosine (5-hmC). Later, 5-hmC is transformed to 5-formylcytosine (5-fC) and, finally, to 5-carboxylcytosine (5-caC). These intermediate compounds can be eliminated in a passive manner, dependent on cell replication, or excised by the thymidine DNA glycosylase (TDG) enzyme. TDG leaves an abasic site that will be further repaired by the base excision repair (BER) machinery, resulting in a demethylated DNA and, if located in a promoter site, leading to the expression of the associated gene (Hashimoto et al. 2012; Wu and Zhang 2017).

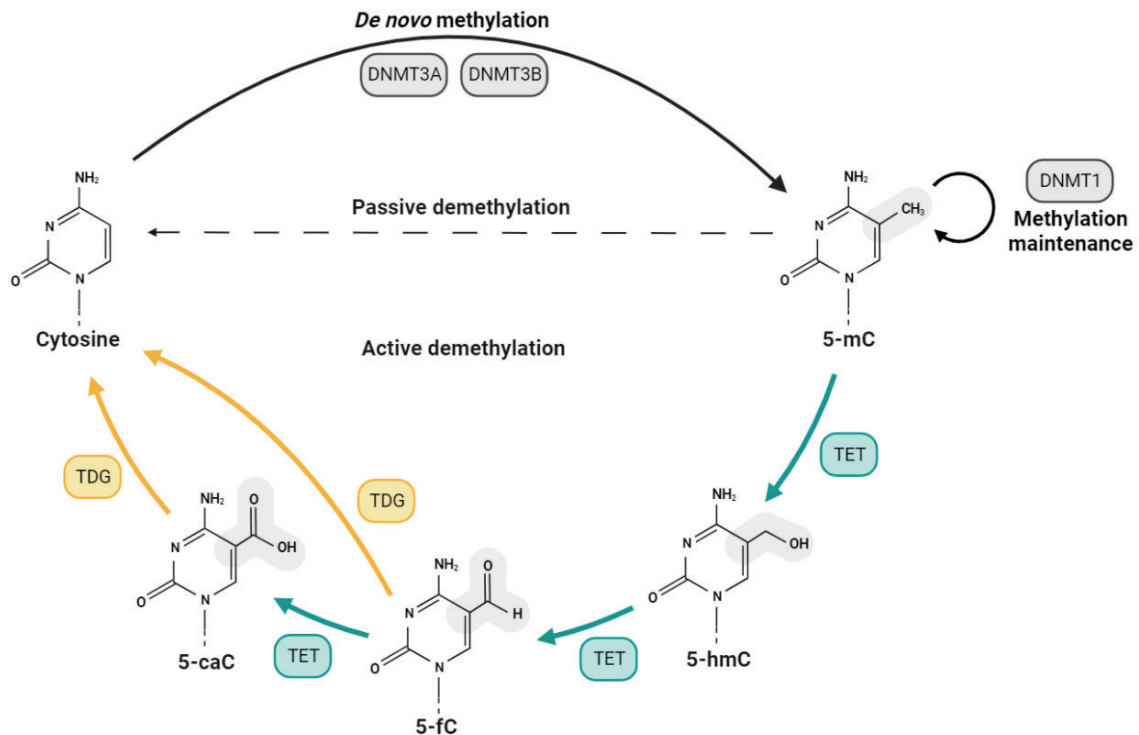


**Figure 7. De novo methylation and passive/active demethylation schema.** Cytosine molecule is methylated by DNMT3A/B into 5-methylcytosine (5-mC). Passive demethylation happens upon dilution of the methylation mark during replication steps. DNMT1 mediates the methylation maintenance through cell replication. Active DNA demethylation from 5-mC (5-methylcytosine) to 5-hmC (5-hydroxymethylcytosine), 5-fC (5-formylcytosine) and to 5-caC (5-carboxylcytosine) is mediated by TET proteins. Final restoration of the unmethylated cytosine is achieved by TDG enzyme from 5-caC or either 5-fC.

### 3.2.1. TET proteins

TET enzymes contain a C-terminal catalytic domain that oxidizes the substrates, and an N-terminal domain that contains a CXXC DNA binding domain. Differently from TET1 and TET3, TET2's putative CXXC domain is separated from the protein due to an evolutionary inversion, becoming a new protein named IDAX (Hu et al. 2013; Ko et al. 2013).

The TET-DNA interaction does not involve the methyl group, thus allowing TET to bind to different forms of modified cytosines. Nonetheless, TET enzymes have substrate preferences. First, they present higher affinity for 5-mC in a CpG context, rather than in CpC or CpA (Hu et al. 2013) and, second, TET proteins put forward 5-mC than 5-hmC or 5-fC, and enzyme kinetics analysis have



revealed that the fastest catalysed conversion is from 5-mC to 5-hmC (Hu et al. 2015; Ito et al. 2011). Therefore, 5-hmC epigenetic mark is less predisposed to be oxidized, a relevant fact for regulatory functions of TFs binding (Hu et al. 2015; Wu and Zhang 2017).

TET2 is highly expressed in the hematopoietic system and neuronal lineages, and its deficiency impairs correct development of both systems. Loss of TET2 and TET3 in mice impairs pro-B to pre-B cell commitment by blocking demethylation of *IgK* enhancers and globally decreasing chromatin accessibility to B cell TFs at enhancers. In addition, conditional knock out of TET2 and TET3 prevents B cell lineage-specific genes demethylation, causing disruption in cell differentiation (Lio et al. 2016; Martin-Subero and Oakes 2018; Orlanski et al. 2016; Tsagaratou et al. 2017). Remarkably, *TET2* has been reported as one of the most frequently mutated genes in DLBCL (6-12% of cases) (Asmar et al. 2013; Reddy et al. 2017a).

### **3.3. Histone modifications**

Histones possess intrinsically unfolded N-terminal tails susceptible of being post-translationally modified. Histone modifications affect their interaction with DNA, altering chromatin compaction and, consequently, the transcriptional activity of histone surrounding genes. The unwinding of nucleosomes caused by some histone modifications changes the chromatin structure resulting in a more open chromatin status (euchromatin), that allows TF recruitment and gene activation. Contrarily, other histone modifications strengthen the binding between histones and DNA, therefore, lead to a more compacted chromatin state (heterochromatin), which is associated to transcriptional silencing.

Histone modifiers have been identified and classified into 'writers', 'erasers' or 'readers' depending on whether they deposit, remove or recognize histone marks, respectively (Bannister and Kouzarides 2011; Hyun et al. 2017). Histone modifications comprise methylation, acetylation, phosphorylation, ubiquitylation and sumoylation, among others, being acetylation and methylation the most well studied so far. Generally, histone acetylation is associated with gene activation,

whereas histone methylation may exert both activating or repressing roles, depending on the specific altered residue.

Histone methyltransferases (HMT) are enzymes that harbor the enzymatic activity to deposit methyl groups into histones, which can be erased by histone demethylases (HDMT). Methyl groups are deposited in lysine and arginine residues on histones H3 and H4, using SAM as cofactor. HMTs can be classified into arginine-specific HMTs (PRMTs) or lysine-specific HMTs (KMTs), being the latter divided in subgroups, depending on the presence or absence of a conserved catalytic SET domain. Lysine can be modified in a mono-, di- or tri-methylated manner, whereas arginine can only be mono- and di-methylated. As none of the methylation states changes the charge of the amino acid affected, the effect recalls in effector molecules that recognize the methylated sites, and these 'readers' contain methyl-binding motifs such as PHD, chromo or PWWP. As mentioned above, histone methylation does not determine an active or repressive state but, depending on the methylated residue position, a correlation is established. For example, H3K79 and H3K4 methylation pinpoint active transcription, whereas H3K9 and H3K27 methylation are generally associated with gene silencing (Hyun et al. 2017).

Histone/protein acetyl transferases (HATs) and histone/protein deacetylases (HDACs) are two families of enzymes that exert opposite actions on the acetylation of histone tails (Figure 8). HATs use acetyl-CoA as the acetyl group donor to "write" it to the lysine in the histone tail leading to the neutralization of lysine's positive charge and weakening the histone interaction with DNA. Meanwhile, HDACs erase lysine acetylation, restoring the positive charge and stabilizing the chromatin architecture and condensation. Therefore, HATs are associated with transcriptional activation, whereas HDACs are commonly linked to transcriptional repression. (Bannister and Kouzarides 2011; Morgan and Shilatifard 2020). Of note, it is well established that HATs and HDACs not only acetylate or deacetylate histone variants, but also occur in a considerable number of non-histone proteins, such as TF and cytoplasmic proteins (Peng and Seto 2011).

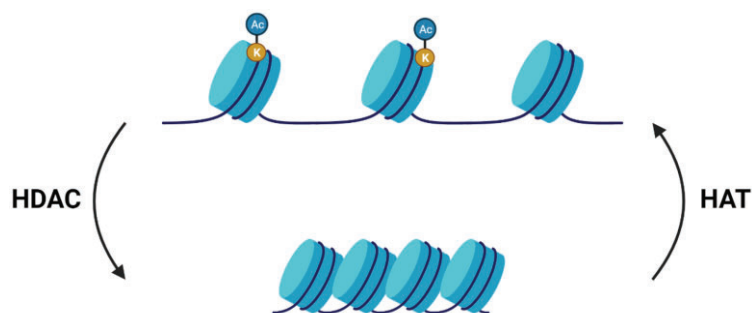


**Figure 8. Schematic representation of the chromatin status depending on HDAC or HAT enzymatic activity.** HAT (histone acetyltransferase) adds an acetyl group to a histone lysine (K) residue and in consequence chromatin adopts an open status, associated to transcriptional activation. Contrarily, HDAC (histone deacetylase) removes the acetyl group, compacting chromatin and repressing gene expression.

#### 4. Histone or protein deacetylases

HDACs' ability to remove acetyl groups from lysine residues is associated to a gene repressive function. Indeed, HDACs are considered transcriptional repressors and co-repressors in many physiological and pathological systems (Barneda-Zahonero and Parra 2012). To date, 18 human HDACs have been identified and grouped into four classes (I-IV) according to their homology with yeast proteins (Figure 9).

Class I HDACs (HDAC1, 2, 3 and 8) share sequence similarity with *S. cerevisiae* reduced potassium dependency 3 (*Rpd3*) (Taunton, Hassig, and Schreiber 1996). Their structure consists of a conserved catalytic domain flanked by short amino and carboxy-terminal domains. They are expressed ubiquitously, mainly displaying enzymatic activity in the nucleus (Haberland, Montgomery, and Olson 2009).

Class II HDACs are subdivided into IIa and IIb subclasses, and share homology with yeast histone deacetylase-A1 (*Hda1*) (Grozinger, Hassig, and Schreiber 1999). Class IIa HDACs, which comprise HDAC4, 5, 7 and 9, possess particular features not shared with other HDACs protein families. These particularities will be further developed in the next section, since this is the main focus of this thesis. Class IIb HDACs comprise HDAC6 and 10 and are characterized by a duplication of their catalytic domains, presenting a copy at

each protein termination. Both HDAC6 and 10 are mainly located in the cytoplasm but can shuttle to the nucleus (Delcuve, Khan, and Davie 2012).

Class III HDACs or Sirtuins (SIRT1, 2, 3, 4, 5, 6 and 7) are homologs with yeast Silent information regulator 2 (*Sir2*). Sirtuins have two enzymatic activities, they are nicotinamide-adenine dinucleotide (NAD<sup>+</sup>) dependent protein deacetylases, and some of them have also mono-ADP-ribosyltransferase activity. SIRT5 also owns protein lysine desuccinylase and demalonylase activity (Du et al. 2011). Their cellular compartment location is also variable and can be found at the nucleus, the cytoplasm and the mitochondria (Seto and Yoshida 2014).

Finally, class IV HDACs is solely constituted by HDAC11. Structurally, it presents a catalytic domain, homolog to class I and II HDACs, and short N- and C-terminal extensions. Its subcellular location varies between the nucleus and the cytoplasm depending on the cell type (Núñez-Álvarez and Suelves 2021). Specifically, HDAC11 is found expressed in brain, testis, kidney and also muscle (Gao et al. 2002).

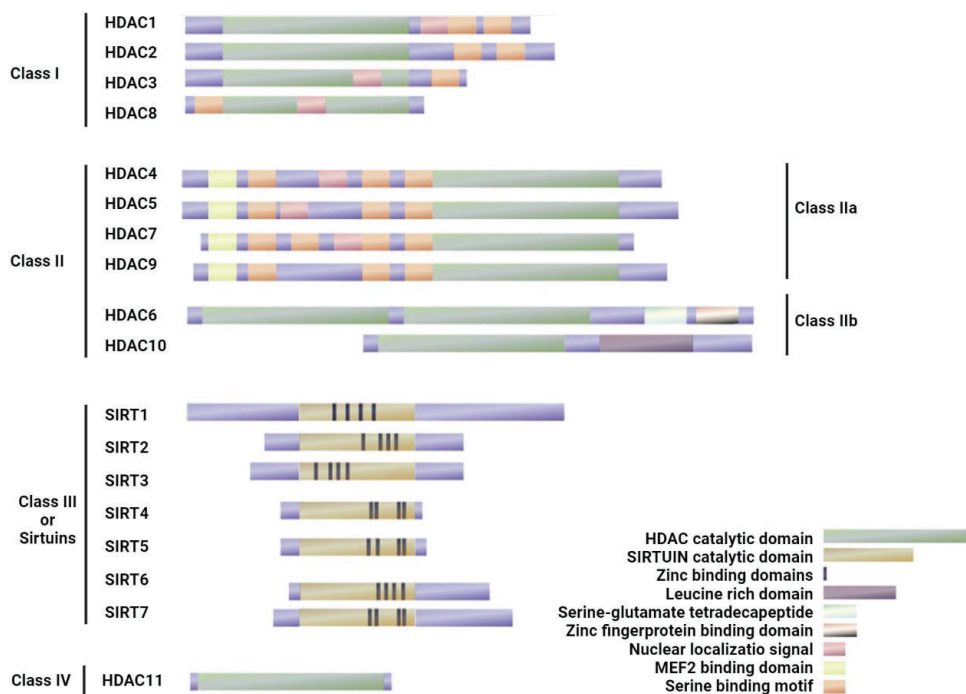


**Figure 9. HDACs family classification.** HDACs are grouped into four different classes. Most relevant domains are colored as detailed in legend. Figure modified from (Barneda-Zahonero and Parra 2012).

## 4.1. Class IIa HDACs

Among all HDACs, class IIa present unique features. First of all, they possess a long N-terminal domain that contains interacting sites for TFs, such as members of the MEF2 family. The binding domain allows class IIa HDACs to interact with MEF2 or other TFs and permits its recruitment to their target genes, thus modulating its expression (Dressel et al. 2001; Di Giorgio and Brancolini 2016; Lemercier et al. 2000; Miska et al. 1999). Second, the signaling-dependent phosphorylation of several serine residues located at the N-terminal domain controls their subcellular location. Under basal conditions, serine residues are unphosphorylated and class IIa HDACs remain located in the nucleus, where they can exert their transcriptional repressive function. However, in response to external stimuli, class IIa HDACs become phosphorylated and exported to the cytoplasm where, consequently, their target genes become de-repressed (Parra and Verdin 2010). Third, class IIa HDACs lack of measurable enzymatic activity on histones, although they have a highly conserved catalytic domain. Actually, it has been described that they bridge to the SMRT/N-CoR-HDAC3 enzymatic complex to exert their activity, acting as adaptors of repressor complexes and not real enzymes (Fischle et al. 2002). Finally, they are expressed in a tissue-specific manner and exert their transcriptional repressive function in distinct tissues, such as the bone, the vascular system, the brain, skeletal, smooth and cardiac muscle and in the immune system, among others (Parra 2015).

### 4.1.1. HDAC7

HDAC7 was discovered in the early 2000's in Evans' laboratory as an interactor of the SMRT/N-CoR complex (Kao et al. 2000) and, since then, its role in multiple physiological and pathological systems has been studied.

In muscle, MEF2 TFs exert a critical role in terminal differentiation. When muscle differentiation is induced, HDAC7 shuttles from the nucleus to the cytoplasm, allowing MEF2 to exert its gene activating function (Dressel et al. 2001). *Hdac7*-deficient mice show embryonic lethality at day 11, resulting from a vascular dilatation caused by a failure in the proper formation of cell-to-cell

junctions between endothelial cells in the developing circulatory system. HDAC7, through MEF2C, represses matrix metalloproteinase 10 (MMP10), a critical regulator for blood vessel formation and extracellular matrix degradation (Chang et al. 2006). In addition, HDAC7 also interacts with RUNX2, an essential regulator of bone formation, and represses its expression during osteoblast maturation (Jensen et al. 2008; Jensen, Gopalakrishnan, and Westendorf 2009).

In the hematopoietic system, HDAC7 is highly expressed in CD4<sup>+</sup>CD8<sup>+</sup> double positive thymocytes. It is localized in the nucleus of resting T cells, where it represses many genes involved in the positive and negative selection of these cells. Among those genes, HDAC7 represses Nur77, an orphan receptor involved in the apoptosis and negative selection of thymocytes via MEF2D interaction. After T cell receptor (TCR) activation, HDAC7 is phosphorylated by protein kinase D (PKD-1) and exported from the nucleus to the cytoplasm, leading to Nur77 expression (Dequiedt et al. 2003, 2005; Parra et al. 2005). Thymocytes lacking HDAC7 in the double positive stage evolve into a population with reduced proportion of CD4<sup>+</sup> and increased ratio of CD8<sup>+</sup> T cells, due to an inefficient negative selection, short lifespan and loss of viability (Kasler et al. 2011; Myers et al. 2017). The fact that HDAC7 deficiency in thymocytes does not impede positive selection, promotes the escape of autoreactive T cells into the periphery, developing tissue-restricted autoimmunity (Kasler et al. 2012, 2018). In line with that, CD8<sup>+</sup> cytotoxic T lymphocytes (CTL) retain HDAC7 in the cytoplasm by mediated phosphorylation, and a disruption of this process drives to CTL malfunction (Navarro et al. 2011).

Besides its role in thymocytes, it has also been reported by our laboratory that HDAC7 plays a crucial role in the biology of B lymphocytes. In 2009, the laboratory of Thomas Graf developed an *in vitro* immune cellular reprogramming system in which pre-B cells transdifferentiate into macrophage-like cells after induction of the myeloid TF CEBP $\alpha$  (Bussmann et al. 2009). Interestingly, our group found that HDAC7 was downregulated during the conversion of pre-B cells into macrophages, and the exogenous expression of HDAC7 in this system interferes with the establishment of the myeloid transcriptional program.

HDAC7 is recruited to MEF2C binding sites at the promoter of non-B cell genes in pre-B cells leading to their transcriptional repression (Barneda-Zahonero et al. 2013). Accordingly, using a conditional knock out mouse model for *Hdac7* in the pro-B cell stage, it was reported that HDAC7 deficiency dramatically blocked early B cell development in the bone marrow, developing severe lymphopenia in peripheral organs. In pro-B cells, HDAC7, via MEF2C, was found to be recruited to promoters and enhancers of myeloid and T lymphocyte genes, leading to their transcriptional repression. Moreover, HDAC7 acts as epigenetic modulator, since its deficiency resulted in an increased enrichment of histone active marks (H3K9/K14ac and H4K16ac) and a decrease in the repressive epigenetic marks (H3K27me3) at the promoter regions of these non-B cells genes. This way, HDAC7 ensures proper early B cell development (Azagra et al. 2016).

For many years, alterations in HDAC family members have been reported in several cancers, and HDAC7 is not an exception. It is overexpressed in adenocarcinoma of the pancreas (Ouaïssi et al. 2008), in myeloproliferative neoplasms (Skov et al. 2012), in renal cancer (Nam et al. 2021) and in non-small cell lung cancer (Guo et al. 2022). Other studies have reported a connection between HDAC7 and B-cell derived hematologic malignancies. For instance, an insertional mutagenesis study unveiled HDAC7 as a potential gene related with hematological cancers (Rad et al. 2010). Additionally, Lohr *et al.* pinpointed HDAC7 as a mutated gene in DLBCL (Lohr et al. 2012) and, afterwards, Morin *et al.* described that HDAC7 is mutated in 7% of DLBCL cases (Morin et al. 2013). Furthermore, Reddy *et al.* have catalogued HDAC7 as a potential tumor suppressor in a study performed in a cohort of 1001 DLBCL patient samples (Reddy et al. 2017b).

Different roles in several development systems highlight the importance of HDAC7 and, despite all the recapitulated information, its role in B cell development and the potential implication in B cells associated pathologies is still not completely understood. Further studies are required in order to fully understand its role in the development of healthy B cells and to find the mechanistic reasons that underlie its altered expression in B cell malignancies.





## **OBJECTIVES**



## **OBJECTIVES**

The work performed during this PhD thesis aimed to address the following objectives:

1. To dissect the HDAC7-mediated molecular mechanisms during pro-B lymphocyte differentiation.
2. To investigate the potential anti-oncogenic role of HDAC7 in pediatric pro-B-ALL.
3. To analyze the contribution of HDAC7 as a transcriptional regulator of the germinal center reaction.
4. To unveil the potential anti-lymphomagenic implication of HDAC7 in DLBCL.



## **RESULTS**



I hereby certify that the PhD student Ainara Meler Marquina will present her thesis as a compendium of three publications. Her contribution to each work is as follows:

**Article 1:** Alba Azagra †, **Ainara Meler** †, Oriol de Barrios, Laureano Tomas-Daza, Olga Collazo, Beatriz Monterde, Mireia Obiols, Llorenç Rovirosa, Maria Vila-Casadesús, Mónica Cabrera-Pasadas, Mar Gusi-Vives, Thomas Graf, Ignacio Varela, José Luis Sardina, Biola M. Javierre, Maribel Parra.

†The authors contributed equally to this article

**Title:** “The HDAC7–TET2 epigenetic axis is essential during early B lymphocyte development”

**Journal:** Nucleic Acids Research, 2022, Vol. 50, No. 15 8471–8490. Impact factor (2022): 19.33

In this article Ainara Meler participated in some experiments reported. Particularly in bone marrow extraction, cell sorting of *Hdac7<sup>+/+</sup>* and *Hdac7<sup>fl/-</sup>* pro-B and pre-B cells and of *ex-vivo* cell culture, ATAC-seq experiments, ChIP-seq experiments of the histone marks H3K27ac and H3K27me3, primary culture of bone marrow B cells, *ex vivo* infection of bone marrow B cells with Tet2 shRNA, RT-qPCR of several genes and analysis of the RNAseq, ATAC-seq and H3K27ac and H3K27me3 ChIP-seq data, as well as integrative study of omics datasets and data interpretation. Several data from this article have been used for the thesis of Alba Azagra Rodríguez but does not include the above-mentioned experiments.

**Article 2:** Oriol de Barrios, Alexandros Galaras, Juan L. Trincado, Alba Azagra, Olga Collazo, **Ainara Meler**, Antonio Agraz-Doblas, Clara Bueno, Paola Ballerin, Giovanni Cazzaniga, Ronald W. Stam, Ignacio Varela, Paola De Lorenzo, Maria Grazia Valsecchi, Pantelis Hatzis, Pablo Menéndez, Maribel Parra.

**Title:** “HDAC7 is a major contributor in the pathogenesis of infant t(4;11) proB acute lymphoblastic leukemia”

**Journal:** Leukemia. 2021;35(7):2086-2091. Impact factor (2021): 12.255

In this article Ainara Meler has been involved in the analysis of HDAC7 expression in MLL-AF4 pro-B-ALL patients compared to healthy B cell progenitor and other pro-B-ALL with alternative rearrangements. Moreover, she has assisted in the generation of HDAC7-overexpressing pro-B-ALL SEM cell line.

**Article 3:** **Ainara Meler**, Mar Gusi-Vives, Oriol de Barrios, Alba Azagra, Olga Collazo, Javier Melchor, Alberto del Monte, Miriam Verdu-Bou, Tomás Navarro, Ignacio Martin-Subero, Gaël Roué, Almudena R. Ramiro, Sergio Roa, Maribel Parra.


**Title:** “HDAC7 is involved early pre-germinal center and its deregulation is associated with DLBCL”

**Journal:** Manuscript in preparation.

In this article Ainara Meler participated in all the experiments reported. In particular, in different B cell populations cell sorting from *Hdac7*<sup>+/+</sup> and *Hdac7*<sup>fl/ko</sup>, RT-qPCR of various genes, FACS analysis, *ex vivo* cell culture of CD43<sup>-</sup> splenic cells, immunoglobulin production assessment upon *ex vivo* stimulation of splenic B cells, western blot, RNA-seq experiments and data analysis, immunohistochemistry of spleen sections, cell counting, cell viability and cell cycle assessment, gain of function experiments in DLBCL cell line and xenografts approach with this same cell line, as well as general data collection, analysis, figures edition and manuscript preparation.

In witness whereof, I hereby sign this in Badalona,

PARRA BOLA,  
MARIA ISABEL  
(AUTENTICAC  
IÓN)



Firmado  
digitalmente por  
PARRA BOLA, MARIA  
ISABEL  
(AUTENTICACIÓN)  
Fecha: 2023.04.12  
11:45:52 +02'00'

Badalona, March 31<sup>st</sup>, 2023

Maribel Parra Bola, PhD

Lymphocyte Development and Disease Group leader  
Josep Carreras Leukaemia Research Institute  
Ctra de Can Ruti, Camí de les Escoles s/n  
08916 Badalona, Barcelona



## SUMMARY OF RESULTS

The study of HDAC7 in our laboratory has demonstrated that it is a master transcriptional repressor of lineage-inappropriate genes in early B cell development. Our goals in this PhD thesis have consisted in the study of the role and mechanisms of action of HDAC7 in early and terminal B cell development, as well as in B cell malignancies. For the execution of our studies, we have used *in vivo*, *ex vivo* and *in vitro* experimental approaches, using conditional knock out mice models, cell lines and human samples.

### 1. HDAC7 regulates chromatin condensation and 5-hmC levels in pro-B cells

To decipher the HDAC7-mediated molecular mechanisms during early B cell development, we generated a conditional knock out mouse model to delete HDAC7 expression at the pro-B cell stage. We crossed *Hdac7<sup>loxp/ko</sup>* mice with the *mb1-Cre* strain, which expresses Cre recombinase in pro-B cells. RNA-seq of pro-B and pre-B sorted cell populations unveiled an altered profile of genes involved in chromosome condensation, suggesting a potential deregulation of chromatin conformation in the absence of HDAC7. To test whether HDAC7 may be required to maintain a proper chromatin state in pro-B and pre-B cells we performed ATAC-seq. The global chromatin accessibility intensity was higher in both HDAC7-deficient pro-B and pre-B cells, compared to wild-type cells, and the genomic distribution of accessible sites differed. A reduction of open promoter regions, more notably in pro-B cells, and an increase of accessible distal intergenic regions was observed. Integration of ATAC-seq and RNA-seq data unveiled that around 200 upregulated genes presented a more open and accessible chromatin in both HDAC7-deficient pro-B and pre-B cells.

It has been reported that increases in DNA 5-hmC are associated with chromatin decompaction and, consequently, with alterations in hematopoietic cell differentiation and maintenance of cell identity (Izzo et al. 2020). Accordingly, we proved that HDAC7 deficiency in pro-B cells leads to a significant increase in 5-hmC global levels. Taken together, these data indicate that HDAC7 controls

chromatin compaction and DNA 5-hmC levels at early stages of B cell development.

## **2. HDAC7 regulates *Tet2* expression and epigenetic marks deposition**

Analysis of public data from the Immgen database classifies HDAC7 as a potential and unique negative regulator of *Tet2* expression. Accordingly, *Tet2* was upregulated in HDAC7 deficient pro-B and pre-B cells compared to wild-type cells. These data suggest that HDAC7 may govern early B cell development through the regulation and maintenance of TET2 physiological levels. Molecularly, we found that HDAC7 is recruited to the promoter of *Tet2*. To gain insight into the epigenetic mechanisms driven by the HDAC7-TET2 axis, we performed ChIP-seq on H3K27ac and H3K27me3 histone marks in wild-type and HDAC7-deficient pro-B cells. We observed a global higher enrichment of H3K27ac in HDAC7-deficient pro-B cells, as well as at *Tet2* promoter region. This is in concordance with ATAC-seq results, and reinforces HDAC7 repressive role. Enrichment of H3K27me3 repressive mark did not show significant changes between wild-type and HDAC7-deficient pro-B cells. Collectively, these results demonstrate that HDAC7 controls the proper deposition of epigenetic marks and that *Tet2* is directly targeted by HDAC7 in pro-B cells.

## **3. HDAC7 deficiency alters 5-hmC at specific loci controlling the expression of lineage inappropriate genes in pro-B cells.**

We next performed 5-hmC DNA immunoprecipitation sequencing (hMeDIP-seq) revealing higher 5-hmC overall signal in HDAC7-deficient pro-B cells compared to wild-type. Next, we focused our attention on potential alterations in 5-hmC at lineage-inappropriate genes. We observed an increase in the enrichment of 5-hmC at the *Jun* loci in HDAC7-deficient pro-B cells that, together with its higher expression observed in our transcriptomic analysis, its open chromatin observed in ATAC-seq, and the recruitment of TET2 to the *Jun* loci, indicating that its expression is regulated by the HDAC7-TET2 axis. Additionally, we performed loss-of-function or rescue experiments. Knocking down *Tet2* prevented the upregulation of *Jun* in HDAC7-deficient B cells, proving the involvement of the HDAC7-TET2 axis in the proper control of the expression of lineage inappropriate genes in pro-B cells.

Overall, our data demonstrated that, during early B cell development, HDAC7 exerts a crucial role in preserving chromatin conformation and controlling TET2 levels, leading to maintain 5-hmC physiological levels at lineage inappropriate genes.

#### **4. HDAC7 contributes to the pathogenesis pro-B-ALL**

*As mentioned above, HDAC7 is essential for the correct development of pro-B lymphocytes. Therefore, HDAC7 could be implicated in the pathogenesis of a malignancy with origin in the pro-B cell, such as pro-B-ALL.*

We assessed by RNA-seq whether HDAC7 expression was altered across different pro-B-ALL subtypes, grouped according to *MLL* status. The subgroup with a t(4;11) rearrangement showed a dramatic underexpression of HDAC7. Clinically, was observed that the low HDAC7 expression was associated to poorer outcome. Concomitantly, the lowest levels of HDAC7 were in marked contrast to a higher expression of the oncogene c-MYC, highlighting an aggressive phenotype.

The unfavorable impact of low HDAC7 expression on clinical outcome prompted us to investigate whether HDAC7 has any protective effects on pro-B-ALL. For that, two cell lines with low HDAC7 expression levels, SEM-K2 and RS4;11 were transduced with a two-step retroviral vector that enables exogenous HDAC7 expression in an inducible manner upon doxycycline addition. We found that the exogenous expression of HDAC7 compromised the viability of the cells. RNA-seq analysis of the transduced SEM-K2 cell line reinforced the previous results, highlighting a downregulation of key hallmarks of cancer such as proliferation, migration and apoptosis evasion. Overall, these findings support the role of HDAC7 as a novel biomarker and prognostic factor in t(4;11) pro-B-ALL.

*Deeping into the B lymphocyte development path, we interrogated whether HDAC7 could also be involved in the regulation of the late B cell differentiation.*

## 5. HDAC7 is required for the germinal center reaction

*Given the importance of HDAC7 in maintaining the chromatin status through Tet2 silencing in pro-B cells, we started a new research project focused in HDAC7 role in the GC reaction. Additionally, we interrogated HDAC7 participation in GC-derived DLBCL, as we previously described its importance in pro-B-ALL.*

To determine whether HDAC7 is required for the GC reaction we generated a conditional knock out mouse model for specific deletion of HDAC7 in activated B cells, by crossing *Hdac7<sup>fl/ko</sup>* mice with the Cγ1-Cre strain, which expresses Cre recombinase in activated B cells. We immunized wild-type and HDAC7-deficient mice with a T-cell dependent antigen (SRBC) to induce GC formation and performed a series of phenotypic analysis 10 days later. Upon immunization, the percentage of GC B cells and PCs in HDAC7-deficient mice was reduced. To assess the potential effect of HDAC7 deficiency in CSR we stimulated splenic B cells from wild-type and HDAC7-deficient mice *ex vivo* with different stimulus and measured IgG isotypes by flow cytometry. We found that HDAC7-deficient B cells showed a significant decrease in IgGs production at 72h after treatment. Together these data indicate that HDAC7 is essential for the GC reaction, and its loss impairs CSR and terminal B cell differentiation into PCs.

## 6. HDAC7 deficiency induces transcriptional changes in GC B cells and alters proliferation

To shed light into the HDAC7-mediated mechanisms underlying the GC reaction we performed RNA-seq of sorted GC B cells from wild-type and HDAC7-deficient immunized mice. Upregulated genes in the absence of HDAC7 revealed an enrichment of genes related to cell cycle and cell division, and response to DNA damage. The downregulated genes showed enrichment in pathways related to chromatin organization, and regulation of proliferation. These data indicate that HDAC7 may exert its function by properly controlling cell cycle and proliferation processes during the GC reaction.

Therefore, we next interrogated whether HDAC7 deficiency affects the proliferation and cell cycle status of GC B cells *in vivo* and *ex vivo*. The

percentage of cells found in S phase was significantly decreased upon HDAC7 deletion and also HDAC7-deficient B cells underwent less divisions than wild-type cells. Unexpectedly, Ki67 staining of spleen sections showed a higher number and a larger area of Ki67<sup>+</sup> GC within the follicle of HDAC7-deficient mice. These data indicated the possibility that in the absence of HDAC7 activated B cells may be blocked in an early or pre-GC stage unable to properly enter into the GC reaction. To test this, we interrogated the presence of CD38<sup>+</sup>IgD<sup>+</sup> pre-GC B cells. Strikingly, GC B cells from HDAC7-deficient mice showed an aberrant double positive CD38<sup>+</sup>IgD<sup>+</sup> cell population. These data suggested that HDAC7 may play a crucial role at early post-immunization events before B cells enter and form the GC.

## 7. Altered GC dynamics in HDAC7-deficient mice

Next we wondered whether the aberrant GC B cells observed in the absence of HDAC7 could also presented an altered GC dynamics. Flow cytometry analysis of GC B cells revealed a significant loss and gain of DZ (CXCR4<sup>+</sup>CD86<sup>-</sup>) and LZ (CXCR4<sup>-</sup>CD86<sup>+</sup>) populations, respectively, upon HDAC7-loss. Intriguingly, in HDAC7-deficient GC B cells, we observed two clear distinguishable populations, CXCR4<sup>low</sup> and CXCR4<sup>mid/high</sup>. To further define the nature of HDAC7-deficient GC B cells sub-populations we performed cell cycle analysis. The percentage of CXCR4<sup>mid/high</sup> DZ GC B cell was significantly increased in G2 phase and decrease in G0/G1 phases indicating a higher proliferation rate in the absence of HDAC7. The majority of the atypical CXCR4<sup>low</sup> GC B cell population of HDAC7-deficient cells was found in a G1 resting state and decreased in S phase, resembling those in the LZ. To gain further insight into the control of the GC dynamics mediated by HDAC7, we performed GSEA on RNA-seq data of GC B cells using previously reported DZ-LZ gene signatures (Victoria et al. 2012). The analysis unveiled that GC B cells from HDAC7-deficient mice harbor gene signatures characteristic of the DZ compartment. These results suggest that HDAC7 deletion promotes an aberrant DZ-LZ program that impedes proper polarization of GC B cells.

## **8. HDAC7 is underexpressed in DLBCL patients correlating with poor prognosis**

We found that HDAC7 is significantly underexpressed in DLBCL patients compared to GC healthy B cells, in a subtype-independent manner. Additionally, we assessed the effect of HDAC7 expression levels in DLBCL genetic signature, using previously mined RNA-seq data. Strikingly, DLBCL patients harbouring normal levels of HDAC7 exhibited a transcriptomic profile similar to that of healthy donors suggesting that low levels of HDAC7 could be associated with more aggressive lymphomagenesis and poor prognosis of the patients. Accordingly, the clinical outcome of 292 DLBCL patients treated with conventional R-CHOP immunotherapy unveiled that the lower expression of HDAC7 was associated to a poorer outcome of the patients. These data indicate that absence or low levels of HDAC7 may be involved in the pathogenesis of DLBCL representing a novel biomarker and prognostic factor for these patients.

## **9. HDAC7 expression reduces DLBCL proliferation and survival *in vitro* and *in vivo***

To further evaluate the role of HDAC7 in B cell lymphomagenesis we chose the MD901 DLBCL cell line that expresses very low levels of HDAC7. To assess HDAC7-loss related lymphomagenic features we performed a gain-of-function experimental approach (*as described in paragraph 4*). HDAC7 expression significantly inhibited the proliferation of MD901, concomitant with increased programmed cell death. To determine if HDAC7 reduces the growth of DLBCL *in vivo*, we implanted MD901 cells transduced with either empty or HDAC7 inducible retroviral vector in immunodeficient mice. We observed that HDAC7 expression significantly suppressed DLBCL growth in terms of tumor volume and tumor weight. To delineate the anti-lymphomagenic mechanisms of HDAC7 in DLBCL we next performed RNA-seq of the tumors generated, unveiling a clear upregulation of apoptosis-associated mechanisms upon HDAC7 expression. Taken together, our data indicate that HDAC7 could be a valuable novel biomarker and prognostic factor in DLBCL.

## **ARTICLE 1**

*“The HDAC7-TET2 epigenetic axis is essential during early B lymphocyte development”*





# The HDAC7–TET2 epigenetic axis is essential during early B lymphocyte development

Alba Azagra<sup>1,2,†</sup>, Ainara Meler<sup>1,2,†</sup>, Oriol de Barrios<sup>1,2</sup>, Laureano Tomás-Daza<sup>3,4</sup>, Olga Collazo<sup>1,2</sup>, Beatriz Monterde<sup>5</sup>, Mireia Obiols<sup>6</sup>, Llorenç Roviroso<sup>3</sup>, Maria Vila-Casadesús<sup>7</sup>, Mónica Cabrera-Pasadas<sup>3,4</sup>, Mar Gusi-Vives<sup>1</sup>, Thomas Graf<sup>7,8</sup>, Ignacio Varela<sup>5</sup>, José Luis Sardina<sup>6</sup>, Biola M. Javierre<sup>3</sup> and Maribel Parra<sup>1,2,\*</sup>

<sup>1</sup>Lymphocyte Development and Disease Group, Josep Carreras Leukaemia Research Institute, 08916 Badalona, Spain, <sup>2</sup>Cellular Differentiation Group, Cancer Epigenetics and Biology Program (PEBC), Bellvitge Biomedical Research Institute (IDIBELL), Av. Gran Via 199, 08908 L'Hospitalet, Barcelona, Spain, <sup>3</sup>3D Chromatin Organization Group, Josep Carreras Leukaemia Research Institute, 08916 Badalona, Spain, <sup>4</sup>Barcelona Supercomputing Center (BSC), Barcelona, Spain, <sup>5</sup>Instituto de Biomedicina y Biotecnología de Cantabria. Universidad de Cantabria-CSIC. 39011 Santander, Spain, <sup>6</sup>Epigenetic Control of Haematopoiesis Group, Josep Carreras Leukaemia Research Institute, 08916 Badalona, Spain, <sup>7</sup>Centre for Genomic Regulation (CRG), PRBB Building, Dr. Aiguader 88, 08003 Barcelona, Spain and <sup>8</sup>Universitat Pompeu Fabra, Barcelona, Spain

Received July 29, 2021; Revised June 23, 2022; Editorial Decision June 25, 2022; Accepted July 05, 2022

## ABSTRACT

**Correct B cell identity at each stage of cellular differentiation during B lymphocyte development is critically dependent on a tightly controlled epigenomic landscape. We previously identified HDAC7 as an essential regulator of early B cell development and its absence leads to a drastic block at the pro-B to pre-B cell transition. More recently, we demonstrated that HDAC7 loss in pro-B-ALL in infants associates with a worse prognosis. Here we delineate the molecular mechanisms by which HDAC7 modulates early B cell development. We find that HDAC7 deficiency drives global chromatin de-condensation, histone marks deposition and deregulates other epigenetic regulators and mobile elements. Specifically, the absence of HDAC7 induces TET2 expression, which promotes DNA 5-hydroxymethylation and chromatin de-condensation. HDAC7 deficiency also results in the aberrant expression of microRNAs and LINE-1 transposable elements. These findings shed light on the mechanisms by which HDAC7 loss or misregulation may lead to B cell-based hematological malignancies.**

## INTRODUCTION

A longstanding fundamental question in the field of cell development has been: how do cells decide at a molecular level to acquire a specific cell fate during tissue and organ generation? The mammalian hematopoietic system is considered a paradigm model for answering this question. For instance, B cell lymphopoiesis is a complex developmental process that comprises several cellular transitions, including cell commitment and early and late cellular differentiation. Proper transcriptional control at each cellular transition is essential for the correct generation of B lymphocytes. Of note, aberrant establishment of specific transcriptional programs may lead to the development of B cell malignancies.

Lineage-specific networks of transcription factors (TFs) have a central role in positively regulating the transition and maintenance of the distinct B cell developmental stages. In the bone marrow, lymphoid-primed multipotent progenitors (LMPPs) have the capacity and plasticity to become either common lymphoid progenitors (CLPs) or common myeloid progenitors (CMPs) (1). At that stage, the TFs IKAROS, MEF2C, and PU.1 are crucial for the early cellular choice towards the lymphoid lineage (2,3). Later on, commitment to the B cell lineage from CLPs to B cell progenitors (pro-B) and B cell precursors (pre-B) depends on the hierarchical and coordinated actions of the TFs PAX5, E2A, EBF and MEF2C (4–6). Classically thought as genuine activators for specific gene expression, B cell TFs are now believed to be involved in the repression of inappropriate lineage or of functionally undesirable gene transcrip-

\*To whom correspondence should be addressed. Tel: +34 935572800; Fax: +34 934651472; Email: mparra@carrerasresearch.org

<sup>†</sup>The authors contributed equally to this article.

Present address: Maria Vila-Casadesús, Bioinformatics Platform, CIBER Hepatic and Digestive Diseases (CIBERehd), 08036 Barcelona, Catalonia, Spain.

tion, thereby ensuring that the proper B cell identity and differentiation are maintained. In addition to positively promoting B lymphocyte gene-specific programs, the PAX5, E2A, EBF1 and MEF2C TFs induce the repression of inappropriate genes of alternative lineages, thereby ensuring maintenance of proper B cell identity and differentiation (3,7–11). These findings support the concept of transcriptional repression as an essential mechanism for proper B lymphocyte generation. However, the identity of master transcriptional repressors essential for establishing and maintaining the genetic identity of B lymphocytes has remained elusive for many years.

Besides specific TF networks, B cell differentiation also requires that epigenetic regulators and architectural proteins establish the correct permissive/non-permissive chromatin structure (euchromatin/heterochromatin) (12). There is a close relationship between transcriptional regulators and dynamic changes in the DNA epigenetic landscape during B cell development, with DNA methylation levels and the chromatin conformation state dynamically changing at every differentiation cell stage, giving them a specific epigenetic signature (13–17). Also, TFs such as PAX5 interact with architectural proteins that mediate long-range chromatin interactions (18). In mammals, DNA demethylation depends on the action of the Ten-Eleven Translocation (TET) enzyme family of TET1, TET2 and TET3, which convert 5-methylcytosine (5-mC) to 5-hydroxymethylcytosine (5-hmC), leading to DNA demethylation and consequent gene expression (19). Notably, TET2 has been shown to play crucial roles during hematopoiesis (20–22). Although broadly expressed within the hematopoietic system, myeloid cells express higher levels of TET2 compared with lymphoid cell populations (23–25). To date, the molecular mechanisms controlling different TET2 physiological levels within the hematopoietic systems are largely unknown.

We have previously reported that HDAC7 is a master transcriptional repressor in early B cell development, controlling the expression of lineage-inappropriate genes and thus the identity of pro-B cells. A lack of HDAC7 in pro-B cells leads to a block in B cell differentiation, aberrant activation of alternative lineage genes, a reduction of proliferation, and an increase in apoptosis (26). More recently, we have identified HDAC7 as a prognostic factor and biomarker of survival in infants with pro-B acute lymphoblastic leukemia (pro-B-ALL) and MLL-AF4 rearrangement, who display a general loss in HDAC7 expression; notably, the lowest levels of HDAC7 are associated with the poorest outcome for the infants (27). We hypothesized that these findings could be indicative of a yet-unknown HDAC7-mediated molecular mechanisms that allows proper acquisition of cell identity during early B cell development in the bone marrow.

Using a combination of transcriptomic and epigenetic genome-wide analysis, we now shed light into the molecular mechanisms that are governed by HDAC7 during early B cell development. We identified HDAC7 as a regulator of proper chromatin compaction in different stages of B cell development (pro-B and pre-B cells). Importantly, we demonstrated that HDAC7 represses TET2 expression

in pro-B and pre-B cells, and that its deficiency leads to TET2 up-regulation and subsequent alteration in global and specific 5-hmC patterns. In fact, HDAC7-deficient pro-B cells showed enhanced 5-hmC global levels, resulting not only in the activation of inappropriate lineage genes, but also in the aberrant expression of non-coding elements (such as active transposon LINE-1 elements and miRNAs). Thus, our findings unveil novel molecular mechanisms that govern the maintenance of correct B cell development and identity, working through the HDAC7–TET2 axis.

## MATERIALS AND METHODS

### Study Design

The study aimed to define unprecedented molecular mechanisms by which class IIa HDAC7 preserves B cell identity in mice. Experiments included 4–6 weeks-old wild-type and knockout mouse strains (C57BL/6). Mice selected in each experiment were littermates. Primary pro-B and pre-B lymphocytes were isolated by using cell sorting. Tet2 was identified as a direct target of HDAC7 with chromatin immunoprecipitation and expression analysis experiments. 5-hydroxymethylation levels in pro-B cells were quantified by ELISA and hydroxymethyl-DIP experiments. 5-hmeDIP-seq, ATAC-seq, H3K27ac and H3K27me3 ChIP-seq were performed to determine global and specific changes. All results were validated by qPCR assays and were successfully reproduced. No sample size calculations were performed, since these were selected on the basis of previous studies performed in our lab. The numbers of experimental replicates are included in the figure legends.

### Mice

*Hdac7<sup>fl/fl</sup>* on C57BL/6 mice have been previously described (28) and were kindly provided by Dr Eric Olson (UT Southwestern Medical Center, Dallas, TX, USA). Mb1-Cre<sup>ki/+</sup> on C57BL/6 (B6.C(Cg)-Cd79a<sup>tm1(cre)</sup>Reth/EhobJ) mice were kindly provided by Dr Michael Reth (Max Planck Institute of Immunology and Epigenetics, Freiburg, Germany). Experiments were performed with 4–6 week-old mice. Littermate controls were used for *Hdac7<sup>fl/fl</sup>* mb1-cre mice. Animal housing and handling and all procedures involving mice, were approved by the Bellvitge Biomedical Research Institute (IDIBELL) ethics committee and the Animal Experimentation Ethics Committee (CEEA) of the Comparative Medicine and Bioimage Centre of Catalonia (CMCiB), at Germans Trias i Pujol Research Institute (IGTP), in accordance with Spanish national guidelines and regulations.

### Cells

HAFTL pre-B cell line transduced with a MSCV-GFP-C/EBP $\alpha$  retroviral vector (to generate C10 cells) and with a MSCV-hCD4-C/EBP $\alpha$ ER retroviral vector (to generate C11 cells), were described previously described (29). C10-MSCV and C10-HDAC7 cells were generated as previously described (30).

### shRNA-Tet2 infection of primary B cells and transduced pre-B cell line (C11)

Retroviral vector for PGK-shRNATet2-GFP retroviral vector has been described in (31). CD19<sup>+</sup> B cells from *Hdac7<sup>+/-</sup>* and *Hdac7<sup>fl/-</sup>* mice or C11 cells were infected with the shRNA Tet2 targeting vector (shTet2) or with an empty retroviral vector (shCtrl). Cells were infected twice, in a time gap of 24 h, and then, 48 h after second infection, GFP<sup>+</sup> cells were sorted using a FACSAria™ Fusion cell sorter (BD Biosciences). After isolation, CD19<sup>+</sup> B cells were cultured on RPMI media supplemented with 2% FBS, 0.03% Primatone RL (Sigma), 1 mM penicillin/streptomycin, 50 μM β-mercaptoethanol and 1% IL-7 (PeproTech), whereas C11 cells were cultured in RPMI media supplemented with 10% FBS and 1 mM penicillin/streptomycin. *Tet2* knockdown was confirmed by qRT-PCR using SYBR green quantification.

### β-Estradiol treatment of cell lines

C10-MSCV, C10-HDAC7, C11-shCtrl and C11-shTet2 cells were cultured and treated as previously described (30).

### Flow cytometry analysis and cell-sorting

Cells were extracted from bone marrow (femur and tibia of both hind legs) of *Hdac7<sup>+/-</sup>* and *Hdac7<sup>fl/-</sup>* mice. Red blood cells were lysed with ACK lysis buffer. Cell counts were determined using a manual cell counter and Türk's staining to facilitate the counting of white cells nuclei. Isolated cells were incubated with anti-CD16/CD32 (2.4G2, Fc Block) (BD Bioscience) for 10 min on ice to reduce non-specific staining. The following antibodies were used for analysis (from BD Biosciences): anti-B220 (RA3-6B2), anti-CD43 (S7), anti-IgM (R6-60.2), anti-CD19 (1D3) and anti-Cd11b (M1/70). For Cd11b, Streptavidin-V50 (560797, BD Biosciences) was used as a secondary antibody. Cells were stained with primary antibodies for 30 min on ice in the dark. Cells were analyzed on a BDFACS Canto II (BD Biosciences) or sorted on BD FACSAria™ Fusion cell sorter (BD Biosciences). Data were analyzed using FlowJo software (Tree Star, Inc.). See Supplementary Figure S1A for sorting gating strategy (pro-B cells: IgM<sup>-</sup>, CD19<sup>+</sup>, B220<sup>+</sup>, CD43<sup>+</sup>; pre-B cells: IgM<sup>-</sup>, CD19<sup>+</sup>, B220<sup>+</sup>, CD43<sup>-</sup>).

### Magnetic cell separation (MACS)

Cells were extracted from bone marrow (femur and tibia of both hind legs) of *Hdac7<sup>+/-</sup>* and *Hdac7<sup>fl/-</sup>* mice. Red blood cells were lysed with ACK lysis buffer. Cell counts were determined using a manual cell counter and Türk's staining to facilitate the counting of white cells nuclei. Isolated cells were incubated with anti-CD16/CD32 (2.4G2, Fc Block) (BD Bioscience) for 10 min on ice to reduce non-specific staining. The following antibodies were used for separation (from Miltenyi Biotec): anti-CD19-Microbeads (mouse), anti-Cd11b biotin (M1/70, BD Biosciences), and Streptavidin-Microbeads. Samples were incubated for 20 min at 4°C in the dark. CD11b needed double incubation, first with anti-Cd11b and second with Streptavidin-beads.

Samples were put into Ls columns (Miltenyi Biotec) to perform magnetic cell separation. After three washes, cell from positive fractions (CD19<sup>+</sup> and Cd11b<sup>+</sup>) were kept for further experimentation.

### RNA-sequencing and analysis

Total RNA was extracted from HDAC7-deficient and control pro-B and pre-B cells in the Genomics facility of Institute for Research in Biomedicine (IRB) in Barcelona. Samples were quantified and subjected to quality control using a Bioanalyzer apparatus (IRB, Barcelona). Samples were processed at BGI Genomics Service, (China). Briefly, low input library was performed in all samples. Later, they were sequenced in paired-end mode with a read length of 100 bp. Thirty-five million paired-end reads were generated for each sample. Quality control of the samples was performed with the FastQC tool (available at <https://www.bioinformatics.babraham.ac.uk/projects/fastqc/>). Paired-end reads from RNA-Seq were aligned to the murine reference genome (GRCm38) using Hisat2 (version 2.0.5). Quality of the alignments was assessed using FastQC (v0.11.2). A count table file indicating the number of reads per gene in each sample was generated using HTSeq (version 0.6.0) (32). Genes with no or very low expression were filtered out and differentially expressed genes were identified using DESeq (33), requiring a minimum adjusted *P*-value of 0.05 and a  $\log_2$ FCI value >1. Functional analysis was performed using gene set enrichment analysis (GSEA) (34) using a pre-ranked list of human orthologs genes and the gene set database c5.all.v7.2.symbols.gmt (Gene Ontology). GSEA analyses were performed from the *Hdac7<sup>+/-</sup>* pro-B versus *Hdac7<sup>+/-</sup>* pre-B cells, *Hdac7<sup>+/-</sup>* pro-B versus *Hdac7<sup>fl/-</sup>* pro-B cells and *Hdac7<sup>+/-</sup>* pro-B versus *Hdac7<sup>fl/-</sup>* pre-B cells comparisons. Genes were ranked using this formula:  $-\log_{10}(\text{FDR}) \times \text{sign}[\log(\text{FC})]$ . As gene sets collection, hallmarks (H) from the Molecular Signatures Database (MSigDB) were selected, adding the specified custom gene sets. Data from RNA-seq is available under accession code GSE171855.

### RT-qPCR analysis

RNA from sorted pro-B and pre-B cells was extracted with an RNeasy Mini kit (Qiagen) and subsequently converted into cDNA using the High Capacity cDNA Reverse Transcription Kit (AB Applied Biosystems) according to the manufacturer's instructions. Real-time-quantitative PCR (RT-qPCR) was performed in triplicate using SYBR Green I Master (Roche). PCR reactions were run and analyzed using the LightCycler 480 Detection System (Roche). RT-qPCR primer pairs are shown in supplemental information Supplementary Table S1.

### Micrococcal nuclease assay

Two million of B cells from *Hdac7<sup>+/-</sup>* and *Hdac7<sup>fl/-</sup>* mice were resuspended in 500 μl of lysis buffer (10 mM Tris, 10 mM NaCl, 3 mM MgCl<sub>2</sub>, 1% Triton, pH 7.5) and incubated on ice for 10 min. Nuclei were collected by centrifugation at 300 g for 5 min at 4°C. The nuclear pellet was then

resuspended in 400  $\mu$ l of nuclear lysis buffer (20 mM Tris, 20 mM KCl, 70 mM NaCl, 3 mM CaCl<sub>2</sub> and protease inhibitors, pH 7.5). Aliquots of 100  $\mu$ l were incubated with 9 units of micrococcal nuclease (MNase, ThermoFisher) and digested at room temperature for 0, 1, 2 and 5 min, respectively. Then 3  $\mu$ l of 0.5M EDTA was added to stop digestion, and DNA was purified by using the QIAquick PCR purification kit (Qiagen). About 500 ng were used for gel electrophoresis and 12 ng of DNA were used for qPCR analysis using SybrGreen (Roche). Primers obtained from (35) were designed to target the  $\beta$ -globin gene to obtain PCR amplicons longer than the length of a single nucleosome. Mononucleosomes generated during MNase digestion cannot be amplified by qPCR. Then, reduced amplification involves more open/accessible chromatin state, at least at this locus.

### Western Blot

White cells from bone marrow of control and *Hdac7<sup>fl/-</sup>* mice were extracted as in sorting procedure. Next, cells were stained with anti-CD19-microBeads (Miltenyi Biotec) according to manufacturer's instructions. CD19<sup>+</sup> B cells were isolated by magnetic separation with LS column adapters (Miltenyi Biotec). Purified cells were lysed with RIPA buffer. Lysates were resolved on 8–15% SDS-PAGE (Mini-Protean electrophoresis chamber, Bio-Rad) and transferred on nitrocellulose membranes (Amersham Biosciences). Membranes were blocked in 5% milk in TBS with 0.1% Tween (TBS-T) and incubated overnight at 4°C, with primary antibodies (anti-Tet2 ab94580, abcam 1:1000; anti-HDAC7 sc-11421, Santa Cruz Biotechnology 1:1000; anti-H3K9me3 ab8898 (Abcam) 1:1000; anti-PUMA 12450 (Cell Signaling) 1:500; anti-IRF4 sc-48338 (Santa Cruz Biotechnology) 1:500; anti-c-MYB sc-74512 (Santa Cruz Biotechnology) 1:500; anti-H3 ab1791 (Abcam) 1:1000; anti-Lamin B1 ab16048 (Abcam) 1:1000, and anti-Actin AC-15 (Sigma-Aldrich) 1:40000). Secondary antibody incubations (HRP-anti mouse, P0260, or anti rabbit, P0448, Dako 1:3000), were carried out for 1h at room temperature. Protein signal was detected using ECL western detection kit (Amersham Biosciences).

### Chromatin immunoprecipitation assays (ChIP)

For chromatin immunoprecipitation (ChIP) assays, purified pro-B cells from the bone marrow of *Hdac7<sup>+/+</sup>* and *Hdac7<sup>fl/-</sup>* mice were crosslinked for 15 min in 1% formaldehyde, followed by inactivation in 125 mM glycine for 5 min and by two washes in cold PBS. Afterward, samples were incubated in cell lysis buffer from LowCell# ChIP kit (Diagenode) for 30 min at 8°C and sonicated with M220-Focused Ultra Sonicator (Covaris) according to manufacturer's instructions. Next steps of ChIP experiments were performed using resources from the LowCell# ChIP kit (Diagenode) according to the manufacturer's instructions. The following antibodies were used for immunoprecipitation: anti-HDAC7 (Abcam, HDAC7-97, 2.5  $\mu$ g), anti-H3K9/K14ac (Millipore, 06-599 2.5  $\mu$ g), anti-H3K27me3 (Millipore, 07-449, 2.5  $\mu$ g), anti-H3K27ac (Abcam, ab4729, 2.5  $\mu$ g) and anti-H3k9me3 (Abcam,

ab8898, 2.5  $\mu$ g). Real-time quantitative PCR (RT-qPCR) was performed in triplicate and the results analyzed. Data are presented as the ratio between the HDAC7-bound fraction and histone modification antibody relative to the input control. ChIP-qPCR primer pairs are shown in supplemental information Supplementary Table S1.

### ChIP-seq experiments and analysis

H3K9/K14ac ChIP-seq data were extracted from ChIP-seq experiments, as described elsewhere (26), whose data are available under the accession code: SRA submission SUB1614653. For new ChIP-seq experiments, purified pro-B and pre-B cells from the bone marrow of *Hdac7<sup>+/+</sup>* and *Hdac7<sup>fl/-</sup>* mice were crosslinked for 15 min in 1% formaldehyde, followed by inactivation in 125 mM glycine for 5 min and by two washes in cold PBS. Afterward, samples were lysed and sonicated with M220-Focused Ultra Sonicator (Covaris) to obtain fragments of 250–500 bp. Samples were processed according to Blueprint Histone ChIP-Seq protocol (<https://www.blueprint-epigenome.eu/>). The following antibodies were used for immunoprecipitation: 2.5  $\mu$ g of anti-H3K27me3 (07449) and 2.5  $\mu$ g of anti-H3K27ac (ab4729). As experimental control we used input sonicated chromatin (not immunoprecipitated) in all experimental conditions. For the analysis, reads were checked for quality using FastQC (0.11.5) and then trimmed using trim galore (v.0.6.6) to remove the sequencing adapters. Reads were aligned to the mouse reference genome GRCm38 using Bowtie v2.3.2 with '–very-sensitive' parameters (36). Aligned reads were then filtered based on ENCODE standards and removed those mapping to the blacklist and duplicates using samtools (v.1.9) and sambamba (v.0.7.0). Peaks were called using MACS2 v2.2.7.1 (37) with default parameters, providing an input sample to avoid false positives. Background correction was applied by first defining a set of non-redundant enriched regions for all samples by taking the union of all peaks from both replicates of all samples. Bigwig files were generated using bamCoverage v3.2.1 from deeptools (38). Genomic peak annotation was performed with HOMER software (v4.11). Intensity plots were performed using computeMatrix in a window of  $\pm 1$  kb center in the TSS from deeptools (38). Data from H3K27ac and H3K27me3 ChIP experiments are available under accession code: GSE204673.

### ATAC-seq experiment and analysis

50 000 purified pro-B and pre-B cells from the bone marrow of *Hdac7<sup>+/+</sup>* and *Hdac7<sup>fl/-</sup>* mice were isolated and freshly lysed using cold lysis buffer (10 mM Tris–HCl, pH 7.4, 10 mM NaCl, 3 mM MgCl<sub>2</sub> and 0.1% IGEPAL CA-630). Immediately after lysis, nuclei were spun at 500 g for 10 min using a refrigerated centrifuge, and pellet was resuspended in the transposase reaction mix (12.5  $\mu$ l 2  $\times$  TD buffer, 2  $\mu$ l transposase (Illumina) and 5.5  $\mu$ l nuclease-free water). The transposition reaction was carried out for 1 h at 37°C, followed by addition of clean up buffer (900 mM NaCl, 300 mM EDTA, 2  $\mu$ l 5%SDS, 20 ng Proteinase K) and incubation for 30 min at 40°C. Tagmented DNA was isolated using 2  $\times$  SPRI beads from Beckman–Coulter. Following purification, we amplified library fragments using

1× NEBnext PCR master mix and 1.25 μM of Nextera PCR primers as described elsewhere (39). Sequence reads quality was assessed with MultiQC v1.12 (40), and adapter content (if any) was trimmed using Trimmomatic v0.39 (41). Paired-end reads were aligned to GRCm38 using Bowtie2 v2.2.3 with a maximum insert size of 2000 (-X 2000) (36). These parameters ensured that fragments up to 2 kb were allowed to align and that only unique aligning reads were collected (-m1). For all data files, duplicates and mtDNA were removed using picard (<http://picard.sourceforge.net>) and sambamba (v.0.7.0), respectively. For peak-calling, MACS2 v2.2.7.1 (37) tool was used with default parameters. Background correction was applied by first defining a set of non-redundant enriched regions for all samples by taking the union of all peak summits from both replicates of all samples. We then quantified the signal at all summits in each sample by counting the number of fragments (using the R bioconductor package csaw, v. 1.0.7) (42). The resulting counts matrix file was analyzed for differential peaks with DESeq2 (43). Genomic peak annotation was performed with HOMER software (v4.11). Intensity plots were performed using computeMatrix in a window of ±1 kb center in the TSS from deepTools (38). Data from ATAC-seq are available under accession code GSE204672.

### Quantification of global 5-hydroxymethylation levels

To quantify 5-hmC, a Quest 5hmC DNA ELISA kit (Zymo Research) was used according to the manufacturer's protocol. First, genomic DNA from sorted cells was extracted using Quick-DNA Miniprep Plus kit (D4068, Zymo Research). Next, the bottom of the provided well was coated with anti-5-hmC polyclonal antibody (pAb) for 1 h at 37°C in the dark. Wells were then blocked and 100 ng of denatured genomic DNA was added for 30 min at 37°C in the dark. After corresponding washes, anti-DNA HRP antibody was applied to wells for 30 min at 37°C in the dark. After corresponding washes, HRP developer (3,3',5,5'-tetramethylbenzidine (TMB) (Sigma-Aldrich)) was added to detect the DNA bound to the anti-5-hmC pAb for 20–30 min at room temperature in the dark. Afterward, the color reaction was stopped by the addition of sulfuric acid and the resulting color was analyzed at 450 nm by using a Glomax microplate reader (Promega). The percentage of 5-hmC DNA was estimated from linear regression.

### hMeDIP-qPCR experiments

Genomic DNA was purified by using the same kit as in ELISA assay. 1 μg of genomic DNA from wild-type and HDAC7-deficient sorted pro-B cells was sonicated with M220-Focused Ultra Sonicator (Covaris) to obtain fragments of 300–400 bp. Fragmented DNA were incubated with 2 μg anti-5hmC (Active Motif, 39769) and 20 μl of Dynabeads G (Life Technologies) for 16 h at 4°C, and 10% of DNA was kept to be used as input. After incubation, Dynabeads were washed 3 times with IP buffer (10 mM Na-Phosphate pH 7, 0.14 M NaCl, 0.05% Triton X-100) and then were resuspended in Proteinase K digestion buffer (50 mM Tris pH8, 10 mM EDTA, 0.5% SDS) for 30 min at 55°C. DNA from immunocomplexes was purified with

the QIAquick MinElute kit (Qiagen). Real-time quantitative PCR was performed and the results analyzed. Data are presented as the ratio of the enrichment of 5-hmC relative to the input control.

### hMeDIP sequencing experiments and analysis

Purified genomic DNA (1 μg) from wild-type and HDAC7-deficient pro-B cells was sonicated to obtain fragments of 300–400 bp. Adaptor ligations were performed and libraries constructed by qGenomics Laboratories (Barcelona, Spain). 2 μg of anti-5hmC (Active Motif, 39769) were incubated with 20 μl of Dynabeads G (Life Technologies) for 2 h at 4°C. Fragmented DNA was incubated with Dynabeads and antibody for 16 h at 4°C, and 10% of DNA was kept to be used as input. DNA was purified as described in hMeDIP qPCR assay. Amplified libraries were constructed and sequenced at qGenomics Laboratories (Barcelona, Spain). Fastq data were obtained with Trim Galore-0.4.2 and Cutadapt-1.6. Reads were mapped with bwa-0.7.12. Sorting Sam to Bam was carried out with Picard-2.8.0 SortSam and duplicates were removed with Picard-2.8.0 MarkDuplicates. Bigwig files were made with deeptools and normalized based on RPKM. Peak calling was performed using MACS2 bdgpeakcall option (-c 250 -l 10 -g 10). To avoid false positives, peaks that intersect with peaks in the corresponding input samples were removed. DESEQ analysis (DESeq2 v1.20.0) was then used to define peaks and perform quantitative analyses. The Diffbind-2.6.6 R package was used for differential binding analysis. Differential enrichment was defined by a threshold value of  $P = 0.005$  and a >1-fold difference in KO relative to WT samples. Motif enrichment was analyzed and peak depth quantified with HOMER software (v4.10). Data from hMeDIP-seq is available under accession code GSE135263.

### Co-immunoprecipitation (Co-IP)

Co-IP assays were performed using CD19<sup>+</sup> cells from control and HDAC7 deficient mice. Cell extracts were prepared in lysis buffer [50 mM Tris-HCl, pH 7.5, 1 mM EDTA, 150 mM NaCl, 1% Triton-X-100, protease inhibitor cocktail (complete<sup>TM</sup>, Merck)] with corresponding units of Benzozase (Sigma) and incubated at 4°C for 6 h. 50 μl of supernatant was saved as input and diluted with 2× Laemmli sample buffer (4% SDS, 20% glycerol, 120 mM Tris-HCl, pH 6.8). Supernatant was first incubated with PureProteome<sup>TM</sup> Protein A/G agarose suspension (Merck Millipore) for 1 h to remove background signal. Samples were then incubated overnight at 4°C with corresponding antibodies against TET2 (ab124297, Abcam) and rabbit (12-371, Merck Millipore) IgGs (negative control) and A agarose beads. After that, beads were washed three times with lysis buffer. For sample elution, 100 μl of 1× Laemmli sample buffer was added to the beads. Samples and inputs were denatured at 95°C in the presence of 1% β-mercaptoethanol.

### Expression profiling of microRNAs

We used miRCURY LNA<sup>TM</sup> Universal RT microRNA PCR System (Exiqon) to determine miRNA expression profiles.

The miRNA annotation of mirBase version 20.0 was used. Single-stranded cDNA was synthesized by reverse transcription of 8  $\mu$ l of RNA, using the universal cDNA Synthesis Kit II (Exiqon). Diluted cDNA was mixed with ExiLent SYBR<sup>®</sup> Green master mix (Exiqon), and quantitative PCR was performed using the Roche LightCycler<sup>®</sup> 480 RealTime PCR system (Roche). Primers design for validations of miRNA's differential expression was performed with miRprimer software (<https://sourceforge.net/projects/mirprimer/>).

### Immgen data analysis

Immgen is a public resource that is the result of a collaborative group of immunology and computational biology laboratories that share knowledge and expertise to perform a broad and deep dissection of the genome's activity and its regulation in the immune system. This public resource is broadly used by many immunology laboratories to interrogate biological questions of a gene of interest or more broad mechanistic insights within the hematopoietic system.

Gene Skyline tool: expression data from microarrays collected from several participating laboratories is normalized with Robust Multiarray Average (RMA) algorithm (44,45). RMA is a three-step algorithm, which removes background noise (normally distributed), performs quantile normalization and log<sub>2</sub> transformation. Raw reads from microarray are normalized by median of ratios with DeSeq2 package from Bioconductor. Spike-in data is also used to evaluate the RMA method in order to address questions about the correctness of microarray data. Immgen developers ensure that the comparison of expression levels of one gene among different cell types is sensitive and quantitative.

Modules and regulators tool: this tool uses an algorithm called Ontogenet in order to outline the regulatory networks that drive the hematopoietic cell differentiation (see detailed explanation in (46)). Briefly, it classifies and clusters genes in groups called 'modules' based on expression levels of genes among all cell types from all lineages and developmental stages from the hematopoietic system given by several microarray analyses. Each module is called 'coarse module', which can be further divided into 'fine modules'. The algorithm assumes that genes included in one module are regulated in the same way. For these modules, Immgen create automatically an expression matrix represented as a heatmap, showing potential regulators of the module and their expression pattern among blood cell types. Immgen also provides a table of expression level and regulatory activity (weight), classifying each regulator into positive and negative.

My GeneSet tool: this browser allows you to examine the pattern of expression of a selected set of genes over some or all of the ImmGen expression data (obtained from either RNA-seq or microarray experiments).

### Statistical analysis

Data were analyzed by Student's two-tailed unpaired *t*-test and Mann-Whitney test using GraphPad Prism (v7). *P*-values lower than 0.05 were considered statistically significant. Statistical methods for analysis of genome wide

datasets involving hMeDIP-seq, RNA-seq, ChIP-seq and ATAC-seq are explained in detail under the respective section.

## RESULTS

### HDAC7 regulates chromatin condensation and 5-hmC levels in pro-B cells

We previously identified HDAC7 as a critical transcriptional repressor of lineage-inappropriate genes that ensures correct early B cell development. However, its exact molecular mechanisms remained to be addressed (26,30). To unveil the mechanisms and functions that HDAC7 exerts during early B lymphocyte development along the different cell stages of differentiation, we performed RNA-sequencing (RNA-seq) experiments on pro-B and pre-B cells from HDAC7 conditional knockout mice (*Hdac7<sup>fl/-</sup>*; hereafter, HDAC7-deficient) and their control littermates (*Hdac7<sup>+/-</sup>*; hereafter, wild-type) (Figure 1A; see also gating strategy, Supplementary Figure S1A). First, we performed an unsupervised cluster analysis of the samples based on their gene expression profiles. Notably, pro-B and pre-B wild-type cell populations were grouped into two different clusters, confirming that early B cell differentiation steps were affected by gene transcription changes, a hallmark of early B lymphocyte development. In contrast, HDAC7-deficient pro-B and pre-B cells were more similar and grouped closer, indicating that the B cell developmental block observed upon HDAC7 deficiency is a consequence of altered gene transcription programs (Figure 1B). Based on RNA-seq analyses, a comparison of the differentially expressed genes between the cell populations showed that 1992 and 2140 genes were up-regulated and down-regulated, respectively, during the cellular transition from pro-B to pre-B wild-type cells (Supplementary Figure S1B). The lack of HDAC7 from the pro-B or pre-B cells resulted in a downregulation of 272 and 1576 genes, respectively, as compared to the wild-type pro-B cells (Supplementary Figure S1B). Among the downregulated genes, we observed a dramatic disruption in heavy chain immunoglobulin (*Igh*) production (Supplementary Figure S1C), which is a critical process in early B cell development; this demonstrated that HDAC7 deficiency would drastically affect the immune response (Supplementary Figure S1D).

HDAC7 is a transcriptional repressor. Accordingly, 393 and 1609 genes in pro-B and pre-B cells, respectively, were upregulated in the HDAC7-deficient cells as compared to pro-B wild-type cells (Figure 1C). Gene Ontology (GO) analysis of up-regulated genes at both cell stages showed that they were related, on one hand, to cell proliferation, survival and immune processes (Supplementary Figure S1E) and, on the other hand, to enhanced protein binding (Supplementary Figure S1F). To specifically analyze the gene expression changes exclusively depending on HDAC7, and omit differences due to different cell stages, we overlapped upregulated genes from pro-B and pre-B cells. GO analysis revealed that overlapped upregulated genes upon HDAC7 deficiency were associated with an altered immune response (Figure 1D, upper panel), with a clear tendency for increased protein binding and transcription factor (TF) activity, which may correlate with a more open chromatin

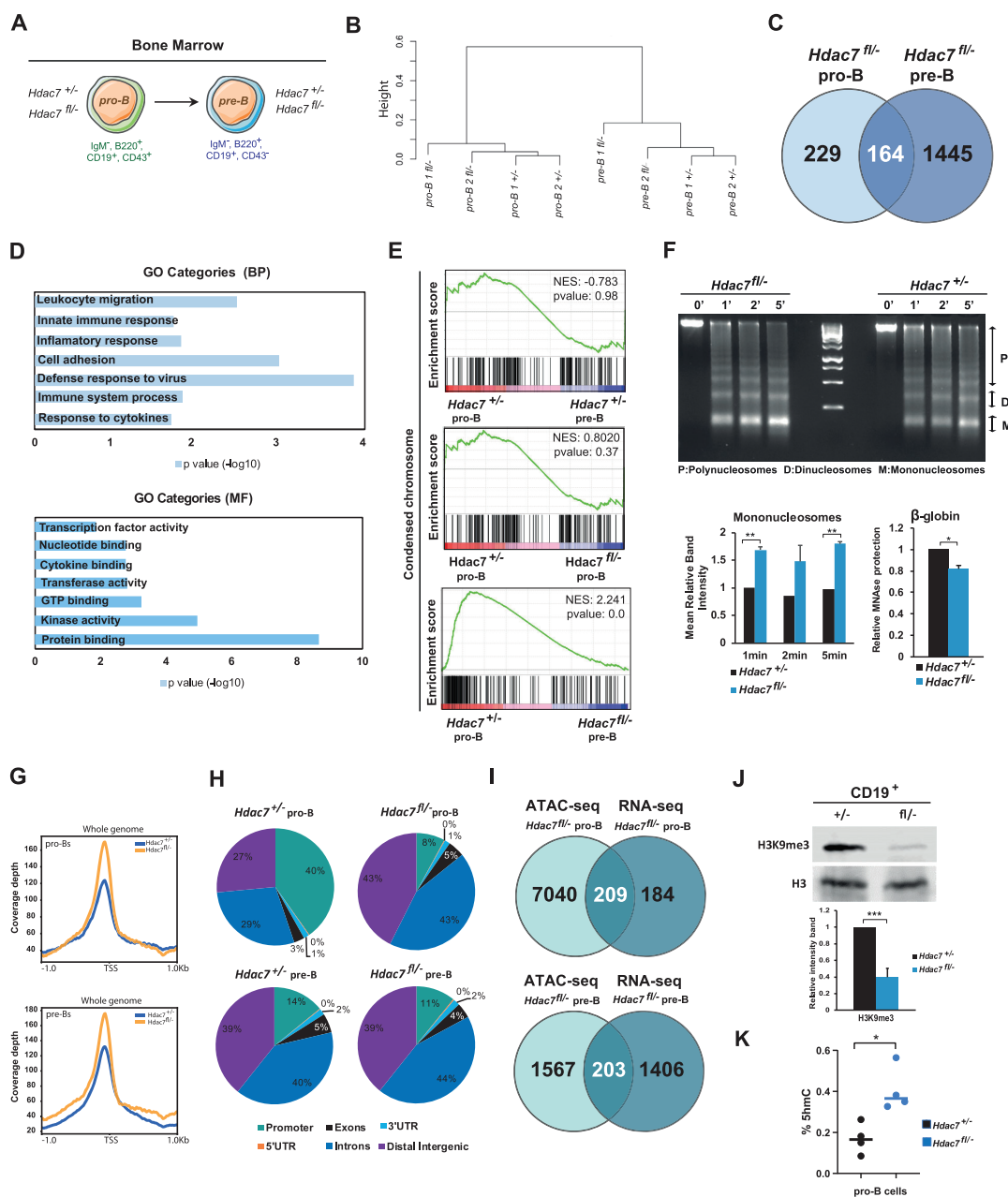


**Figure 1.** HDAC7 deficiency results in global chromatin de-condensation and increase 5-hmC levels. (A) Experimental design for RNA-seq experiments, showing the type of cells used. B cell progenitors (pro-B); B cell precursors (pre-B). (B) Cluster dendrogram obtained from RNA-seq gene expression profiles for each replicate and cell type. (C) Venn Diagram comparing up-regulated genes in *Hdac7*<sup>fl/-</sup> pro-B cells respect to control pro-B cells (left) and in *Hdac7*<sup>fl/-</sup> pre-B cells respect to control pro-B cells (right). (D) Gene ontology (GO) enrichment analysis of up-regulated genes in HDAC7 deficient pro-B and pre-B cells respect to control pro-B cells. BP refers to Biological Processes and MF corresponds to Molecular Functions. (E) GSEA analysis comparing wild-type pre-B and HDAC7-deficient pro-B and pre-B cells respect to wild-type pro-B cells in expression profiles related to condensed chromosome signatures. (F) Chromatin accessibility assay in control and HDAC7-deficient B cells. Isolated nuclei from these cells were digested with 5 units of micrococcal nuclease (MNase) for 0, 1, 2 or 5 min. Different nucleosomal fractions (mono, di and polynucleosomes) were separated by gel electrophoresis (upper panel). Band density quantification from chromatin accessibility assay using ImageJ software. Results are expressed as the mean ± SEM of three independent experiments. \*\**P* < 0.01 by unpaired *t*-test (left lower panel). qPCR showing protection of MNase-digested DNA after 5 min incubation in control or HDAC7-deficient B cells (right lower panel). Data represent mean ± SEM of three independent experiments per condition after normalization to *Actb* gene expression. \**P* < 0.05 by unpaired *T*-test. (G) ATAC-seq coverage depth (per base pair per peak for 10 million mapped reads) of peaks located in the TSS (-1 kb to +1 kb) in wild-type and HDAC7-deficient pro-B (upper panel) and pre-B cells (lower panel). (H) Genomic distribution of chromatin accessible peaks in *Hdac7*<sup>+/-</sup> and *Hdac7*<sup>fl/-</sup> pro-B and pre-B cells determined by ATAC-seq experiments. (I) Venn Diagram comparing differentially enriched peaks in ATAC-seq in *Hdac7*<sup>fl/-</sup> pro-B cells and up-regulated genes in RNA-seq in *Hdac7*<sup>fl/-</sup> pro-B cells (upper panel) and pre-B cells (lower panel) compared to control cells. (J) H3K9me3 global levels decrease upon HDAC7 deficiency, analyzed by Western blot representative assay (upper panel). Total H3 levels were used as a control. Band quantification of the Western blot experiment was performed using ImageJ program. Results are expressed as the mean ± SEM of three independent experiments. \*\*\**P* < 0.001 by unpaired *t*-test (lower panel). (K) ELISA assay showing global levels of DNA 5-hmC in pro-B cells from wild-type and HDAC7-deficient mice. Each dot represents one animal (*n* = 4, test); the line represents the mean. Data is represented as mean ± SEM of four independent experiments. \**P* < 0.05, Mann-Whitney test.

state (Figure 1D, lower panel). Gene set enrichment analysis (GSEA) showed that the gene signatures in HDAC7-deficient pro-B or pre-B cells were associated to a deficiency in chromosome condensation, suggesting a potential loss of the heterochromatin state in the absence of HDAC7 (Figure 1E). This de-condensation was independent of the cell stage, as there was no difference in these gene signatures between control pro-B and pre-B cells, when separately analyzed for each genotype (Figure 1E). These results indicate that HDAC7 deficiency may result in chromatin decompaction. Accordingly, HDAC7-deficient B cells presented increased chromatin accessibility, as genomic DNA from these cells was more sensitive to micrococcal nuclease (MNase) digestion than that from control B cells (Figure 1F, upper and lower left panels). These results were reinforced by qPCR showing protection of MNase-digested DNA at  $\beta$ -globin site (Figure 1F, lower right panel). To definitively prove the potential role of HDAC7 in maintaining proper chromatin status in pro-B and pre-B cells, we performed transposase-accessible chromatin assay coupled with next generation sequencing (ATAC-seq). We found that the global chromatin accessibility intensity was higher in both HDAC7-deficient pro-B and pre-B cells compared to control cells (Figure 1G). Consistent with its role as a transcriptional repressor, we observed ~13 000 more accessible peaks in HDAC7-deficient pro-B cells. Next, we determined ATAC-seq differential regions between HDAC7-deficient and wild-type pro-B (Figure 1H, upper panel) and pre-B cells (Figure 1H, lower panel). We found that the genomic distribution of the accessible sites differed significantly in the absence of HDAC7. In particular, we observed a reduction of peaks located at promoters and, more notably in pro-B cells, a dramatic increase of accessible peaks at distal intergenic regions (Figure 1H). To interrogate a potential functional link between the altered chromatin landscape and transcriptional programming in the absence of HDAC7, we integrated the data obtained in ATAC-seq and RNA-seq experiments. We compared the open chromatin regions in HDAC7-deficient pro-B and pre-B cells versus upregulated genes in the absence of HDAC7 (Figure 1I, upper panel). Half of the differentially upregulated genes (209 genes) in pro-B cells also presented a more open chromatin state in HDAC7-deficient cells, whereas 203 genes among the pre-B cells upregulated genes set showed a more accessible chromatin (Figure 1I, lower panel). Additionally, and given that chromatin condensation is associated to heterochromatin state, we next isolated CD19<sup>+</sup> B cells from HDAC7-deficient or wild-type mice and assessed the levels of H3K9me<sub>3</sub>, a well-known epigenetic mark involved in the establishment of heterochromatin, genome stability, and cell identity maintenance (47). We found that HDAC7-deficient B cells showed a significant and dramatic decrease in H3K9me<sub>3</sub> as compared to their wild-type counterparts (Figure 1J). Increases in 5-hmC have been associated with chromatin decompaction and, consequently, with alterations in hematopoietic cell differentiation and the maintenance of cell identity (48). Importantly, 5-hmC and H3K9me<sub>3</sub> have an opposite genomic localization pattern, with TET proteins recruited mostly to euchromatin regions (49,50). We next carried out ELISA assays to determine the global 5-hmC levels; which revealed that HDAC7 loss in pro-B cells led to a significant increase in

the global levels of 5-hmC (Figure 1K). Thus, altogether our data indicated that HDAC7 controls chromatin compaction and DNA 5-hmC levels at early stages of B cell development.

### HDAC7 regulates TET2 expression in pro-B and pre-B cells

Our results suggested that an essential function of HDAC7 during early B cell development could be the regulation of TET proteins expression, which are responsible for incorporating 5-hmC into DNA. Among the different family members, TET2 appears to play crucial roles during hematopoiesis and is highly expressed in myeloid cells (20–22). Therefore, we hypothesized that HDAC7 may be responsible for tightly regulating and fine-tuning the physiological levels of TET2 in pro-B and pre-B cells, thereby ensuring proper cell differentiation and identity. We directly addressed our hypothesis firstly by analyzing whether TET2 is expressed at different levels in the lymphoid and myeloid compartments within the hematopoietic system. For this purpose, we examined transcriptomic data from the Immunological Genome Project Database (Immgen) (<http://www.immgen.org/>). Indeed, TET2 was expressed at much higher levels in myeloid cells than in lymphoid populations (Figure 2A). Next, taking advantage of the ‘modules and regulators’ interactive tool in the Immgen database, we searched for putative positive and negative TET2 regulators. This tool uses all expression data of hematopoietic cell populations deposited by several groups and enables the search for putative positive and negative regulators of the gene of interest. Strikingly, HDAC7 appeared to be the only negative regulator or transcriptional repressor controlling TET2 expression within the hematopoietic system (Figure 2B). Further analysis of data from Immgen database to compare the expression pattern between HDAC7 and TET enzymes coding genes in lymphoid and myeloid populations revealed an inverse correlation with gene expression between HDAC7 and TET2 (Figure 2C), indicating a fully opposite expression pattern of both genes throughout hematopoiesis. In contrast, TET1 had an expression pattern similar to that of HDAC7, while TET3 displayed uniform expression levels throughout all tested cell populations (Supplementary Figure S2A and B). These data suggested that HDAC7 was responsible for controlling TET2 levels in lymphoid cells. We next examined data from RNA-seq in Figure 1B–E, as well as from our published microarray (26). We found that *Tet2* was upregulated in HDAC7-deficient pro-B and pre-B cells with respect to control pro-B cells (Figure 2D and E) reaching similar levels to that of macrophages (Supplementary Figure S2C), whereas the expression of the essential B cell genes *E2a* and *Pax5* remained unaltered (Supplementary Figure S2D and E). RT-qPCR assays revealed that the absence of HDAC7 from pro-B and pre-B cells did not alter the expression levels of the other class IIa HDACs family members (HDAC4, 5 and 9) indicating the specific requirement of HDAC7 during early B cell development (Supplementary Figure S2F). According to mRNA levels, analysis of our ATAC-seq revealed a more open chromatin at *Tet2* gene loci in HDAC7-deficient pro-B cells and pre-B cells (Figure 2F). Western blot experiments confirmed that the absence of HDAC7 from B cells



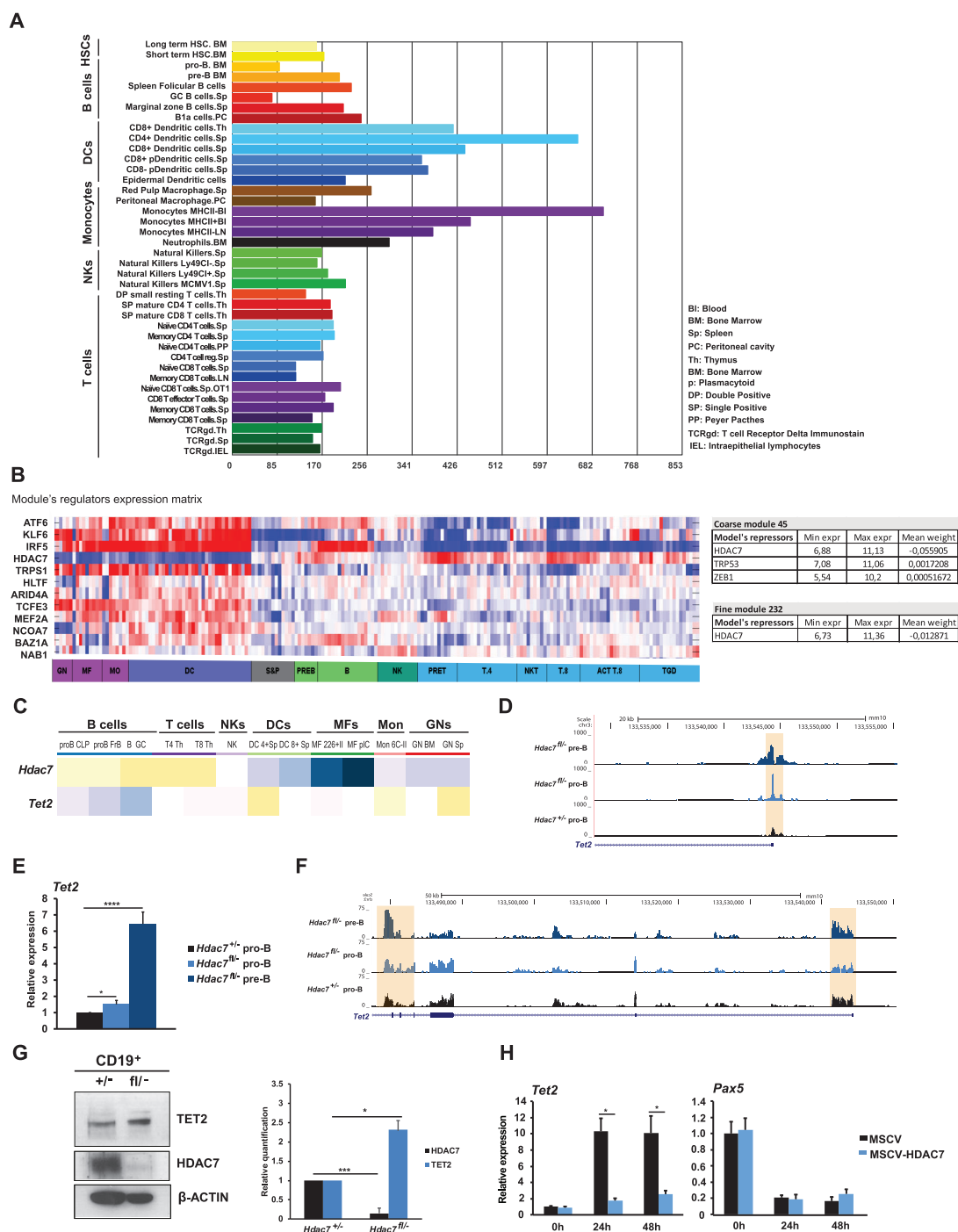


**Figure 2.** (A) HDAC7 controls DNA 5-hmC through *Tet2* regulation in pro-B and pre-B cells. Gene skyline showing the *Tet2* gene expression profile along different murine hematopoietic cell lineages (obtained from 'gene skyline' tool of Immgen database). (B) Heatmap showing the expression of potential *Tet2* gene regulators in hematopoietic cell subsets (left panel). Tables showing mean weight (enzymatic activity) of potential negative regulators of *Tet2* gene in hematopoietic cells. *Tet2* gene is included in two modules or cluster of genes: coarse module includes 315 genes and three negative regulators and fine module contains 35 genes and one negative regulator (right panel). Data were extracted from Immgen public database using *Modules and Regulators* tool. (C) Heatmap showing the inverse expression of *Hdac7* and *Tet2* in the indicated cell subsets. Data was extracted from Immgen public database using *My Gene Set* tool. (D) Genome browser snapshot of the *Tet2* gene showing signal for RNA-seq in wild-type and HDAC7-deficient pro-B and pre-B cells. Orange shadow indicates *Tet2* promoter. (E) Analysis by RT-qPCR of the *Tet2* mRNA levels in wild-type and HDAC7-deficient pro-B and pre-B cells. (F) Genome browser snapshot of the *Tet2* gene showing signal for ATAC-seq in *Hdac7*<sup>+/-</sup> pro-B cells, *Hdac7*<sup>fl/fl</sup> pro-B and pre-B cells. Orange shadows indicate *Tet2* promoter and additional exonic regions. (G) TET2 upregulation in *Hdac7*<sup>fl/fl</sup> CD19<sup>+</sup> B cells compared to *Hdac7*<sup>+/-</sup> B cells analyzed by Western Blot assay (left panel). Quantification of two Western Blot experiments was performed by using ImageJ program (right panel). (H) RT-qPCR experiments for gene expression changes for *Tet2* and *Pax5* in the absence or presence of HDAC7 during the conversion of pre-B cells into macrophage-like cells. 24 and 48 h time points indicate time since transdifferentiation induction with  $\beta$ -estradiol. Data from E and H is represented as mean  $\pm$  SEM of four independent experiments. \**P* < 0.05, \*\*\*\**P* < 0.0001, unpaired *t*-test. Data from G is represented as mean  $\pm$  SEM of two independent experiments. \**P* < 0.05, unpaired *t*-test.

corresponded with significantly increased TET2 protein levels (Figure 2G). Therefore, different physiological levels of TET2 protein may have an effect and specific function in hematopoietic cell populations. Next, using a transdifferentiation system developed by Graf laboratory (24), we found that HDAC7 exogenous expression blocked the upregulation of *Tet2* during pre-B cells conversion into macrophages (Figure 2H). Forced expression of HDAC7 did not interfere with the downregulation of *Pax5* during cellular conversion (Figure 2H), confirming that its expression is totally independent of that of HDAC7. Together, these findings indicated that HDAC7 may govern early B cell development in the bone marrow through the control of the physiological levels of TET2.

### ***Tet2* is a direct HDAC7 target gene in pro-B cells**

We next performed chromatin immunoprecipitation (ChIP) assays to test whether *Tet2* is a direct HDAC7 target gene in B cells; we found that HDAC7 was recruited to the promoter of the *Tet2* gene, which contains MEF2 binding sites in pro-B cells (Figure 3A, upper panel). This was consistent with the previously demonstrated requirement of HDAC7 to interact with MEF2C to repress its target genes in pro-B cells (26), and with *Tet2* being a MEF2C direct target in pro-B cells (6). We also demonstrated HDAC7 recruitment at a previously described *Tet2* enhancer (24) (Figure 3A, lower panel). We previously reported by ChIP-seq experiments that HDAC7 loss in pro-B cells causes an increase of H3K9/K14ac at the promoter and enhancers of its target genes (26). ChIP-seq data examination and ChIP-qPCR revealed an increase of H3K9/K14ac at both promoter and enhancer regions of *Tet2* in the absence of HDAC7 from pro-B cells (Figure 3B and C). As expected, the absence of HDAC7 from pro-B cells had no effect on H3K9/K14ac enrichment at *Pax5* gene (Supplementary Figure S3A). Next, integration of ATAC-seq and H3K9/K14ac ChIP-seq data from HDAC7-deficient pro-B cells revealed an overlapping of 4487 enriched regions, remarkably including *Tet2* (Supplementary Figure S3B). To further gain insight into the mechanisms altered by HDAC7 deficiency, we performed ChIP-seq of H3K27ac and H3K27me3 histone marks in wild-type and HDAC7-deficient pro-B cells. The analysis revealed an increased global intensity of the activating histone mark H3K27ac in the HDAC7-deficient pro-B cells (Supplementary Figure S3C), as well as at both specific promoter and enhancer regions of *Tet2* gene (Figure 3D, E). In addition, the absence of HDAC7 from pro-B cells resulted in a decrease of global H3K27ac mark in promoter regions and an increase in distal intergenic regions (Supplementary Figure S3D). Increased number of H3K27ac peaks in distal regions upon HDAC7 deficiency agrees with previous results of more open chromatin regions under the same conditions, reinforcing the repressive role of HDAC7. The integration of ATAC-seq and H3K27ac-seq data revealed 3113 common peaks (representing ~40% of the enriched regions in both assays) in the absence of HDAC7, in which *Tet2* was also included (Supplementary Figure S3E). In parallel, H3K27me3 ChIP-seq data unveiled similar coverage intensity between wild-type and HDAC7 deficient pro-B cells (Supplementary Figure S3F). The genomic

distribution of H3K27me3 remained also unaltered in the absence of HDAC7 (Supplementary Figure S3G). In the case of H3K27me3 enrichment in HDAC7-deficient pro-B cells, we performed the integrative analysis comparing with ATAC-seq data from wild-type cells and observed an overlap of ~25% of enriched peaks (Supplementary Figure S3H). ChIP-qPCR demonstrated a significant decrease of H3K27me3 at *Tet2* gene loci in HDAC7-deficient pro-B cells (Figure 3F, G). Finally, we aimed to determine if the global decrease in H3K9me3 in the absence of HDAC7 shown in Figure 1J could be observed at the *Tet2* gene loci. Indeed, ChIP-qPCR showed that HDAC7 deficiency in pro-B cells led to lower enrichment levels of the repressive histone mark H3K9me3, at both the promoter and enhancer of *Tet2* gene (Supplementary Figure S3I). Collectively, our findings demonstrated that HDAC7 controls the proper deposition of epigenetic marks and that *Tet2* is a direct HDAC7-target gene in pro-B cells.

### **HDAC7 deficiency alters 5-hmC at specific loci**

We next performed a 5-hmC DNA immunoprecipitation (hMeDIP) followed by next-generation sequencing (hMeDIP-seq) in pro-B cells purified from *Hdac7<sup>fl/fl</sup>* mice and their *Hdac7<sup>+/-</sup>* control littermates. While the total frequencies of 5-hmC peaks were similar, the global 5-hmC coverage was higher in HDAC7-deficient pro-B cells than in wild-type pro-B cells, in concordance with the results from Figure 1K (Figure 4A and Supplementary Figure S4A). The genomic distribution of the peaks did not differ significantly between the two genotypes, with most peaks located in intergenic and intronic regions as well as within LINE-1 elements (Figure 4B). Further, we found differential peaks in 5-hmC enrichment: HDAC7-deficient pro-B cells had an increase of ~13 000, and a decrease in ~15 800, 5-hmC peaks, as compared to wild-type B cells. Next, we performed an integrative analysis of the ATAC-seq and hMeDIP-seq data obtained. In particular, we overlapped the genes presenting a more open chromatin with the genes associated with higher 5-hmC enrichment in the HDAC7-deficient pro-B cells. We found that around 40% of genes with a more accessible chromatin harbored increased 5-hmC, indicating that HDAC7 may regulate a proper DNA compaction to avoid aberrant deposition of this epigenetic mark (Figure 4C). Focusing on alterations in potential lineage-inappropriate genes, we observed an increase in the enrichment of 5-hmC at the *Jun* gene in HDAC7-deficient pro-B cells as compared to wild-type cells, indicating that *Jun* may be aberrantly overexpressed in the absence of HDAC7 (Figure 4D). Indeed, RNA-seq data showed a higher expression of *Jun* in HDAC7-deficient pro-B and pre-B cells as compared to wild-type pro-B cells (Figure 4D). This correlated with a more open chromatin of the *Jun* gene in the absence of HDAC7 in both cell types (Figure 4D). Similar results were observed for the *Fosb* gene (Supplementary Figure S4B). The results from hMeDIP-seq and RNA-seq were confirmed by hMeDIP-qPCR and RT-qPCR experiments (Figure 4E, F, and Supplementary Figure S4C). Upregulation of additional lineage inappropriate genes, *Cd69* and *Itgb2*, in HDAC7-deficient pro-B and pre-B cells is shown in Supplementary Figure S4D. Importantly, we found in-

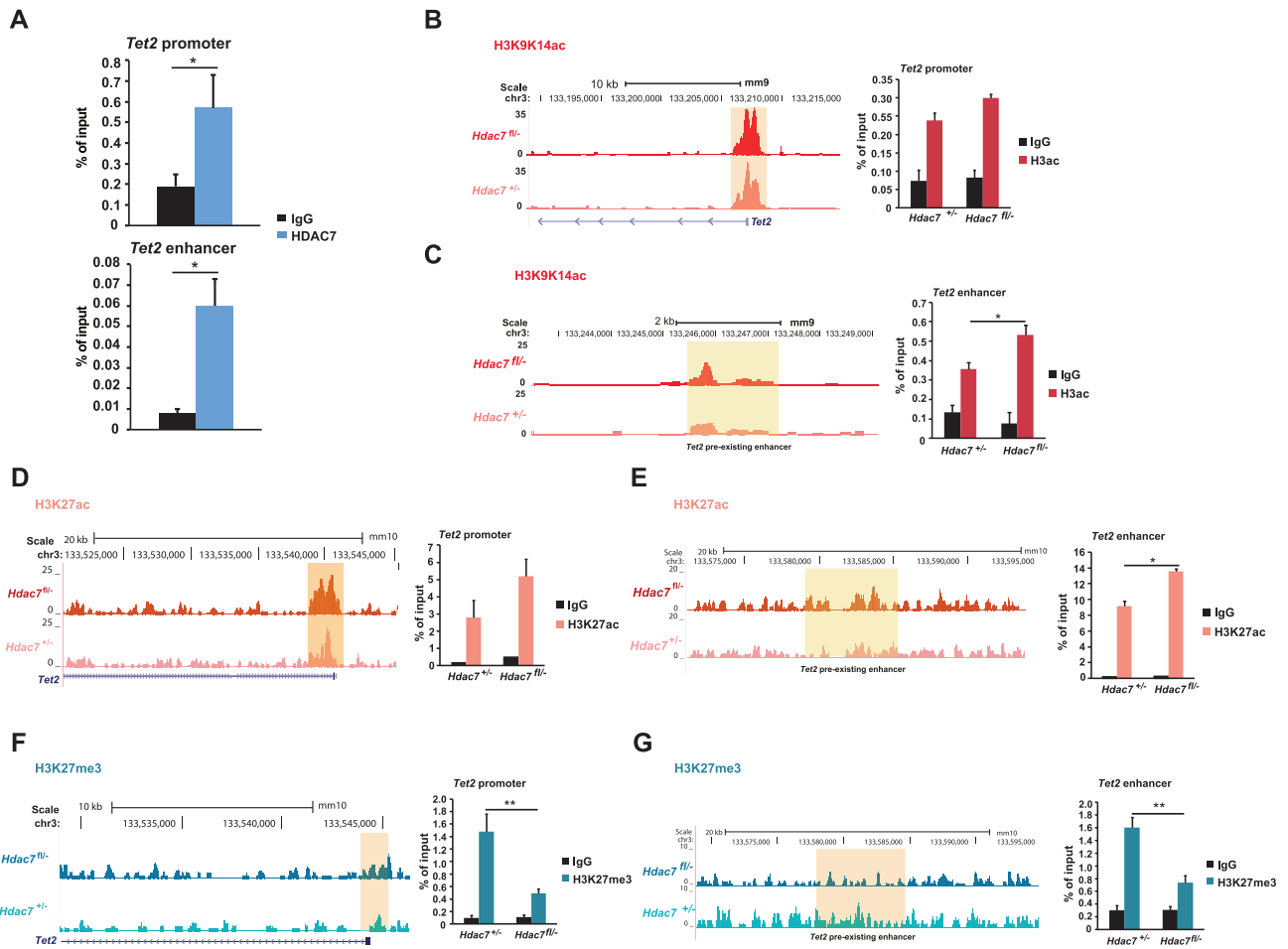


**Figure 3.** *Tet2* is a direct HDAC7 target gene in pro-B and pre-B cells. (A) Chromatin immunoprecipitation (ChIP) experiments showing the recruitment of HDAC7 to the *Tet2* promoter or the *Tet2* enhancer, quantified as % of input. (B) Genome browser snapshot of H3K9/K14ac ChIP-seq (left panel) showing differential enrichment levels at the promoter region of *Tet2* gene for HDAC7-deficient pro-B and control cells. ChIP-qPCR assay validating ChIP-seq data after immunoprecipitation with anti-H3K9/14ac antibody is shown in right panel, quantified as % of input. (C) As in (B), but for a *Tet2* pre-existing enhancer region. (D, E) As in (B, C), but for H3K27ac ChIP-seq enrichment and after immunoprecipitation with H3K27ac antibody. (F, G) As in (B, C), but for H3K27me3 ChIP-seq enrichment and after immunoprecipitation with H3K27me3 antibody. All data are represented as mean  $\pm$  SEM of  $n = 3$ . \* $P < 0.05$ , \*\* $P < 0.01$ , unpaired  $t$ -test.

creased TET2 recruitment to the *Jun* gene loci identified in the hMedIP-seq analysis, as well as to further myeloid gene promoters (*Fosl2*, *Ahnak* and *Itgb2*), in HDAC7-deficient pro-B cells (Figure 4G and Supplementary Figure S4E).

To definitively prove the functionality of HDAC7–TET2 axis, we performed rescue analysis (gain and loss of function) using three different experimental approaches. A graphical scheme depicting the three experimental approaches is shown in Supplementary Figure S4F. First, we transduced purified B cells from bone marrow of wild-type and HDAC7-deficient mice with a retroviral vector for specific shRNA against *Tet2* (sh*Tet2*) and compared them to counterpart cells transduced with control retroviral vector (shCtrl). We found that knocking down *Tet2* prevented the upregulation of *Jun* and *Fosl2* in HDAC7 deficient B cells (Figure 4H). Therefore, as a second approach, we took advantage of the HAFTL murine pre-B cell line engineered to transdifferentiate into functional macrophages by addition of  $\beta$ -estradiol (C11 cells) and previously reported in (29).

Similarly to the case of C10 cells, HDAC7 and TET2 become downregulated and upregulated during cellular conversion, respectively. C11 were transduced with shCtrl or sh*Tet2* retroviral vectors and sorted GFP-positive cells were later induced to macrophage transdifferentiation by the addition of  $\beta$ -estradiol, in order to achieve double HDAC7 and TET2 deficiency (Figure 4I). RT-qPCR assays showed that *Jun* and *Fosl2* were upregulated after cellular conversion, concomitant to HDAC7 downregulation. Importantly, *Tet2* knockdown resulted in a significant block of both inappropriate genes induction (Figure 4I). And third, we determined the expression of *Jun* and *Fosl2* in C10 samples from Figure 2H similarly to the case of C11 cells, *Jun* and *Fosl2* were upregulated during the conversion of pre-B cells into macrophages. Importantly, HDAC7 exogenous expression blocked their increased expression (Figure 4J). These data demonstrate that the HDAC7–TET2 axis is involved in the proper control of the expression of lineage inappropriate genes in B cells.

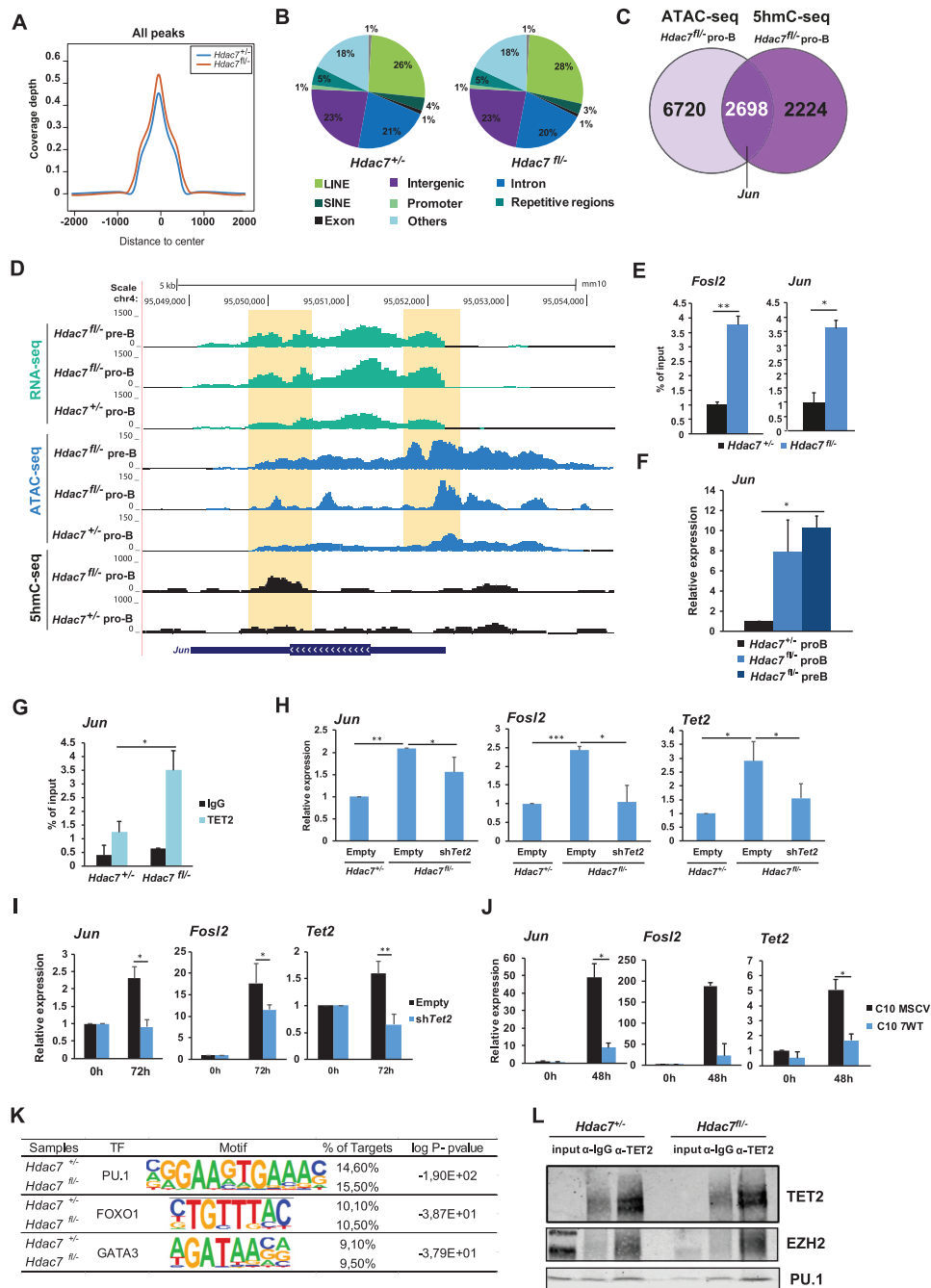


**Figure 4.** HDAC7 deficiency results in increased recruitment of TET2 and altered 5-hmC enrichment at B cell lineage inappropriate genes. (A) 5-hmC coverage depth (per base pair per peak per 10 million mapped reads) of 5-hmC peaks (−2 kb to +2 kb) in control and HDAC7-deficient pro-B cells. (B) Genomic distribution of 5-hmC enrichment in  $Hdac7^{+/+}$ - and  $Hdac7^{fl/fl}$ - pro-B cells. (C) Venn Diagram comparing enriched peaks associated genes in ATAC-seq from  $Hdac7^{fl/fl}$ - pro-B cells and 5hmC enriched genes in hMeDIP-seq in  $Hdac7^{fl/fl}$ - pro-B cells compared to control cells. (D) Genome browser snapshot of the *Jun* gene showing signal for 5-hmC from hMeDIP-seq, ATAC-seq and RNA-seq data in wild-type or HDAC7-deficient pro-B and pre-B cells. The peak locations are indicated in the orange-shaded rectangles. Orange shadows indicate *Jun* gene regions with differential peaks. (E) 5hmC-qPCR experiments showing the enrichment of 5-hmC in wild-type or HDAC7-deficient pro-B cells in the *FosI2* and *Jun* genes. (F) Analysis by RT-qPCR of *Jun* mRNA levels in control or HDAC7-deficient pro-B cells and pre-B cells. (G) Analysis of TET2 recruitment at the *Jun* gene by ChIP-qPCR in control and HDAC7-deficient pro-B cells. (H) Ex vivo shCtrl and shTet2 retroviral infection in B cells from HDAC7-deficient mice. As control, wild-type B cells were transduced with shCtrl vector. Cells were infected with shTet2 and expression levels of target genes were analyzed by RT-qPCR 72h after retroviral infection. (I) In vitro shTet2 infection of C11 pre-B cells. Cells were infected with shCtrl or shTet2 and then treated with  $\beta$ -estradiol to induce trans-differentiation to macrophages. Expression levels of target genes were analyzed after 72 h of transdifferentiation (J) C10 pre-B cells expressing empty plasmid (MSCV) and HDAC7-expressing plasmid (7WT) were treated with  $\beta$ -estradiol to induce transdifferentiation to macrophages. Expression levels of target genes were analyzed after 48 h of transdifferentiation. (K) The most relevant TF binding motifs in wild-type or HDAC7-deficient pro-B cells, based on their enrichment in 5-hmC using the HOMER database of known motifs. (L) Co-immunoprecipitation assays performed in  $Hdac7^{+/+}$ - and  $Hdac7^{fl/fl}$ - CD19<sup>+</sup> B cells. Protein extracts were immunoprecipitated using an anti-TET2 antibody, using IgG as a negative control and total protein extract as input. Data in (E, F) are represented as mean  $\pm$  SEM of  $n = 4$ . Data in (G–J) are represented as mean  $\pm$  SEM of  $n = 3$ . \* $P < 0.05$ , \*\* $P < 0.01$ , \*\*\* $P < 0.001$  unpaired  $t$  test.

Finally, we performed a motif enrichment analysis to determine whether HDAC7 deficiency produces an alteration in chromatin positioning that could lead to changes in TF occupancy. Although we found no differences associated with HDAC7, we did note enrichment of relevant TFs in the hematopoietic system, such as PU.1 (Figure 4K), which has been previously reported to interact with TET2 (51,52). The occupancy of PU.1 under both conditions is consistent with its relevance in both lymphoid and myeloid lineages. Accordingly, we corroborated that TET2 interacts with PU.1 in HDAC7-deficient B cells, as well as in wild-type B cells. As expected, EZH2 (a known TET2 partner) was also identified as an interactor (Figure 4L). Together, our results demonstrate an essential role of HDAC7 in silencing B cell-inappropriate genes by its regulation of TET2 expression and, consequently, of the DNA 5-hmC levels.

### HDAC7 directs 5-hmC and expression of specific miRNA in pro-B cells

Further examination of our hMeDIP-seq data revealed that the coverage depth of 5-hmC peaks at miRNAs in HDAC7-deficient pro-B cells was higher than in control pro-B cells (Figure 5A). Additionally, integrative analysis with our ATAC-seq obtained data demonstrated that more than 50% of miRNA-related peaks that are enriched in 5-hmC mark in the absence of HDAC7, are also located in open chromatin regions (Figure 5B). In fact, we found that several miRNAs involved in leukemia and lymphoma, as well as in myeloid differentiation, such as miR-125b and miR34a, were more enriched in 5-hmC and located in more open chromatin regions in pro-B cells from *Hdac7<sup>fl/fl</sup>* mice (53) (see an example of miR125b in Figure 5C). Using ChIP-qPCR, we found that TET2 recruitment increased at both miR125b- and miR34a-associated loci, which correlated to the enhanced 5-hmC enrichment in HDAC7-deficient pro-B cells (Figure 5D). Additionally, GSEA analysis of our RNA-seq data confirmed that gene sets related to miR-34a and miR-125b functions were more expressed upon HDAC7 deficiency (Figure 5E). To examine a potential connection between changes in 5-hmC and chromatin condensation and HDAC7-mediated control of miRNA expression, we performed a miRNA profiling using a qPCR-based panel containing over 375 miRNAs (miR-CURY LNA™ microRNA Array [Exiqon]) in wild-type or HDAC7-deficient pro-B cells (Figure 5F and Supplementary Table S2). We found 25 miRNAs whose levels of expression differed significantly between wild-type and HDAC7-deficient pro-B cells, which correlated with differential 5hmC enrichment and chromatin state. miRNAs that were up-regulated and 5hmC-enriched under HDAC7-deficient conditions included miR-125b-5p, miR-126, miR-29b, miR-34a and miR-99a (Figure 5F and Supplementary Figure S5A). On the contrary, B-cell related miRNAs that were down-regulated upon HDAC7 deficiency, such as miR-150a and miR-181a, also presented decreased 5hmC enrichment and more closed chromatin state (Figure 5F and Supplementary Figure S5B). The differential expression observed in HDAC7-deficient pro-B cells of several miRNAs involved in the hematopoietic system or related disorders were validated by RT-qPCR (Figure 5G). Thus, aberrant

microRNAs (such as miR-125b and miR-34a) were upregulated, while B cell-specific miRNAs (such as miR-28a, miR150, miR-142 and miR181a) were downregulated in HDAC7-deficient pro-B cells. Finally, we tested whether targets of these miRNAs are altered as a consequence of HDAC7 deficiency. On one hand, we observed that protein levels of MYB, target of miR-142 and miR-150, were increased in *Hdac7<sup>fl/fl</sup>* cells (Figure 5H). On the other hand, we found decreased expression of PUMA and IRF4, both targets of miR-125b, upon HDAC7 deficiency (Figure 5I). Globally, our data indicate that, through the regulation of *Tet2*, HDAC7 controls the expression levels of crucial miRNAs of the immune system.

### HDAC7 regulates 5-hmC levels and expression of LINE-1 elements

Our hMeDIP-seq approach also revealed that, according to the average signal from all the peaks obtained, the signal intensity of 5-hmC peaks associated with LINE-1 elements in HDAC7-deficient pro-B cells was higher than in their wild-type counterparts (Figure 6A). Gene ontology analysis of genes located in regions associated to LINE-1 elements revealed that 5-hmC enriched genes in *Hdac7<sup>fl/fl</sup>* pro-B cells were more associated to gene activation and cell proliferation, whereas down-regulated LINE-1-related genes were involved in negative regulation of cell proliferation and cell differentiation (Figure 6B). In addition, we found that specific LINE-1-related loci were more susceptible to MNase treatment in HDAC7-deficient B cells than wild-type cells and, therefore, more predisposed for aberrant upregulation (Figure 6C). Accordingly, we found that >50% of LINE-1 related peaks (associated 514 to genes) with 5-hmC enrichment were located in more open chromatin regions (Figure 6D). Hence, HDAC7 depletion was correlated with increased chromatin accessibility and enhanced or uncontrolled gene activation in LINE-1 associated loci (see examples in Figure 6E and Supplementary Figure S6A). Aberrant expression of LINE-1 elements is associated with genome instability. Accordingly, GSEA analysis of our RNA-seq data showed that the gene signatures in HDAC7-deficient pro-B or pre-B cells were associated to impaired DNA repair mechanisms (Figure 6F), suggesting a potential increase of genomic instability in the absence of HDAC7 that could correlate with LINE-1 aberrant expression. In fact, genes included in DNA repair gene set (from GSEA) that were down-regulated in HDAC7-deficient pro-B cells were related to DNA damage response and DNA repair abilities (Supplementary Figure S6B, C), supporting the potential affection of DNA repair capacity upon HDAC7 deficiency. Regions with differential 5-hmC peaks were validated by hMeDIP-qPCR assays, confirming that the absence of HDAC7 from pro-B cells resulted in higher levels of 5-hmC in LINE-1 elements (Figure 6G). Moreover, we observed a significant increase in the expression of LINE-1 transcripts from the most active families in HDAC7-deficient pro-B cells (Figure 6H), reinforcing the correlation between 5-hmC enrichment and gene activation. Previously published data revealed that TET1 and TET2 are recruited to the 5' UTR of young LINE-1 elements in embryonic stem cells (54). We confirmed by ChIP-qPCR that

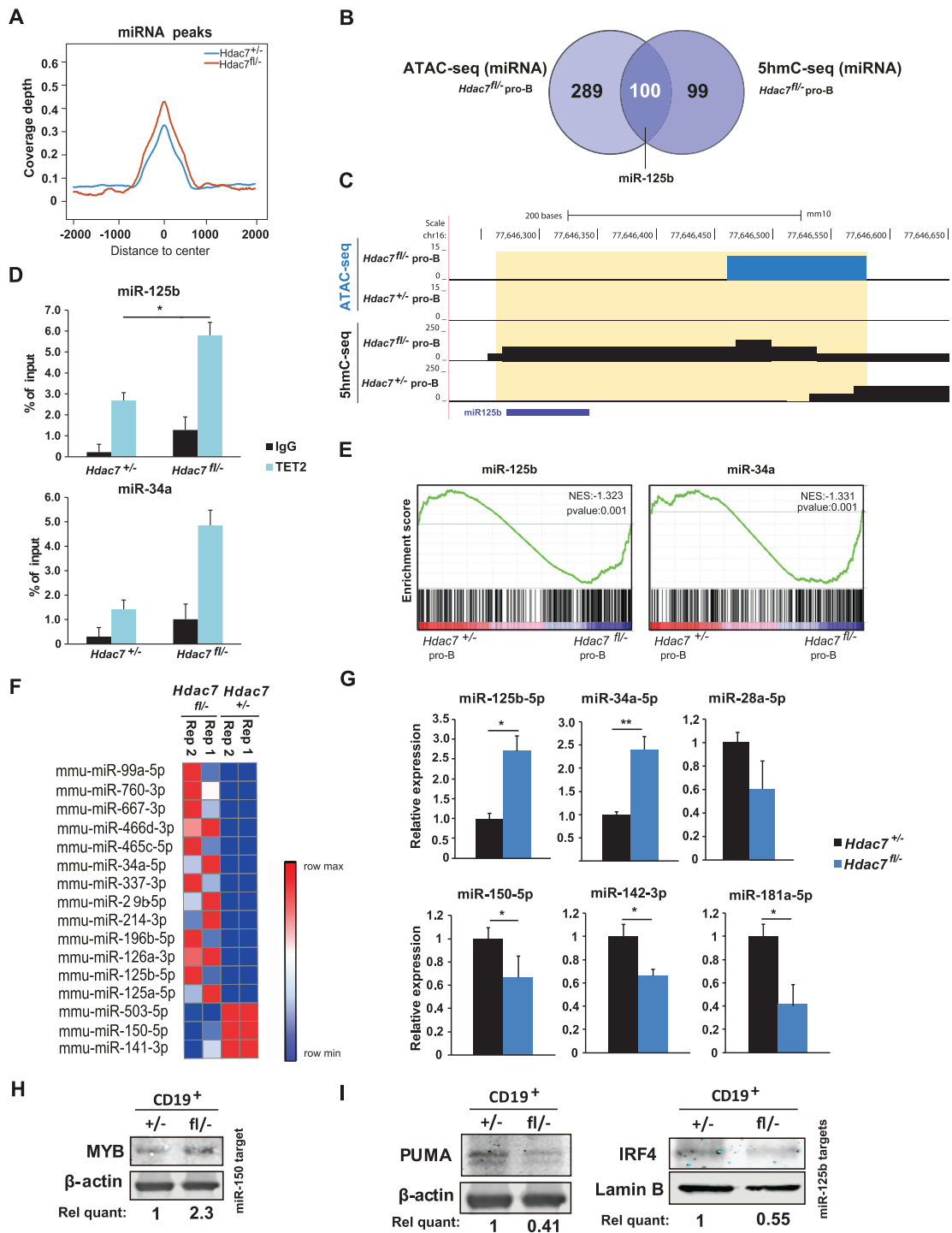


**Figure 5.** HDAC7 directs B cell-specific miRNA hydroxymethylation and expression patterns. (A) 5-hmC coverage depth (per base pair per peak per 10 million mapped reads) of 5hmC peaks located in microRNAs (–2 kb to +2 kb) from control or HDAC7-deficient pro-B cells. (B) Venn diagram comparing miRNA-related enriched peaks in ATAC-seq from *Hdac7*<sup>fl/-</sup> pro-B cells and miRNA-related peaks enriched in 5hmC-seq (or hMeDIP-seq) in *Hdac7*<sup>fl/-</sup> pro-B cells compared to control cells. (C) Example of 5-hmC and open chromatin enriched peaks at miR-125b from hMeDIP-seq and ATAC-seq experiments. (D) ChIP-qPCR analysis of TET2 recruitment to hydroxymethylated miRNAs in HDAC7-deficient pro-B cells. (E) GSEA analysis showing gene sets related to miR-34a and miR-125b functions, comparing HDAC7-deficient pro-B cells to control pro-B cells. miR-125b and miR-34a datasets were retrieved from [www.gsea-msigdb.org](http://www.gsea-msigdb.org). (F) Heat map of the differential expression of miRNAs for two HDAC7-deficient vs. wild-type replicates. Only miRNAs with a FC > 2 or FC < 0.5 2 from the miRCURY LNA™ Universal RT panel were selected. See also Supplementary Table S2. (G) RT-qPCR analysis of selected microRNAs from the miRCURY LNA™ Universal RT panel in HDAC7-deficient and control pro-B cells. The levels of U6 RNA were used for normalization. (H) Protein levels of miR-150 and miR-142 target MYB were assessed by western blot assays in control and HDAC7-deficient CD19<sup>+</sup> cells. (I) Protein levels of miR-125b targets PUMA (left panel) and IRF4 (right panel) were assessed by western blot assays in control and HDAC7-deficient CD19<sup>+</sup> cells. Using  $\beta$ -actin or Lamin-B as housekeeping, relative quantification of protein levels in G and H was performed with ImageJ software and is indicated below each panel. Data in (G) is represented as mean  $\pm$  SEM of  $n = 3$ . \* $P < 0.05$ , \*\* $P < 0.01$ , unpaired  $t$  test.

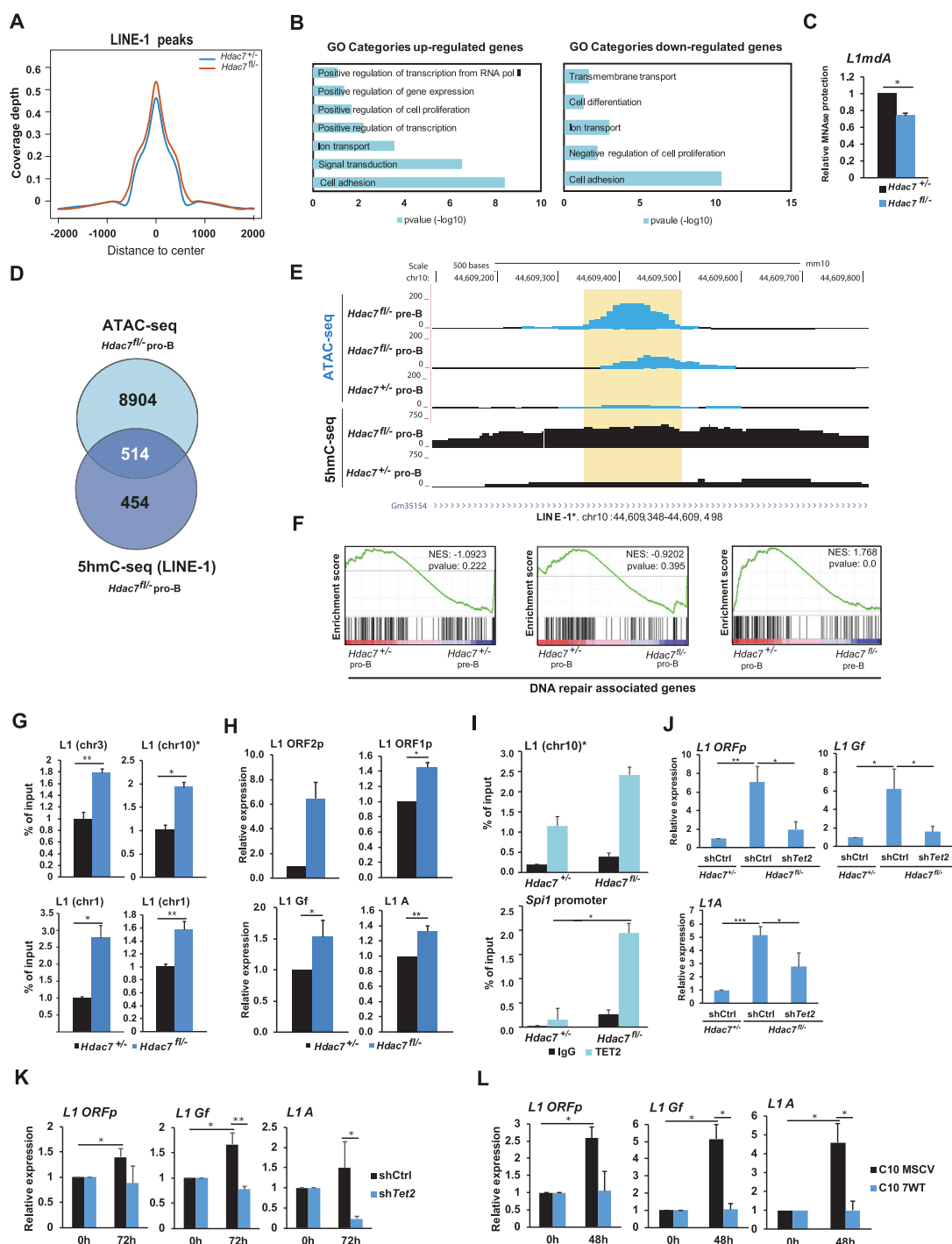


**Figure 6.** HDAC7 regulates 5-hydroxymethylation levels of transposable LINE-1 elements. (A) 5-hmC coverage depth (per base pair per peak per 10 million mapped reads) of 5-hmC peaks located in LINE-1 elements (−2 kb to +2 kb) in wild-type or HDAC7-deficient pro-B cells. (B) Gene Ontology (GO) enrichment analysis of genes associated to up-regulated (left panel) and down-regulated (right panel) regions in HDAC7-deficient pro-B cells respect to control pro-B cells in hMeDIP-seq shown in (A). (C) RT-qPCR showing protection of MNase-digested DNA at the 5min time point in wild-type or HDAC7-deficient B cells. (D) Venn diagram comparing enriched peaks associated genes in ATAC-seq from *Hdac7*<sup>fl/-</sup> pro-B cells and LINE-1 enriched peaks associated genes in 5hmC-seq (or hMeDIP-seq) in *Hdac7*<sup>fl/-</sup> pro-B cells compared to control cells. (E) Example of 5-hmC and ATAC-seq enrichment in young retrotransposon (L1) from peaks detected in hMeDIP-seq and ATAC-seq data. The peak location found common in the two omics analyses is located in the orange-shaded rectangle. (F) GSEA analysis comparing wild-type pre-B or HDAC7-deficient pre-B and pre-B cells to wild-type pro-B cells in expression profiles related to DNA repair signatures. DNA repair dataset was retrieved from [www.gsea-msigdb.org](http://www.gsea-msigdb.org). (G) hMeDIP-qPCR analysis of 5-hmC enrichment at LINE-1 retrotransposable elements in wild-type or HDAC7-deficient pro-B cells. (H) RT-qPCR analysis of the expression of proteins encoded by LINE-1 (ORFp1, ORFp2) and the most active L1 elements subfamilies (Gf, A) in wild-type or HDAC7-deficient pro-B cells. (I) ChIP-qPCR analysis of TET2 recruitment at hydroxymethylated L1 elements. TET2 enrichment at the *Spi1* promoter was used as a positive control. (J–L) As in Figure 4H–J, but analyzing the expression levels of L1 associated regions (L1 ORFp, L1 Gf and L1A). Data from (G–L) are represented as mean ± SEM of  $n = 3$ . \* $P < 0.05$ , \*\* $P < 0.01$ , \*\*\* $P < 0.001$ , unpaired  $t$  test.

TET2 was recruited to LINE-1 elements with enhanced 5-hmC in HDAC7-deficient pro-B cells; TET2 recruitment to the *Spil* promoter was used as a positive control (Figure 6I). Finally, using samples from the gain and loss of function experimental approaches shown in Figure 4H–J, we further demonstrated that HDAC7-mediated LINE-1 regulation depends on *Tet2* expression (Figure 6J–L). Overall, our data indicated that HDAC7 plays a role in preserving the chromatin state and genome integrity in B cells by restricting the expression levels of TET2, which consequently leads to the maintenance of physiological levels of 5-hmC at retrotransposon elements.

## DISCUSSION

Here we reveal an unprecedented HDAC7-mediated molecular mechanism that preserves the correct chromatin conformation, histone marks deposition and DNA 5-hydroxymethylation state. Notably, this state is essential for B cell identity and, consequently, for a correct gene expression pattern during early B cell development. HDAC7 deficiency resulted in a global chromatin de-compaction that significantly increased its accessibility. This correlated with a global increase of H3K27ac in the absence of HDAC7 from pro-B cells. Chromatin organization is dynamically reshaped during B cell development, obtaining unique populations at each differentiation stage (55); however, this process is highly controlled, and alterations in chromatin state (such as that observed here in HDAC7-deficient cells) can alter the transcriptional regulation and gene expression patterns, which can drive malignant transformation (56). In line with the increased chromatin accessibility, HDAC7 deficiency also caused a significant decrease in H3K9me3, a hallmark of heterochromatin state, which is involved in maintaining lineage stability and preventing cell reprogramming (47,57,58). TET enzymes are mainly recruited to open chromatin regions; therefore, euchromatin (unlike heterochromatin) is enriched in 5-hmC (49). HDAC7 deficiency results in a global decrease of heterochromatin regions and enhanced TET2 recruitment. It has been reported that TET2 loss at stem cell stages produced an aberrant number of myelomonocytic cells and impairment in the expression of macrophage markers such as Mac-1 in myeloid cells (20,22). Within the B cell lineage, TET2 conditional deficiency at pro-B cell stage does not cause any phenotype during development and differentiation. Only conditional deletion of both TET2 and TET3 lead to defective B cell development (52). Even though there is no phenotype observed by TET2 deficiency *in vivo*, TET2 has been reported to play a critical role in mediating the hydroxymethylation of cytosine residues from myeloid genes during pre-B cells conversion into macrophages (24,29). Despite loss of TET2 and TET3 leads to aberrant lymphocyte development and related disorders (59,60), and loss of TET2 enzymatic activity appears to mainly affect myelopoiesis (23,60), our results strongly suggest that HDAC7 is a critical factor that preserves B cell identity and correct DNA hydroxymethylation state via *Tet2* gene silencing.

Previous studies have established a close relationship between transcription regulators and dynamic changes in

DNA methylation during B cell development and commitment, specifically at the pro-B to pre-B cell transition (14,59). Hematopoietic cells present low hydroxymethylation levels (~0.2%) compared to other cell types, such as Purkinje cells or embryonic stem cells (~5%) (50,61). However, we observed a significant decrease of heterochromatin, and an increase in 5-hmC, upon HDAC7 deficiency, leading to several molecular and biological consequences. First, we found a high percentage of 5-hmC peaks located in intergenic and distal promoter regions. These results may imply that distal regulatory regions with enhancer features are dependent on TET2-mediated DNA demethylation and may correlate with the presence of additional mechanisms that control DNA methylation status at promoter-associated regions (62,63). *Jun* and *Fosl2* were found among the myeloid and T cell genes with increased 5-hmC levels in HDAC7-deficient B cells. *Fosl2* is a TET2-activated gene during the transdifferentiation of pre-B cells to macrophages (24), and *Jun* undergoes enhancer demethylation prior to B cell being reprogrammed into induced pluripotent stem cells (iPSCs) (64). The finding that lineage-inappropriate genes are already marked with 5-hmC in B cell progenitors supports the notion that they may be epigenetically poised in early stages of development.

HDAC7 deficiency also led to differential 5-hmC levels in some regions containing miRNAs. miRNAs are epigenetic players that have crucial roles in multiple developmental processes, and their de-regulation is involved in many biological disorders. Recent studies have demonstrated that miRNAs have a role in normal and malignant B cell development, by modulating the expression of key regulatory genes (65–67). For instance, miR-34a is strongly expressed in myeloid cells, and its constitutive expression in B cells blocks the pro-B to pre-B cell transition (26,68); notably, this is the biological effect that we observed upon HDAC7 deficiency. miR-150, which is down-regulated in pro-B cells from *Hdac7*-null mice, is related to B cell development and performs tumor-suppressor functions in leukemic cells. miR-142 and miR-181 are highly expressed in a cell-specific manner (69), such as in hematopoietic cells. Specifically, B cell function is impaired in miR-142 deficiency conditions (67), and miR181a regulates positively the B lymphocyte differentiation (70). Previous studies indicated that miR-126 is downregulated in lymphoid cells, (71,72), which is consistent with our results. Moreover, miR-29b is activated by C/EBP $\alpha$  and represses *Tet2* expression, which concurs with C/EBP $\alpha$  and *Tet2* up-regulation when HDAC7 is deficient (73). miR-34a is strongly expressed in myeloid cells, and its constitutive expression in B cells blocks the pro-B to pre-B cell transition (68). Finally, some members of the miR-99 family, such as miR-99b, are abundant in macrophages, neutrophils, and monocytes. Here, we observed that another member of the family related to leukemic stem cells, miR-99a, was upregulated in HDAC7-deficient pro-B cells. Thus, our results demonstrate that HDAC7 can also exert its gene repressive function during early B cell development by regulating gene expression, presumably by interacting with its classical partner MEF2C, which may be recruited to miRNA regulatory regions, as it does at other specific miRNA regions in the skeletal muscle (74).



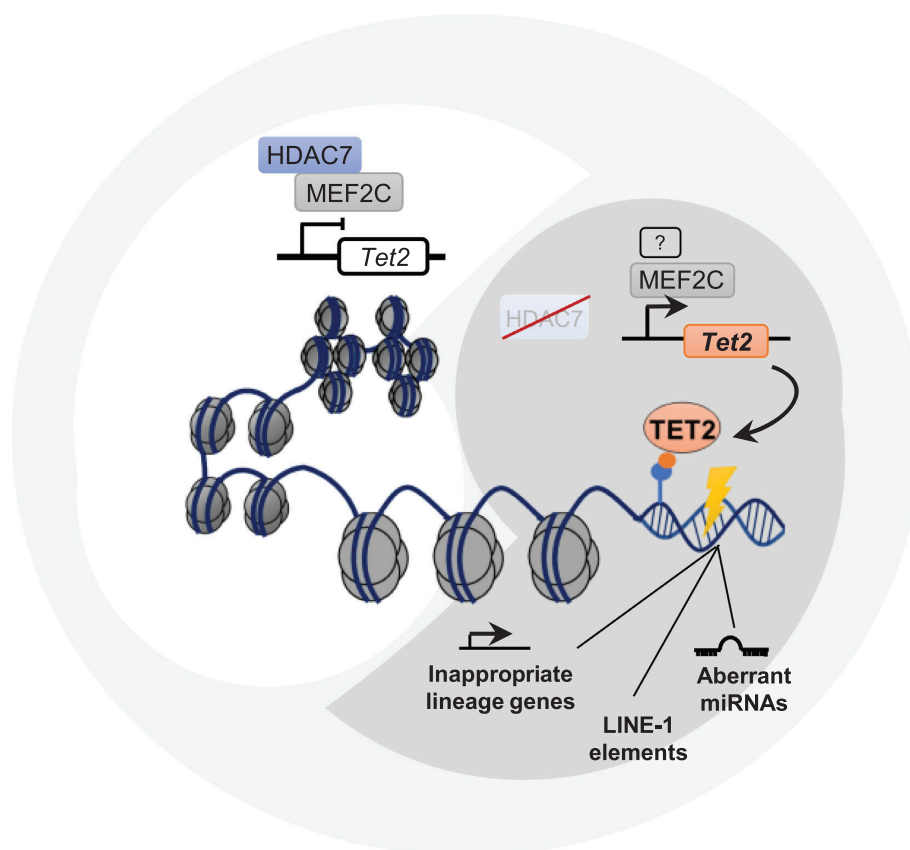


**Figure 7.** Visual representation summarizing the role of HDAC7–TET2 axis in the regulation of proper gene silencing in early B cell development.

We have detected increased 5-hmC enrichment and a more open chromatin state in some regions containing LINE-1 transposable elements in HDAC7-deficient pro-B cells. LINE-1 elements are the only active autonomous retrotransposons in the mammalian genome and, consequently, a potential disturber of chromatin stability (75). In fact, LINE-1 transcripts from the A and Gf sub-families, which present increased expression in HDAC7-deficient pro-B cells, contain some members that still have the full-length transcript, which maintains its retrotransposon activity in the mouse genome (76). The fact that increased 5-hmC is associated to TET2 recruitment suggests that HDAC7 might be required to preserve chromatin integrity by mediating the silenced status of LINE-1 elements. Of note, recent studies have shown that tight regulation of TET2 activity is essential for correct maintenance of genome stability: TET2 deficiency produces defects in DNA damage response, and its overexpression produces chromosome instability and aneuploidy due to a collapse in BER activity (77,78). Thus, results from this paper suggest that TET2 aberrant expression by HDAC7-deficient B cells may impair their capacity to repair DNA damage, which agree with the observed higher cell death rates in these cells that we reported in our previous published work (26).

Significant loss of H3K9me3 enrichment upon HDAC7 deficiency could also correlate with LINE-1 deregulated expression, since this heterochromatin mark is required to repress aberrant expression of retrotransposons in mammal

embryonic stem cells (79,80). However, given that DNA methylation is the main source of LINE-1 repression in more differentiated cells, we suggest that LINE-1 are silenced due to DNA demethylation caused by TET2 upregulation; this would reinforce the effects of DNA methylation loss following TET2 up-regulation upon HDAC7 deficiency. This result indicates that LINE-1 deregulation is produced as a consequence of HDAC7 deficiency.

Our results represent a significant step forward in our understanding of how B cells acquire their genetic identity, from three different perspectives. First, we identified HDAC7 as a chromatin modulator that regulates the heterochromatin state and histone marks deposition in early B cell development. Second, we demonstrated that HDAC7 is the specific transcription repressor that controls TET2 activity, which it achieves by fine-tuning its physiological expression levels in pro-B cells. This may represent the mechanistic explanation for the different TET2 expression levels observed in myeloid and lymphoid cells. Third, our results reveal an unexpected role for HDAC7 in controlling proper DNA 5-hydroxymethylation status and expression of lineage- or functionally-inappropriate genes, microRNAs, and non-coding elements (such as LINE-1 elements) in pro-B cells. We recently identified HDAC7 to be a novel biomarker and prognostic factor in infants (<1-year-olds) with pro-B acute lymphoblastic leukemia (pro-B-ALL) and MLL-AF4 rearrangement (27). This subgroup of pediatric patients presents an extremely adverse outcome, with sur-

vival rate below 35%, and the loss of HDAC7 is associated with a worse prognosis. Therefore, the elucidation of the exact molecular mechanisms that HDAC7 exert during physiological early B cell development will be crucial to understand how their deregulation can result in B cell-associated malignancies, with potential implications in the clinics.

Altogether, our findings lead us to a proposed model by which HDAC7 functions during early B cell development are not restricted to controlling expression by direct recruitment to its target genes. Rather, HDAC7 governs the expression of another crucial epigenetic regulator, TET2. The identified HDAC7–TET2 epigenetic axis is essential to preserve proper 5-hmC and histone marks levels, chromatin compaction, and expression of miRNAs and LINE-1 elements (Figure 7). We anticipate that our findings may open new avenues to understanding the consequences of HDAC7 deregulation in altering the molecular mechanism found in B cell-related malignancies, eventually leading to strategies to develop therapies for these pathologies.

#### DATA AVAILABILITY

Data are available in GEO repository as follows: RNA-seq (GSE171855), ATAC-seq (GSE204672), ChIP-seq (GSE204673) and hMeDIP-seq (GSE135263).

#### SUPPLEMENTARY DATA

Supplementary Data are available at NAR Online.

#### ACKNOWLEDGEMENTS

We thank CERCA Programme/Generalitat de Catalunya and the Josep Carreras Foundation for institutional support. We thank Dr Eric Olson (UT Southwestern Medical Center, Dallas, TX, USA) and Dr Michael Reth (Max Planck Institute of Immunology and Epigenetics, Freiburg, Germany) for kindly providing the *Hdac7<sup>loxP/-</sup>* and *mb1-Cre* mice, respectively. We thank Lucía Fanlo for her assistance in technical issues and bioinformatics analysis of ChIP-seq and ATAC-seq experiments. We thank Alberto Bueno for deep analysis of our RNA-seq and hMeDIP-seq data, in order to assess the presence of differentially expressed dsRNA species. We also thank Drs Pura Muñoz Cánoves and Tokameh Mahmoudi for helpful comments on the manuscript.

#### FUNDING

Spanish Ministry of Economy and Competitiveness (MINECO) [SAF2017-87990-R]; Spanish Ministry of Science and Innovation (MICINN) [EUR2019-103835]; Josep Carreras Leukaemia Research Institute (IJC, Badalona, Barcelona); IDIBELL Research Institute (L'Hospitalet de Llobregat, Barcelona); A.M. is funded by the Spanish Ministry of Science, Innovation and Universities, which is part of the Agencia Estatal de Investigación (AEI) [PRE2018-083183] (cofunded by the European Social Fund); OdB. was funded by a Juan de la Cierva Formación Fellowship from the Spanish Ministry of Science, Innovation and Universities [FJCI-2017-32430]; Postdoctoral Fellowship

from the Asociación Española Contra el Cáncer (AECC) Foundation [POSTD20024DEBA]; B.M. is awardee of the Ayudas para la formación del profesorado universitario [FPU18/00755, Ministerio de Universidades]; B.M.J. is funded by La Caixa Banking Foundation Junior Leader project [LCF/BQ/PI19/11690001]; FEDER/Spanish Ministry of Science and Innovation [RTI2018-094788-A-I00]; L.T.-D. is funded by the FPI Fellowship [PRE2019-088005]; L.R. is funded by an AGAUR FI fellowship [2019FI-B00017]; J.L.S. is funded by ISCIII [CP19/00176], co-funded by ESF, 'Investing in your future' and the Spanish Ministry of Science, Innovation and Universities [PID2019-111243RA-I00]. CRG acknowledge the support of the Spanish Ministry of Science and Innovation through the Centro de Excelencia Severo Ochoa (CEX2020-001049-S, MCIN/AEI /10.13039/501100011033). Funding for open access charge: Spanish Ministry of Science, Innovation and Universities (MICIU) [SAF2017-87990-R, EUR2019-103835].

*Conflict of interest statement.* None declared.

#### REFERENCES

- Nimmo, R.A., May, G.E. and Enver, T. (2015) Primed and ready: understanding lineage commitment through single cell analysis. *Trends Cell Biol.*, **25**, 459–467.
- Parra, M. (2009) Epigenetic events during b lymphocyte development. *Epigenetics*, **4**, 462–468.
- Ramírez, J., Lukin, K. and Hagman, J. (2010) From hematopoietic progenitors to b cells: mechanisms of lineage restriction and commitment. *Curr. Opin. Immunol.*, **22**, 177–184.
- Cobaleda, C., Schebesta, A., Delogu, A. and Busslinger, M. (2007) Pax5: the guardian of b cell identity and function. *Nat. Immunol.*, **8**, 463–470.
- Kwon, K., Hutter, C., Sun, Q., Bilic, I., Cobaleda, C., Malin, S. and Busslinger, M. (2008) Instructive role of the transcription factor E2A in early b lymphopoiesis and germinal center b cell development. *Immunity*, **28**, 751–762.
- Kong, N.R., Davis, M., Chai, L., Winoto, A. and Tjian, R. (2016) MEF2C and EBF1 co-regulate B cell-specific transcription. *PLoS Genet.*, **12**, e1005845.
- Ikawa, T., Kawamoto, H., Wright, L.Y.T. and Murre, C. (2004) Long-term cultured E2A-deficient hematopoietic progenitor cells are pluripotent. *Immunity*, **20**, 349–360.
- Nutt, S.L. and Kee, B.L. (2007) The transcriptional regulation of b cell lineage commitment. *Immunity*, **26**, 715–725.
- Pongubala, J.M.R., Northrup, D.L., Lancki, D.W., Medina, K.L., Treiber, T., Bertolino, E., Thomas, M., Grosschedl, R., Allman, D. and Singh, H. (2008) Transcription factor EBF restricts alternative lineage options and promotes b cell fate commitment independently of pax5. *Nat. Immunol.*, **9**, 203–215.
- Stehling-Sun, S., Dade, J., Nutt, S.L., DeKoter, R.P. and Camargo, F.D. (2009) Regulation of lymphoid versus myeloid fate 'choice' by the transcription factor *mef2c*. *Nat. Immunol.*, **10**, 289–296.
- Boller, S. and Grosschedl, R. (2014) The regulatory network of B-cell differentiation: a focused view of early B-cell factor 1 function. *Immunol. Rev.*, **261**, 102–115.
- Vilarrasa-Blasi, R., Soler-Vila, P., Verdaguier-Dot, N., Russiñol, N., Di Stefano, M., Chapaprieta, V., Clot, G., Farabella, I., Cuscó, P., Agirre, X. *et al.* (2021) Dynamics of genome architecture and chromatin function during human B cell differentiation and neoplastic transformation. *Nat. Commun.*, **12**, 651.
- Martin-Subero, J.I. and Oakes, C.C. (2018) Charting the dynamic epigenome during B-cell development. *Semin. Cancer Biol.*, **51**, 139–148.
- Benner, C., Isoda, T. and Murre, C. (2015) New roles for DNA cytosine modification, eRNA, anchors, and superanchors in developing b cell progenitors. *Proc. Natl. Acad. Sci. U.S.A.*, **112**, 12776–12781.

15. Almamun, M., Levinson, B.T., Gater, S.T., Schnabel, R.D., Arthur, G.L., Wade Davis, J. and Taylor, K.H. (2015) Genome-wide DNA methylation analysis in precursor B-cells. *Epigenetics*, **9**, 1588–1595.
16. Schuyler, R.P., Merkel, A., Raineri, E., Altucci, L., Vellenga, E., Martens, J.H.A., Pourfarzad, F., Kuijpers, T.W., Burden, F., Farrow, S. *et al.* (2016) Distinct trends of DNA methylation patterning in the innate and adaptive immune systems. *Cell Rep.*, **17**, 2101–2111.
17. Boller, S., Li, R. and Grosschedl, R. (2018) Defining b cell chromatin: lessons from EBF1. *Trends Genet.*, **34**, 257–269.
18. Azagra, A., Marina-Zárate, E., Ramiro, A.R., Javierre, B.M. and Parra, M. (2020) From loops to looks: transcription factors and chromatin organization shaping terminal b cell differentiation. *Trends Immunol.*, **41**, 46–60.
19. Wu, X., Li, G. and Xie, R. (2018) Decoding the role of TET family dioxygenases in lineage specification. *Epigenetics Chromatin*, **11**, 58.
20. Moran-Crusio, K., Reavie, L., Shih, A., Abdel-Wahab, O., Ndiaye-Lobry, D., Lobry, C., Figueroa, M.E., Vasanthakumar, A., Patel, J., Zhao, X. *et al.* (2011) Tet2 loss leads to increased hematopoietic stem cell self-renewal and myeloid transformation. *Cancer Cell*, **20**, 11–24.
21. Quivoron, C., Couronné, L., Della Valle, V., Lopez, C.K., Plo, I., Wagner-Ballon, O., Do Cruzeiro, M., Delhommeau, F., Arnulf, B., Stern, M.-H. *et al.* (2011) TET2 inactivation results in pleiotropic hematopoietic abnormalities in mouse and is a recurrent event during human lymphomagenesis. *Cancer Cell*, **20**, 25–38.
22. Ko, M., Bandukwala, H.S., An, J., Lamperti, E.D., Thompson, E.C., Hastie, R., Tsangaratos, A., Rajewsky, K., Koralov, S.B. and Rao, A. (2011) Ten-Eleven-Translocation 2 (TET2) negatively regulates homeostasis and differentiation of hematopoietic stem cells in mice. *Proc. Natl. Acad. Sci. U.S.A.*, **108**, 14566–14571.
23. Ko, M., Huang, Y., Jankowska, A.M., Pape, U.J., Tahiliani, M., Bandukwala, H.S., An, J., Lamperti, E.D., Koh, K.P., Ganetzky, R. *et al.* (2010) Impaired hydroxylation of 5-methylcytosine in myeloid cancers with mutant TET2. *Nature*, **468**, 839–843.
24. Kallin, E.M., Rodríguez-Ubrevia, J., Christensen, J., Cimmino, L., Aifantis, I., Helin, K., Ballestar, E. and Graf, T. (2012) Tet2 facilitates the depression of myeloid target genes during CEBP $\alpha$ -Induced transdifferentiation of Pre-B cells. *Mol. Cell*, **48**, 266–276.
25. Cull, A.H., Snetsinger, B., Buckstein, R., Wells, R.A. and Rauh, M.J. (2017) Tet2 restrains inflammatory gene expression in macrophages. *Exp. Hematol.*, **55**, 56–70.
26. Azagra, A., Román-González, L., Collazo, O., Rodríguez-Ubrevia, J., de Yébenes, V.G., Barneda-Zahonero, B., Rodríguez, J., Castro de Moura, M., Grego-Bessa, J., Fernández-Duran, I. *et al.* (2016) In vivo conditional deletion of HDAC7 reveals its requirement to establish proper b lymphocyte identity and development. *J. Exp. Med.*, **213**, 2591–2601.
27. de Barrios, O., Galaras, A., Trincado, J.L., Azagra, A., Collazo, O., Meler, A., Agraz-Doblas, A., Bueno, C., Ballerini, P., Cazzaniga, G. *et al.* (2021) HDAC7 is a major contributor in the pathogenesis of infant t(4;11) proB acute lymphoblastic leukemia. *Leukemia*, **35**, 2086–2091.
28. Chang, S., Young, B.D., Li, S., Qi, X., Richardson, J.A. and Olson, E.N. (2006) Histone deacetylase 7 maintains vascular integrity by repressing matrix metalloproteinase 10. *Cell*, **126**, 321–334.
29. Bussmann, L.H., Schubert, A., Vu Manh, T.P., De Andres, L., Desbordes, S.C., Parra, M., Zimmermann, T., Rapino, F., Rodríguez-Ubrevia, J., Ballestar, E. *et al.* (2009) A robust and highly efficient immune cell reprogramming system. *Cell Stem Cell*, **5**, 554–566.
30. Barneda-Zahonero, B., Román-González, L., Collazo, O., Rafati, H., Islam, A.B.M.M.K., Bussmann, L.H., di Tullio, A., De Andres, L., Graf, T., López-Bigas, N. *et al.* (2013) HDAC7 is a repressor of myeloid genes whose downregulation is required for transdifferentiation of Pre-B cells into macrophages. *PLoS Genet.*, **9**, e1003503.
31. Figueroa, M.E., Abdel-Wahab, O., Lu, C., Ward, P.S., Patel, J., Shih, A., Li, Y., Bhagwat, N., Vasanthakumar, A., Fernandez, H.F. *et al.* (2010) Leukemic IDH1 and IDH2 mutations result in a hypermethylation phenotype, disrupt TET2 function, and impair hematopoietic differentiation. *Cancer Cell*, **18**, 553–567.
32. Anders, S. and Huber, W. (2010) Differential expression analysis for sequence count data. *Genome Biol.*, **11**, R106.
33. Anders, S., Pyl, P.T. and Huber, W. (2015) HTSeq-A python framework to work with high-throughput sequencing data. *Bioinformatics*, **31**, 166–169.
34. Subramanian, A., Tamayo, P., Mootha, V.K., Mukherjee, S., Ebert, B.L., Gillette, M.A., Paulovich, A., Pomeroy, S.L., Golub, T.R., Lander, E.S. *et al.* (2005) Gene set enrichment analysis: a knowledge-based approach for interpreting genome-wide expression profiles. *Proc. Natl. Acad. Sci. U.S.A.*, **102**, 15545–15550.
35. Vazquez, B.N., Thackray, J.K., Simonet, N.G., Chahar, S., Kane-Goldsmith, N., Newkirk, S.J., Lee, S., Xing, J., Verzi, M.P., An, W. *et al.* (2019) SIRT7 mediates L1 elements transcriptional repression and their association with the nuclear lamina. *Nucleic Acids Res.*, **47**, 7870–7885.
36. Langmead, B., Trapnell, C., Pop, M. and Salzberg, S.L. (2009) Ultrafast and memory-efficient alignment of short DNA sequences to the human genome. *Genome Biol.*, **10**, R25.
37. Zhang, Y., Liu, T., Meyer, C.A., Eeckhoute, J., Johnson, D.S., Bernstein, B.E., Nussbaum, C., Myers, R.M., Brown, M., Li, W. *et al.* (2008) Model-based analysis of chip-Seq (MACS). *Genome Biol.*, **9**, R137.
38. Ramírez, F., Ryan, D.P., Grüning, B., Bhardwaj, V., Kilpert, F., Richter, A.S., Heyne, S., Dündar, F. and Manke, T. (2016) deepTools2: a next generation web server for deep-seq data analysis. *Nucleic Acids Res.*, **44**, W160–W165.
39. Buenrostro, J.D., Giresi, P.G., Zaba, L.C., Chang, H.Y. and Greenleaf, W.J. (2013) Transposition of native chromatin for fast and sensitive epigenomic profiling of open chromatin, DNA-binding proteins and nucleosome position. *Nat. Methods*, **10**, 1213–1218.
40. Ewels, P., Magnusson, M., Lundin, S. and Käller, M. (2016) MultiQC: summarize analysis results for multiple tools and samples in a single report. *Bioinformatics*, **32**, 3047–3048.
41. Bolger, A.M., Lohse, M. and Usadel, B. (2014) Trimmomatic: a flexible trimmer for illumina sequence data. *Bioinformatics*, **30**, 2114–2120.
42. Thierion, E., Le Men, J., Collombet, S., Hernandez, C., Couplier, F., Torbey, P., Thomas-Chollier, M., Noordermeer, D., Charnay, P. and Gilardi-Hebenstreit, P. (2017) Krox20 hindbrain regulation incorporates multiple modes of cooperation between cis-acting elements. *PLoS Genet.*, **13**, e1006903.
43. Love, M.I., Huber, W. and Anders, S. (2014) Moderated estimation of fold change and dispersion for RNA-seq data with DESeq2. *Genome Biol.*, **15**, 550.
44. Irizarry, R.A., Hobbs, B., Collin, F., Beazer-Barclay, Y.D., Antonellis, K.J., Scherf, U. and Speed, T.P. (2003) Exploration, normalization, and summaries of high density oligonucleotide array probe level data. *Biostatistics*, **4**, 249–264.
45. Painter, M.W., Davis, S., Hardy, R.R., Mathis, D., Benoist, C. and Immunological Genome Project Consortium. and Immunological Genome Project Consortium. (2011) Transcriptomes of the b and t lineages compared by multiplatform microarray profiling. *J. Immunol.*, **186**, 3047–3057.
46. Jovic, V., Shay, T., Sylvania, K., Zuk, O., Sun, X., Kang, J., Regev, A., Koller, D., Best, A.J., Knell, J. *et al.* (2013) Identification of transcriptional regulators in the mouse immune system. *Nat. Immunol.*, **14**, 633–643.
47. Nicetto, D. and Zaret, K.S. (2019) Role of H3K9me3 heterochromatin in cell identity establishment and maintenance. *Curr. Opin. Genet. Dev.*, **55**, 1–10.
48. Izzo, F., Lee, S.C., Poran, A., Chaligne, R., Gaiti, F., Gross, B., Murali, R.R., Deochand, S.D., Ang, C., Jones, P.W. *et al.* (2020) DNA methylation disruption reshapes the hematopoietic differentiation landscape. *Nat. Genet.*, **52**, 378–387.
49. Kubiura, M., Okano, M., Kimura, H., Kawamura, F. and Tada, M. (2012) Chromosome-wide regulation of euchromatin-specific 5mC to 5hmC conversion in mouse ES cells and female human somatic cells. *Chromosom. Res.*, **20**, 837–848.
50. Ficz, G., Branco, M.R., Seisenberger, S., Santos, F., Krueger, F., Hore, T.A., Marques, C.J., Andrews, S. and Reik, W. (2011) Dynamic regulation of 5-hydroxymethylcytosine in mouse ES cells and during differentiation. *Nature*, **473**, 398–402.
51. de la Rica, L., Rodríguez-Ubrevia, J., García, M., Islam, A.B., Urquiza, J.M., Hernando, H., Christensen, J., Helin, K., Gómez-Vaquero, C. and Ballestar, E. (2013) PU.1 target genes undergo Tet2-coupled demethylation and DNMT3b-mediated

- methylation in monocyte-to-osteoclast differentiation. *Genome Biol.*, **14**, R99.
52. Lio, C.-W., Zhang, J., González-Avalos, E., Hogan, P.G., Chang, X. and Rao, A. (2016) Tet2 and tet3 cooperate with B-lineage transcription factors to regulate DNA modification and chromatin accessibility. *Elife*, **5**: e18290.
  53. Chaudhuri, A.A., So, A.Y.-L., Mehta, A., Minisandram, A., Sinha, N., Jonsson, V.D., Rao, D.S., O'Connell, R.M. and Baltimore, D. (2012) Oncomir miR-125b regulates hematopoiesis by targeting the gene *lin28A*. *Proc. Natl. Acad. Sci. U.S.A.*, **109**, 4233–4238.
  54. de la Rica, L., Deniz, Ö., Cheng, K.C.L., Todd, C.D., Cruz, C., Houseley, J. and Branco, M.R. (2016) TET-dependent regulation of retrotransposable elements in mouse embryonic stem cells. *Genome Biol.*, **17**, 234.
  55. Schoonhoven, A. van, Huylebroeck, D., Hendriks, R.W. and Stadhouders, R. (2020) 3D genome organization during lymphocyte development and activation. *Brief. Funct. Genomics*, **19**, 71–82.
  56. Vilarrasa-Blasi, R., Soler-Vila, P., Verdaguer-Dot, N., Russiñol, N., Di Stefano, M., Chapaprieta, V., Clot, G., Farabella, L., Cuscó, P., Kulis, M. *et al.* (2021) Dynamics of genome architecture and chromatin function during human b cell differentiation and neoplastic transformation. *Nat. Commun.*, **12**, 651.
  57. Becker, J.S., Nicetto, D. and Zaret, K.S. (2016) H3K9me3-Dependent heterochromatin: barrier to cell fate changes. *Trends Genet.*, **32**, 29–41.
  58. Allan, R.S., Zueva, E., Cammas, F., Schreiber, H.A., Masson, V., Belz, G.T., Roche, D., Maison, C., Quivy, J.-P., Almouzni, G. *et al.* (2012) An epigenetic silencing pathway controlling t helper 2 cell lineage commitment. *Nature*, **487**, 249–253.
  59. Orlanski, S., Labi, V., Reizel, Y., Spiro, A., Lichtenstein, M., Levin-Klein, R., Korolov, S.B., Skversky, Y., Rajewsky, K., Cedar, H. *et al.* (2016) Tissue-specific DNA demethylation is required for proper B-cell differentiation and function. *Proc. Natl. Acad. Sci. U.S.A.*, **113**, 5018–5023.
  60. Ito, K., Lee, J., Chrysanthou, S., Zhao, Y., Josephs, K., Sato, H., Teruya-Feldstein, J., Zheng, D., Dawlaty, M.M. and Ito, K. (2019) Non-catalytic roles of tet2 are essential to regulate hematopoietic stem and progenitor cell homeostasis. *Cell Rep.*, **28**, 2480–2490.
  61. Kriaucionis, S. and Heintz, N. (2009) The nuclear DNA base 5-Hydroxymethylcytosine is present in purkinje neurons and the brain. *Science*, **324**, 929–930.
  62. Rasmussen, K.D. and Helin, K. (2016) Role of TET enzymes in DNA methylation, development, and cancer. *Genes Dev.*, **30**, 733–750.
  63. Rasmussen, K.D., Berest, I., Keßler, S., Nishimura, K., Simón-Carrasco, L., Vassiliou, G.S., Pedersen, M.T., Christensen, J., Zaugg, J.B. and Helin, K. (2019) TET2 binding to enhancers facilitates transcription factor recruitment in hematopoietic cells. *Genome Res.*, **29**, 564–575.
  64. Sardina, J.L., Collombet, S., Tian, T.V., Gómez, A., Di Stefano, B., Berenguer, C., Brumbaugh, J., Stadhouders, R., Segura-Morales, C., Gut, M. *et al.* (2018) Transcription factors drive tet2-mediated enhancer demethylation to reprogram cell fate. *Cell Stem Cell*, **23**, 727–741.
  65. Zhang, J., Jima, D.D., Jacobs, C., Fischer, R., Gottwein, E., Huang, G., Lugar, P.L., Lagoo, A.S., Rizzieri, D.A., Friedman, D.R. *et al.* (2009) Patterns of microRNA expression characterize stages of human B-cell differentiation. *Blood*, **113**, 4586.
  66. Chen, C.-Z., Li, L., Lodish, H.F. and Bartel, D.P. (2004) MicroRNAs modulate hematopoietic lineage differentiation. *Science*, **303**, 83–86.
  67. Zheng, B., Xi, Z., Liu, R., Yin, W., Sui, Z., Ren, B., Miller, H., Gong, Q. and Liu, C. (2018) The function of microRNAs in B-cell development, lymphoma, and their potential in clinical practice. *Front. Immunol.*, **9**, 936.
  68. Rao, D.S., O'Connell, R.M., Chaudhuri, A.A., Garcia-Flores, Y., Geiger, T.L. and Baltimore, D. (2010) MicroRNA-34a perturbs b lymphocyte development by repressing the forkhead box transcription factor *foxp1*. *Immunity*, **33**, 48–59.
  69. Landgraf, P., Rusu, M., Sheridan, R., Sewer, A., Iovino, N., Aravin, A., Pfeffer, S., Rice, A., Kamphorst, A.O., Landthaler, M. *et al.* (2007) A mammalian microRNA expression atlas based on small RNA library sequencing. *Cell*, **129**, 1401–1414.
  70. Li, J., Wan, Y., Ji, Q., Fang, Y. and Wu, Y. (2013) The role of microRNAs in B-cell development and function. *Cell. Mol. Immunol.*, **10**, 107–112.
  71. Lechman, E.R., Gentner, B., Ng, S.W.K., Schoof, E.M., van Galen, P., Kennedy, J.A., Nucera, S., Ciceri, F., Kaufmann, K.B., Takayama, N. *et al.* (2016) miR-126 regulates distinct self-renewal outcomes in normal and malignant hematopoietic stem cells. *Cancer Cell*, **29**, 214–228.
  72. Petriv, O.I., Kuchenbauer, F., Delaney, A.D., Lecault, V., White, A., Kent, D., Marmolejo, L., Heuser, M., Berg, T., Copley, M. *et al.* (2010) Comprehensive microRNA expression profiling of the hematopoietic hierarchy. *Proc. Natl. Acad. Sci. U.S.A.*, **107**, 15443–15448.
  73. Amodio, N., Rossi, M., Raimondi, L., Pitari, M.R., Botta, C., Tagliaferri, P. and Tassone, P. (2015) miR-29s: a family of epi-miRNAs with therapeutic implications in hematologic malignancies. *Oncotarget*, **6**, 12837–12861.
  74. Liu, N., Williams, A.H., Kim, Y., McAnally, J., Bezprozvannaya, S., Sutherland, L.B., Richardson, J.A., Bassel-Duby, R. and Olson, E.N. (2007) An intragenic MEF2-dependent enhancer directs muscle-specific expression of microRNAs 1 and 133. *Proc. Natl. Acad. Sci. U.S.A.*, **104**, 20844–20849.
  75. Richardson, S.R., Doucet, A.J., Kopera, H.C., Moldovan, J.B., Garcia-Perez, J.L. and Moran, J.V. (2015) The influence of LINE-1 and SINE retrotransposons on mammalian genomes. *Microbiol. Spectr.*, **3**, MDNA3-0061-2014.
  76. Goodier, J.L., Ostertag, E.M., Du, K. and Kazazian, H.H. (2001) A novel active L1 retrotransposon subfamily in the mouse. *Genome Res.*, **11**, 1677–1685.
  77. Kafer, G.R., Li, X., Horii, T., Suetake, I., Tajima, S., Hatada, I. and Carlton, P.M. (2016) 5-Hydroxymethylcytosine Marks sites of DNA damage and promotes genome stability. *Cell Rep.*, **14**, 1283–1292.
  78. Mahfoudhi, E., Talhaoui, I., Cabagnols, X., Della Valle, V., Secardin, L., Rameau, P., Bernard, O.A., Ishchenko, A.A., Abbes, S., Vainchenker, W. *et al.* (2016) TET2-mediated 5-hydroxymethylcytosine induces genetic instability and mutagenesis. *DNA Repair (Amst)*, **43**, 78–88.
  79. Bulut-Karlıoglu, A., De, L.a., Rosa-Velázquez, I.A., Ramirez, F., Barenboim, M., Onishi-Seebacher, M., Arand, J., Galán, C., Winter, G.E., Engist, B. *et al.* (2014) Suv39h-Dependent H3K9me3 marks intact retrotransposons and silences LINE elements in mouse embryonic stem cells. *Mol. Cell*, **55**, 277–290.
  80. Kato, M., Takemoto, K. and Shinkai, Y. (2018) A somatic role for the histone methyltransferase *setdb1* in endogenous retrovirus silencing. *Nat. Commun.*, **9**, 1683.

## **Supplementary Information**

### **The HDAC7-TET2 epigenetic axis is essential during early B lymphocyte development**

**Alba Azagra, Ainara Meler, Oriol de Barrios, Laureano Tomás-Daza, Olga Collazo, Beatriz Monterde, Mireia Obiols, Llorenç Rovirosa, Maria Vila-Casadesús, Mónica Cabrera-Pasadas, Mar Gusi-Vives, Thomas Graf, Ignacio Varela, José Luis Sardina, Biola M Javierre, and Maribel Parra**

## Supplementary Figure Legends

### Supplementary Figure 1. HDAC7 deficiency results in global chromatin decondensation and increase 5-hmC levels

(A) Flow cytometry plots showing the gating strategy to sort pro-B (IgM<sup>-</sup>, CD19<sup>+</sup>, B220<sup>-</sup>, CD43<sup>+</sup>) and pre-B cells (IgM<sup>-</sup>, CD19<sup>+</sup>, B220<sup>-</sup>, CD43<sup>-</sup>) from the bone marrow of control and *Hdac7<sup>fl/-</sup>* conditional mice. (B) Schematic representation of up-regulated and down-regulated genes between different cell types and conditions of the RNA sequencing experiment in Figures 1B-E. (C) Heat map showing most down-regulated genes in *Hdac7<sup>fl/-</sup>* pro-B and pre-B cells compared to control cells (left panel). Absolute expression of *Igkv4-40*, *Igkv4-55* and *Igkv4-57-1* genes in HDAC7-deficient pro-B and pre-B cells versus control counterpart cells, using data from RNA-seq (right panel). Quantification values shown are expressed in FPKM values. (D) Gene ontology (GO) analysis of down-regulated genes in HDAC7 deficient pro-B and pre-B cells versus control pro-B cells. (E) BP ontology analysis of up-regulated genes in HDAC7-deficient pro-B and pre-B cells compared to control pro-B cells. (F) MF ontology analysis of up-regulated genes in HDAC7-deficient pro-B and pre-B cells compared to control pro-B cells. MF and BP correspond to Molecular Function and Biological Process, respectively.

### Supplementary Figure 2. HDAC7 controls DNA 5-hmC through *Tet2* regulation in pro-B and pre-B cells.

(A) *Tet1* and *Tet3* expression profiles in hematopoietic cells subsets. Data were obtained from the Immunological Genome Project (Immgen) database. (B) Heat map showing the expression of *Hdac7*, *Tet1*, *Tet2* and *Tet3* in different hematopoietic cell types. Data was obtained from Immgen database using “My Gene set” tool. (C) Analysis by RT-qPCR of *Tet1*, *Tet2* and *Tet3* mRNA levels in bone marrow from wild-type and HDAC7-deficient pro-B cells and in Cd11b<sup>+</sup> cells. (D) RNA-seq signal profiles for *Pax5* gene of HDAC7-deficient pro-B and pre-B cells, and control pro-B cells. Orange shadow highlights *Pax5* promoter region. (E) Analysis by RT-qPCR of *E2a* and *Pax5* genes in pro-B and pre-B cells from wild-type and HDAC7-deficient mice. (F) As in (E), but for *Hdac4*, *Hdac5* and *Hdac9* genes. Data from panels C, E and F are represented as mean of n=3 ± SEM; unpaired t test were used to determine significance (\*p<0.05, \*\*p<0.01).

### Supplementary Figure 3. *Tet2* is a direct HDAC7 target gene in pro-B and pre-B cells

(A) ATAC-seq signal profile of HDAC7-deficient and control pro-B cells over the transcription factor *Pax5* genomic sequence. (B) Venn Diagram comparing genes enriched in H3K9/K14ac ChIP-seq epigenetic mark and genes detected as open regions by ATAC-seq in *Hdac7<sup>fl/-</sup>* pro-B cells compared to control pro-B cells. *Tet2* is included among the subset of overlapping genes. (C) Depth coverage of H3K27ac peaks signal in all regions from ChIP-sequencing experiments in Figures 3D-E. (D) Genomic distribution of H3K27ac enriched peaks in *Hdac7<sup>+/-</sup>* and *Hdac7<sup>fl/-</sup>* pro-B cells determined by ChIP-seq experiments in Figures 3D-E. (E) Venn Diagram comparing genes enriched in H3K27ac epigenetic mark and genes detected as open regions by ATAC-seq in *Hdac7<sup>fl/-</sup>* pro-B cells compared to control pro-B cells. (F) Depth coverage of H3K27me3 peaks signal in all regions from ChIP-sequencing experiments in Figures 3F-G. (G) As in (D), but with gene regions enriched for H3K27me3 epigenetic mark. (H) Venn Diagram comparing genes enriched in H3K27me3 epigenetic mark from wild-type pro-B cells and genes detected as open regions by ATAC-seq in *Hdac7<sup>fl/-</sup>* pro-B cells compared to control pro-B cells. (H) H3K27ac and H3K27me3 ChIP-seq signal profile of HDAC7-deficient and control pro-B cells over the transcription factor

*Pax5* genomic sequence. (I) ChIP-qPCR data after immunoprecipitation with H3K9me3 antibody. Enrichment of *Tet2* promoter (left panel) and *Tet2* enhancer (right panel) regions is quantified as % of input. Data is represented as mean  $\pm$  SEM of n = 3. \*p < 0.05, unpaired T-test.

#### **Supplementary Figure 4. HDAC7 deficiency results in increased recruitment of TET2 and altered 5-hmC enrichment at B cell lineage inappropriate genes**

(A) Depth coverage of 5-hmC peaks signal in intergenic and promoter (TSS) regions from 5-hmC-sequencing experiments in Figures 4A-C. (B) Genome browser snapshot of 5-hmC peaks, ATAC-seq peaks and RNA-seq peaks at *FosB* promoter in wild-type pro-B and HDAC7-deficient pro-B and pre-B cells. (C) Analysis by RT-qPCR of inappropriate lineage genes *FosL2* and *FosB* in wild-type pro-B cells and HDAC7-deficient pro-B and pre-B cells. (D) RNA-seq signal profile of HDAC7-deficient pro-B and pre-B and control pro-B cells of *Itgb2* and *Cd69* genes. (E) Analysis of TET2 recruitment at other targets such as *FosI2*, *Ahnak* and *Itgb2* genes by ChIP-qPCR, quantified as % of input. (F) Schematic representation of the three experimental approaches used in gain and loss of function experiments in Figures 4H-J. Approach 1 uses primary pro-B cells from *Hdac7<sup>+/-</sup>* and *Hdac7<sup>fl/-</sup>* mice and approaches 2 and 3 use pre-B cell lines that transdifferentiate into macrophages upon  $\beta$ -estradiol treatment. Blue lines indicate the effects caused by the inhibition of *Tet2* expression through sh*Tet2* retroviral infection or HDAC7 induction by MSCV-7WT infection. TF=transcription factor. Data in panel (D) is represented as mean  $\pm$  SEM of n = 3. \*p < 0.05, unpaired T-test.

#### **Supplementary Figure 5. HDAC7 directs B cell-specific miRNA hydroxymethylation and expression patterns**

(A) Example of 5-hmC and open chromatin peaks enriched at aberrant miRNAs such as miR-29b and miR-99a from hMeDIP-seq and ATAC-seq experiments. (B) Example of 5-hmC and open chromatin enriched peaks at B-cell related miRNAs such as miR-150 and miR-181a from hMeDIP-seq and ATAC-seq experiments.

#### **Supplementary Figure 6. HDAC7 regulates 5-hydroxymethylation levels of transposable LINE-1 elements**

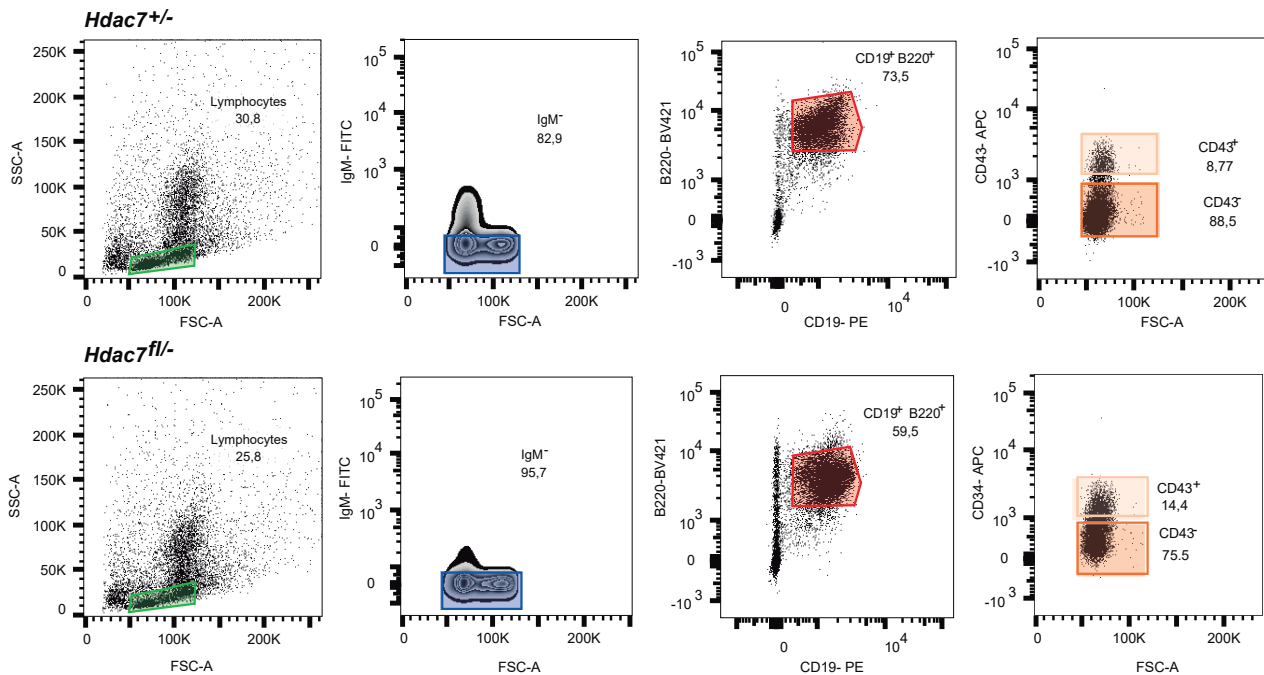
(A) Example of 5-hmC and open chromatin peaks enriched at LINE-1 associated regions from hMeDIP-seq and ATAC-seq experiments. (B) GO analysis of genes included in DNA repair geneset (from GSEA) that are down-regulated in *Hdac7<sup>fl/-</sup>* pro-B cells. (C) Table showing genes lists included in clusters from GO analysis from panel (B).

**Table S1.** Primer sequences used for RT-qPCR and ChIP qPCR experiments.

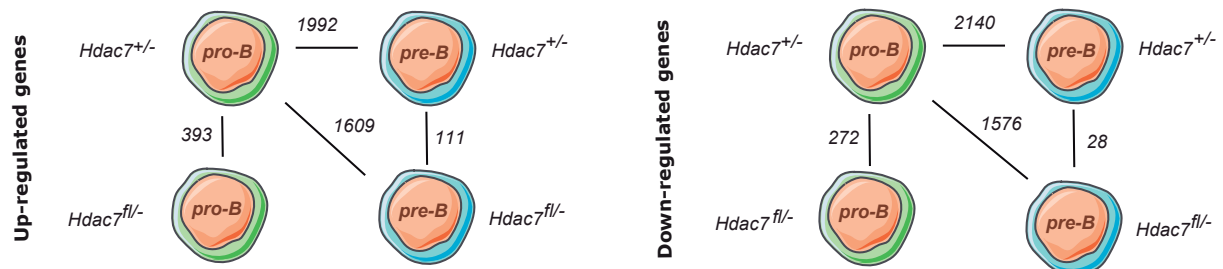
**Table S2.** Relative expression values of microRNAs showing differential expression profiles in control and *Hdac7<sup>fl/-</sup>* pro-B cells.

# Supplementary Figure 1

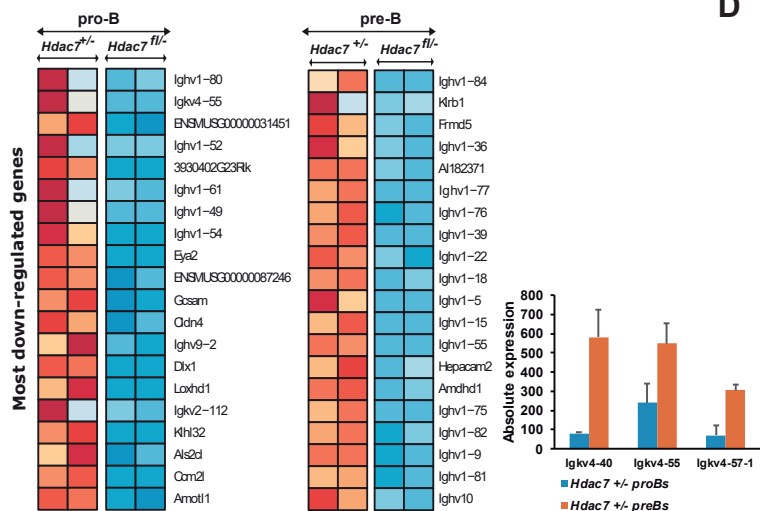
**A**



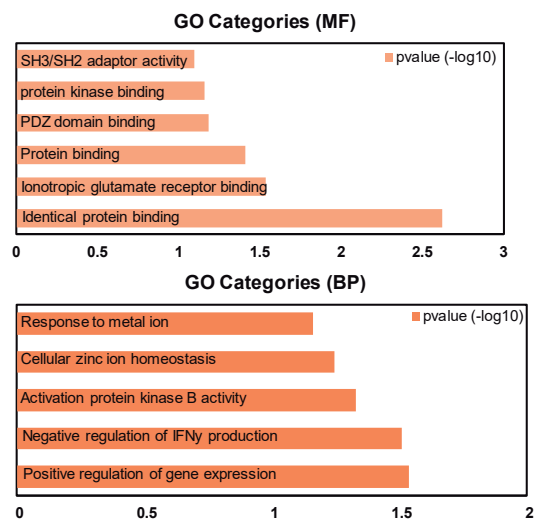
**B**



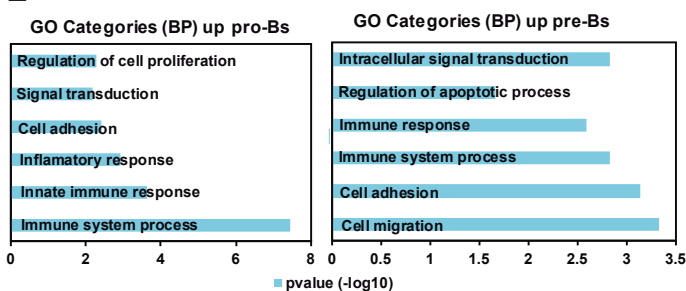
**C**



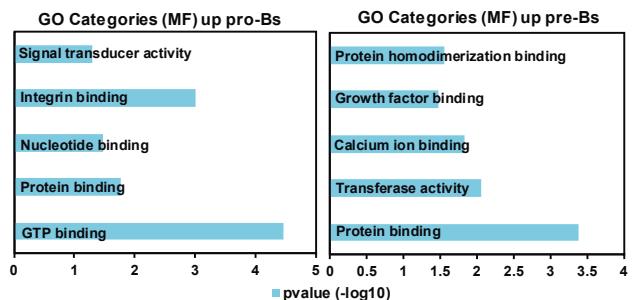
**D**



**E**

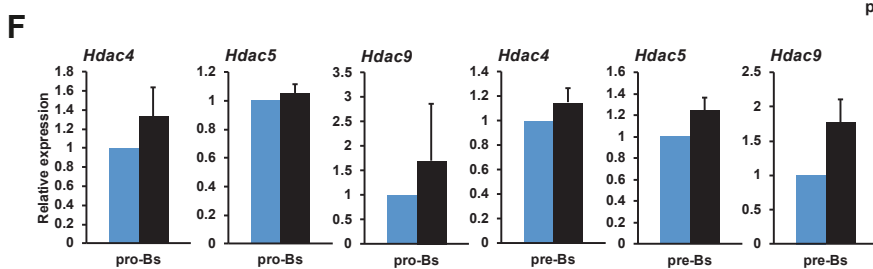
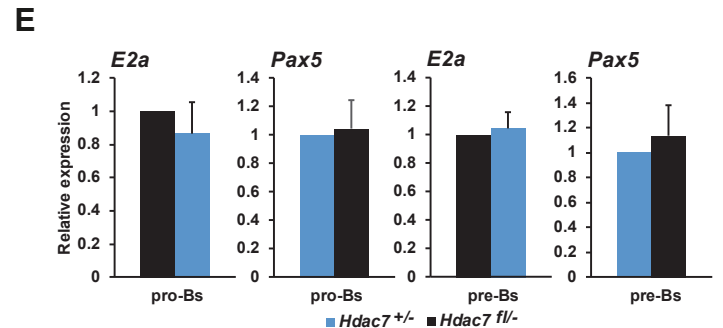
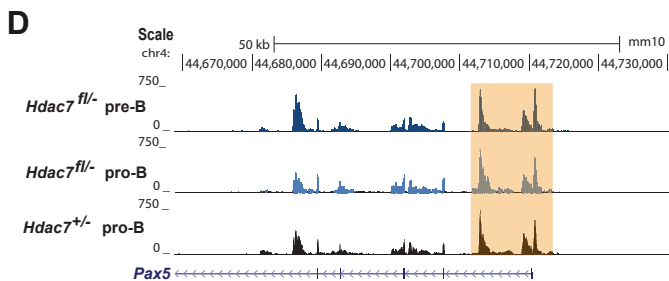
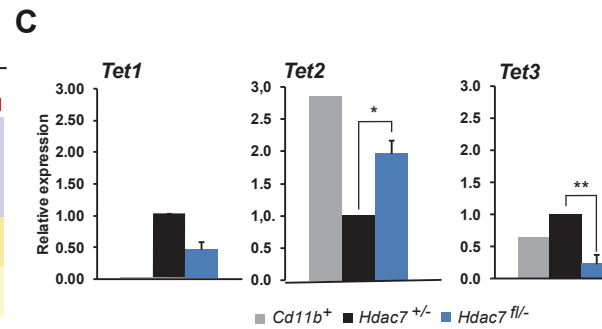
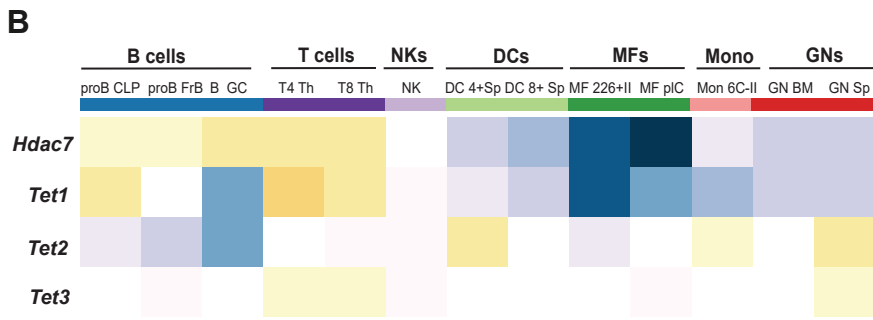
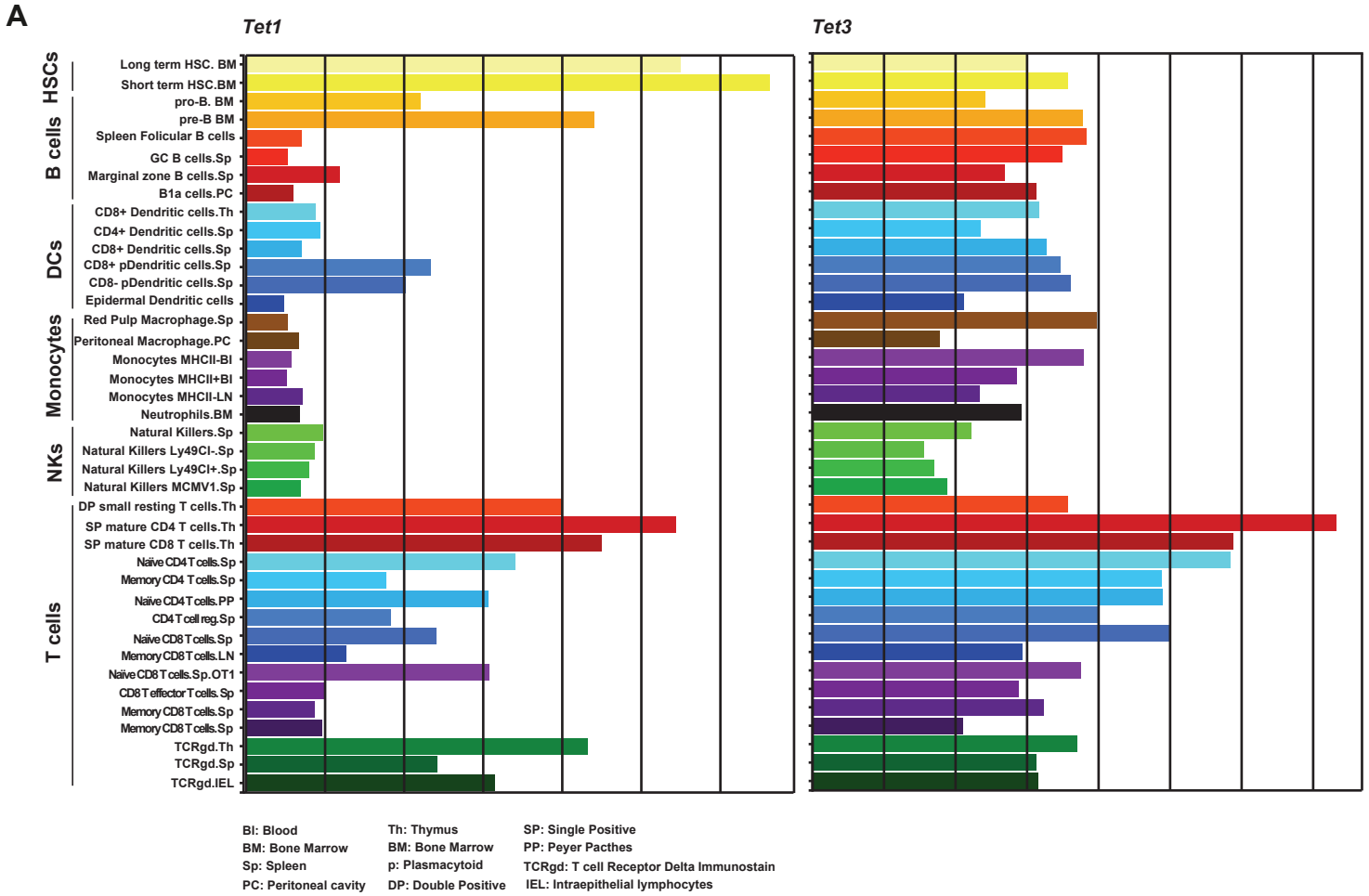


**F**

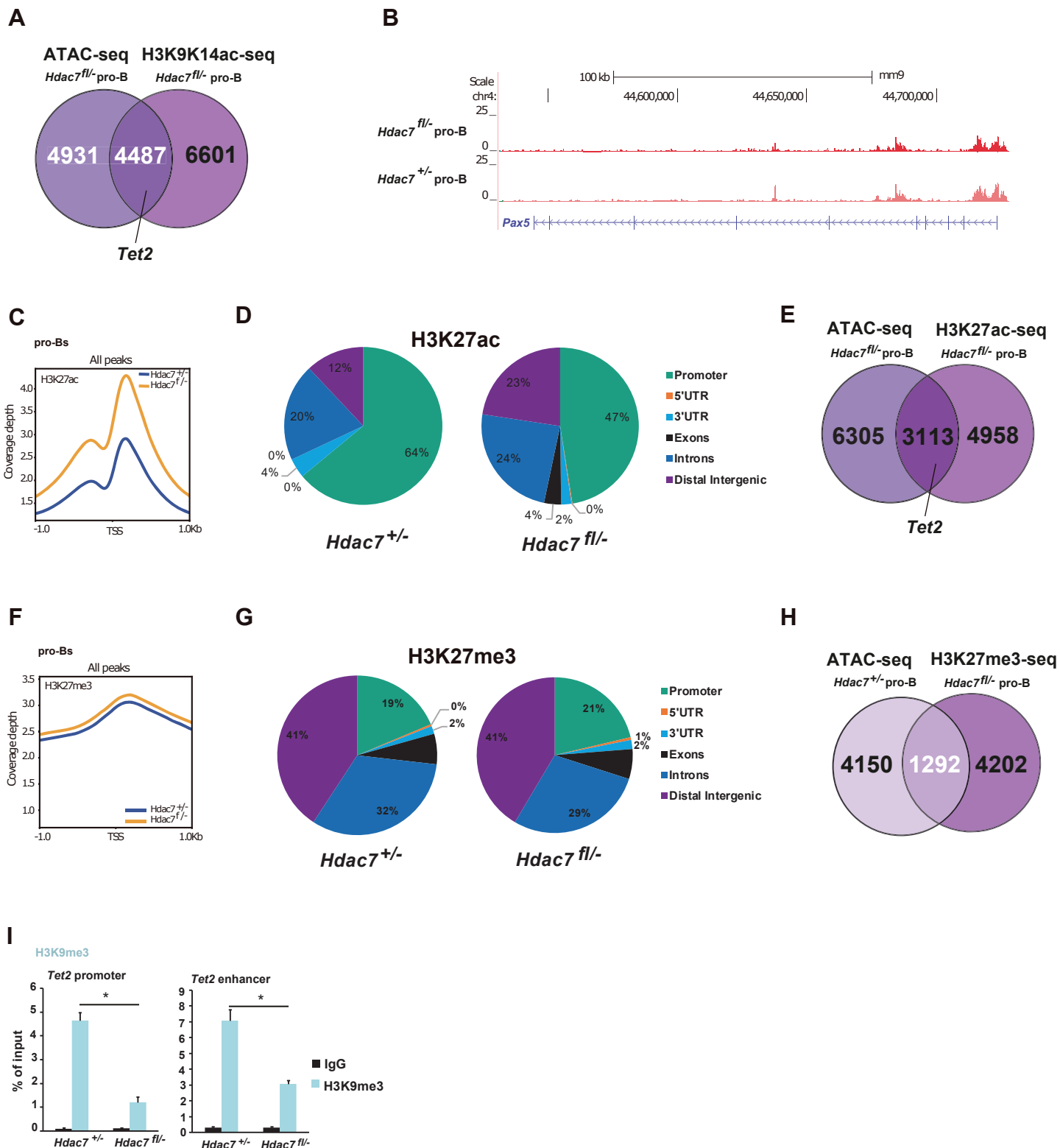




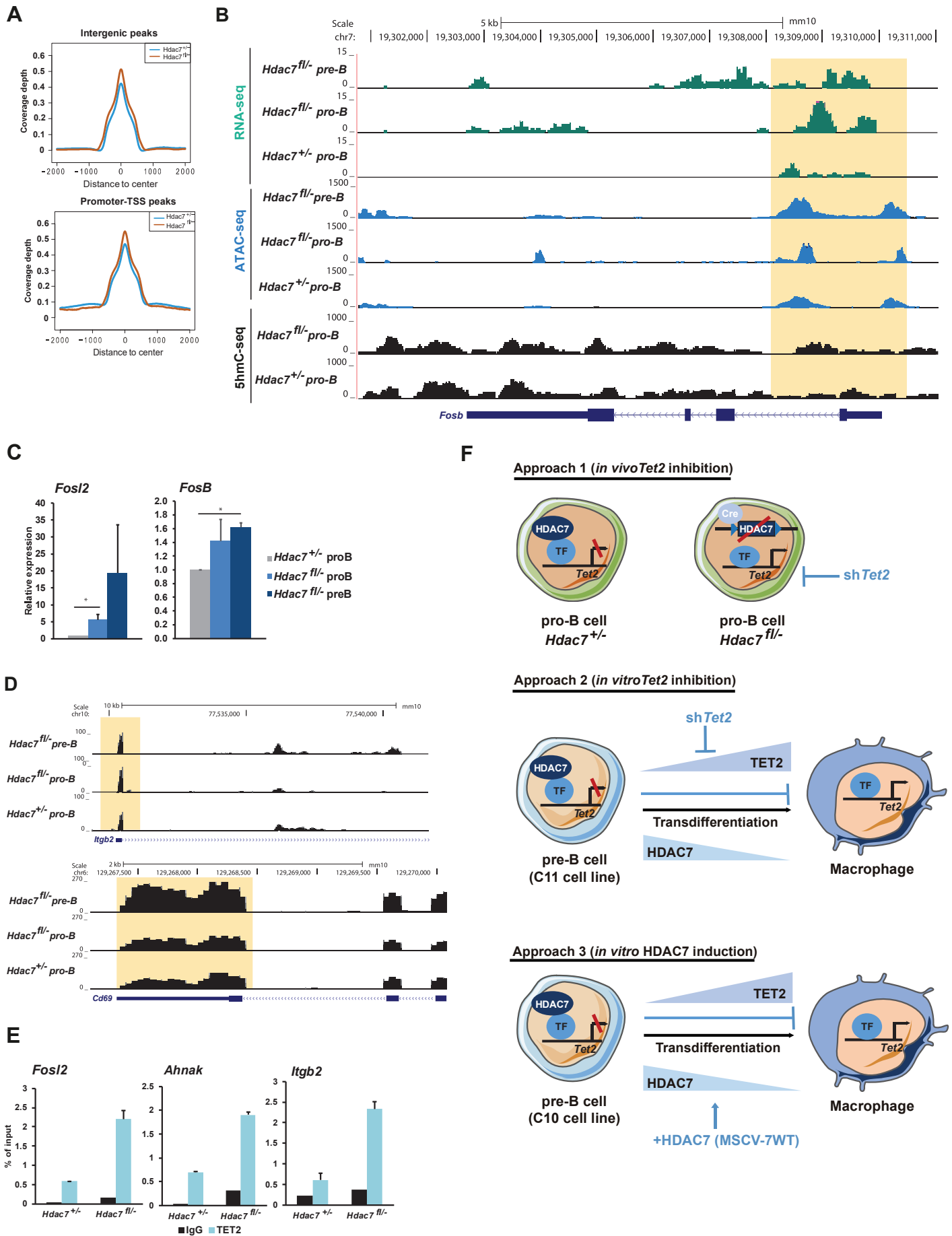
# Supplementary Figure 2



# Supplementary figure 3

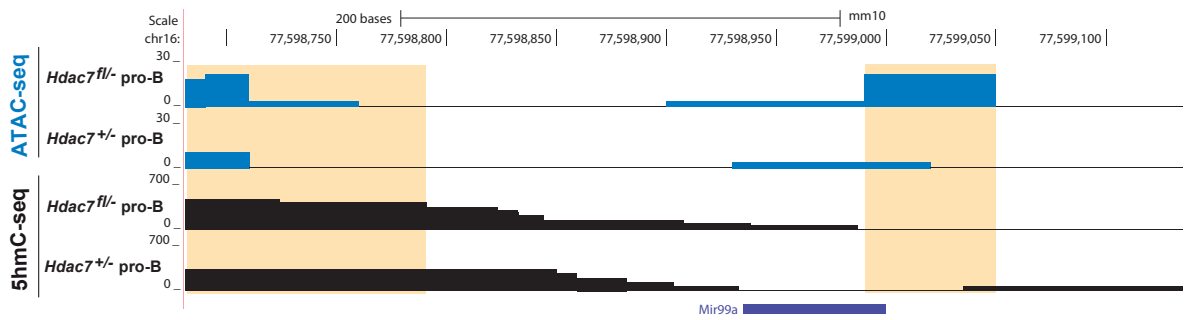
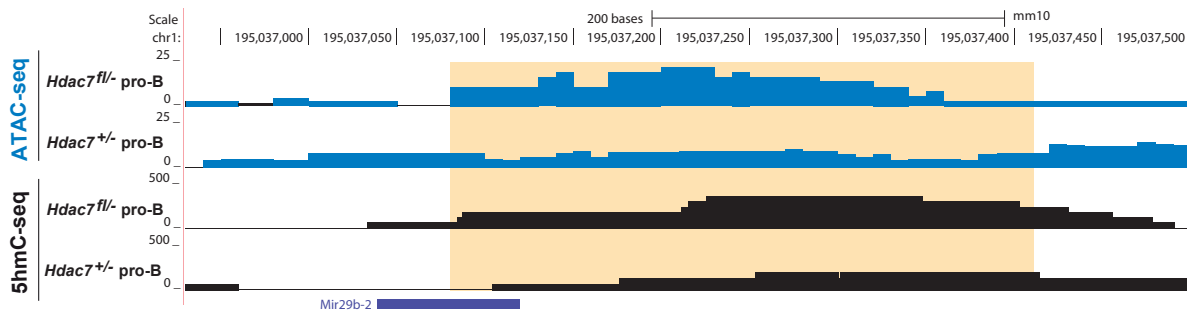


# Supplementary Figure 4

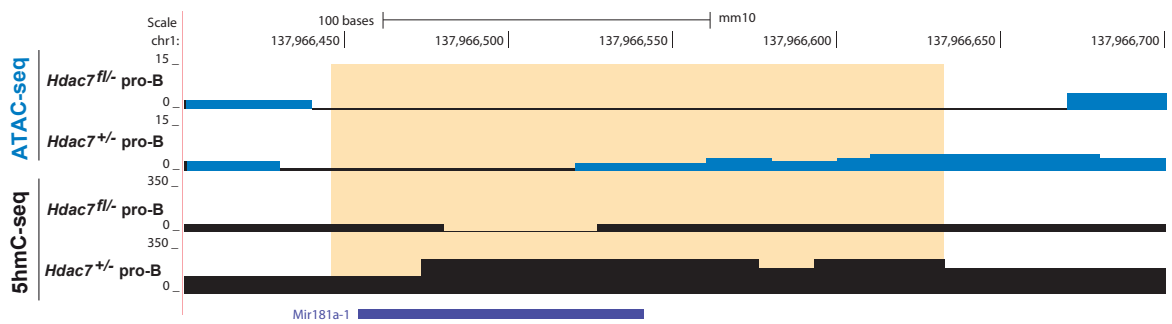
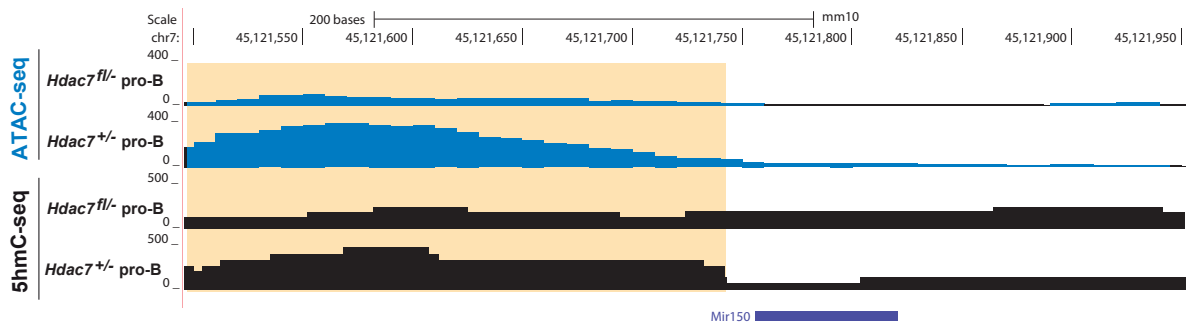


# Supplementary Figure 5

**A**

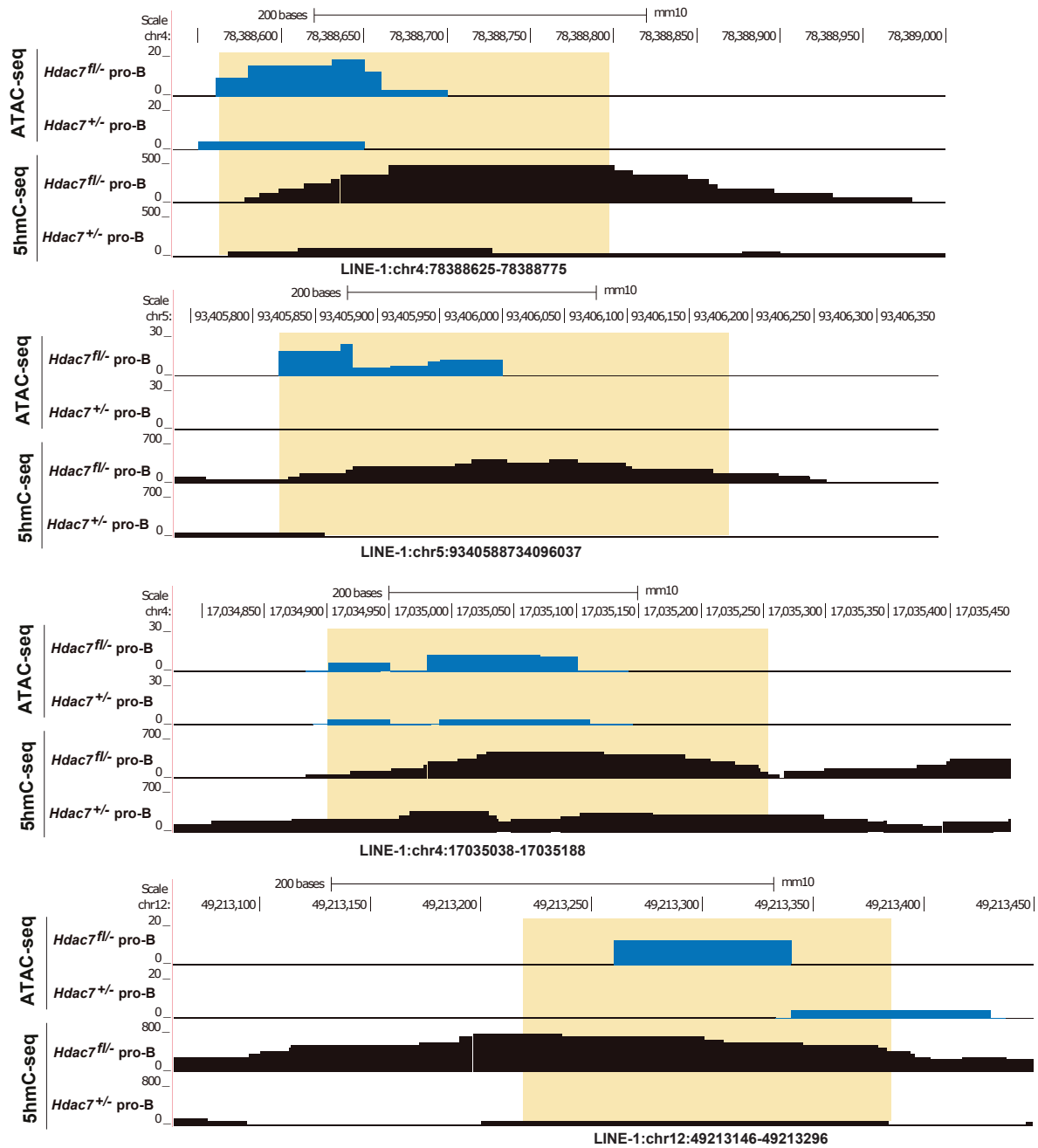


**B**



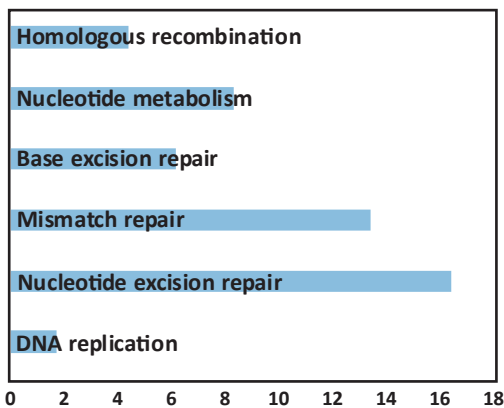
# Supplementary Figure 6

**A**



**B**

## GO analysis (KEGG pathways)



**C**

Nucleotide excision repair	Mismatch repair	Base excision repair	Cellular response to DNA damage
DDB1	LIG1	FEN1	RAD51
ERCC2	POLD1/3	LIG1	DDB1
ERCC8	PCNA	POLD1/3	ERCC2/5
GTF2H1/3	RCF3/4/5	POLL	FEN1
PCNA	RPA2/3	PCNA	GTF2H1/3
LIG1			POLD1
POLD1/3			POLL
RFC3/4/5			POLH
RPA2/3			PCNA
			SSRP1

**Table S1- primer sequences**

Name	Sequence	Purpose	Source
Tet1 RTqPCR Fw	ACAAGCAGATGGCTCCAGTT	Real time qPCR	Kallin et al, Moll Cell 2012
Tet1 RTqPCR Rv	GCAACAGGTGACACCAGAGA	Real time qPCR	Kallin et al, Moll Cell 2012
Tet2 RTqPCR Fw	ATCCAAACCGAAGCTGAATG	Real time qPCR	Kallin et al, Moll Cell 2012
Tet2 RTqPCR Rv	CTTGCCCTACCACCGTTTTTA	Real time qPCR	Kallin et al, Moll Cell 2012
Tet3 RTqPCR Fw	TCCGGATTGAGAAGGTCATC	Real time qPCR	Kallin et al, Moll Cell 2012
Tet3 RTqPCR Rv	TCCTCCAGTGTGTCTTCG	Real time qPCR	Kallin et al, Moll Cell 2012
Pax5 RTqPCR Fw	GCCTGGGAGTGAATTTTCTGGA	Real time qPCR	This paper
Pax5 RTqPCR Rv	GGGCTGCAGGGCTGTAATAGTAT	Real time qPCR	This paper
E2a RTqPCR Fw	AGGAAATCGCATCAGTAGCC	Real time qPCR	This paper
E2a RTqPCR Rv	AGGGACAGCACCTCATCTGT	Real time qPCR	This paper
Gapdh RTqPCR Fw	ACATCTCACTCAAGATTGTCAGCA	Real time qPCR	Dawlaty et al, Develop Cell 2014
Gapdh RTqPCR Rv	ATGGCATGGACTGTGGTCAT	Real time qPCR	Dawlaty et al, Develop Cell 2014
FosL2 RTqPCR Fw	TGGAGTGATCAAGACCATCG	Real time qPCR	Kallin et al, Moll Cell 2012
FosL2 RTqPCR Rv	GTTTCTCTCCCTCCGGATTC	Real time qPCR	Kallin et al, Moll Cell 2012
Jun RTqPCR Fw	ACGACCTTCTACGACGATGC	Real time qPCR	Kim et al, PNAS 2013
Jun RTqPCR Rv	CCAGGTTCAAGGTCATGCTC	Real time qPCR	Kim et al, PNAS 2013
L1-ORFp1 RTqPCR Fw	ACTCAAAGCGAGGCAACACTAGA	Real time qPCR	de la Rica et al, Genome Biol 2016
L1-ORFp1 RTqPCR Rv	GTTCCAGATTTCTTTCCTAGGGTTTC	Real time qPCR	de la Rica et al, Genome Biol 2016
L1MdGf RTqPCR Fw	TGGAATACAGAGTGCCAGCC	Real time qPCR	de la Rica et al, Genome Biol 2016
L1MdGf RTqPCR Rv	GTGCTCTCACCGGAAGGTG	Real time qPCR	de la Rica et al, Genome Biol 2016
L1MdA RTqPCR Fw	TCTGGTGAGTGGAACACAGC	Real time qPCR	de la Rica et al, Genome Biol 2016
L1MdA RTqPCR Rv	AGTCTCGAGTGGAGCGGAAG	Real time qPCR	de la Rica et al, Genome Biol 2016
miR-125b-5p Fw	GCAGTCCCTGAGACCCT	Real time qPCR	miRprimer ( <a href="https://sourceforge.net/projects/mirprimer/">https://sourceforge.net/projects/mirprimer/</a> )
miR-125b-5p Rv	CGAGTTTTTTTTTTTTTTTTCACAAGT	Real time qPCR	miRprimer software (same source)
miR-34a-5p Fw	GCAGTGGCAGTGTCTTAG	Real time qPCR	miRprimer software (same source)
miR-34a-5p Rv	GGTCCAGTTTTTTTTTTTTTTTACAAC	Real time qPCR	miRprimer software (same source)
miR-28a Fw	CAGAAGGAGCTCACAGTCT	Real time qPCR	miRprimer software (same source)
miR-28a Rv	GGTCCAGTTTTTTTTTTTTTTTCTCA	Real time qPCR	miRprimer software (same source)
miR-150-5p Fw	CTCCAACCCTGTACCA	Real time qPCR	miRprimer software (same source)
miR-150-5p Rv	GGTCCAGTTTTTTTTTTTTTTTCACT	Real time qPCR	miRprimer software (same source)
miR-142-3p Fw	CGAGTGTAGTGTTCCT	Real time qPCR	miRprimer software (same source)
miR-142-3p Rv	GGTCCAGTTTTTTTTTTTTTTTCCA	Real time qPCR	miRprimer software (same source)
miR-181a-5p Fw	CATTCAACGCTGTGGT	Real time qPCR	miRprimer software (same source)
miR-181a-5p Rv	GGTCCAGTTTTTTTTTTTTTTTACTCA	Real time qPCR	miRprimer software (same source)
Hdac4 Fw	GCCATCTGTGATGCTTCTGA	Real time qPCR	This paper
Hdac4 Rv	ATTGGCATTGGGTCTCTGAT	Real time qPCR	This paper
Hdac5 Fw	AGCCATGGGATTCTGCTTCT	Real time qPCR	This paper
Hdac5 Rv	AGTCCACGATGAGGACCTTG	Real time qPCR	This paper
Hdac9 Fw	CCCCTATGGGAGATGTTGAG	Real time qPCR	This paper
Hdac9 Rv	CAATGCATCAAATCCAGCAG	Real time qPCR	This paper
Tet2-promoter ChIP Fw	CAAGCTTGAGGCTGGGAGAA	ChIP-qPCR	This paper
Tet2-promoter ChIP Rv	CAGTCAGGCTGCTATCGAGT	ChIP-qPCR	This paper
Tet2-enhancer ChIP Fw	CTGAGAGCATCTCCAGGTC	ChIP-qPCR	This paper
Tet2-enhancer ChIP Rv	GGAGTGAGGCAATACCAGGA	ChIP-qPCR	This paper

**Table S1- primer sequences**

L1-chr10-ChIP Fw	GTTGACCCCGTGTCAGTCTT	ChIP-qPCR	This paper
L1-chr10-ChIP Rv	GGCGACCTCAACTGAATGAT	ChIP-qPCR	This paper
Spi1 promoter ChIP Fw	GTAGCGCAAGAGATTTATGCAAAC	ChIP-qPCR	This paper
Spi1 promoter ChIP Rv	GCACAAGTTCCTGATTTTATCGAA	ChIP-qPCR	This paper
miR-125b-Tet2-ChIP Fw	TTCCCAAGCTGTCCGTTTAC	ChIP-qPCR	This paper
miR-125b-Tet2-ChIP Rv	TGGTGGTTTATGCCGAGAAT	ChIP-qPCR	This paper
miR-34a-Tet2-ChIP Fw	AGCCTCTCCATCTTCCTGTG	ChIP-qPCR	This paper
miR-34a-Tet2-ChIP Rv	CGTTGCTGACCTCTGACCTT	ChIP-qPCR	This paper
Jun ChIP Fw	GAGGTTGGGGGCTACTTTTC	ChIP-qPCR	This paper
Jun ChIP Rv	TGTCCTGCCAGTGTTTGTA	ChIP-qPCR	This paper
Itgb2 ChIP Fw	CTACAAGCCCCTCCCTCTCT	ChIP-qPCR	Kallin et al, Moll Cell 2012
Itgb2 ChIP Rv	CCCAGGAGGAAGTTGAGTGA	ChIP-qPCR	Kallin et al, Moll Cell 2012
Jun 5hmC Fw	AAAGTCTGCCGCCAATAG	hMeDIP-qPCR	This paper
Jun 5hmC Rv	GAACTTGACTGGTTGCGACA	hMeDIP-qPCR	This paper
Fosl2 5hmC Fw	GGAGCTTGAGAGCAGAAAC	hMeDIP-qPCR	Kallin et al, Moll Cell 2012
Fosl2 5hmC Rv	CCTAACCAAGGCAGACAGGA	hMeDIP-qPCR	Kallin et al, Moll Cell 2012
L1 chr3 5hmC Fw	TTGTGCTTTTTCTTGGGCTA	hMeDIP-qPCR	This paper
L1 chr3 5hmC Rv	AGTTTTCCCTCCCTCTGCTC	hMeDIP-qPCR	This paper
L1 chr10 5hmC Fw	AAACCCACAGAATTGGAACG	hMeDIP-qPCR	This paper
L1 chr10 5hmC Rv	CCTCGTCTTTTCCTTCACTTTG	hMeDIP-qPCR	This paper
L1 chr1 5hmC Fw	AGCCTCCTTGATGTTCTCTT	hMeDIP-qPCR	This paper
L1 chr1 5hmC Rv	TGAGAGCACAAACACTAAGCAA	hMeDIP-qPCR	This paper
$\beta$ -globin Fw	AAGGTATGAGAATCCAGGCAG	MNAse, qPCR	Vazquez et al, Nucleic Acids Res 2019
$\beta$ -globin Rv	GCCAAAACAATCACCAGCAC	MNAse, qPCR	Vazquez et al, Nucleic Acids Res 2019
L1mdA Fw	CAAACCCCTTCCACTCCACTCGAGC	MNAse, qPCR	Vazquez et al, Nucleic Acids Res 2019
L1mdA Rv	CCTTCGCCATCTGGTAATC	MNAse, qPCR	Vazquez et al, Nucleic Acids Res 2019

**Table S2. Relative expression values of microRNAs showing differential expression profiles in control and *Hdac7*<sup>fl/-</sup> pro-B cells.**

miRNA Name	Wt1	Wt2	Ko1	Ko2	Mean Wt	Mean Ko	FC	Log2FC
mmu-miR-141-3p	0.03518	0.05	0.01914	0.02	0.04394	0.02011	2.18	1.13
mmu-miR-150-5p	3.95758	6.91	1.27930	1.42	5.43628	1.34796	4.03	2.01
mmu-miR-503-5p	3.14987	0.02	0.15820	0.00	1.58459	0.07981	19.85	4.31
mmu-miR-125p-5p	0.00243	0.01	0.02324	0.06	0.00708	0.04114	0.22	-2.18
mmu-mi125b-5pR-	0.00776	0.00	0.05818	0.08	0.00505	0.07002	0.07	-3.79
mmu-miR-126a-3p	0.01418	0.04	0.07275	0.17	0.02514	0.12053	0.21	-2.26
mmu-miR-196b-5p	0.00134	0.00	0.00777	0.02	0.00102	0.01587	0.06	-3.96
mmu-miR-214-3p	0.00050	0.00	0.01465	0.00	0.00047	0.00868	0.05	-4.20
mmu-miR-29b-5p	0.31845	0.55	1.93672	1.63	0.43660	1.78306	0.24	-2.03
mmu-miR-337-3p	0.00112	0.00	0.00075	0.03	0.00134	0.01552	0.09	-3.54
mmu-miR-34a-5p	0.00643	0.02	0.33496	0.13	0.01142	0.23492	0.05	-4.36
mmu-miR-465c-5p	0.00044	0.00	0.03096	0.07	0.00032	0.04874	0.01	-6.77
mmu-miR-466d-3p	0.01122	0.02	0.12842	0.35	0.01366	0.24153	0.07	-3.81
mmu-miR-667-3p	0.00199	0.00	0.00598	0.01	0.00166	0.00769	0.22	-2.21
mmu-miR-760-3p	0.00337	0.00	0.02158	0.02	0.00265	0.02143	0.12	-3.02
mmu-miR-99a-5p	0.00645	0.00	0.04043	0.07	0.00417	0.05587	0.07	-3.75



## **ARTICLE 2**

*“HDAC7 is a major contributor in the pathogenesis of infant t(4;11) proB acute lymphoblastic leukemia”*





Acute lymphoblastic leukemia

## HDAC7 is a major contributor in the pathogenesis of infant t(4;11) proB acute lymphoblastic leukemia

Oriol de Barrios<sup>1,2</sup> · Alexandros Galaras<sup>3,4</sup> · Juan L. Trincado<sup>5</sup> · Alba Azagra<sup>1,2</sup> · Olga Collazo<sup>1,2</sup> · Ainar Meler<sup>1,2</sup> · Antonio Agraz-Doblas<sup>5,6</sup> · Clara Bueno<sup>5</sup> · Paola Ballerini<sup>7</sup> · Giovanni Cazzaniga<sup>8</sup> · Ronald W. Stam<sup>9</sup> · Ignacio Varela<sup>6</sup> · Paola De Lorenzo<sup>8,10</sup> · Maria Grazia Valsecchi<sup>10</sup> · Pantelis Hatzis<sup>3</sup> · Pablo Menéndez<sup>5,11,12</sup> · Maribel Parra<sup>1,2</sup>

Received: 14 July 2020 / Accepted: 14 November 2020 / Published online: 1 December 2020  
© Springer Nature Limited 2020

### To the Editor:

Acute lymphoblastic leukemia derived from B-cell progenitors (proB ALL) is the most frequently diagnosed type

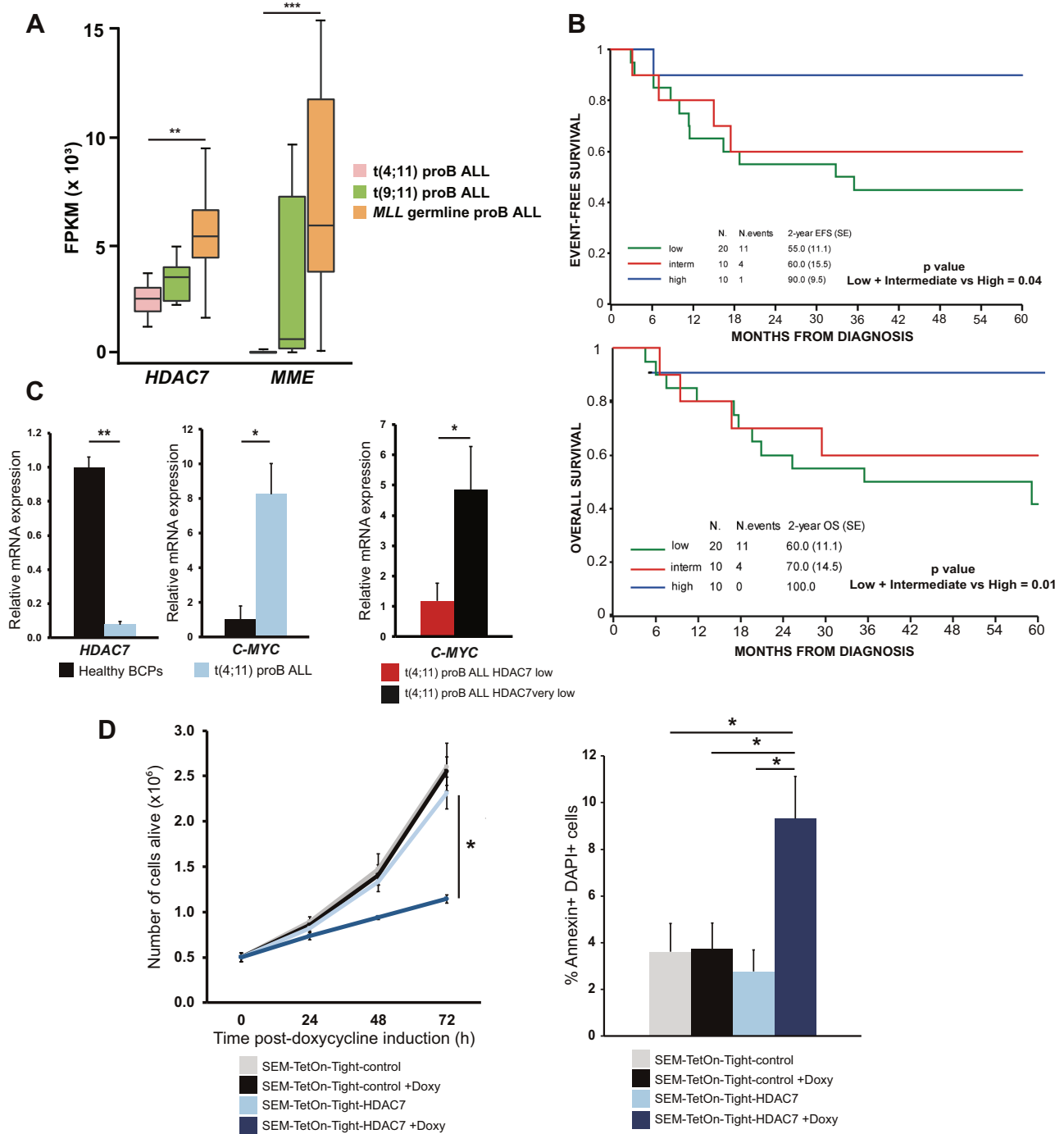
**Supplementary information** The online version of this article (<https://doi.org/10.1038/s41375-020-01097-x>) contains supplementary material, which is available to authorized users.

✉ Maribel Parra  
mparra@carrerasresearch.org

- 1 Lymphocyte Development and Disease Group, Josep Carreras Leukaemia Research Institute (IJC), Ctra. de Can Ruti, Camí de les Escoles, s/n, 08916 Badalona, Barcelona, Spain
- 2 Cellular Differentiation Group, Instituto de Investigación Biomédica de Bellvitge (IDIBELL), Barcelona, Spain
- 3 Biomedical Sciences Research Center “Alexander Fleming”, 16672 Vari, Greece
- 4 Department of Biochemistry and Biotechnology, University of Thessaly, Larissa, Greece
- 5 Josep Carreras Leukaemia Research Institute, School of Medicine, University of Barcelona, 08036 Barcelona, Spain
- 6 Instituto de Biomedicina y Biotecnología de Cantabria, Universidad de Cantabria-CSIC, Santander, Spain
- 7 Department of Pediatric Hematology, A. Trousseau Hospital, Paris, France
- 8 Centro Ricerca Tettamanti, Department of Pediatrics, University of Milano-Bicocca, Fondazione MBBM, Monza, Italy
- 9 Princess Maxima Center for Pediatric Oncology, Utrecht, The Netherlands
- 10 Interfant Trial Data Center, University of Milano-Bicocca, Monza, Italy
- 11 Institutió Catalana de Recerca i Estudis Avançats (ICREA), Barcelona, Spain
- 12 CIBER-ONC-ISCIII, Barcelona, Spain

of childhood cancer [1]. Current 5-year overall survival (OS) rates for pediatric B-ALL approach ~90%. However, proB ALL in infants (<1 year of age) is associated with an aggressive early clinical presentation, suboptimal response to chemotherapy and unfavorable clinical outcome [2]. Importantly, chromosomal rearrangements involving the mixed-lineage leukemia gene (*KMT2A*, also known as *MLL*) account for ~80% of proB ALL diagnoses [3], and clinical outcome of proB ALL infants with *MLL* rearrangements (*MLLr*), especially with t(4;11) translocation, is particularly dismal [4–6]. *MLLr* is an initiating oncogenic driver in proB ALL, occurring prenatally during fetal hematopoiesis [2, 7, 8]. This fact, coupled to a short latency, suggests that *MLLr* might suffice for leukemogenesis. In support of this hypothesis, genome-wide DNA sequencing of proB ALL infants has revealed a sparse mutational landscape [6], reinforcing the idea that *MLLr* proB ALL requires very few cooperating mutations to lead to overt leukemia.

The fine-tuned generation of distinct hematopoietic cell populations is of utmost relevance in leukemia research. There is increasing evidence that lymphocyte-specific transcription factors (TFs) not only induce B-cell-specific genes, but also repress lineage-specific or functionally inappropriate genes, ensuring the formation and identity of B lymphocytes [9]. The aberrant expression of and/or mutations in many of these TFs have been linked to the onset of hematopoietic malignancies [10]. Additionally, histone deacetylases (HDACs) have emerged as crucial transcriptional repressors at diverse stages of immune cells differentiation and, therefore, have been suggested as potential therapeutic candidates for proB ALL [11]. However, our understanding of how individual HDACs contribute to cancer is limited, partly because their contribution is not restricted to an overexpression context. Toward alleviating this, we have previously reported the role of HDAC7, a class IIa HDAC, in early B lymphocyte



development, where it silences lineage-inappropriate genes at the proB lymphocyte stage [12]. Here, we report HDAC7 as an important contributor to the pathogenesis of t(4;11) leukemia. It is strongly underexpressed in t(4;11) proB ALL infants and its low expression correlates with a significantly poorer clinical outcome. The identification of HDAC7 as a clinical prognostic marker for t(4;11) leukemia opens new therapeutic avenues in proB ALL.

We set out to assess whether HDAC7 expression was altered across 42 proB ALL infants, grouped according to

MLL status, into t(4;11) (n = 27), t(9;11) (n = 5), and MLL germline (n = 10), all homogeneously treated according to the interinfant protocol [6]. RNA-seq-based expression of HDAC7 in proB ALL infants was compared with that of healthy fetal liver B-cell progenitors (FL-BCP). RNA-seq profiling showed a significantly different expression in HDAC7 between t(4;11) patients and the other subgroups (Figs. 1A and S1). Overall, MLL germline patients presented with the highest HDAC7 levels, whereas t(4;11) patients presented with a dramatic underexpression of

**Fig. 1** *HDAC7* exerts a leukemia suppressive phenotype in t(4;11) proB ALL cells, and its absence associates with poor prognosis in proB ALL infants. **A** *HDAC7* is underexpressed in proB ALL infants harboring t(4;11) translocation. Boxplot from RNA-seq data for *HDAC7* and *MME* mRNA expression obtained from 27 t(4;11), 5 t(9;11) and 10 *MLL* germline proB ALL infants. *MME* gene expression was used as a control of proper differentiation of proB to preB cells. Data are expressed in Fragments Per Kilobase of exon per Million fragments mapped (FPKM). **B** *HDAC7* expression represents a clinical prognostic factor in proB ALL. For the Kaplan–Meier EFS (upper panel) and OS (lower panel) plots, the outcome of 40 patients illustrated in (A) was analyzed. Patients were assigned to one of the three groups according to the level of *HDAC7* expression: *HDAC7*<sup>high</sup> (blue line, with FPKM values above 4000), *HDAC7*<sup>intermediate</sup> (red line, FPKM values between 2600 and 4000), and *HDAC7*<sup>low</sup> (green line, FPKM values below 2600). The numbers of patients allocated to each group is indicated. **C** Low expression of *HDAC7* induces *c-MYC* oncogene in t(4;11) proB ALL patients. Left panel: qRT-PCR levels of *HDAC7* and *c-MYC* in an independent cohort of 29 t(4;11) proB ALL patients. Human FL-BCPs were used as a control. *GAPDH* and *RPL38* were used as housekeeping genes. Right panel: t(4;11) proB ALL patients with the lowest levels of *HDAC7* (*HDAC7*<sup>very low</sup>) display higher expression of *c-MYC*. The patients in left panel, grouped as *HDAC7*<sup>low</sup> and *HDAC7*<sup>very low</sup>, were used to analyze *c-MYC* expression by qRT-PCR. *GAPDH* and *RPL38* were used as housekeeping genes. **D** Doxycycline-induced ectopic expression of *HDAC7* impairs proliferation and induces apoptosis in SEM-K2 cells. Left panel: proliferation of SEM-TetOn-Tight-control and SEM-TetOn-Tight-*HDAC7* cells treated with or without doxycycline was assessed at 24, 48, and 72 h after seeding 0.5 million cells ( $n = 4$ ). Right panel: apoptosis was assayed by Annexin V/DAPI staining ( $n = 4$ ) 96 h after doxycycline treatment. Error bars indicate standard error (SE). Group differences were investigated with the Mann–Whitney test; statistical significance is indicated as: \* $p < 0.05$ ; \*\* $p < 0.01$ ; \*\*\* $p < 0.001$ ; or n.s. non-significant.

*HDAC7*, suggestive of *HDAC7* deficiency in t(4;11) leukemia. The expression pattern of *HDAC7* was associated to that of the B lymphocyte differentiation gene *MME* (Figs. 1A and S1), which was consistent with its role in defining B-cell identity [12].

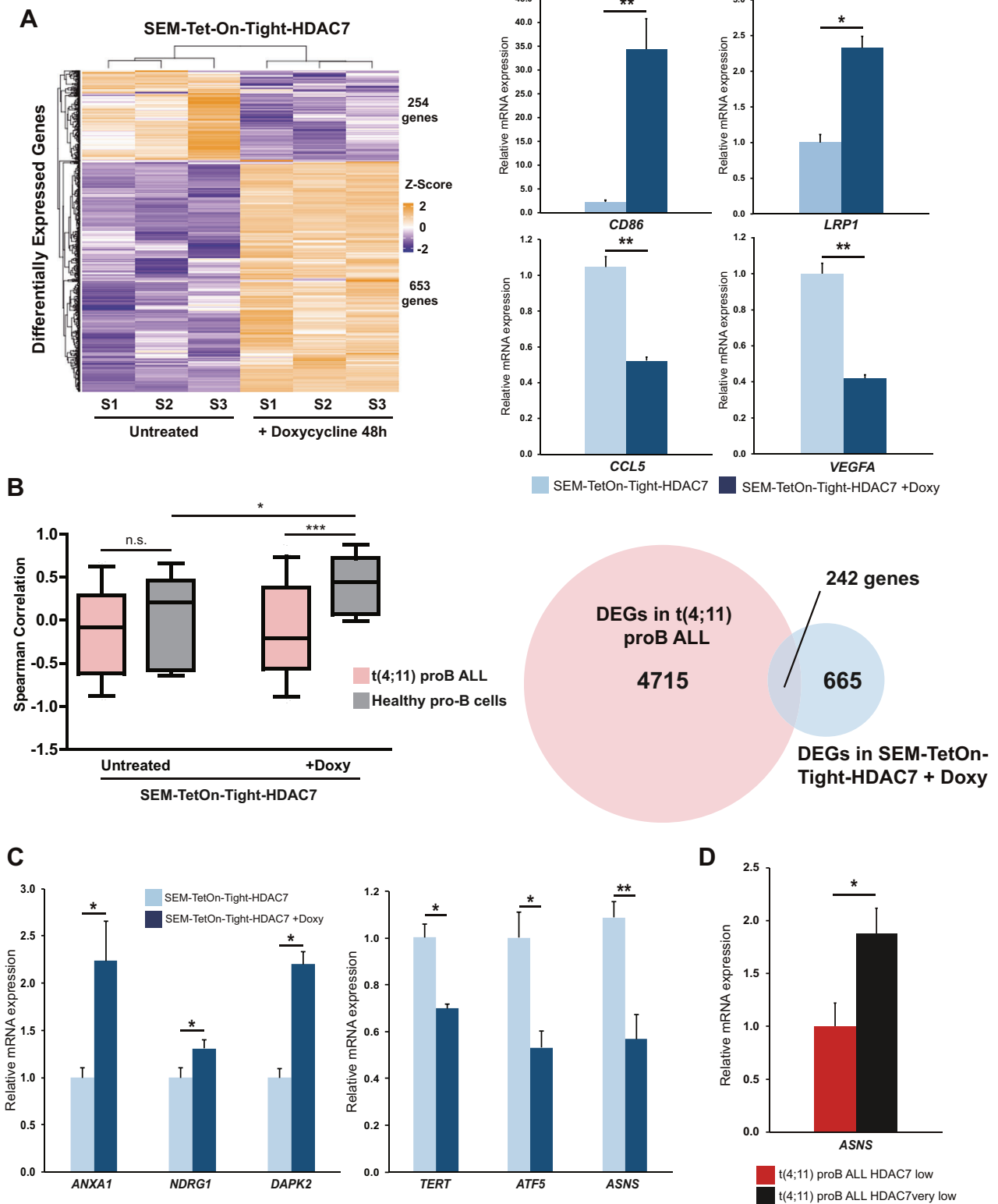
We next analyzed the clinical impact of *HDAC7* expression in proB ALL patients, irrespective of *MLL* gene status. Patients were divided by *HDAC7* mRNA expression level into *HDAC7*<sup>high</sup>, *HDAC7*<sup>intermediate</sup> or *HDAC7*<sup>low</sup>. The 5-year event-free survival (EFS (SE)) of *HDAC7*<sup>high</sup> patients was 90% (9.5), whereas both *HDAC7*<sup>intermediate</sup> and *HDAC7*<sup>low</sup> patients had a significantly poorer outcome, with a 5-year EFS (SE) of 60% (15.5) and 45% (11.2), respectively ( $p = 0.04$ ). A similar impact was observed on OS (Fig. 1B). Taken together, these results indicate that a low *HDAC7* expression marks t(4;11) proB ALL infants, associated to poorer outcome.

To validate these findings, we analyzed *HDAC7* mRNA expression by qRT-PCR in a cohort of 29 t(4;11) proB ALL cases [6]. In line with previous observations in B-ALL with different immunophenotypes [13], *HDAC7* was drastically underexpressed in t(4;11) proB ALL, compared with healthy FL-BCPs. Remarkably, the low levels of *HDAC7* were

in marked contrast to a higher expression of *c-MYC* oncogene (Fig. 1C, left panel). Given the overall low expression of *HDAC7*, patients were subdivided into *HDAC7*<sup>low</sup> and *HDAC7*<sup>very low</sup> groups, based on its median expression. As expected, patients within the *HDAC7*<sup>very low</sup> group tended to express the highest levels of the oncogene *c-MYC* (Fig. 1C, right panel). Mechanistically, ChIP-seq data showed that both *MLL-AF4* and *MLL-Af4* fusion proteins (originated from t(4;11) rearrangement) specifically bind to *c-MYC* but not to *HDAC7*, in both SEM-K2 cells and *MLL-Af4*-transduced CD34+ cells [14], respectively (Fig. S2A). Accordingly, we also confirmed strongly decreased mRNA and protein levels of *HDAC7* in proB ALL cell lines SEM-K2 and RS4;11 (Fig. S2B, C). These data indicate that t(4;11) proB ALL patients display low *HDAC7* expression, which associates with proB ALL clinical outcome.

The unfavorable impact of low *HDAC7* expression on clinical outcome showed in Fig. 1B prompted us to investigate whether *HDAC7* has any protective effects on proB ALL. SEM-K2 and RS4;11 cells were transduced with a double plasmid system that enables the expression of *HDAC7* upon doxycycline treatment (generated cell lines were named “TetOn-Tight-control” or “TetOn-Tight-*HDAC7*”). Increased mRNA and protein levels of *HDAC7* specifically upon doxycycline treatment functionally validated our system (Fig. S3A, B). We observed that exogenous *HDAC7* expression severely compromised the cell viability of both SEM-K2 and RS4;11 cells, as measured by MTT activity (Fig. S4A). Impaired viability was associated with *HDAC7*-mediated significantly decreased cell proliferation (Figs. 1D, left panel, and S4B) and increased cell death (Figs. 1D, right panel, and S4C) in both t(4;11) cell lines. Collectively, these data indicate that *HDAC7* endows t(4;11) proB ALL cells with a leukemia-suppressing phenotype.

We next performed bulk RNA-seq on untreated versus doxycycline-treated SEM-TetOn-Tight-*HDAC7* cells to gain insight into the molecular mechanisms and biological pathways affected in t(4;11) proB ALL cells upon exogenous expression of *HDAC7*. SEM-TetOn-Tight-control cells (both untreated and doxycycline-treated) were also subjected to RNA-seq, to discard the unspecific effect of doxycycline on gene expression. Bioinformatic analysis revealed 907 differentially expressed genes (DEGs) in doxycycline-treated SEM-TetOn-Tight-*HDAC7* cells. Of these, 653 (72%) genes were upregulated and 254 (28%) were downregulated after *HDAC7* overexpression (Figs. 2A, left panel, and S5A). Gene ontology (GO) analysis of the upregulated DEGs revealed significant enrichment in signal transduction, cell adhesion, and immune-inflammatory pathways upon overexpression of *HDAC7*. Although fewer genes were downregulated after *HDAC7* induction, GO analysis revealed that key hallmarks of



cancer such as cell proliferation, migration and apoptosis evasion were enriched in this set of genes (Fig. S5B). The altered expression of upregulated (*CD86* and *LRP1*) and downregulated (*VEGFA* and *CCL5*) genes was confirmed by qRT-PCR, given their importance in key processes such

as B lymphocyte differentiation or regulation of apoptosis (Fig. 2A, right panel, and Table S1).

In order to gain further insight into the molecular contribution of *HDAC7* in t(4;11) proB ALL, we next investigated whether *HDAC7* expression shifts the transcriptomic

**Fig. 2 Enforced overexpression of *HDAC7* partially reverts the expression pattern of genes affected by t(4;11) translocation in proB ALL.** **A** A total of 907 genes were detected as differentially expressed in SEM-K2 cells upon overexpression of *HDAC7*. Left panel: heatmap of the 907 DEGs identified by comparing bulk RNA-seq data from three sets of untreated vs doxycycline-treated SEM-TetOn-Tight-*HDAC7* cells, after discarding DEGs coincident with untreated vs doxycycline-treated SEM-TetOn-Tight-control cells dataset. Z-scores are represented from  $-2$  to  $2$ . Right panel: qRT-PCR validation for the DEGs *CD86*, *LRP1*, *CCL5*, and *VEGFA* in untreated vs doxycycline-treated SEM-TetOn-Tight-*HDAC7* cells. The average levels of expression of *GAPDH* and *RPL38* was used as reference. **B** *HDAC7* expression partially restores the transcriptome of healthy BCPs in SEM-K2 cells. Left panel: boxplot depicting the Spearman correlation values between the transcriptomic profile of SEM-K2 cells and primary samples from t(4;11) proB ALL or healthy FL-BCPs examined in Agraz-Doblas et al. [6]. Condition at x-axis refers to SEM-K2 status (untreated or treated with doxycycline), whereas legend colors refer to the comparison of SEM-K2 samples with t(4;11) proB ALL samples (pink) or healthy FL-BCPs (gray). Right panel: *HDAC7* reverts the expression pattern of a significant number of genes affected by t(4;11) translocation in proB ALL. Venn diagram shows the number of coincident genes between DEGs in (A) and DEGs between t(4;11) proB ALL patients and healthy FL-BCPs published in Agraz-Doblas et al. [6]. **C** Regulation of apoptosis is affected by *HDAC7* overexpression in SEM-K2 cells. As in (A) (right panel), but for mRNA levels of *TERT*, *ATF5*, *ASNS*, *NDRG1*, *ANXA1* and *DAPK2*. **D** t(4;11) proB ALL patients with the lowest levels of *HDAC7* (*HDAC7*<sup>very low</sup>) display higher expression of *ASNS*, a chemoresistance marker in proB ALL. The patients in Fig. 1C (right panel) were used to analyze *ASNS* expression by qRT-PCR. *GAPDH* and *RPL38* were used as housekeeping genes. Error bars represent SE. Statistical significance is indicated as: \* $p < 0.05$ ; \*\* $p < 0.01$ ; \*\*\* $p < 0.001$ ; or n.s. non-significant.

profile of SEM-K2 cells closer to that of healthy FL-BCPs. For this purpose, we used RNA-seq data generated from t(4;11) infants (Fig. 1A, B) and from healthy BCPs [6]. After assigning a Spearman correlation value to each single comparison between SEM-K2 (either basal or doxycycline-treated) and primary human (BCPs or t(4;11) proB ALL) samples (Fig. S6), we found that the transcriptomic profile of *HDAC7*-expressing cells (i.e., doxycycline-treated) was significantly more similar to that of BCPs than to that of t(4;11) proB ALL samples, whereas there were no differences in the same comparison within doxycycline-untreated cells (Fig. 2B, left panel). When comparing the complete list of DEGs shown in Fig. 2A with the DEGs between t(4;11) proB ALL and healthy BCPs [6], we found a total of 242 coincident genes. Remarkably, 17.4% of genes activated by *HDAC7* in SEM-K2 cells (114 out of 653) overlapped with genes repressed in t(4;11) proB ALL infants, while 17.3% of genes repressed by *HDAC7* (44 out of 254) overlapped with those activated in t(4;11) proB ALL patients, suggesting that *HDAC7* reverses the expression pattern of a set of 158 genes (65% from the total 242 coincident genes) affected by t(4;11) translocation in proB ALL (Figs. 2B, right panel, and S7A). GO analysis of this set of 158 genes revealed several altered pathways,

including those regulating apoptotic processes (Fig. S7B), according to data in Fig. 1D. Six genes from this overlapping set, involved in apoptotic mechanisms, were validated in vitro in SEM-K2 cells. As expected, the proapoptotic genes *ANXA1*, *NDRG1*, and *DAPK2* were activated upon *HDAC7* overexpression, while antiapoptotic markers such as *ATF5*, *TERT*, and *ASNS* were repressed by *HDAC7* (Fig. 2C and Table S1).

*ASNS* is a marker of chemoresistance associated with worse prognosis in childhood ALL [15, 16]. Therefore, the effect of *HDAC7* on *ASNS* suggests that the poor survival associated with the low expression of *HDAC7* might be linked with that of *ASNS* enzyme. The *HDAC7*-mediated repression of *ASNS* was confirmed in our cohort of t(4;11) proB ALL samples used in Fig. 1C. Remarkably, patients within the *HDAC7*<sup>very low</sup> group tended to express the highest levels of *ASNS* (Fig. 2D), indicating an association between *HDAC7* expression and chemotherapy response.

Overall, our findings highlight the role of *HDAC7* as a prognostic determinant in proB ALL. *HDAC7* plays a role in the pathogenesis of t(4;11) proB ALL by exerting a leukemia-suppressing phenotype; it is strongly repressed in t(4;11) leukemia infants and its low expression is associated with a significantly poorer clinical outcome. The elucidation of the mechanisms responsible for *HDAC7* repression in t(4;11) leukemia may open new therapeutic avenues in proB ALL with *MLL* gene rearrangement. For instance, future works aiming to enhance *HDAC7*, by modulating oncogenic drivers or specific external signaling that block *HDAC7* expression, may be highly valuable in terms of improving prognosis of infant t(4;11) leukemia.

**Acknowledgements** The authors wish to thank all clinical and laboratory members of the Interfant treatment protocol for their support and accessibility of samples/clinical data. We thank CERCA Programme/Generalitat de Catalunya for institutional support. This paper was funded by grants to MP by the Spanish Ministry of Science, Innovation and Universities (SAF2017-87990-R and EUR2019-103835) and elaborated at the Josep Carreras Leukaemia Research Institute (IJC, Badalona, Barcelona) and IDIBELL Research Institute (L'Hospitalet de Llobregat, Barcelona). OdB is funded by a Juan de la Cierva—Formación fellowship from the Spanish Ministry of Science, Innovation and Universities (FJCI-2017-32430). AM is funded by the Spanish Ministry of Science, Innovation and Universities, which is part of the Agencia Estatal de Investigación (AEI), through grant PRE2018-083183 (cofunded by the European Social Fund). Work in PM and CB's lab was supported by the European Research Council (CoG-2014646903), the Spanish Ministry of Economy and Competitiveness (SAF-2016-80481-R), Uno entre Cien Mil Foundation, the Leo Messi Foundation, the Asociación Española Contra el Cáncer (AECC-CI-2015), and the ISCIII/FEDER (PI17/01028). We thank Juan Ramón Tejedor for the analysis of ChIP sequencing data.

**Author contributions** OdB designed and performed most of the experimental work of the study. AG, JLT, AA-D, and PH performed and interpreted bioinformatics data analysis. AA, OC, and AM carried out some of the experimental work. CB, PB, GC, RWS, IV, and PM supplied critical materials to the study. PdL and MGv performed the analysis of

patients' outcome. PM assisted in the conception and supervision of the study. OdB and MP wrote the paper. MP obtained funding, conceived and supervised the study. All authors critically reviewed the paper.

### Compliance with ethical standards

**Conflict of interest** The authors declare no competing financial interest. PM is founder of OneChain Immunotherapeutics SL.

**Publisher's note** Springer Nature remains neutral with regard to jurisdictional claims in published maps and institutional affiliations.

### References

- Pui CH, Mullighan CG, Evans WE, Relling MV. Pediatric acute lymphoblastic leukemia: where are we going and how do we get there? *Blood*. 2012;120:1165–74.
- Bueno C, Montes R, Catalina P, Rodríguez R, Menendez P. Insights into the cellular origin and etiology of the infant pro-B acute lymphoblastic leukemia with MLL-AF4 rearrangement. *Leukemia*. 2011;25:400–10.
- Meyer C, Burmeister T, Gröger D, Tsaur G, Fechina L, Renneville A, et al. The MLL recombinome of acute leukemias in 2017. *Leukemia*. 2018;32:273–84.
- Kowarz E, Burmeister T, Lo Nigro L, Jansen MWJC, Delabesse E, Klingebiel T, et al. Complex MLL rearrangements in t(4;11) leukemia patients with absent AF4-MLL fusion allele. *Leukemia*. 2007;21:1232–8.
- Pieters R, Schrappe M, De Lorenzo P, Hann I, De Rossi G, Felice M, et al. A treatment protocol for infants younger than 1 year with acute lymphoblastic leukemia (Interfant-99): an observational study and a multicentre randomized trial. *Lancet*. 2007;370:240–50.
- Agraz-Doblas A, Bueno C, Bashford-Rogers R, Roy A, Schneider P, Bardini M, et al. Unravelling the cellular origin and clinical prognostic markers of infant B-cell acute lymphoblastic leukemia using genome-wide analysis. *Haematologica*. 2019;104:1176–88.
- Sanjuan-Pla A, Bueno C, Prieto C, Acha P, Stam RW, Marschalek R, et al. Revisiting the biology of infant t(4;11)/MA4+ B-cell acute lymphoblastic leukemia. *Blood*. 2015;126:2676–85.
- Menendez P, Catalina P, Rodríguez R, Melen GJ, Bueno C, Arriero M, et al. Bone marrow mesenchymal stem cells from infants with MLL-AF4+ acute leukemia harbor and express the MLL-AF4 fusion gene. *J Exp Med*. 2009;206:3131–41.
- Parra M. Epigenetic events during B lymphocyte development. *Epigenetics*. 2009;4:462–8.
- Kuiper RP, Schoemakers EFPM, Van Reijmersdal SV, Hehir-Kwa JY, Geurts van Kessel A, Van Leeuwen FN, et al. High-resolution genomic profiling of childhood ALL reveals novel recurrent genetic lesions affecting pathways involved in lymphocyte differentiation and cell cycle progression. *Leukemia*. 2007;21:1258–66.
- Bachmann PS, Piazza RG, Janes ME, Wong NC, Davies C, Mogavero A, et al. Epigenetic silencing of BIM in glucocorticoid poor-responsive pediatric acute lymphoblastic leukemia and its reversal by histone deacetylase inhibition. *Blood*. 2010;116:3013–22.
- Azagra A, Román-González L, Collazo O, Rodríguez-Ubrea J, de Yébenes VG, Barneda-Zahonero B, et al. In vivo conditional deletion of HDAC7 reveals its requirement to establish proper B lymphocyte identity and development. *J Exp Med*. 2016;213:2591–601.
- Barneda-Zahonero B, Collazo O, Azagra A, Fernández-Duran I, Serra-Musach J, Islam ABMMK, et al. The transcriptional repressor HDAC7 promotes apoptosis and c-Myc downregulation in particular types of leukemia and lymphoma. *Cell Death Dis*. 2015;6:e1635.
- Godfrey L, Crump NT, O'Byrne S, Lau IJ, Rice S, Harman JR, et al. H3K79me2/3 controls enhancer-promoter interactions and activation of the pan-cancer stem cell marker PROM1/CD133 in MLL-AF4 leukemia cells. *Leukemia*. 2020. <https://doi.org/10.1038/s41375-020-0808-y>.
- Rousseau J, Gagné V, Labuda M, Beaubois C, Sinnett D, Laverdière C, et al. ATF5 polymorphisms influence ATF function and response to treatment in children with childhood acute lymphoblastic leukemia. *Blood*. 2011;118:5883–90.
- Pastorczak A, Fendler W, Zalewska-Szewczyk B, Gómiak P, Lejman M, Trelinska J, et al. Asparagine synthetase (ASNS) gene polymorphism is associated with the outcome of childhood acute lymphoblastic leukemia by affecting early response to treatment. *Leuk Res*. 2014;38:180–3.



## SUPPLEMENTARY INFORMATION

for

### **HDAC7 is a major contributor in the pathogenesis of infant t(4;11) proB Acute Lymphoblastic Leukemia**

Oriol de Barrios<sup>1,2</sup>, Alexandros Galaras<sup>3,4</sup>, Juan L. Trincado<sup>5</sup>, Alba Azagra<sup>1,2</sup>, Olga Collazo<sup>1,2</sup>, Ainara Meler<sup>1,2</sup>, Antonio Agraz-Doblas<sup>5,6</sup>, Clara Bueno<sup>5</sup>, Paola Ballerini<sup>7</sup>, Giovanni Cazzaniga<sup>8</sup>, Ronald W. Stam<sup>9</sup>, Ignacio Varela<sup>6</sup>, Paola de Lorenzo<sup>10</sup>, Maria Grazia Valsecchi<sup>10</sup>, Pantelis Hatzis<sup>3</sup>, Pablo Menéndez<sup>5,11,12</sup>, Maribel Parra<sup>1,2\*</sup>

<sup>1</sup>Lymphocyte Development and Disease Group, Josep Carreras Leukaemia Research Institute (IJC), Ctra. de Can Ruti, Camí de les Escoles s/n, 08916 Badalona, Barcelona, Spain

<sup>2</sup>Cellular Differentiation Group, Instituto de Investigación Biomédica de Bellvitge (IDIBELL), Barcelona, Spain

<sup>3</sup>Biomedical Sciences Research Center “Alexander Fleming”, 16672 Vari, Greece

<sup>4</sup>Department of Biochemistry and Biotechnology, University of Thessaly, Greece

<sup>5</sup>Josep Carreras Leukaemia Research Institute and School of Medicine, University of Barcelona, 08036 Barcelona, Spain

<sup>6</sup>Instituto de Biomedicina y Biotecnología de Cantabria, Universidad de Cantabria-CSIC, Santander, Spain

<sup>7</sup>Pediatric Hematology, A. Trousseau Hospital, Paris, France

<sup>8</sup>Centro Ricerca Tettamanti, Department of Pediatrics, University of Milano Bicocca, Fondazione MBBM, Monza, Italy

<sup>9</sup>Princess Maxima Center for Pediatric Oncology, Utrecht, the Netherlands

<sup>10</sup>Interfant Trial Data Center, University of Milano-Bicocca, Monza, Italy

<sup>11</sup>Institució Catalana de Recerca i Estudis Avançats (ICREA), Barcelona. Spain

<sup>12</sup>CIBER-ONC-ISCI, Barcelona, Spain

\*Correspondence to:

Dr. Maribel Parra

Ctra de Can Ruti, Camí de les Escoles

08916 Badalona, Barcelona, Spain

Phone: +34 935572800 Fax: +34 934651472

E-mail: [mparra@carrerasresearch.org](mailto:mparra@carrerasresearch.org)

## SUPPLEMENTARY MATERIALS AND METHODS

### Human samples, RNA expression and survival-associated data

RNA samples from proB ALL infants (n=42) and healthy B-cell progenitors (BCPs, n=6) as well as survival-associated data were obtained through collaboration with the INTERFANT treatment protocol consortium<sup>1</sup>. RNAseq expression data were obtained from publicly available datasets published in Agraz-Doblas *et al.*<sup>2</sup> The expression of *HDAC7* in proB ALL patients was calculated taking that of healthy fetal liver B-cell progenitors (FL-BCP) as reference. For outcome analysis, two patients were excluded due to inconsistent data in diagnosis criteria. The remaining 40 patients were allocated in the corresponding *HDAC7*<sup>high</sup> or *HDAC7*<sup>low</sup> (n=20) groups according to their median *HDAC7* mRNA expression. Given that *HDAC7*<sup>high</sup> group contained higher variability in terms of *HDAC7* expression, this group was split in *HDAC7*<sup>high</sup> (n=10) and *HDAC7*<sup>intermediate</sup> (n=10) subgroups. Therefore, outcome analysis was performed for three separate groups, with the following expression cutoff values: *HDAC7*<sup>high</sup> patients, above 4000 Fragments Per Kilobase of exon per Million fragments mapped (FPKM); *HDAC7*<sup>intermediate</sup> patients, between 2600 and 4000 FPKM; *HDAC7*<sup>low</sup> patients, below 2600 FPKM. The project was IRB-approved by the IJC Ethics Committee. All samples were obtained upon informed consent and were stored in accredited biobanks linked to Interfant.

### Cell cultures

Human SEM-K2 and RS4;11 and murine HAFTL cell lines were grown and maintained in regular cell culture conditions (RPMI 1640 medium + 10% fetal bovine serum), whereas HEK 293T cells and their derivative Platinum-A cells were maintained in DMEM medium, also with 10% fetal bovine serum. Blasticidin was added at 10 µg/mL for Platinum-A culture. Once they had been selected, SEM-TetOn-Tight-control, SEM-TetOn-Tight-*HDAC7*, RS4;11-TetOn-Tight-control and RS4;11-TetOn-Tight-*HDAC7* were cultured in RPMI 1640 complete medium and selection with

G418 (1.5 mg/mL) and puromycin (0.4 µg/mL) was maintained. Where indicated, cells were treated with 1 µg/mL doxycycline for 24, 48, 72 or 96 h.

### **Retroviral supernatant production and generation of stable inducible cell lines**

pRetro-X-Tight-Pur-HDAC7 construct was generated from pRetro-X-Tight-Pur-control as described previously<sup>3</sup>. Platinum-A cells containing retrovirus packaging vectors were used to produce retroviral supernatant. Briefly, pRetro-X-Tet-On-Advanced (Tanaka Bio), pRetro-X-Tight-Pur-control and pRetro-X-Tight-HDAC7 were transfected into these cells using polyethyleneimine (PEI) transfection reagent, and the supernatant was collected 48 h after transfection. Inducible SEM-K2 and RS4;11 cell lines were generated after two consecutive infections. First, cells were infected with supernatant containing pRetro-X-Tet-On-Advanced viral particles and selected with geneticin (G418, Sigma-Aldrich) at 1.5 mg/mL for 3-4 weeks. After completing this selection, cells were subsequently infected with supernatant containing either pRetro-X-Tight-control or pRetro-X-Tight-HDAC7 viral particles and selected with puromycin at 0.4 µg/mL for 1-2 weeks.

### **MTT and cell proliferation assays**

For MTT assays,  $5 \times 10^4$  cells were seeded in 12-well plates, in triplicate for each condition tested. At the indicated times (24, 48 and 72 h), MTT reagent was added at a final concentration of 5 mg/mL. Cells were incubated for 3 h under regular conditions and, afterwards, the resulting formazan blue product was solubilized in DMSO. Absorbance was measured as the difference between absorbance at 570 nm and background absorbance measured at 750 nm. Data are presented as the average of at least three independent experiments, each one of them performed in triplicate. For cell proliferation assays,  $5 \times 10^5$  cells were seeded in 6-well plates and the living cells were assessed by counting after 24, 48 and 72 h. Data are presented as average of at least four independent experiments.

### **Apoptosis and cell death evaluation**

Established cell lines derived from SEM-K2 and RS4;11 cell lines were cultured in 75 cm<sup>2</sup> flasks for 96 h, starting from 5 x 10<sup>5</sup> cells, either untreated or treated with doxycycline. At the indicated time, 1 x 10<sup>6</sup> cells were collected, stained with Annexin V-PE (MACS, Milteny Biotech) and DAPI for 15 min in the dark, and analyzed by flow cytometry (FACS Canto, Beckton-Dickinson, IGTP Research Centre flow cytometry facility). Summary results of cells in early apoptosis (Annexin V-positive cells) and in late apoptosis or necrosis (Annexin V and DAPI-double positive cells) are shown. Data are represented as the average of at least four independent assays.

### **RNA extraction and RT-qPCR expression analysis**

Total RNA from SEM-K2 and RS4;11 cell lines samples was extracted using Trizol (Life Technologies, Thermo Fisher), following the manufacturer's instructions. After being quantified, 1-2 µg of RNA were retrotranscribed with random hexamers using a High-Capacity cDNA Reverse Transcription kit (Applied Biosystems, Thermo Fisher). mRNA levels were determined by qRT-PCR using Light Cycler 480 SYBR Green Master Mix (Roche) either in a Light Cycler 480 II (Roche) or in a QuantStudio 7 Flex Real-Time PCR (Applied Biosystems) apparatus. Results were analyzed using LightCycler 480 software (Roche), taking *GAPDH* and *RPL38* as housekeeping genes. Genes selected for validation by qRT-PCR were based on previously reported data<sup>4-13</sup>. Primers used for gene expression analysis are listed in Supplementary Table S1. All primer pairs were designed with Primer3® software.

### **Protein extraction and western blot**

For protein extraction, cells were washed with ice-cold PBS and resuspended in RIPA lysis buffer (150 mM NaCl, 50 mM Tris-HCl pH 8.0, 1% NP40, 0.1% SDS, 0.5% sodium deoxycholate) containing Complete Mini EDTA-free protease inhibitors cocktail (Roche), PMSF and DTT. Lysates were sonicated in a UP50H ultrasonic processor (Hielscher), clarified by maximum speed

centrifugation and quantified with Bradford reagent (Bio-Rad). Protein lysates were boiled and loaded onto 10% polyacrylamide gels and transferred to 0.2- $\mu$ m nitrocellulose membranes (Amersham Protran, GE Healthcare Lifescience). After blocking with 5% non-fat milk, membranes were blotted with antibodies against HDAC7 (clone H-273, Santa Cruz Biotechnologies; 1:500) and  $\beta$ -actin (clone AC-15, Sigma-Aldrich, 1:2000) overnight at 4°C. After washing with TBS-Tween, membranes were incubated with HRP-conjugated secondary antibodies (anti-mouse HRP and anti-rabbit HRP; 1:3000) for 1-2 h at r.t. The reaction was developed with the ECL Western Blotting Analysis System (Amersham). Images shown are representative of at least three independent experiments.

### **RNA sequencing**

Total RNA was extracted from SEM-Tet-On-Tight-control and SEM-Tet-On-Tight-HDAC7 cell lines with RNeasy Mini Column kit (Qiagen), either untreated or after 48 h of doxycycline treatment. After checking that HDAC7 had been correctly induced, samples were quantified and subjected to quality control using a Bioanalyzer apparatus (Faculty of Medicine, University of Barcelona). Samples were processed at the *Centre Nacional d'Anàlisi Genòmica* (CNAG, Barcelona). Briefly, after preparing human stranded total RNA libraries, they were sequenced in paired-end mode with a read length of 75 bp. 20 million paired-end reads were generated for each sample. Quality control of the samples was performed with the FASTQC tool (available at <https://www.bioinformatics.babraham.ac.uk/projects/fastqc/>). Data is publicly available in GEO repository (**GSE151793**).

### **RNA sequencing analysis and bioinformatic analysis**

Sequenced reads were mapped to the Genome Reference Consortium Human Build 37 (GRCh37), using an alignment procedure consisting of two steps. In the first round, reads were mapped with hisat2<sup>14</sup>, using default parameters. In the second round, the unmapped reads were mapped with bowtie2<sup>15</sup> using the --local and --very-sensitive parameters. The resulting bam files were analyzed

with the Bioconductor package *metaseqR*<sup>16</sup>, as described in Nikolaou *et al.*<sup>17</sup> without the exon filters. The resulting gene counts table was subjected to differential expression analysis for the contrasts: SEM-TetOn-Tight-control + doxycycline vs untreated and SEM-TetOn-Tight-HDAC7 + doxycycline vs untreated, using the DESeq algorithm. Genes with DESeq p-value less than 0.05 and fold change (for each contrast) greater than 0.58 or less than -0.58 in log<sub>2</sub> scale, corresponding to 1.5 times up and down, respectively, on a natural scale, were considered differentially expressed. In order to remove the potential unspecific effect of doxycycline, the list of Differentially Expressed Genes (DEGs) in SEM-TetOn-Tight-control + doxycycline condition (compared to untreated cells) was compared to that of DEGs in SEM-TetOn-Tight-HDAC7 + doxycycline condition, and coincident genes were removed. Protein coding differentially expressed genes were used for pathway enrichment analysis with GO and KEGG analysis with the web-available tool Genecodis. Original RNA sequencing data from t(4;11) proB ALL patients and healthy B cell progenitors<sup>2</sup> were used to assess the degree of similarity with our own sequencing data from SEM-K2 cells samples (basal and after doxycycline treatment). Mitochondrial genes and genes with < 10% variance were removed. After calculating the principal components (PCs) of the samples, the optimal number of six PCs, as selected by Horn's parallel analysis<sup>18</sup>, available in using PCAtools (version 1.1.10), were retained. Pairwise Pearson correlation coefficients between all samples were calculated. Values were plotted as a heatmap, assigning the colors blue and red to the negative and red positive values, respectively. These values were grouped to generate a box plot and to facilitate statistical analysis.

### **ChIP sequencing analysis**

ChIP sequencing tracks were obtained from publicly available GEO datasets. GSE84116 was used to analyze MLL-Af4-transduced CD34+ murine cells<sup>19</sup>, while GSE74812 was used for the analysis of N-terminal MLL and C-terminal AF4 immunoprecipitations in SEM-K2 human cells<sup>20</sup>.

## **Statistical analysis**

The data presented were analyzed using Prism software (GraphPad Software). Statistical significance was assessed with non-parametric Mann–Whitney U-tests. All histograms represent average values with corresponding SEs. Where indicated, relevant comparisons are labelled as either significant at the  $p < 0.001$  (\*\*\*) ,  $p < 0.01$  (\*\*) or  $p < 0.05$  (\*) levels, or as non-significant (n.s.) for values of  $p \geq 0.05$ . Event-free survival (EFS) was defined as time from diagnosis to first event, i.e. resistance, relapse, death from any cause, or second malignant neoplasm. Overall survival (OS) was defined as time from diagnosis to death from any cause. Observation periods were censored at time of last contact when no events were reported. EFS was estimated according to Kaplan-Meier (with Greenwood standard error) and compared with the log-rank test. Analysis were performed with SAS 9.4.

## SUPPLEMENTARY REFERENCES

1. Pieters R, Schrappe M, De Lorenzo P, Hann I, De Rossi G, Felice M, et al. A treatment protocol for infants younger than 1 year with acute lymphoblastic leukemia (Interfant-99): an observational study and a multicentre randomized trial. *Lancet*. 2007;370(9583):240-250.
2. Agraz-Doblas A, Bueno C, Bashford-Rogers R, Roy A, Schneider P, Bardini M, et al. Unravelling the cellular origin and clinical prognostic markers of infant B-cell acute lymphoblastic leukemia using genome-wide analysis. *Haematologica*. 2019;104(6):1176-1188.
3. Barneda-Zahonero B, Collazo O, Azagra A, Fernández-Duran I, Serra-Musach J, Islam ABMMK, et al. The transcriptional repressor HDAC7 promotes apoptosis and c-Myc downregulation in particular types of leukemia and lymphoma. *Cell Death Dis*. 2015;6(2):e1635.
4. Engel P, Gribben JG, Freeman GJ, Zhou LJ, Nozawa Y, Abe M, et al. The B7-2 (B70) costimulatory molecule expressed by monocytes and activated B lymphocytes is the CD86 differentiation antigen. *Blood*. 1994;84(5):1402-1407.
5. Nilsson A, Vesterlund L, Oldenborg PA. Macrophage expression of LRP1, a receptor for apoptotic cells and unopsonized erythrocytes, can be regulated by glucocorticoids. *Biochem Biophys Res Comm*. 2012;417:1304-1309.
6. Zhang G, Wang H, Zhu K, Yang Y, Li J, Jiang H, et al. Investigation of candidate molecular biomarkers for expression profile analysis of the Gene expression omnibus (GEO) in acute lymphocytic leukemia (ALL). *Biomed Pharmacother*. 2019;120:109530.



7. Dullo I, Hooi PB, Sabapathy K. Hypoxia-induced DNp73 stabilization regulates Vegf-A expression and tumor angiogenesis similar to TAp73. *Cell Cycle*. 2015;14(22):3533-3539.
8. Lee J, Sung YH, Cheong C, Choi YS, Jeon HK, Sun W, et al. TERT promotes cellular and organismal survival independently of telomerase activity. *Oncogene*. 2008;27:3754-3760.
9. Dluzen D, Li G, Tacelosky D, Moreau M, Liu DX. et al. BCL-2 is a downstream target of ATF5 that mediates the prosurvival function of ATF5 in a cell type-dependent manner. *J Biol Chem*. 2011;286(9):7705-7713.
10. Ueno T, Ohtawa K, Mitsui K, Kodera Y, Hiroto M, Matsushima A, et al. Cell cycle arrest and apoptosis of leukemia cells induced by L-asparaginase. *Leukemia*. 1997;11:1858-1861.
11. Stein S, Thomas EK, Herzog B, Westfall MD, Rocheleau JV, Jackson 2<sup>nd</sup> RS, et al. NDRG1 is necessary for p53-dependent apoptosis. *J Biol Chem*. 2004;47(19):48930-48940.
12. Vago JP, Nogueira CRC, Tavares LP, Soriani FM, Lopes F, Russo RC, et al. Annexin A1 modulates natural and glucocorticoid-induced resolution of inflammation by enhancing neutrophil apoptosis. *J Leukoc Biol*. 2012;92(2):249-258.
13. Schlegel CR, Fonseca AV, Stöcker S, Georgiou ML, Misterek MB, Munro CE, et al. DAPK2 is a novel modulator of TRAIL-induced apoptosis. *Cell Death Differ*. 2014;21(11):1780-1791.
14. Kim D, Langmead B, Salzberg SL. HISAT: a fast-spliced aligner with low memory requirements. *Nat Methods*. 2015;12(4):357-360.
15. Langmead B, Salzberg SL. Fast gapped-read alignment with Bowtie 2. *Nat Methods*. 2012;9(4):357-359.

16. Moulos P, Hatzis P. Systematic integration of RNA-Seq statistical algorithms for accurate detection of differential gene expression patterns. *Nucleic Acids Res.* 2015;43(4):e25.
17. Nikolau KC, Moulos P, Harokopos V, Chalepakis G, Talianidis I. Kmt5a controls hepatic metabolic pathways by facilitating RNA pol II release from promoter-proximal regions. *Cell Rep.* 2017;20(4):909-922.
18. Buja A, Eyuboglu N. Remarks on parallel analysis. *Multivariate Behav Res.* 1992;27:509-540.
19. Lin S, Luo RT, Ptasinska A, Kerry J, Assi SA, Wunderlich M, et al. Instructive Role of MLL-fusion proteins revealed by a model of t(4;11) pro-B acute lymphoblastic leukemia. *Cancer Cell.* 2016;30(5):737-749
20. Benito JM, Godfrey L, Kojima K, Hogdal L, Wunderlich M, Geng H, et al. MLL-rearranged acute lymphoblastic leukemias activate BCL-2 through H3K79 methylation and are sensitive to the BCL-2-specific antagonist ABT-199. *Cell Rep.* 2015;13(12):2715-2727.

## SUPPLEMENTARY TABLE S1

DNA oligos used for quantitative real-time PCR

Human gene	Forward 5' – 3'	Reverse 5' – 3'	Amplicon size (bp)
<i>RPL38</i>	TGGGTGAGAAAGGTCCTGGTCCG	CGTCGGGCTGTGAGCAGGAA	100
<i>GAPDH</i>	TCTTCTTTTGCCTCGCCAG	AGCCCCAGCCTTCTCCA	171
<i>HDAC7</i>	CACAGCGGATGTTTGTGATG	TCACGAGAAGCCACTTTGAA	142
<i>CD86</i>	ACAAAAAGCCACAGGAATG	TTAGGTTCTGGGTAACCGTGT	160
<i>LRP1</i>	GCTTTCAGCTTCAGGCAGAT	CCTTGCAGGAGCGGTTATC	156
<i>CCL5</i>	TACACCAGTGGCAAGTGCTC	TGTACTCCCGAACCCATTTTC	129
<i>VEGFA</i>	CGCAAGAAATCCCGGTATAA	GCGAGTCTGTGTTTTTGCAG	172
<i>TERT</i>	ACTGGCTGATGAGTGTGTACGTCGT	ACCCTCTTCAAGTGCTGTCTGATT	151
<i>ATF5</i>	TCCACCTTCTTTCTTCAGC	ACTGATGGCAACAGGAGAGG	153
<i>ASNS</i>	AGCGTGGTGATCTTCTCTGG	TCCCTCAGAAGCCTCTCACT	116
<i>ANXA1</i>	TAAGGGTGACCGATCTGAGG	ACGTCTGTCCCCTTCTCCT	102
<i>NDRG1</i>	ACAACCCTGAGATGGTGGAG	AGCTTGGGTCCATCCTGAG	144
<i>DAPK2</i>	ACAATGTCATCACGCTGCAC	CCTTCTGGGCCAGGAAAT	105

## SUPPLEMENTARY FIGURE LEGENDS

### **SUPPLEMENTARY FIGURE S1 - HDAC7 expression is downregulated in t(4;11) proB ALL patients compared to alternative *MLL* gene status.**

Heatmap representation showing that *HDAC7* is underexpressed in proB ALL infants harboring t(4;11) translocation. RNAseq data for *HDAC7* and *MME* mRNA expression was obtained from 27 t(4;11) (labeled as MA4\_X), 5 t(9;11) (labeled as MA9\_X) and 10 *MLL* germline (labeled as MLLwt\_X) proB ALL infants. *MME* gene expression was used as a control of proper differentiation of proB to preB cells.

### **SUPPLEMENTARY FIGURE S2 – *HDAC7* is not transcriptionally activated by MLL-AF4 fusion protein in t(4;11) proB ALL cells**

(A) MLL-AF4 binds to *MYC* but not to *HDAC7*, in both SEM cells and *MLL-Af4*-transduced CD34<sup>+</sup> cells. ChIP sequencing data for *HDAC7* (*upper panel*) and *MYC* (*lower panel*) genes in SEM-K2 cells and *MLL-Af4*-transduced CD34<sup>+</sup> murine cells. Binding peaks are shown for FLAG-*MLL-Af4* transduced CD34<sup>+</sup> cells, after immunoprecipitation with FLAG antibody (in red); and for SEM-K2 cells, after immunoprecipitation with antibodies against N-terminal region of MLL (in blue) and C-terminal region of AF4 (in green). (B) *HDAC7* is underexpressed in human proB ALL cell lines harboring the MLL-AF4 rearrangement. Protein levels of HDAC7 in human SEM-K2 and RS4;11 and murine HAFTL cell lines.  $\beta$ -actin was used as a loading control. (C) mRNA expression of *HDAC7* in human t(4;11) proB ALL cell lines (SEM-K2 and RS4;11) and fetal cord blood CD19<sup>+</sup> CD34<sup>+</sup>, analyzed by qRT-PCR. The average level of expression of *GAPDH* and *RPL38* was used as housekeeping.

**SUPPLEMENTARY FIGURE S3 - HDAC7 is induced by doxycycline in SEM-K2 and RS4;11 cells infected with TetOn-Tight double plasmid system**

(A) Lysates of SEM-TetOn-Tight-control and SEM-TetOn-Tight-HDAC7 (*left panel*) and RS4;11-TetOn-Tight-control and RS4;11-TetOn-Tight-HDAC7 (*right panel*) assessed by western blot for HDAC7 and  $\beta$ -actin, as a loading control. Where indicated, cells were treated with 1  $\mu$ g/mL of doxycycline for 72 h. (B) mRNA levels of *HDAC7* in SEM-TetOn-Tight-control and SEM-TetOn-Tight-HDAC7 (*left panel*) and RS4;11-TetOn-Tight-control and RS4;11-TetOn-Tight-HDAC7 (*right panel*) assessed by qRT-PCR, using the average of *GAPDH* and *RPL38* as housekeeping. Where indicated, cells were treated with 1  $\mu$ g/mL of doxycycline for 48 h.

**SUPPLEMENTARY FIGURE S4 - HDAC7 overexpression reduces viability of t(4;11) proB ALL cells**

(A) Cell viability assessed by MTT assay in SEM-TetOn-Tight-control and SEM-TetOn-Tight-HDAC7 (*left panel*) and in RS4;11-TetOn-Tight-control and RS4;11-TetOn-Tight-HDAC7 (*right panel*) cells after treatment with 1  $\mu$ g/mL of doxycycline (n=4) at the indicated time points. Results are presented as relative absorbance for the differences between values measured at 560 and 750 nm. (B) Cell counts of RS4;11-TetOn-Tight-control and RS4;11-TetOn-Tight-HDAC7 cells at 24, 48 and 72 h after seeding a starting quantity of 0.5 million cells. Where indicated, cells were treated with 1  $\mu$ g/mL of doxycycline. (C) Average of four experiments performed for each condition, showing the percentage of Annexin V single-positive and Annexin V/DAPI double-positive cells, after analyzing  $2.5 \times 10^5$  RS4;11-TetOn-Tight-HDAC7 stained cells by flow cytometry. Where indicated, cells were treated with doxycycline for 96 h.

**SUPPLEMENTARY FIGURE S5 - 907 genes are differentially expressed in SEM-K2 cells upon forced expression of HDAC7**

(A) Volcano plot including 907 DEGs found after treating SEM-TetOn-Tight-HDAC7 cells with doxycycline for 48 h. Upregulated and downregulated genes are depicted in red and green, respectively. (B) Biological processes (BP) enriched in DEGs from Figures 2A and S5A include regulation of key leukemic hallmarks. The upper and lower panels represent BPs significantly enriched in upregulated and downregulated DEGs, respectively. Dot sizes reflect the number of genes involved in each pathway, whereas the color indicates the level of significance. Dots are distributed along the X axis as a measure of the proportion of all DEGs that are involved.

**SUPPLEMENTARY FIGURE S6 - HDAC7 expression partially restores healthy B cell progenitors' genomic profile in SEM-K2 cells**

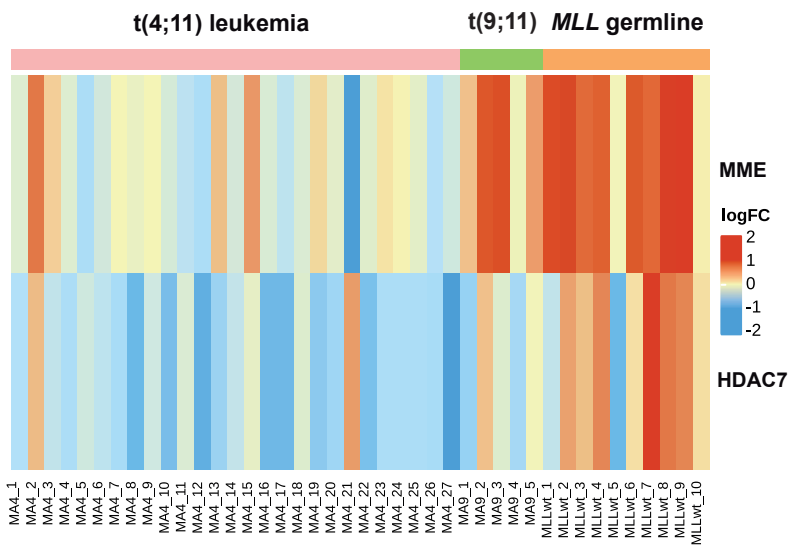
Plot of single Spearman correlation coefficients from Figure 2B, after comparing genomic profiles of each individual sample (both primary human samples and SEM-K2 cells) against all other samples. Values are plotted as a heatmap, assigning blue and red colors, respectively, to the negative and positive correlations.

**SUPPLEMENTARY FIGURE S7 - HDAC7 reverts the expression pattern of a significant number of genes affected by t(4;11) translocation in proB ALL.**

(A) Venn diagram showing the overlapping genes between the set of 242 coincident DEGs from Figure 2B (in grey), the set of 653 DEGs activated (in orange) and the set of 254 DEGs repressed (in purple) in SEM-TetOn-Tight-HDAC7 cells treated with doxycycline. The combination of 158 overlapping genes constitutes the gene set altered in t(4;11) proB ALL whose expression pattern is

reversed by HDAC7 overexpression. **(B)** Bar chart representing biological processes (BP) significantly enriched in the set of 158 overlapping genes in Figure S7A. Pathways that include genes upregulated in SEM-TetOn-Tight-HDAC7 cells treated with doxycycline are colored in orange, while the pathways that include downregulated genes are colored in purple, according to Figure 2A. Only pathways including 4 genes or more are depicted.

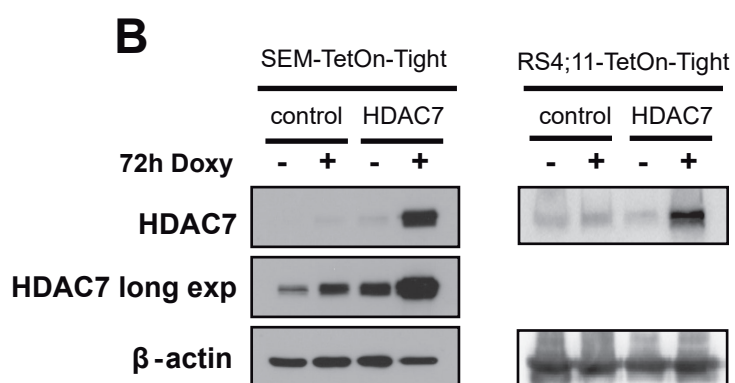
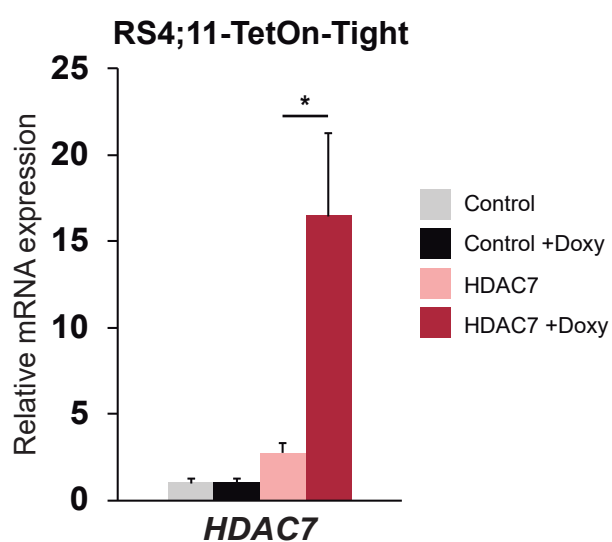
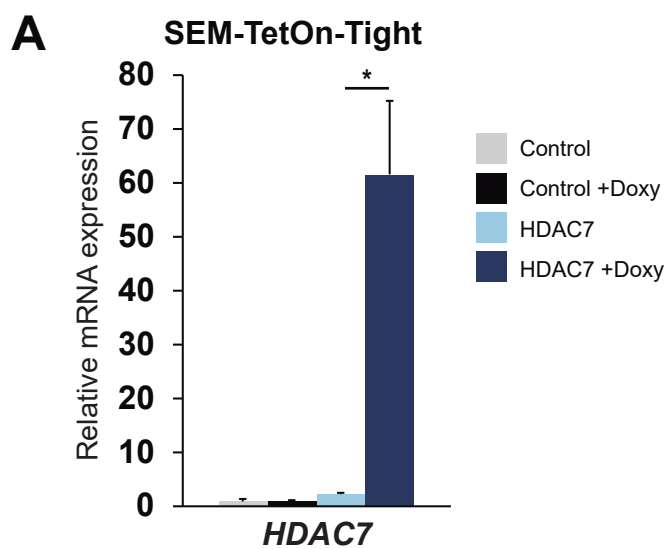
# Supplementary Figure 1





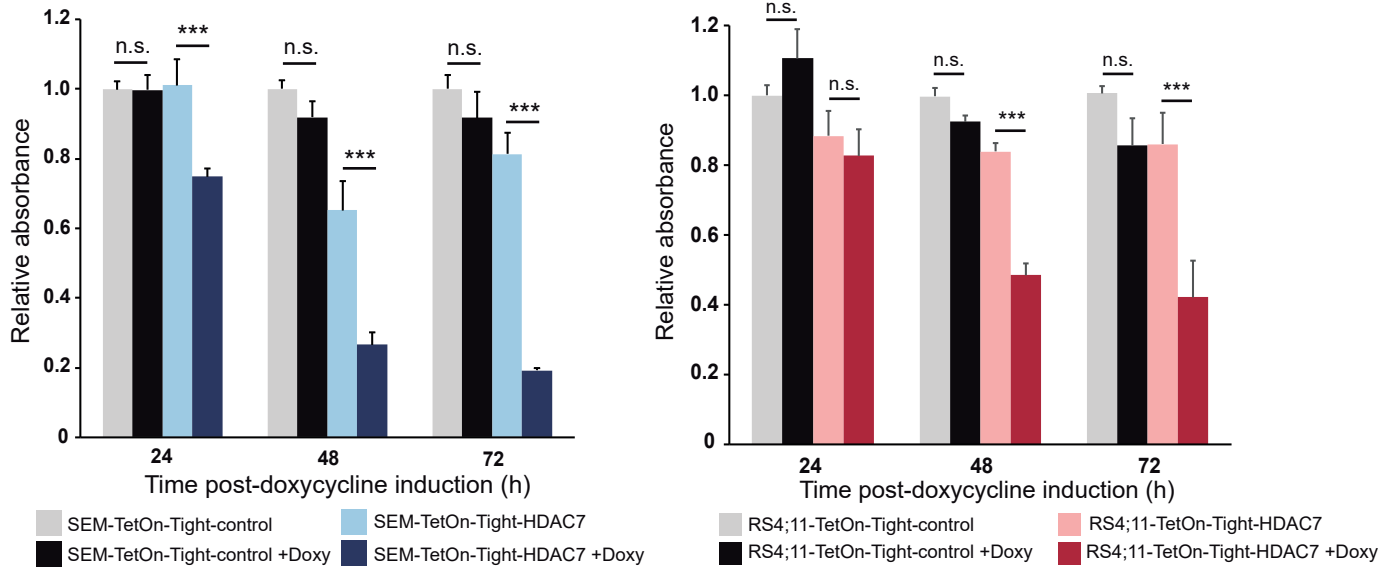


# Supplementary Figure 3

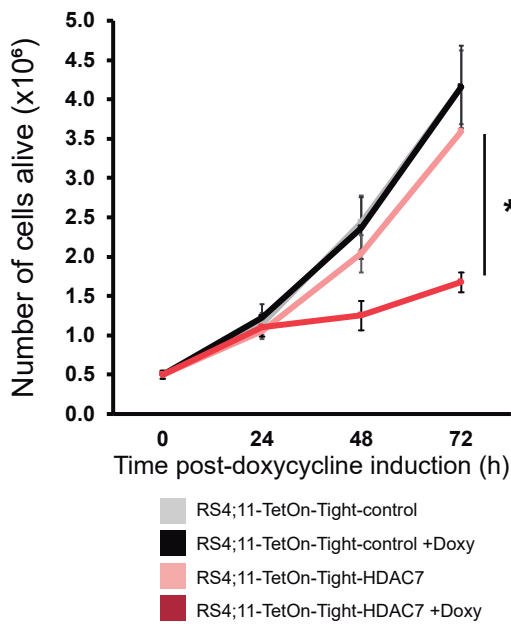


# Supplementary Figure 4

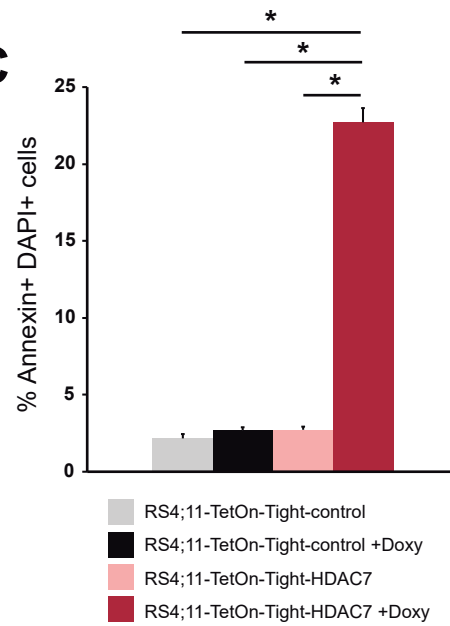
## A



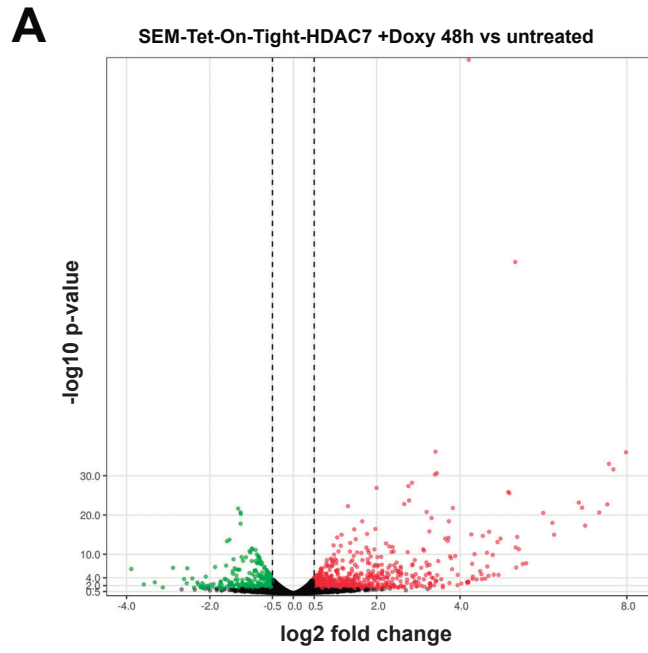
## B



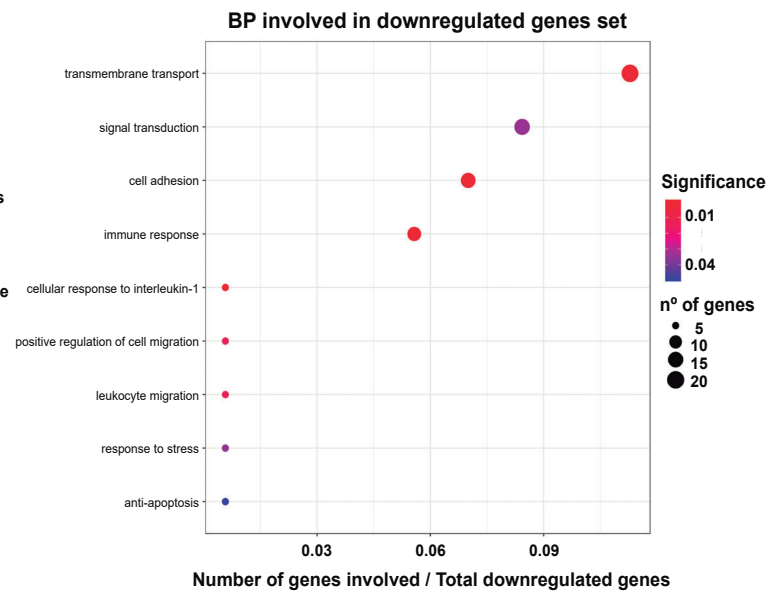
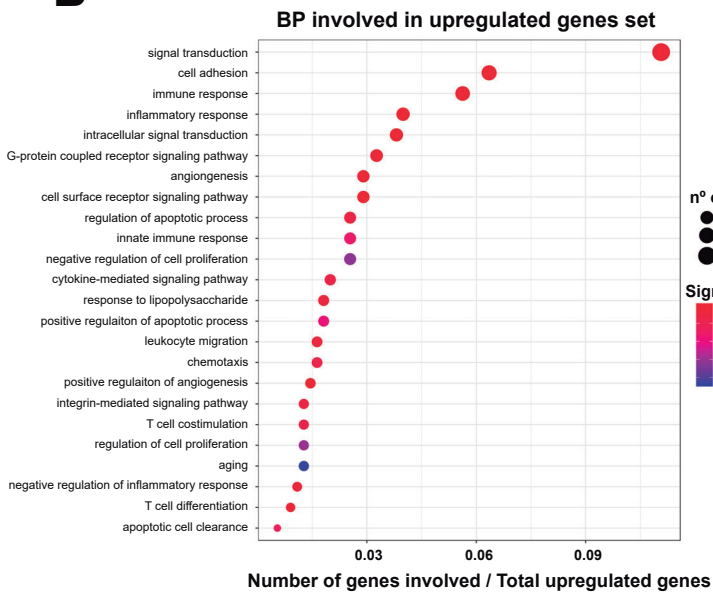
## C



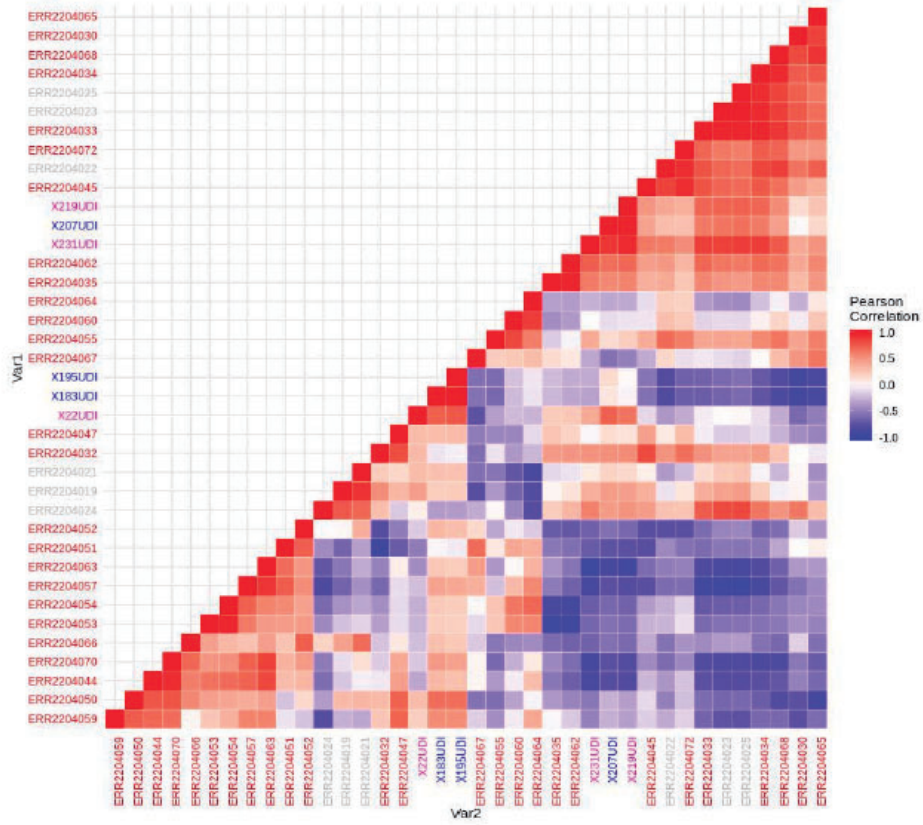
# Supplementary Figure 5



**B**

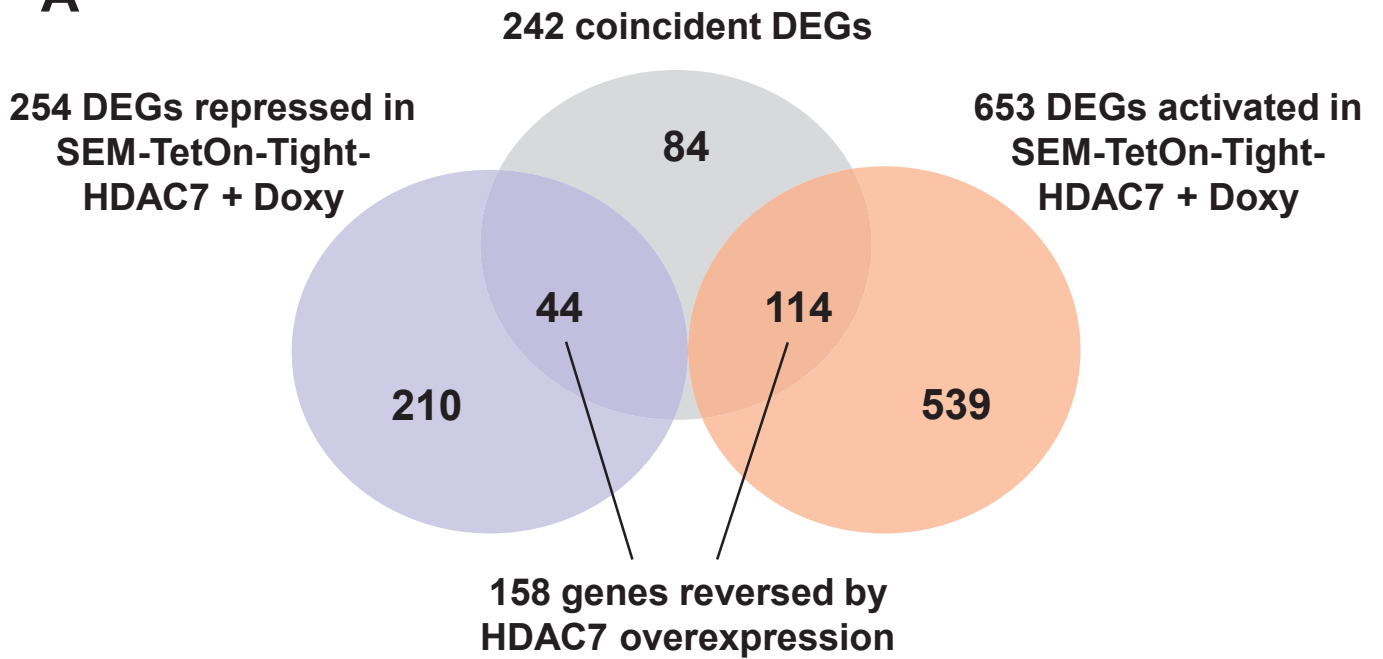


# Supplementary Figure 6

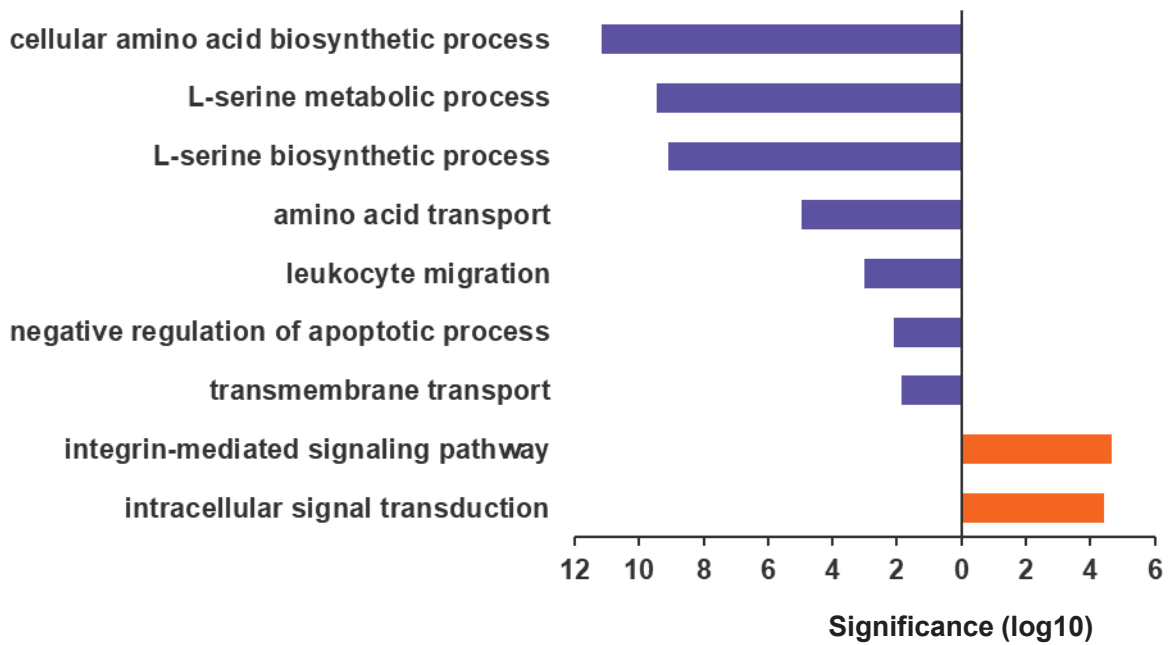


# Supplementary Figure 7

## A



## B



## **ARTICLE 3**

*“HDAC7 is essential in early pre-germinal center formation and its deregulation is associated with DLBCL”*





## **HDAC7 is essential in early pre-germinal center formation and its deregulation is associated with DLBCL**

**Ainara Meler<sup>1</sup>, Mar Gusi-Vives<sup>1,†</sup>, Oriol de Barrios<sup>1,†</sup>, Alba Azagra<sup>1</sup>, Olga Collazo<sup>1</sup>, Javier Melchor<sup>2</sup>, Alberto del Monte<sup>3</sup>, Balázs Győrffy<sup>4,5</sup>, Miriam Verdu-Bou<sup>6</sup>, José-Tomás Navarro<sup>6,7,8</sup>, José Ignacio Martín-Subero<sup>9,10</sup>, Gaël Roué<sup>11</sup>, Almudena R. Ramiro<sup>3</sup>, Sergio Roa<sup>2</sup>, Maribel Parra<sup>1,\*</sup>**

<sup>1</sup>Lymphocyte Development and Disease Group, Josep Carreras Leukaemia Research Institute, 08916 Badalona, Spain

<sup>2</sup>Department of Biochemistry and Genetics, University of Navarra, 31008 Pamplona, Spain

<sup>3</sup>B Cell Biology Laboratory, Centro Nacional de Investigaciones Cardiovasculares, Madrid 28029, Spain

<sup>4</sup>Cancer Biomarker Research Group, TTK, Budapest, Hungary

<sup>5</sup>Department of Bioinformatics and Department of Pediatrics, Semmelweis University, Budapest, Hungary

<sup>6</sup>Lymphoid Neoplasms Group, Josep Carreras Leukaemia Research Institute, 08916 Badalona, Spain

<sup>7</sup>Department of Hematology, Institut Català d'Oncologia-Germans Trias i Pujol Hospital, 08916 Badalona, Spain

<sup>8</sup>Department of Medicine, Universitat Autònoma de Barcelona, 08916 Badalona, Spain

<sup>9</sup>Institut d'Investigacions Biomèdiques August Pi I Sunyer (IDIBAPS) and University of Barcelona, Barcelona, Spain

<sup>10</sup>Institució Catalana de Recerca i Estudis Avançats (ICREA), Barcelona, Spain.

<sup>11</sup>Lymphoma Translational Group, UBIRed, Josep Carreras Leukaemia Research Institute, 08916, Badalona, Spain

<sup>†</sup>The authors contributed equally to this article.

\*Correspondence to:

Dr. Maribel Parra

Josep Carreras Leukaemia Research Institute (IJC)

Ctra de Can Ruti, Camí de les Escoles, s/n

08916 Badalona, Barcelona, Spain,

Phone: +34 935572800

E-mail: [mparra@carrerasresearch.org](mailto:mparra@carrerasresearch.org)

## ABSTRACT

Histone deacetylase HDAC7 is required for early B cell development and governs the acquisition of B cell progenitors gene identity. In addition, HDAC7 has been identified as a novel biomarker and prognostic factor in infant pro-B-ALL. However, its role in mature B cell biology and associated malignancies is unknown. Here, by using a conditional mouse model for specific deletion in activated B cells, we demonstrate that HDAC7 is essential for the entry and initiation of the germinal center (GC) reaction. HDAC7 deficiency results in the blockade of B cell development at the pre-GC stage, leading to the generation of aberrant GC B cells, diminished class switch recombination and plasma cell formation. We demonstrate that, while it is generally underexpressed in diffuse large B cell lymphoma (DLBCL) tumors, the low expression of HDAC7 is associated with a poor prognosis of the patients. Importantly, exogenous expression of HDAC7 in DLBCL cell lines reduces the proliferative capacity of these latter, as well as DLBCL tumorigenicity *in vivo*. In summary, our data revealed first, the essential function of HDAC7 in the establishment of the GC, and second, the potential contribution of HDAC7 deregulation in DLBCL development.

## INTRODUCTION

During terminal differentiation in peripheral lymphoid organs, B cells generate a hugely diverse repertoire of antibodies, which enable specific immune responses against potential pathogens encountered by the organism. The generation of this antibody diversity in mature B cells that have faced antigens occurs in germinal centers (GCs), transient microstructures where activated B cells undergo massive proliferation, eventually leading to the generation of high-affinity memory B cells (MBC) and long-lived antibody-secreting plasma cells (PC). (1, 2). Molecularly, this process is triggered by two mechanisms named class switch recombination (CSR) and somatic hypermutation (SHM) reaction. In response to T-cell dependent activation, naïve B lymphocytes are guided to the GCs, where they undergo cyclic rounds of affinity maturation across two differentiated physical compartments: the dark zone (DZ) and the light zone (LZ), (1, 3, 4). Proliferative expansion and SHM occur within the DZ; whereas in the LZ, B cells undergo affinity selection guided by T-follicular helper and follicular dendritic cells (5, 6). B cells in the LZ without sufficient affinity for initiating antigen, migrate back to the DZ for further cycles of proliferation and SHM. After several rounds of cyclical transit and, according to the properties of the antigen receptors generated, B cells either die, proliferate, or exit the GC and differentiate into MBC or PC.

This classical view of the GC reaction has been recently challenged by several studies demonstrating that B cells can differentiate into MBC and PC before entering the GC. In particular, single-cell transfer experiments unveiled the formation of GC-independent MBC derived from activated B cells, at the time GC are just beginning to coalesce (7, 8). Considering that the initial burst of MBC expresses IgM and IgD, they possibly originate before CSR occurs (9, 10). More commonly known are short-lived PC, also generated prior to GC-dependent PC (11).

A highly coordinated network of transcription factors (TFs) is essential for the correct GC reaction and terminal differentiation. Among them, BCL6 is one of the main regulators and is crucial to prevent premature activation of GC B cells (12). MEF2B induces BCL6 expression at the initiation of the GC reaction (13), whereas MEF2C is required for B cell proliferation upon T-cell activation (14). IRF4 initiates plasmablast differentiation by activating BLIMP1, a well-known TF that represses key B cell identity genes such as *Pax5* and is essential for PC program (15–18). BCL6 and BLIMP1 are mutually exclusive TFs that repress the specific gene signature of PCs and GC B cells, respectively. However, the identity of transcriptional regulators that control the early stages of B cell activation prior to the GC formation remains largely unknown.

Many B cell lymphomas arise from epigenetic and transcriptional alterations that lead to the dysregulation of relevant pathways for the GC physiology. Diffuse large B cell lymphoma (DLBCL) is the most common type of GC-derived B cell non-Hodgkin lymphoma (NHL), accounting for ~40% of all diagnosed cases (19). There are two different DLBCL subtypes, according to the postulated cell of origin; GC B-cell (GBC) subtype and activated B-cell (ABC) subtype, being the former the most frequent (about 60%). It has been reported that several TFs and epigenetic regulators are altered in DLBCL. Mutations in *EZH2*, *MYD88*, *CD79B*, *NOTCH1* and 2, *SGK1* or *TET2*, *BCL2* translocations, structural variations of BCL6 and *TP53* inactivation, are the most frequent alterations (20). Additionally, MEF2B loss-of-function is linked with oncogenic potential (21), while mutations in the methyltransferase gene, *KMT2D*, impair the enzymatic activity of this protein and occur early in DLBCL (22). Mutations in the histone acetyltransferases CREBBP and EP300 are also major pathogenic mechanisms. In consequence, the use of acetylating and deacetylating drugs constitute a promising strategy in DLBCL treatment (23).

Our group has previously identified the histone deacetylase HDAC7 as a master transcriptional repressor in early B-cell development, governing the acquisition of B cell progenitors' (pro-B cells) identity. We demonstrated that HDAC7 is crucial to repress lineage-inappropriate genes from the myeloid and T lymphoid branches and regulates additional epigenetic factors, such as TET2, to ensure proper early B cell differentiation within the bone marrow (24, 25). We have also reported that low HDAC7 expression essentially contributes to the pathogenesis of infant t(4;11) pro-B acute lymphoblastic leukemia (pro-B-ALL) representing a novel biomarker and prognostic factor (26). However, the role of HDAC7 in terminal B cell differentiation and B cell lymphomagenesis remains to be explored.

Here, we report that HDAC7 deficiency in activated B cells results in a differentiation blockade at the pre-GC stage, leading to the generation of aberrant GC B cells. Additionally, we demonstrate that HDAC7 is underexpressed in patients with DLBCL, correlating with a poor prognosis of the patients. Importantly, its forced re-expression reduces the proliferative capacity of lymphomagenic cells, both *in vitro* and *in vivo*.

## RESULTS

### HDAC7 is essential for the germinal center reaction

To test whether HDAC7 plays a role during the GC reaction and terminal B cell differentiation, we first determined its expression levels in different B cell subsets from murine bone marrow and spleen. We corroborated that *Hdac7* is highly expressed in pro-B and pre-B cells and increases its expression in GC B cells. As experimental control, we assessed the levels of *Aicda* and *Prdm1*, which are specifically expressed in GC B cells and PC, respectively (**Fig. 1A**). Next, to determine whether HDAC7 is required for the GC reaction we generated a conditional knock-out mouse model for the specific deletion of *Hdac7* in activated B cells. We crossed *Hdac7<sup>loxp/ko</sup>* mice with the *Cy1-Cre* strain, which expresses Cre recombinase in activated B cells to generate *Cy1-Cre;Hdac7<sup>+/+</sup>* (hereafter, wild-type) and *Cy1-Cre;Hdac7<sup>fl/ko</sup>* (hereafter, HDAC7-deficient) mice. We immunized wild-type and HDAC7-deficient mice with a T-cell dependent antigen (sheep red blood cells, (SRBC) to induce GC formation, and performed a series of phenotypic analysis 10 days later (see **Suppl. Fig. S1A** and **S1B** for gating strategy). The assessment of *Hdac7* mRNA levels in GC B cells upon immunization validated the deletion (**Fig. S1C**). Interestingly, flow cytometry analysis revealed a significant reduction in the percentage of GC B cells (B220<sup>+</sup>Fas<sup>+</sup>GL7<sup>+</sup>) in HDAC7-deficient mice (**Fig. 1B**). The total cell number and B cell number (B220<sup>+</sup>) in the spleen were also significantly decreased in an HDAC7-deficient scenario (**Fig. 1C** and **D**). In addition, we found that the number of PCs (CD138<sup>+</sup>) was significantly reduced in the spleen of HDAC7-deficient mice (**Fig. 1E**). Evaluation of the differentiation stage of those PCs that escape from the GC in the absence of HDAC7 showed that they were blocked at the dividing plasmablast stage in the spleen, incapable of reaching a mature differentiated stage (**Fig. 1F**). Together, these data indicate that HDAC7 is essential for the GC reaction and differentiation of B cells into PC.

### **An optimal CSR depends on the expression of HDAC7**

To assess the potential effect of HDAC7 deficiency in CSR we stimulated splenic B cells from wild-type and HDAC7-deficient mice *ex vivo* in the presence of IL-4 and LPS. First, we corroborated HDAC7 deletion at protein level upon *ex vivo* stimulation (**Fig. 2A**). Next, we assessed whether CSR was induced *ex vivo* by measuring IgG1 expression by flow cytometry at 24, 48 and 72 h after treatment. We found that HDAC7-deficient B cells showed a significant decrease in IgG1 production at 72h after induction (**Fig. 2B**). To further demonstrate the role of HDAC7 in CSR, we treated splenic B cells with IL-4 and anti-CD40 or with LPS alone, that trigger isotype switch to IgG1 and IgG3, respectively. The stimulation resembled the previous results, but interestingly, HDAC7-deficient CD43<sup>+</sup> cells display an obvious impairment in the specific production of IgG1 (**Fig. 2C and 2D**).

### **HDAC7 loss confers a global transcriptional reprogramming in GC B cells**

To shed light into the HDAC7-mediated mechanisms during the GC reaction we next performed RNA-seq of sorted GC B cells from wild-type and HDAC7-deficient mice after 10 days of immunization. We observed that 255 genes were differentially expressed in HDAC7-deficient GC B cells (**Fig. 3A**). Gene ontology analysis of the 156 upregulated genes in the absence of HDAC7 revealed an enrichment of transcripts involved in key processes such as cell cycle and cell division (*Smc1a*, *Ccne2*, and *Ccnf*), apoptosis (*Casp3* and *Casp7*) and response to DNA damage (*Parp1*, *Rad18*) (**Fig. 3B**). Conversely, the set of 99 genes downregulated in HDAC7-deficient GC B cells showed enrichment in transcription-related pathways (*Cbx4*, *Jmjd1c*, *Chd2*), as well as in regulation of cell proliferation (*Chst11*) (**Fig. 3C**). We validated our RNA-seq results on selected representative genes and tested their mRNA levels by RT-qPCR in GC B cells from wild-type and HDAC7-deficient immunized mice (**Figs. 3D and E**). These data indicate that

HDAC7 drives GC reaction by properly controlling cell cycle, proliferation and transcriptional processes.

### **HDAC7 deficiency alters proliferation of GC**

Since we observed a reduction of GC B cells in the absence of HDAC7, we then interrogated whether HDAC7 deficiency affects cell proliferation within GC. Unexpectedly, Ki67 staining of spleen sections 10 days post-immunization of wild-type and HDAC7-deficient mice revealed a higher number of Ki67<sup>+</sup> GC cells upon HDAC7 loss. Moreover, the area of Ki67<sup>+</sup> cells was also larger in the spleen follicles of HDAC7-deficient mice (**Fig. 4A and B**). These data suggest that in the absence of HDAC7, activated B cells may be blocked in an early or pre-GC B cell stage unable to properly enter into the GC reaction. To test this, we performed flow cytometry analysis to interrogate the presence of CD38<sup>+</sup> or IgD<sup>+</sup>, markers of naïve or pre-GC B cells, in the absence of HDAC7. Strikingly, we found that a significant high number of HDAC7-deficient GC B cells expressed CD38 and IgD surface markers (**Fig. 4C**). In addition, GC B cells from HDAC7-deficient mice showed an aberrant double positive CD38<sup>+</sup>IgD<sup>+</sup> cell population (**Fig. 4D**). These data, together with the finding that HDAC7-deficient mice have a significant reduction in GC B cells, suggest that HDAC7 plays a crucial role at early post-immunization events before B cells enter and form the GC.

### **Altered GC dynamics in HDAC7 deficient mice**

Next, we wondered whether the aberrant GC B cells observed in the absence of HDAC7, could also present altered GC dynamics. Flow cytometry analysis of GC B cells from wild-type and HDAC7-deficient mice immunized for 10 days revealed a significant loss of DZ (CXCR4<sup>+</sup>CD86<sup>-</sup>) population, balanced by the gain in LZ (CXCR4<sup>-</sup>CD86<sup>+</sup>) cell numbers (**Fig. 5A**). Intriguingly, whereas GC B cells derived from wild-type mice almost fully display mid/high levels of CXCR4, cells from HDAC7-deficient counterparts are



equally distributed in two subpopulations, classified as CXCR4<sup>low</sup> and CXCR4<sup>mid/high</sup> (**Fig. 5B**). To further define the nature of HDAC7-deficient GC B cells sub-populations, we performed cell cycle analysis. Cells within the LZ were found in G0/G1 phase both in wild-type and HDAC7-deficient mice, characteristic of the cell cycle status within this compartment (**Fig. 5C**). However, HDAC7-deficient cells displayed an increased percentage of DZ cells (CXCR4<sup>mid/high</sup>CD86<sup>-</sup>) in G2 phase, in contrast to a diminished G0/G1 cell fraction, thus indicating a higher proliferation rate upon HDAC7 depletion (**Fig. 5D**). The majority of the atypical CXCR4<sup>low</sup> GC B cell population of HDAC7-deficient cells was also found in a G1 resting state and decreased in S phase (**Fig. 5E**). To gain further insight into the role of HDAC7 in GC dynamics, we performed Gene Set Enrichment Analysis (GSEA) on RNA-seq data of GC B cells from wild-type and HDAC7-deficient mice using previously reported DZ-LZ gene signatures (27). The analysis unveiled that GC B cells from HDAC7-deficient mice harbour gene signatures characteristic of the DZ compartment (**Fig. 5F-H**). These results suggest that HDAC7 deletion promotes an aberrant DZ-LZ program that impairs optimal polarization of GC B cells. Assessment of cell death levels in immunized mice revealed that the HDAC7-deficient GC B cells are prone to die by apoptosis, probably due to their aberrant cellular identity (**Fig. 5I**).

### **HDAC7 is underexpressed in DLBCL and correlates with poor prognosis**

Given the important role of HDAC7 during the pre-GC and GC reaction we hypothesized that its deregulation may have an effect in the development of GC-derived B cell neoplasm. In fact, HDAC7 is mutated in 6% of DLBCL patients (28). In addition, HDAC7 was identified as a potential tumour suppressor in DLBCL cell lines (29). To test whether HDAC7 is involved in B cell lymphomagenesis, we first mined public RNA-seq data profiles in primary human (30, 31) and murine (32, 33) DLBCL samples, compared to control GC B cells. The comparison of DLBCL cases *versus* healthy GC B cell samples

revealed that HDAC7 was significantly underexpressed in this NHL subtype (**Fig. 6A**). Moreover, RT-qPCR assays corroborated the significant underexpression of HDAC7 in both ABC and GCB human DLBCL sub-types, when compared to GC B cells purified from tonsils obtained from healthy donors (**Fig. 6B**). We next analyzed the effect of different HDAC7 expression levels in DLBCL transcriptome signature. RNA-seq data from the 63 human DLBCL samples included in Fig. 6A were allocated in different groups based on the expression levels of HDAC7 (HDAC7<sup>normal</sup> and HDAC7<sup>very low</sup>, as depicted in colored points in Fig. 6A) and compared them to the transcriptome of healthy GC B cells. Strikingly, DLBCL patients harboring normal levels of HDAC7 exhibited a transcriptomic profile similar to that of healthy donors, suggesting that inducing HDAC7 expression could associate to an improved prognosis (**Fig. 6C**). To test this possibility, we next evaluated the clinical outcome in a cohort of 292 DLBCL patients treated with conventional R-CHOP immunotherapy corresponding to two different datasets (34, 35). Importantly, we observed that lower expression of HDAC7 was associated to a poorer survival (**Fig. 6D**). These data indicate that absence or low levels of HDAC7 may not only be involved in the pathogenesis of DLBCL, thereby representing a novel biomarker, but also defining a novel prognostic factor for this disease.

### **HDAC7 expression reduces DLBCL malignancy *in vitro* and *in vivo***

To further evaluate the potential role of HDAC7 in B cell lymphomagenesis we next analyzed its expression levels in DLBCL established cell lines. We found that several DLBCL cell lines display underexpression of HDAC7 and centered our further experiments on MD901 cells, which harbor very low levels (**Fig. 7A**). To assess whether the absence of HDAC7 is associated with lymphomagenesis, we performed a gain-of-function experimental approach, by transducing a two-step retroviral vector that enables forced exogenous HDAC7 overexpression in an inducible manner upon doxycycline addition (**Fig.**

**7B**). We observed that HDAC7 expression significantly inhibited the proliferation of MD901 cells (**Fig. 7C and D**), concomitant to increased levels of programmed cell death (**Fig. 7E**). To determine whether HDAC7 reduces the growth of DLBCL *in vivo*, we subcutaneously implanted  $5 \times 10^6$  newly generated MD901 cells with inducible HDAC7 expression (or its empty vector counterparts) in immunodeficient mice. Following the experimental approach in **Fig. 7F**, we observed that HDAC7 expression significantly suppressed DLBCL cells growth in terms of tumor volume (**Fig. 7G and H**) and tumor weight (**Fig. 7I**). Flow cytometry analysis of the tumors revealed that HDAC7 expression led to apoptotic death as measured by Annexin V and DAPI staining (**Fig. 7J**). To delineate the anti-lymphomagenic mechanisms mediated by HDAC7 in DLBCL cells we next performed RNA-seq of tumors generated in its absence and presence. Exogenous expression of HDAC7 resulted in an increase of programmed cell death pathways, highlighting the upregulation of genes involved in apoptosis and death receptor signaling. At the same time HDAC7 expression disrupted the post-translational machinery, downregulating several genes involved in the protein folding mediated by chaperones (**Fig. 7K**). Additionally, deeper insight into transcriptomic data revealed that HDAC7-overexpressing cells present a significant enrichment in transcripts associated to cell death regulation and apoptosis. (**Fig. 7L**). Taken together, our data indicate that HDAC7 could be a valuable novel biomarker and prognostic factor in DLBCL.

## MATERIALS AND METHODS

### Study design

In this study we aimed to understand the role of the transcriptional regulator HDAC7 in the terminal B cell lymphopoiesis and GC-derived malignancy, DLBCL. For this purpose, we generated a conditional mutant mouse model to delete HDAC7 upon B cell activation and investigated its phenotype. Eight-to-ten days after mice immunization, we assessed by FACS the GC and PC populations. *Ex vivo* cell culture of CD43<sup>+</sup> splenic cells combined with FACS analysis allowed us to investigate CSR status. RNA-seq analysis showed that HDAC7-deficient mouse displayed global changes in its transcriptomic program, highlighting a defective cell cycle, entrance to the GC reaction and GC polarization. We analysed HDAC7 expression in more than fifty DLBCL patients and confirmed its underexpression by RT-qPCR. In addition, we modified a DLBCL cell line with low expression levels of HDAC7 to exogenously induce HDAC7 upon doxycycline treatment to investigate the proliferative capacity *in vitro* but also *in vivo* in a xenograft model. The system unveiled a block in proliferation and apoptosis induction.

### Mice

*Hdac7<sup>fl/ko</sup>* on C57BL/6 mice have been previously described (24) and were kindly provided by Dr. Eric Olson (UT Southwestern Medical Center, Dallas, TX, USA). *Cy1-cre* on C57BL/6 (B6.129P2(Cg)-Ighg1<tm1(cre)Cgn>) mice were obtained from The Jackson Laboratory. Experiments were performed with 8-12-week-old mice. *Hdac7<sup>fl/ko</sup>* was crossed with *Cy1-cre* to generate *Cy1-cre;Hdac7<sup>fl/ko</sup>*. 8-14 weeks old NSG mice were used as recipient mice in xenograft transplantation experiments. Mice procedures were approved by the Animal Experimentation Ethics Committee (CEEA) of the Comparative Medicine and Bioimage Centre of Catalonia (CEEA-CMCiB) of the IGTP (Institut Germans Trias i

Pujol, Badalona, Spain), in accordance with the current Spanish and European legislation regulating ethical research and animal welfare.

### **Human GC B cells and DLBCL patient samples**

Human germinal center B cells were separated from tonsils of children undergoing tonsillectomies. Tonsils were minced extensively and after Ficoll-Isopaque density centrifugation, enrichment of B cells was performed with the AutoMACS system by positive selection of CD19<sup>+</sup> cells, and subsequently germinal center B cells were selected using FACS sorting by their high CD20 and medium CD38 expression.

RNA from DLBCL patients was obtained from formalin-fixed paraffin-embedded (FFPE) samples of lymph nodes using the RecoverAll kit (Ambion, Carlsbad, CA) according to the manufacturer's instructions. Samples acquisition was approved by the institutional research board of Hospital Germans Trias i Pujol (Reference: EO-12-072) in accordance with the Declaration of Helsinki.

### **Cell lines**

The DLBCL cell lines, MD901, SU-SHL 4, SU-DHL 8 and RIVA were grown in RPMI medium supplemented with 10% FBS, 1% penicillin G/streptomycin and L-glutamine. OCI-LY 3 and OCI-LY 8 were grown in IMDM medium supplemented with 20% FBS, 1% penicillin G/streptomycin. HEK-293T cell line was cultured in DMEM medium supplemented with 10% FBS, 1% penicillin G/streptomycin. Cells were grown at 37°C, 5% CO<sub>2</sub>.

### **Flow cytometry and cell-sorting**

Control *Cy1-cre;Hdac7<sup>+/+</sup>* and *Cy1-cre;Hdac7<sup>fl/ko</sup>* were immunized intravenously at 8 to 12 weeks of age with 0.1 ml suspension of 400 million sheep red blood cell (SRBC) in PBS (Gibco) to induce GC formation. Mice were sacrificed after 10 days and spleens were isolated. To cell-sort and to determine the percentage of GC B cell population, single-cell

suspensions from spleens were stained using the following fluorescent-labelled anti-mouse antibodies: BV421 conjugated anti-B220 (BD Biosciences), PE-Cy7 conjugated anti-FAS (BD Biosciences), eFluor660 conjugated anti-CD95 (Invitrogen). To evaluate Dark Zone and Light Zone status, GC B cells were stained with PE conjugated anti-CXCR4 and eFluor710 conjugated with anti-CD86 from BD Biosciences and Invitrogen, respectively. PC were stained with BV510 conjugated with anti-CD138, and positive cells were stained with PE conjugated anti-CD19 and BV421 conjugated anti-B220, from BD Biosciences to assess its developmental stage (dividing plasmablast (B220<sup>+</sup>CD19<sup>+</sup>), early PC (B220<sup>-</sup>CD19<sup>+</sup>), mature resting PC (B220<sup>-</sup>CD19<sup>-</sup>)). Ig were stained with biotinylated anti-IgG1 and anti-IgG3 (BD Biosciences). To cell sort pro-B cells, pre-B cells, and naïve B cells, splenic cells were also stained with APC conjugated anti-CD43 and PE-CF594 conjugated anti-IgM, from BD Biosciences. DAPI or 7AAD were used for the exclusion of dead cells. The data was analyzed by FlowJo software. See Supplementary Figure 1 for sorting gating strategies.

### ***Ex vivo* cell cultures**

Primary B cells were purified by immunomagnetic depletion using anti-CD43 beads (Miltenyi Biotec) and cultured at a final concentration of  $1.2 \times 10^6$  cells per ml in complete RPMI supplemented with 10% FBS, 50 mM of 2-βMercaptoethanol (Gibco), 20 mM Hepes (Gibco). When indicated, cells were treated with: IL4 (PeproTech) plus lipopolysaccharide (LPS, Sigma-Aldrich) at 20 ng/ml and 25 µg/ml, respectively; anti-mouse CD40 (BD Pharmingen) at 1µg/ml; LPS at 25µg/ml.

### **RT-qPCR analysis**

Total RNA was extracted with RNeasy Mini kit (Qiagen). RNA was subsequently converted into cDNA using the High Capacity cDNA Reverse Transcription Kit (AB Applied Biosystems) according to the manufacturer's instructions. Real-time-quantitative PCR (RT-

qPCR) was performed in triplicate using SYBR Green I Master (Roche). PCR reactions were run and analyzed using the LightCycler 480 Detection System (Roche). Primers sequences will be provided upon request.

### **Western blot**

Isolated cells were lysed with RIPA buffer. Lysates were resolved on 8%-12% SDS-PAGE (Mini-Protean electrophoresis chamber, Bio-Rad) and transferred on nitrocellulose membranes (Amersham Biosciences). Membranes were blocked in 5% milk in TBS with 0.1% Tween (TBS-T) and incubated overnight at 4°C, with primary antibodies (anti-HDAC7 sc-11421, Santa Cruz Biotechnology 1:1000, anti- $\beta$ -actin AC-15, Sigma-Aldrich 1:10000, anti  $\alpha$ -Tubulin T6199, Merck 1:10000). Secondary antibody incubations were carried out for 1h at room temperature with 700nm or 800 nm fluorescent labelled anti-mouse or anti-rabbit antibodies from LI-COR. Protein signal was detected using the infrared laser-based Odyssey CLx instrument (LI-COR Biosciences).

### **Plasmids and retroviral supernatant generation**

pRetro-X-Tight-Pur-HDAC7 constructs were generated by cloning full length or deleted HDAC7 cDNAs obtained by EcoRI digestion of the pcDNA3.1-HDAC7 plasmids into the pRetro-X-Tight-Pur vector (Takara Bio, Otsu, Japan). For retrovirus generation, pRetro-X-Tight-Pur-HDAC7 and pRetro-X-Tet-On-Advanced (Takara Bio) plasmids were transfected into the packaged cell line Platinum-E and the supernatant was collected 48 h post transfection. pLKO.1-GFP lentiviral vector was obtained from Addgene (Cambridge, MA, USA).

### **Retroviral transduction and doxycycline treatment**

Inducible HDAC7 expression in cell line was achieved by the generation of the MD901 Tet-On-Tight-HDAC7 cell line. In brief, MD901 cells were first infected with the supernatant containing the pRetro-X-Tet-On-Advanced viral particles overnight and 72 h later selected

with 1.5  $\mu\text{g/ml}$  geneticin (GIBCO, Carlsbad, CA, USA) for 2-3 weeks. Next the selected cells were infected with the pRetro-X-Tight-Pur-HDAC7 viral particles overnight and after 72 h selected with 3  $\mu\text{g/ml}$  puromycin. For HDAC7 expression, cells were treated with 500 ng/ml of doxycycline for the indicated periods. pLKO.1-GFP positive cells were sorted by flow cytometry.

### **Proliferation assays**

For the MTT assays,  $5 \times 10^4$  cells were plated onto 24-well plates. At different time points, MTT was added at a final concentration of 5 mg/ml. After incubation for 3 h (37 °C, 5% CO<sub>2</sub>), the blue formazan derivative was solubilized in dimethyl sulfoxide and the absorbance was measured at 570 nm. Cell proliferation was also assessed by cell counting.

### **Cell viability assay**

Cell cycle and apoptosis were assessed by DAPI (1  $\mu\text{g/ml}$ ), 7AAD (0,5  $\mu\text{g/ml}$ ) or Hoechst (5  $\mu\text{g/ml}$ ) (distribution of cells in G<sub>0</sub>/G<sub>1</sub>, S and G<sub>2</sub>/M phase) and Annexin V-PE staining (BD Biosciences), respectively, followed by flow cytometry analysis using a FACSCanto II (BD Biosciences) flow cytometer. Data was analyzed using FlowJo software.

### **Spleen section histology**

Mice spleens were fixed in 10% formalin, embedded in paraffin and sectioned at 4  $\mu\text{m}$ . Antigen retrieval was done by steaming the slides for 20 min, then cooling for 20 min in citrate buffer (10 mM acid citric, 0.05% Tween 20 pH 6.0). Endogenous peroxidase was blocked with a 0.3% hydrogen peroxide solution for 10 min. For protein block, we used 1% BSA for 60 min at RT. Sections were incubated with anti-HDAC7 (1:100, ab53101) or anti-Ki67 (1:100, ab16667) overnight at 4 °C. Biotinylated reagents were detected with Vectastain ABC kit (PK-6100, Vector laboratories). Peroxidase activity was developed using ImmPACT DAB HRP substrate (Vector laboratories). The sections were



counterstained with hematoxylin for 1 min prior to dehydrating and mounting. Sections were imaged under a Scope.A1 microscope (ZEISS). The number of GCs, the total spleen area occupied by GCs and the average area occupied by the GCs were quantified using ImageJ 1,44o (NIH) software.

### **Mice xenograft and *in vivo* cell cycle analysis**

MD901 cells infected with Tet-On-Tight-HDAC7 and pLKO.1-GFP lentiviruses with inducible control of HDAC7 were used for the xenograft experiment. 8 to 12 week-old NSG mice housed in barrier environment were subcutaneously injected in the left and right flank with  $5 \times 10^6$  MD901 cells with control and HDAC7 MD901 cells, respectively. After 2 weeks, when the tumor volumes were around 50-100 mm<sup>3</sup>, engrafted mice were given doxycycline in drinking water (1 mg/ml) to induce HDAC7 expression. Tumor volumes were monitored every 2-3 days using a calliper and calculated using the following formula: tumor volume (mm<sup>3</sup>) = (smallest diameter<sup>2</sup> × largest diameter)/2. The mice were sacrificed after three weeks and tumors were harvested. For flow cytometry and RNA extraction tumors were homogenized to get single cell suspension.

### **RNA-seq and analysis**

Total RNA was extracted from HDAC7-deficient and control sorted GC B cells in the Genomics facility of Institute for Research in Biomedicine (IRB) in Barcelona, and quantified and subjected to quality control using a Bioanalyzer apparatus (IRB, Barcelona). RNA from xenograft samples was obtained using RNeasy Mini kit (Qiagen). Low input library was performed in all samples, and then 100bp PE sequenced at BGI Genomics Service (China), obtaining a minimum of 60M reads per sample. Quality control of the samples was performed with FASTQC tool (available at <https://www.bioinformatics.babraham.ac.uk/projects/fastqc/>). Data is publicly available in GEO repository (GSE228738). Paired-end reads were aligned to the murine reference

genome (GRCm38) using STAR (version 2.7.0a) (52). A count table file indicating the number of reads per gene in each sample was generated using HTSeq (version 0.10.0) (53). Genes with no or very low expression were filtered out and differentially expressed genes were identified using DESeq2 (54), requiring a minimum adjusted p-value of 0.05 and a  $|\log_2FC|$  value greater than 0.5. Gene set enrichment analysis was performed with DAVID tools (55). Functional analysis was performed using gene set enrichment analysis (GSEA) (56) using a pre-ranked list of curated gene sets (available at: <https://www.gsea-msigdb.org/gsea/msigdb/>). Healthy GC B cells and DLBCL FASTQ files were obtained as referenced in the text and analyzed as described above, aligning to the human reference genome (GRCh38).

### **Statistics analysis**

Statistical was analyzed by using GraphPad Prism (GraphPad Software) and presented as means  $\pm$  SEM. Unpaired Student *t* tests analysis with Bonferroni post-hoc test was used in data analysis. A p value  $<0.05$  was considered statistically significant. ns:  $p>0.05$ , \*:  $p < 0.05$ , \*\*:  $p < 0.01$ , \*\*\*:  $p < 0.001$ . The number of mice used in every experiment are included in the respective figure legend.

### **DATA AVAILABILITY**

Data are available in GEO repository as GSE228738.

### **ACKNOWLEDGEMENTS**

We thank CERCA Programme/Generalitat de Catalunya for institutional support. We thank Dr. Eric Olson (UT Southwestern Medical Center, Dallas, TX, USA) for the *Hdac7<sup>loxp/-</sup>*.

### **FUNDING**

This work was supported by the Spanish Ministry of Economy and Competitiveness (MINECO, SAF2017-87990-R) and the Spanish Ministry of Science and Innovation (MICINN, EUR2019-103835) and elaborated at the Josep Carreras Leukaemia Research

Institute (IJC, Badalona, Barcelona). AM is funded by the Spanish Ministry of Science, Innovation and Universities, which is part of the Agencia Estatal de Investigación (AEI), through grant PRE2018-083183 (cofunded by the European Social Fund). OdB was funded by a Juan de la Cierva Formación Fellowship from the Spanish Ministry of Science, Innovation and Universities (FJCI-2017-32430 grant) and by a Postdoctoral Fellowship from the Asociación Española Contra el Cáncer (AECC) Foundation (POSTD20024DEBA grant). BG was supported by the National Research, Development and Innovation Office (PharmaLab, RRF-2.3.1-21-2022-00015 and TKP2021-NVA-15).

### **COMPETING INTERESTS**

The authors declare no competing interests

## FIGURE LEGENDS

### Fig. 1. HDAC7 is required for the GC reaction and PC generation

**A**, Relative mRNA expression of *Hdac7*, *Aicda* and *Prdm1* in sorted pro-B, pre-B, naïve B cells, GC B cells and PC (n=3). *Rpl38* and *Gapdh* were used as housekeeping genes. **B**, Flow cytometry assessment of GC B cells (B220<sup>+</sup>GL7<sup>+</sup>FAS<sup>+</sup>) from wild-type (n=7) and HDAC7-deficient mice (n=21). **C**, Absolute number quantification of total splenic cells from wild-type (n=11) and HDAC7-deficient mice (n=8). **D**, As in C, but for total number of B cells, calculated as the %B220<sup>+</sup> population on total splenic cell number. **E**, Percentage of PC (CD138<sup>+</sup>) in spleen (left panel) and bone marrow (right panel) (n=3-4 in wild-type and 6-10 in HDAC7-deficient). **F**, Percentage of dividing plasmablasts (B220<sup>+</sup>CD19<sup>+</sup>CD138<sup>+</sup>), early PC (B220<sup>+</sup>CD19<sup>-</sup>CD138<sup>+</sup>) and mature resting PC (B220<sup>-</sup>CD19<sup>+</sup>CD138<sup>+</sup>) from spleen (left panel) and bone marrow (right panel) of wild-type and HDAC7-deficient mice (n=5-6 per condition). Data is represented as mean ± SEM of above-mentioned independent experiments. \*  $P < 0.05$ ; \*\*  $P < 0.01$ ; \*\*\*  $P < 0.001$ ; unpaired Student's *t* test.

### Fig. 2. HDAC7 is required for CSR

**A**, HDAC7 global protein levels analyzed by Western blot in CD43<sup>-</sup> splenic cells from wild-type and HDAC7-deficient mice after *ex vivo* stimulation at the indicated time points (0h and 72h). Total β-Actin levels were used as control. Image is representative of 3 independent experiments. **B**, Representative histogram (left panel) and quantification (right panel) of flow cytometry analysis of IgG1 levels from wild-type and HDAC7-deficient CD43<sup>-</sup> splenic cells at 24h, 48h and 72h after *ex vivo* stimulation with LPS and IL-4 (n=4-10 mice per condition). **C**, As in **B**, but after stimulation with IL-4 and anti-CD40 **D**, As in **B**, but measuring IgG3 levels after stimulation with LPS alone. Data is represented as mean ± SEM of above-mentioned independent experiments. \*  $P < 0.05$ ; unpaired Student's *t* test.

### Fig. 3. HDAC7 loss induces transcriptional changes in GC B cells.

**A**, Differentially expressed genes in sorted GC B cells from three wild-type and four HDAC7-deficient mice. In the heatmap, rows correspond to genes and columns correspond to different mice. Scale bar indicates the Z score (blue, reduced expression; yellow, increased expression; (FDR<0.05, log<sub>2</sub>FC>0.36 or <-0.44)). **B**, Gene ontology of genes upregulated in HDAC7-deficient GC B cells from A. Color scale bar indicates level of significance, while dot sizes indicate the number of genes included in each pathway depicted. **C**, As in **B**, but for downregulated genes. **D**, Relative mRNA expression of selected upregulated genes *Smc1a*, *Parp1* and *Rad18*. *Rpl38* and *Gapdh* were used as housekeeping genes (n=3-8 samples per condition). **E**, As in D, but for downregulated genes *Cbx4*, *Jmjd1c*, *Chd2* and *Chst11*. Data is represented as mean ± SEM of above-mentioned independent experiments. \*  $P<0.05$ ; \*\*  $P<0.01$ ; unpaired Student's *t* test.

**Fig. 4. Cell cycle is disrupted upon HDAC7 deficiency.**

**A**, Immunohistochemical analysis of HDAC7 and Ki67 expression (brown) in representative FFPE spleen sections from wild-type and HDAC7-deficient immunized mice. Non-immunized wild-type mice injected with PBS were used as experimental control. **B**, Quantification of Ki67<sup>+</sup> area per mm<sup>2</sup> (left panel) and size of the Ki67<sup>+</sup> regions in μm<sup>2</sup> (right panel) of the spleens from wild-type and HDAC7-deficient immunized mice (n=6 per condition). **C**, representative flow cytometry plots and quantification of the IgD<sup>+</sup> (upper panel) and the CD38<sup>+</sup> (lower panel) cell population, gated on GC B cells (n=5-6 per condition). **D**, As in **C** but quantifying the double positive IgD<sup>+</sup>CD38<sup>+</sup> GC B cell population. Data is represented as mean ± SEM of above-mentioned independent experiments. \*  $P<0.05$ ; \*\*  $P<0.01$ ; unpaired Student's *t* test.

**Fig. 5. HDAC7 loss alters the GC polarization.**

**A**, Representative flow cytometry plots (left panel) and percentual quantification analysis (right panel) of dark zone (DZ) (CXCR4<sup>+</sup> CD86<sup>-</sup>) and light zone (LZ) (CXCR4<sup>-</sup> CD86<sup>+</sup>)

compartments (n=7 per condition). **B**, Representative flow cytometry plots (left panel) and percentual quantification analysis (right panel) of DZ CXCR4<sup>low</sup> and CXCR4<sup>mid/high</sup> compartments. **C-E**, Cell cycle assessment and representative plots of the previous populations: **C**, LZ; **D**, CXCR4<sup>mid/high</sup> subset from the DZ and **E**, CXCR4<sup>low</sup> subset from the DZ. **F-H**, Gene-set enrichment analysis (GSEA) of curated gene sets of DZ and LZ identity over RNA-seq data from HDAC7-deficient versus wild-type GC B cells. **I**, Percentage of apoptotic (AnnexinV<sup>+</sup>) GC B cells from wild-type and HDAC7-deficient immunized mice (n=4 per condition). Data is represented as mean  $\pm$  SEM of above-mentioned independent experiments. \*  $P < 0.05$ ; \*\*  $P < 0.01$ ; unpaired Student's *t* test.

**Fig. 6. HDAC7 is underexpressed in DLBCL and correlates with poor prognosis.**

**A**, RNA-seq analysis of HDAC7 normalized counts of 63 DLBCL human patients versus 4 healthy GC controls (30, 31) (left panel), and from murine DLBCL samples versus control GC B cells (32, 33) (right panel). **B**, Relative HDAC7 mRNA quantification of GC B cells from healthy tonsils (n=4), and ABC and GCB DLBCL patients (n=3 per lymphoma subtype). **C**, Random clustering of colored points in **A** right panel, determined by HDAC7 expression levels (HDAC7<sup>normal</sup> in black, HDAC7<sup>very low</sup> in orange). **D**, Km-plot based on HDAC7 expression of 292 DLBCL patients from two datasets (34, 35). Data is represented as mean  $\pm$  SEM of above-mentioned independent experiments. \*  $P < 0.05$ ; \*\*\*  $P < 0.001$ ; unpaired Student's *t* test.

**Fig. 7. HDAC7 expression reduces proliferation *in vivo* and *ex vivo*.**

**A**, Assessment of HDAC7 protein levels of some DLBCL cell lines. Representative assay of three-independent experiments. **B**, Analysis of HDAC7 expression by western blot in MD901 cells transduced to express HDAC7 in a doxycycline (D) inducible manner (Tet-On-Tet-Tight-HDAC7). Where indicated, cells were treated with D for, for 72 hours. Representative assay of three-independent experiments. **C**, Determination of cell number

at the indicated time points of treatment with doxycycline. Cell proliferation was determined by cell counting (n=3 per condition). **D**, MTT assay measuring viability of MD901 cells upon induction of HDAC7 *E* (*Tet-On-Tet-Tight-Empty vector*), *H7* (*Tet-On-Tet-Tight-HDAC7*) (n=3 per condition). **E**, Percentage of dead cells was assessed by 7AAD and Annexin-V staining and analyzed by flow cytometry. The figure is representative of three experiments with similar results. **F**, Representative scheme of xenografts experiment performed in immunodeficient NSG mice. **G**, Image of the extracted tumors at day 11 post-treatment (n=11). **H**, Relative volume quantification of tumors shown in **G**. **I**, As in **H**, but analyzing weight of the tumors. **J**, Percentage of late apoptotic cells (AnnexinV<sup>+</sup>, DAPI<sup>+</sup>) in the xenografts. **K**, Gene ontology of the differentially expressed genes from RNA sequenced xenografts that are upregulated (left panel) and downregulated (right panel) in HDAC7-expressing tumors compared to those tumors without HDAC7 overexpression (n=2-3 per condition). **L**, Gene-set enrichment analysis of curated gene sets of *Cell death regulation* and *Apoptosis* over RNA-seq data from xenografts. Data is represented as mean ± SEM of above-mentioned independent experiments. \*  $P < 0.05$ ; \*\*  $P < 0.01$ ; \*\*\*  $P < 0.001$ ; unpaired Student's *t* test.

**Supplementary Fig. 1.** **(A)** Flow cytometry plots representation of the gating strategy followed to identify GC B cells (B220<sup>+</sup>; GL7<sup>+</sup>;FAS<sup>+</sup>), naïve B cells (B220<sup>+</sup>; IgM<sup>+</sup>) and PC (CD138<sup>+</sup>) from mouse spleen. **(B)** Flow cytometry plots representation of the gating strategy followed to identify pro-B (B220<sup>+</sup>; CD19<sup>+</sup>;IgM<sup>-</sup>;CD43<sup>+</sup>) and pre-B cells (B220<sup>+</sup>; CD19<sup>+</sup>;IgM<sup>-</sup>;CD43<sup>-</sup>) from mouse bone marrow. **(C)** Relative mRNA quantification of *Hdac7* expression in sorted GC B cells from control and HDAC7-deficient mice spleens. *Rpl38* and *Gapdh* were used as housekeeping genes. Data in C is represented as mean ± SEM of 4 independent experiments. \*\*  $P < 0.01$ ; unpaired Student's *t* test.

## REFERENCES

1. L. Mesin, J. Ersching, G. D. Victora, Germinal Center B Cell Dynamics. *Immunity*. **45**, 471–482 (2016).
2. G. D. Victora, M. C. Nussenzweig, Germinal Centers. *Annu. Rev. Immunol.* **40**, 413–442 (2022).
3. G. D. Victora, M. C. Nussenzweig, Germinal Centers. *Annu. Rev. Immunol.* **30**, 429–457 (2012).
4. N. S. De Silva, U. Klein, Dynamics of B cells in germinal centres. *Nat. Rev. Immunol.* **15**, 137–148 (2015).
5. C. D. C. Allen, T. Okada, J. G. Cyster, Germinal-Center Organization and Cellular Dynamics. *Immunity*. **27**, 190–202 (2007).
6. G. D. Victora, T. A. Schwickert, D. R. Fooksman, A. O. Kamphorst, M. Meyer-Hermann, M. L. Dustin, M. C. Nussenzweig, Germinal Center Dynamics Revealed by Multiphoton Microscopy with a Photoactivatable Fluorescent Reporter. *Cell*. **143**, 592–605 (2010).
7. J. J. Taylor, K. A. Pape, M. K. Jenkins, A germinal center–independent pathway generates unswitched memory B cells early in the primary response. *J. Exp. Med.* **209**, 597–606 (2012).
8. F. J. Weisel, G. V. Zuccarino-Catania, M. Chikina, M. J. Shlomchik, A Temporal Switch in the Germinal Center Determines Differential Output of Memory B and Plasma Cells. *Immunity*. **44**, 116–130 (2016).
9. J. A. Roco, L. Mesin, S. C. Binder, C. Nefzger, P. Gonzalez-Figueroa, P. F. Canete, J. Ellyard, Q. Shen, P. A. Robert, J. Cappello, H. Vohra, Y. Zhang, C. R. Nowosad, A. Schiepers, L. M. Corcoran, K.-M. Toellner, J. M. Polo, M. Meyer-Hermann, G. D. Victora, C. G. Vinuesa, Class-Switch



- Recombination Occurs Infrequently in Germinal Centers. *Immunity*. **51**, 337-350.e7 (2019).
10. C. Viant, T. Wirthmiller, M. A. ElTanbouly, S. T. Chen, M. Cipolla, V. Ramos, T. Y. Oliveira, L. Stamatatos, M. C. Nussenzweig, Germinal center-dependent and -independent memory B cells produced throughout the immune response. *J. Exp. Med.* **218** (2021), doi:10.1084/jem.20202489.
  11. S. L. Nutt, P. D. Hodgkin, D. M. Tarlinton, L. M. Corcoran, The generation of antibody-secreting plasma cells. *Nat. Rev. Immunol.* **15**, 160–171 (2015).
  12. K. Basso, R. Dalla-Favera, Roles of BCL6 in normal and transformed germinal center B cells. *Immunol. Rev.* **247**, 172–183 (2012).
  13. C. Y. Ying, D. Dominguez-Sola, M. Fabi, I. C. Lorenz, S. Hussein, M. Bansal, A. Califano, L. Pasqualucci, K. Basso, R. Dalla-Favera, MEF2B mutations lead to deregulated expression of the oncogene BCL6 in diffuse large B cell lymphoma. *Nat. Immunol.* **14**, 1084–1092 (2013).
  14. P. R. Wilker, M. Kohyama, M. M. Sandau, J. C. Albring, O. Nakagawa, J. J. Schwarz, K. M. Murphy, Transcription factor Mef2c is required for B cell proliferation and survival after antigen receptor stimulation. *Nat. Immunol.* **9**, 603–612 (2008).
  15. K.-I. Lin, C. Angelin-Duclos, T. C. Kuo, K. Calame, Blimp-1-Dependent Repression of Pax-5 Is Required for Differentiation of B Cells to Immunoglobulin M-Secreting Plasma Cells. *Mol. Cell. Biol.* **22**, 4771–4780 (2002).
  16. Y. Lin, K. Wong, K. Calame, Repression of c- myc Transcription by Blimp-

- 1, an Inducer of Terminal B Cell Differentiation. *Science* (80-. ). **276**, 596–599 (1997).
17. J. F. Piskurich, K. Lin, Y. Lin, Y. Wang, J. P. Ting, K. Calame, C. li, BLIMP-1 mediates extinction of major histocompatibility class II transactivator expression in plasma cells. *Nat. Immunol.* **1** (2000).
  18. M. Minnich, H. Tagoh, P. Bönelt, E. Axelsson, M. Fischer, B. Cebolla, A. Tarakhovsky, S. L. Nutt, M. Jaritz, M. Busslinger, Multifunctional role of the transcription factor Blimp-1 in coordinating plasma cell differentiation. *Nat. Immunol.* **17**, 331–343 (2016).
  19. S. Swerdlow, N. Harris, J. ES, P. SA, S. H, T. J, WHO Classification of Tumours of Haematopoietic and Lymphoid Tissues. *Lyon Int. Agency Res. Cancer.* **2** (2016) (available at <http://apps.who.int/bookorders/anglais/detart1.jsp?codlan=1&codcol=70&codcch=4002>).
  20. G. W. Wright, D. W. Huang, J. D. Phelan, Z. A. Coulibaly, S. Roulland, R. M. Young, J. Q. Wang, R. Schmitz, R. D. Morin, J. Tang, A. Jiang, A. Bagaev, O. Plotnikova, N. Kotlov, C. A. Johnson, W. H. Wilson, D. W. Scott, L. M. Staudt, A Probabilistic Classification Tool for Genetic Subtypes of Diffuse Large B Cell Lymphoma with Therapeutic Implications. *Cancer Cell.* **37**, 551-568.e14 (2020).
  21. P. Brescia, C. Schneider, A. B. Holmes, Q. Shen, S. Hussein, L. Pasqualucci, K. Basso, R. Dalla-Favera, MEF2B Instructs Germinal Center Development and Acts as an Oncogene in B Cell Lymphomagenesis. *Cancer Cell.* **34**, 453-465.e9 (2018).
  22. J. Zhang, D. Dominguez-Sola, S. Hussein, J.-E. Lee, A. B. Holmes, M.

- Bansal, S. Vlasevska, T. Mo, H. Tang, K. Basso, K. Ge, R. Dalla-Favera, L. Pasqualucci, Disruption of KMT2D perturbs germinal center B cell development and promotes lymphomagenesis. *Nat. Med.* **21**, 1190–1198 (2015).
23. L. Pasqualucci, D. Dominguez-Sola, A. Chiarenza, G. Fabbri, A. Grunn, V. Trifonov, L. H. Kasper, S. Lerach, H. Tang, J. Ma, D. Rossi, A. Chadburn, V. V. Murty, C. G. Mullighan, G. Gaidano, R. Rabadan, P. K. Brindle, R. Dalla-Favera, Inactivating mutations of acetyltransferase genes in B-cell lymphoma. *Nature*. **471**, 189–196 (2011).
24. A. Azagra, L. Román-González, O. Collazo, J. Rodríguez-Ubreva, V. G. de Yébenes, B. Barneda-Zahonero, J. Rodríguez, M. Castro de Moura, J. Grego-Bessa, I. Fernández-Duran, A. B. M. M. K. Islam, M. Esteller, A. R. Ramiro, E. Ballestar, M. Parra, In vivo conditional deletion of HDAC7 reveals its requirement to establish proper B lymphocyte identity and development. *J. Exp. Med.* **213**, 2591–2601 (2016).
25. A. Azagra, A. Meler, O. de Barrios, L. Tomás-Daza, O. Collazo, B. Monterde, M. Obiols, L. Rovirosa, M. Vila-Casadesús, M. Cabrera-Pasadas, M. Gusi-Vives, T. Graf, I. Varela, J. L. Sardina, B. M. Javierre, M. Parra, The HDAC7–TET2 epigenetic axis is essential during early B lymphocyte development. *Nucleic Acids Res.* **50**, 8471–8490 (2022).
26. O. de Barrios, A. Galaras, J. L. Trincado, A. Azagra, O. Collazo, A. Meler, A. Agraz-Doblas, C. Bueno, P. Ballerini, G. Cazzaniga, R. W. Stam, I. Varela, P. De Lorenzo, M. G. Valsecchi, P. Hatzis, P. Menéndez, M. Parra, HDAC7 is a major contributor in the pathogenesis of infant t(4;11) proB acute lymphoblastic leukemia. *Leukemia* (2021),

doi:10.1038/s41375-020-01097-x.

27. G. D. Victora, D. Dominguez-Sola, A. B. Holmes, S. Deroubaix, R. Dalla-Favera, M. C. Nussenzweig, Identification of human germinal center light and dark zone cells and their relationship to human B-cell lymphomas. *Blood*. **120**, 2240–2248 (2012).
28. R. D. Morin, K. Mungall, E. Pleasance, A. J. Mungall, R. Goya, R. D. Huff, D. W. Scott, J. Ding, A. Roth, R. Chiu, R. D. Corbett, F. C. Chan, M. Mendez-Lago, D. L. Trinh, M. Bolger-Munro, G. Taylor, A. Hadj Khodabakhshi, S. Ben-Neriah, J. Pon, B. Meissner, B. Woolcock, N. Farnoud, S. Rogic, E. L. Lim, N. A. Johnson, S. Shah, S. Jones, C. Steidl, R. Holt, I. Birol, R. Moore, J. M. Connors, R. D. Gascoyne, M. A. Marra, Mutational and structural analysis of diffuse large B-cell lymphoma using whole-genome sequencing. *Blood*. **122**, 1256–1265 (2013).
29. A. Reddy, J. Zhang, N. S. Davis, A. B. Moffitt, C. L. Love, A. Waldrop, S. Leppa, A. Pasanen, L. Meriranta, M.-L. Karjalainen-Lindsberg, P. Nørgaard, M. Pedersen, A. O. Gang, E. Høgdall, T. B. Heavican, W. Lone, J. Iqbal, Q. Qin, G. Li, S. Y. Kim, J. Healy, K. L. Richards, Y. Fedoriw, L. Bernal-Mizrachi, J. L. Koff, A. D. Staton, C. R. Flowers, O. Paltiel, N. Goldschmidt, M. Calaminici, A. Clear, J. Gribben, E. Nguyen, M. B. Czader, S. L. Ondrejka, A. Collie, E. D. Hsi, E. Tse, R. K. H. Au-Yeung, Y.-L. Kwong, G. Srivastava, W. W. L. Choi, A. M. Evens, M. Pilichowska, M. Sengar, N. Reddy, S. Li, A. Chadburn, L. I. Gordon, E. S. Jaffe, S. Levy, R. Rempel, T. Tzeng, L. E. Happ, T. Dave, D. Rajagopalan, J. Datta, D. B. Dunson, S. S. Dave, Genetic and Functional Drivers of Diffuse Large B Cell Lymphoma. *Cell*. **171**, 481-494.e15

- (2017).
30. O. I. Koues, R. A. Kowalewski, L.-W. Chang, S. C. Pyfrom, J. A. Schmidt, H. Luo, L. E. Sandoval, T. B. Hughes, J. J. Bednarski, A. F. Cashen, J. E. Payton, E. M. Oltz, Enhancer Sequence Variants and Transcription-Factor Deregulation Synergize to Construct Pathogenic Regulatory Circuits in B-Cell Lymphoma. *Immunity*. **42**, 186–198 (2015).
  31. M. Li, Y.-L. Chiang, C. A. Lyssiotis, M. R. Teater, J. Y. Hong, H. Shen, L. Wang, J. Hu, H. Jing, Z. Chen, N. Jain, C. Duy, S. J. Mistry, L. Cerchietti, J. R. Cross, L. C. Cantley, M. R. Green, H. Lin, A. M. Melnick, Non-oncogene Addiction to SIRT3 Plays a Critical Role in Lymphomagenesis. *Cancer Cell*. **35**, 916-931.e9 (2019).
  32. J. Melchor, M. Garcia-Lacarte, S. C. Grijalba, A. Arnaiz-Leché, M. Pascual, C. Panizo, O. Blanco, V. Segura, F. J. Novo, J. G. Valero, P. Pérez-Galán, J. A. Martinez-Climent, S. Roa, Venetoclax improves CD20 immunotherapy in a mouse model of MYC/BCL2 double-expressor diffuse large B-cell lymphoma. *J. Immunother. cancer*. **11** (2023), doi:10.1136/jitc-2022-006113.
  33. M. Pascual, M. Mena-Varas, E. F. Robles, M.-J. Garcia-Barchino, C. Panizo, S. Hervas-Stubbs, D. Alignani, A. Sagardoy, J. I. Martinez-Ferrandis, K. L. Bunting, S. Meier, X. Sagaert, D. Bagnara, E. Guruceaga, O. Blanco, J. Celay, A. Martínez-Baztan, N. Casares, J. J. Lasarte, T. MacCarthy, A. Melnick, J. A. Martinez-Climent, S. Roa, PD-1/PD-L1 immune checkpoint and p53 loss facilitate tumor progression in activated B-cell diffuse large B-cell lymphomas. *Blood*. **133**, 2401–2412 (2019).
  34. A. A. Alizadeh, A. J. Gentles, A. J. Alencar, C. L. Liu, H. E. Kohrt, R.

- Houot, M. J. Goldstein, S. Zhao, Y. Natkunam, R. H. Advani, R. D. Gascoyne, J. Briones, R. J. Tibshirani, J. H. Myklebust, S. K. Plevritis, I. S. Lossos, R. Levy, Prediction of survival in diffuse large B-cell lymphoma based on the expression of 2 genes reflecting tumor and microenvironment. *Blood*. **118**, 1350–1358 (2011).
35. S. Monti, B. Chapuy, K. Takeyama, S. J. Rodig, Y. Hao, K. T. Yeda, H. Inguilizian, C. Mermel, T. Currie, A. Dogan, J. L. Kutok, R. Beroukhim, D. Neuberg, T. M. Habermann, G. Getz, A. L. Kung, T. R. Golub, M. A. Shipp, Integrative Analysis Reveals an Outcome-Associated and Targetable Pattern of p53 and Cell Cycle Deregulation in Diffuse Large B Cell Lymphoma. *Cancer Cell*. **22**, 359–372 (2012).
36. K. Basso, R. Dalla-Favera, Germinal centres and B cell lymphomagenesis. *Nat. Rev. Immunol.* **15**, 172–184 (2015).
37. M. Parra, H. Kasler, T. A. McKinsey, E. N. Olson, E. Verdin, Protein Kinase D1 Phosphorylates HDAC7 and Induces Its Nuclear Export after T-cell Receptor Activation. *J. Biol. Chem.* **280**, 13762–13770 (2005).
38. M. N. Navarro, J. Goebel, C. Feijoo-Carnero, N. Morrice, D. A. Cantrell, Phosphoproteomic analysis reveals an intrinsic pathway for the regulation of histone deacetylase 7 that controls the function of cytotoxic T lymphocytes. *Nat. Immunol.* **12**, 352–361 (2011).
39. F. Dequiedt, J. Van Lint, E. Lecomte, V. Van Duppen, T. Seufferlein, J. R. Vandenheede, R. Wattiez, R. Kettmann, Phosphorylation of histone deacetylase 7 by protein kinase D mediates T cell receptor–induced Nur77 expression and apoptosis. *J. Exp. Med.* **201**, 793–804 (2005).
40. H. G. Kasler, B. D. Young, D. Mottet, H. W. Lim, A. M. Collins, E. N.

- Olson, E. Verdin, Histone Deacetylase 7 Regulates Cell Survival and TCR Signaling in CD4/CD8 Double-Positive Thymocytes. *J. Immunol.* **186**, 4782–4793 (2011).
41. H. G. Kasler, E. Verdin, Histone Deacetylase 7 Functions as a Key Regulator of Genes Involved in both Positive and Negative Selection of Thymocytes. *Mol. Cell. Biol.* **27**, 5184–5200 (2007).
  42. F. Dequiedt, H. Kasler, W. Fischle, V. Kiermer, M. Weinstein, B. G. Herndier, E. Verdin, HDAC7, a Thymus-Specific Class II Histone Deacetylase, Regulates Nur77 Transcription and TCR-Mediated Apoptosis. *Immunity.* **18**, 687–698 (2003).
  43. P. Dhordain, S. Quief, D. Lantoine, J.-P. Kerckaert, O. Albagli, R. J. Lin, R. M. Evans, The LAZ3(BCL-6) oncoprotein recruits a SMRT/mSIN3A/histone deacetylase containing complex to mediate transcriptional repression. *Nucleic Acids Res.* **26**, 4645–4651 (1998).
  44. S.-Y. Park, J.-S. Kim, A short guide to histone deacetylases including recent progress on class II enzymes. *Exp. Mol. Med.* **52**, 204–212 (2020).
  45. T. B. Kepler, A. S. Perelson, Cyclic re-entry of germinal center B cells and the efficiency of affinity maturation. *Immunol. Today.* **14**, 412–415 (1993).
  46. M. Oprea, A. S. Perelson, Somatic mutation leads to efficient affinity maturation when centrocytes recycle back to centroblasts. *J. Immunol.* **158**, 5155–62 (1997).
  47. D. Dominguez-Sola, J. Kung, A. B. Holmes, V. A. Wells, T. Mo, K. Basso, R. Dalla-Favera, The FOXO1 Transcription Factor Instructs the Germinal Center Dark Zone Program. *Immunity.* **43**, 1064–1074 (2015).
  48. G. D. Victora, M. C. Nussenzweig, Germinal Centers. *Annu. Rev.*

- Immunol.* **40**, 413–442 (2022).
49. A. B. Holmes, C. Corinaldesi, Q. Shen, R. Kumar, N. Compagno, Z. Wang, M. Nitzan, E. Grunstein, L. Pasqualucci, R. Dalla-Favera, K. Basso, Single-cell analysis of germinal-center B cells informs on lymphoma cell of origin and outcome. *J. Exp. Med.* **217** (2020), doi:10.1084/jem.20200483.
  50. D. E. Kennedy, M. K. Okoreeh, M. Maienschein-Cline, J. Ai, M. Veselits, K. C. McLean, Y. Dhungana, H. Wang, J. Peng, H. Chi, M. Mandal, M. R. Clark, Novel specialized cell state and spatial compartments within the germinal center. *Nat. Immunol.* **21**, 660–670 (2020).
  51. S. N. Meyer, C. Scuoppo, S. Vlasevska, E. Bal, A. B. Holmes, M. Holloman, L. Garcia-Ibanez, S. Nataraj, R. Duval, T. Vantrimpont, K. Basso, N. Brooks, R. Dalla-Favera, L. Pasqualucci, Unique and Shared Epigenetic Programs of the CREBBP and EP300 Acetyltransferases in Germinal Center B Cells Reveal Targetable Dependencies in Lymphoma. *Immunity.* **51**, 535-547.e9 (2019).
  52. A. Dobin, C. A. Davis, F. Schlesinger, J. Drenkow, C. Zaleski, S. Jha, P. Batut, M. Chaisson, T. R. Gingeras, STAR: ultrafast universal RNA-seq aligner. *Bioinformatics.* **29**, 15–21 (2013).
  53. S. Anders, P. T. Pyl, W. Huber, HTSeq--a Python framework to work with high-throughput sequencing data. *Bioinformatics.* **31**, 166–169 (2015).
  54. M. I. Love, W. Huber, S. Anders, Moderated estimation of fold change and dispersion for RNA-seq data with DESeq2. *Genome Biol.* **15**, 550 (2014).
  55. D. W. Huang, B. T. Sherman, R. A. Lempicki, Systematic and integrative



- analysis of large gene lists using DAVID bioinformatics resources. *Nat. Protoc.* **4**, 44–57 (2009).
56. A. Subramanian, P. Tamayo, V. K. Mootha, S. Mukherjee, B. L. Ebert, M. A. Gillette, A. Paulovich, S. L. Pomeroy, T. R. Golub, E. S. Lander, J. P. Mesirov, Gene set enrichment analysis: A knowledge-based approach for interpreting genome-wide expression profiles. *Proc. Natl. Acad. Sci.* **102**, 15545–15550 (2005).

Figure 1

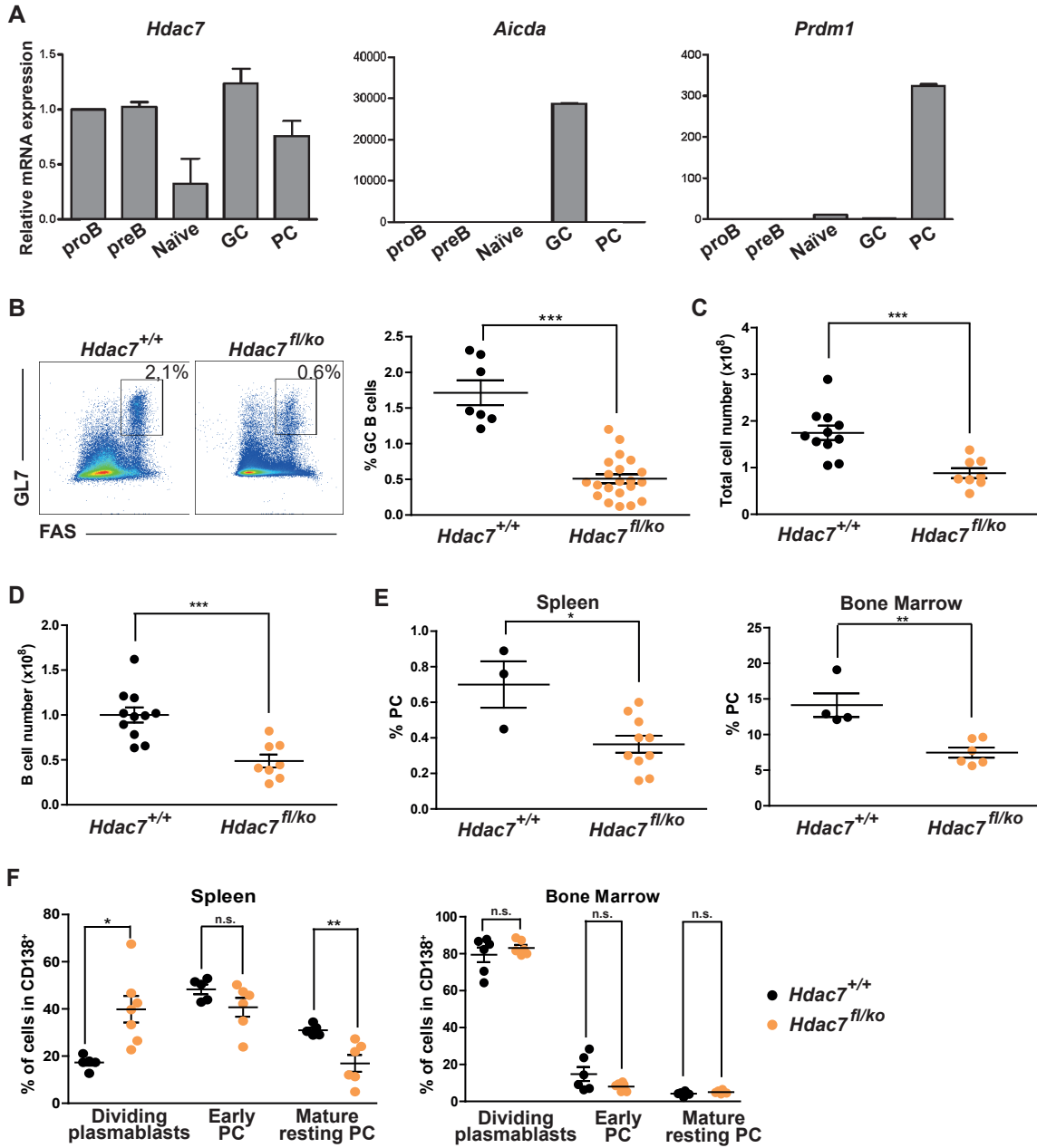


Figure 2

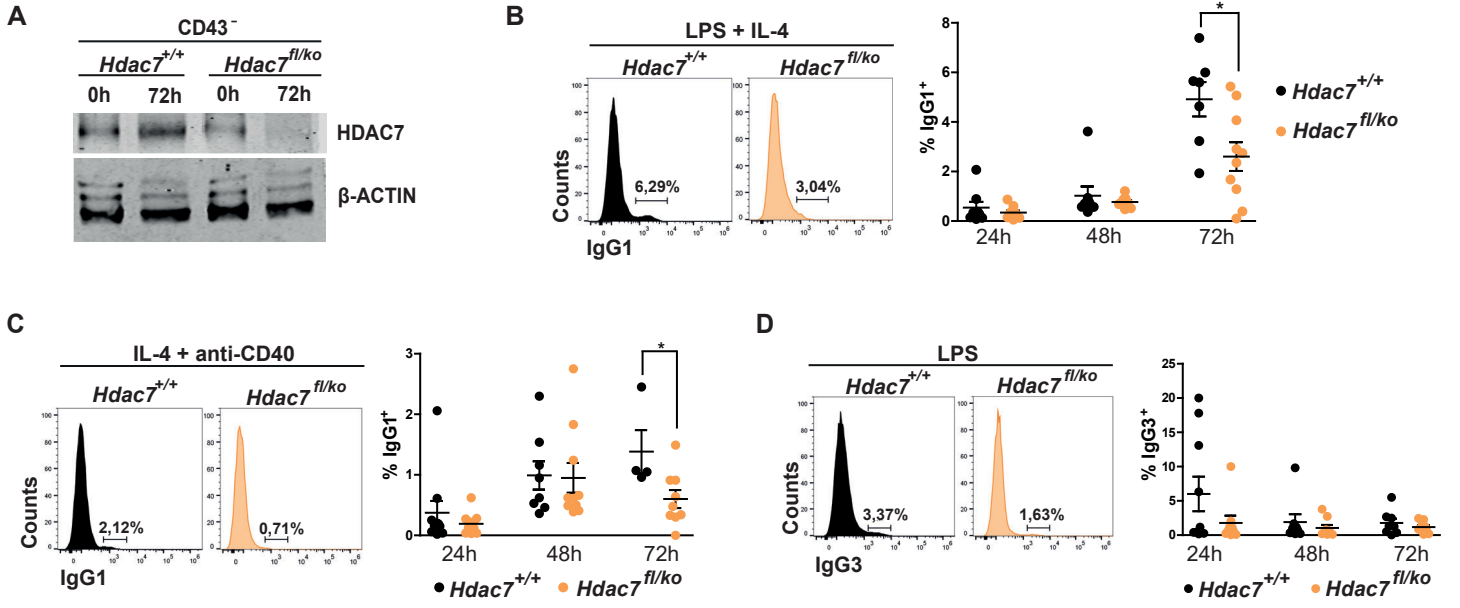
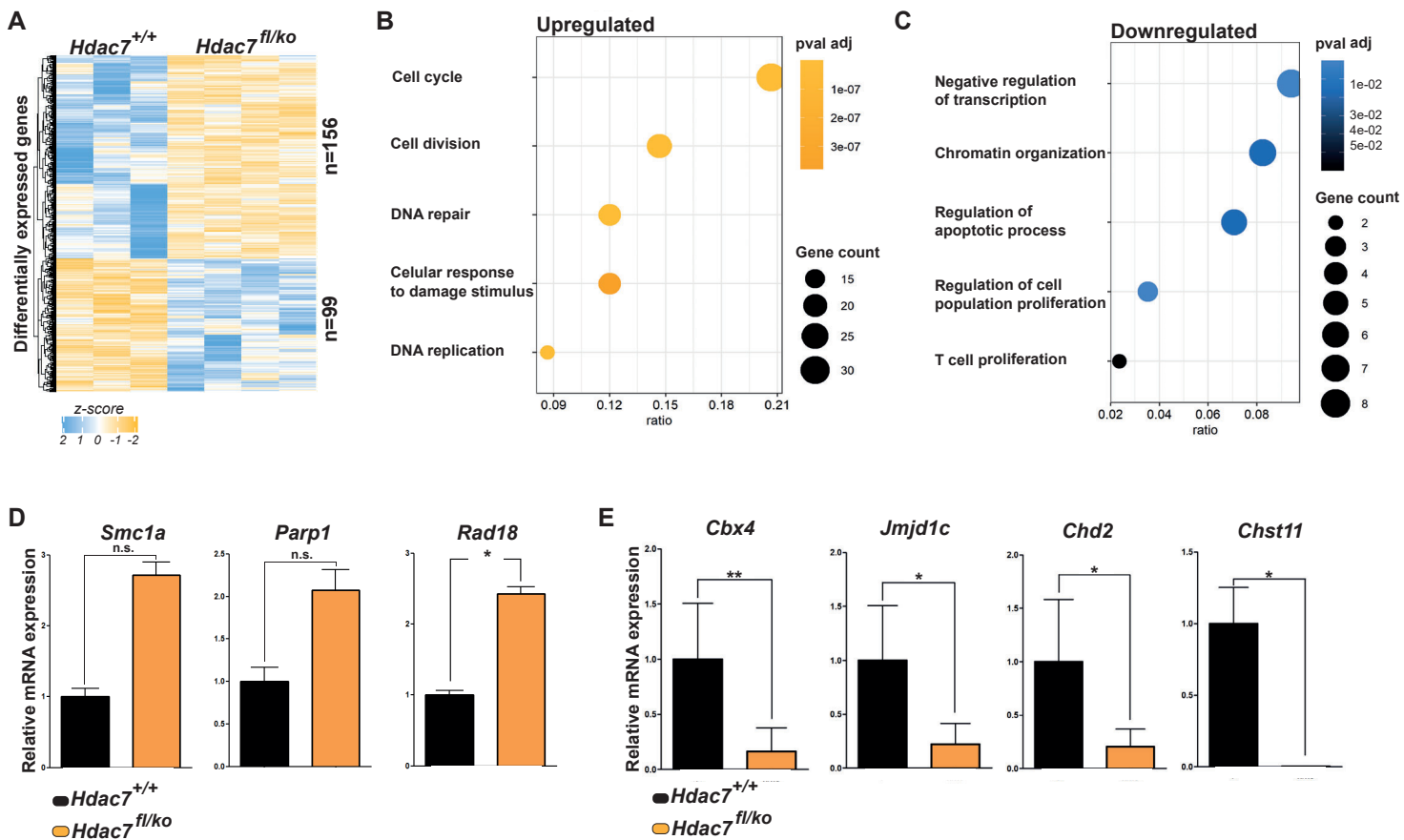
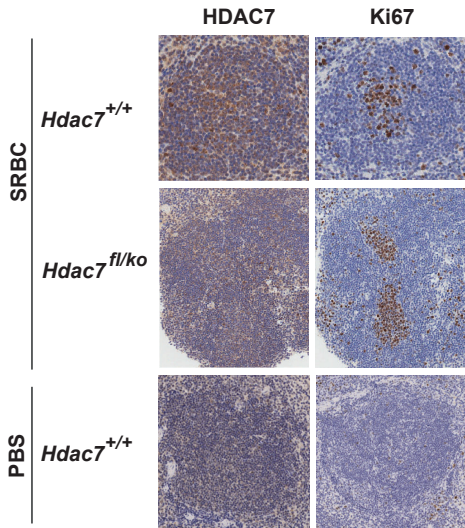


Figure 3

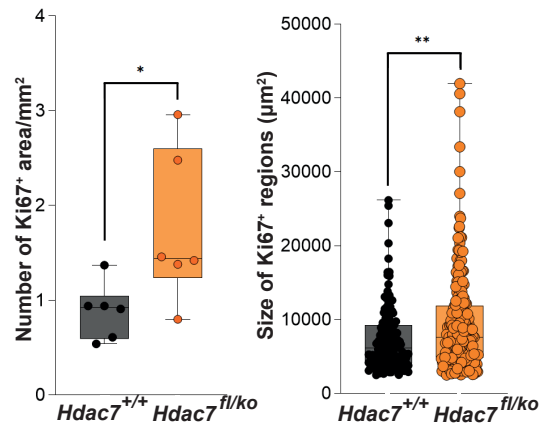


**Figure 4**

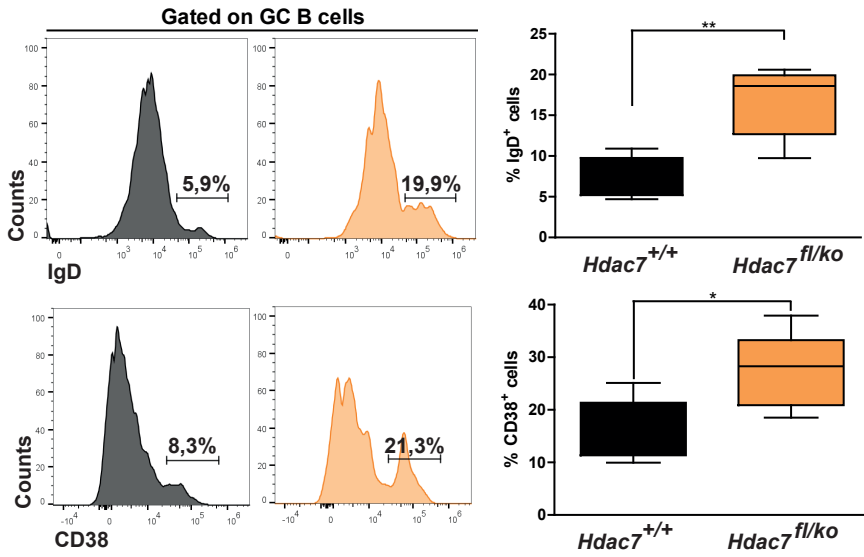
**A**



**B**



**C**



**D**

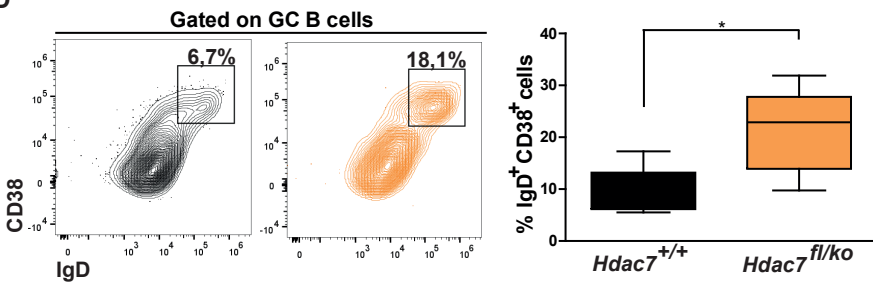


Figure 5

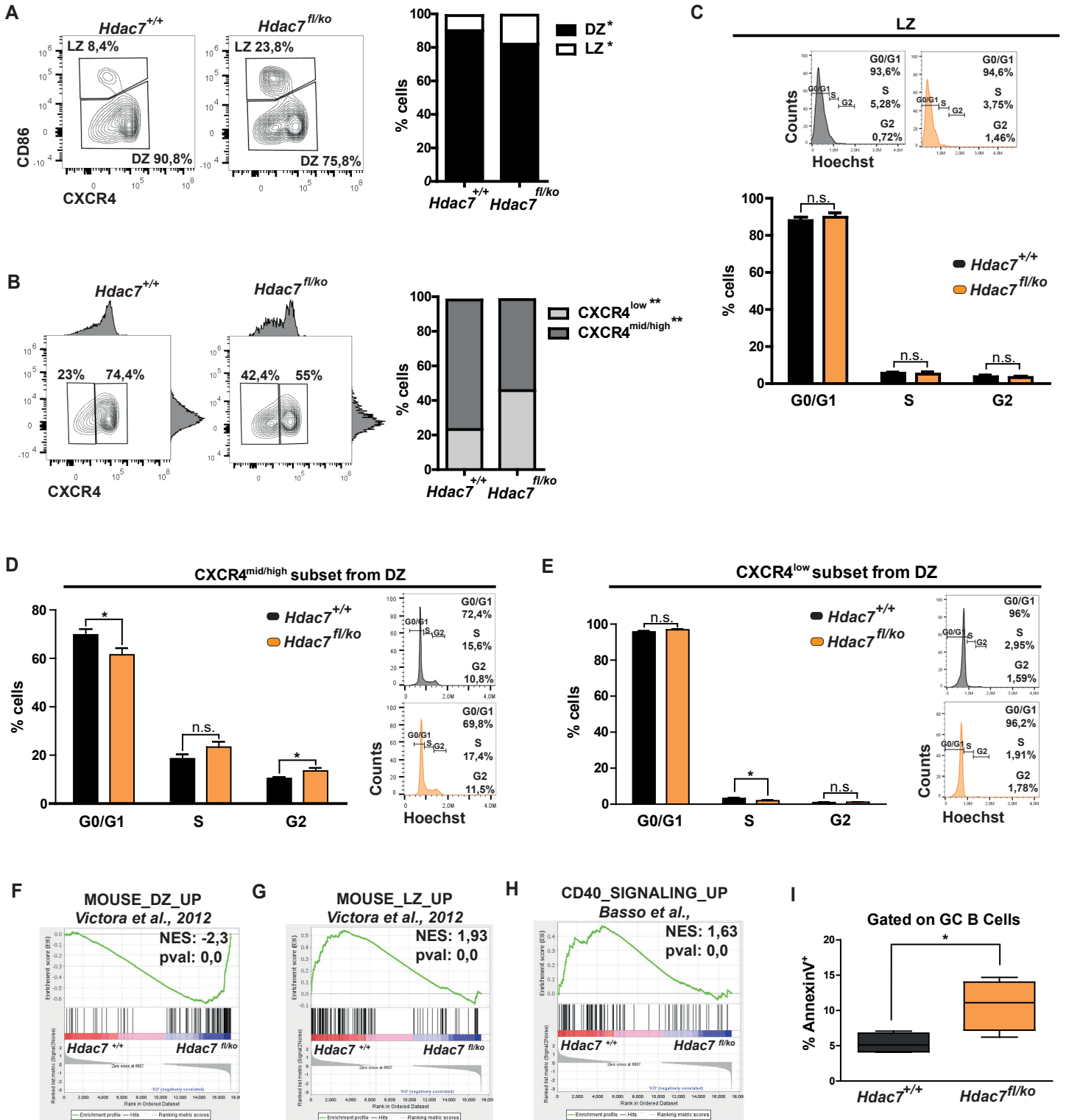


Figure 6

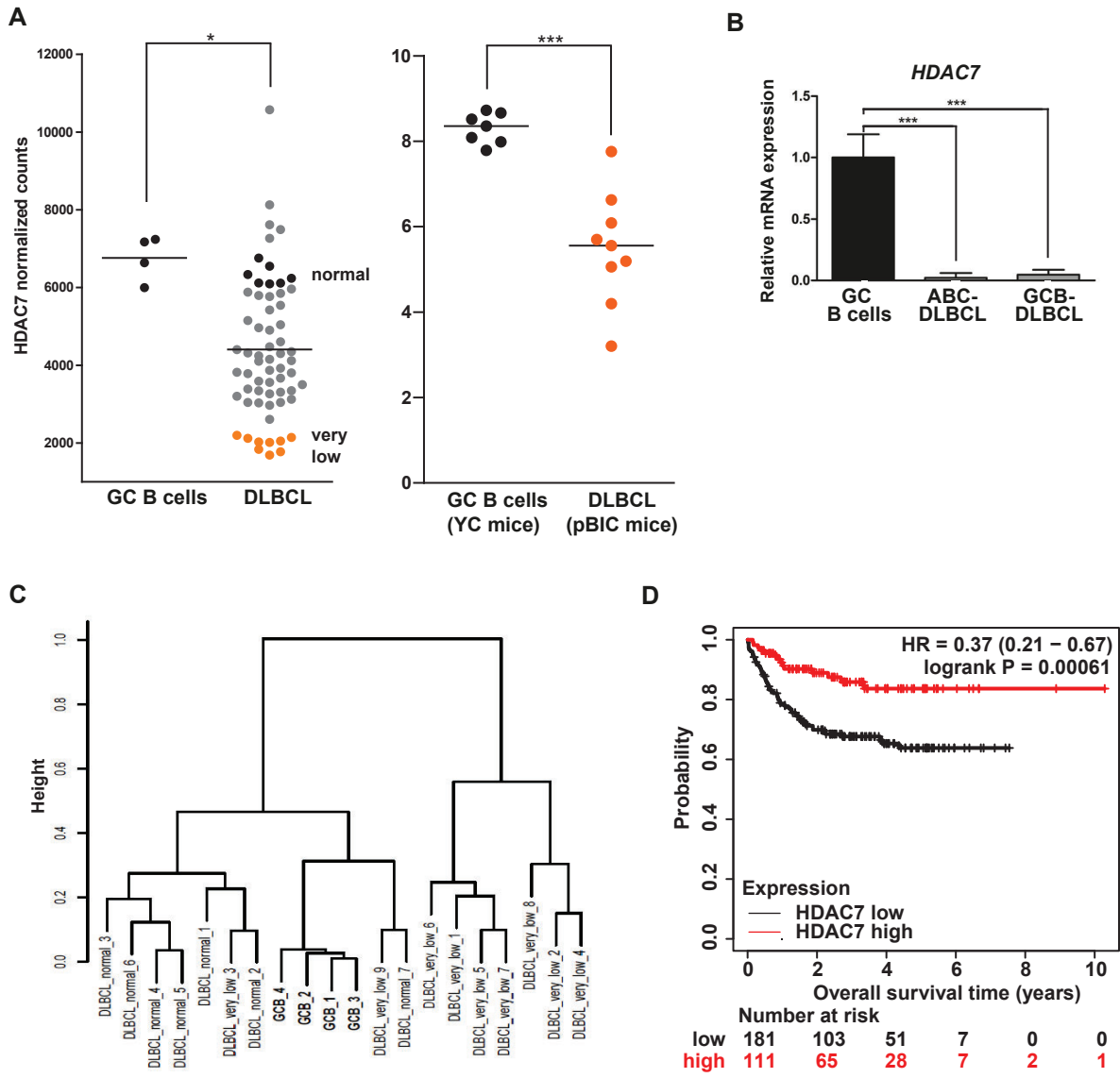
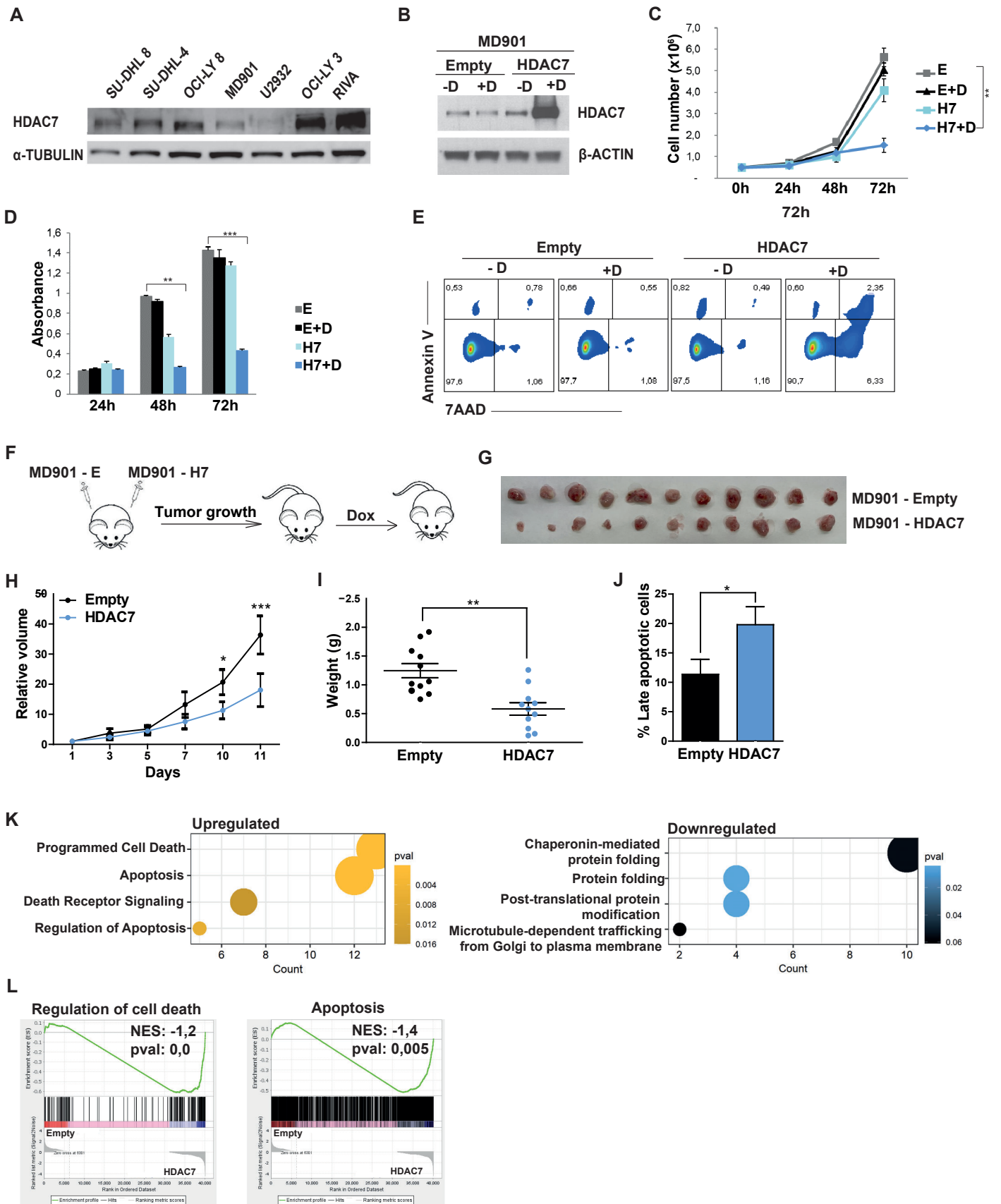


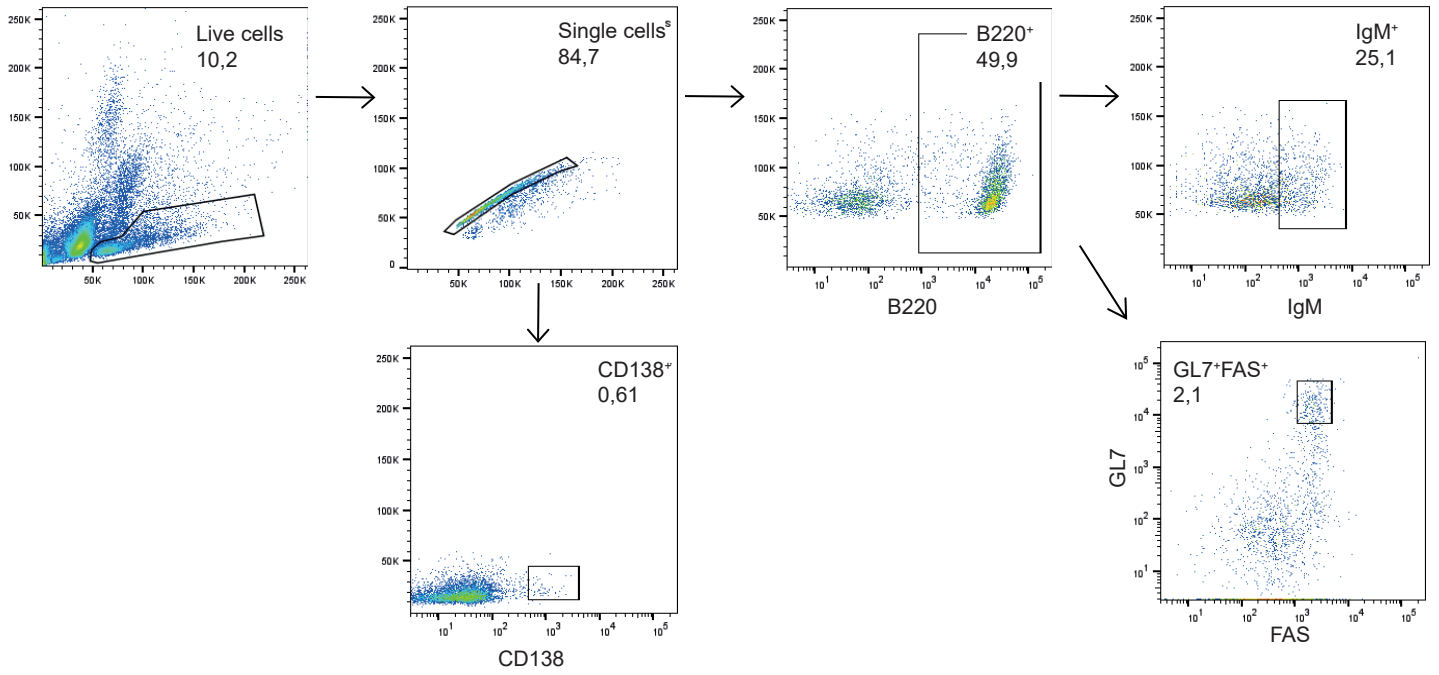
Figure 7



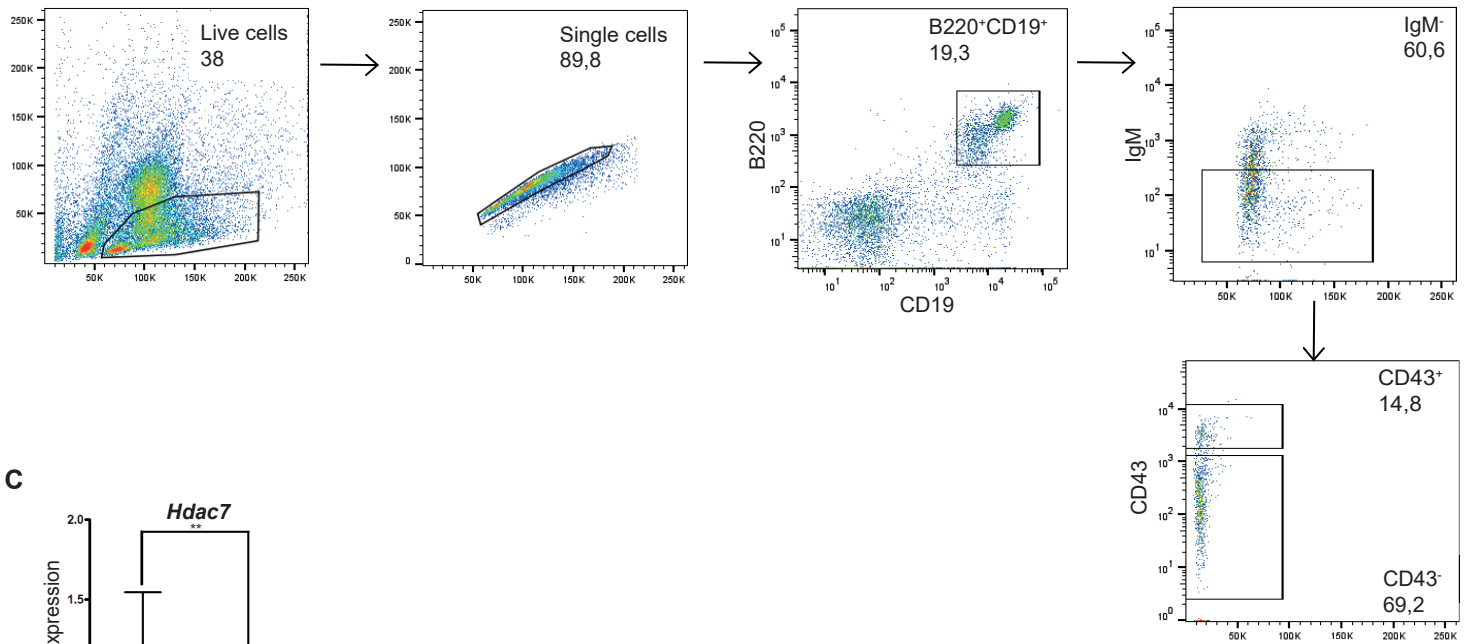


Supplementary Figure 1

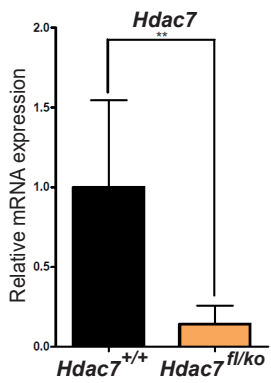
**A**



**B**



**C**





## **DISCUSSION**



## DISCUSSION

For many decades the hematopoietic system has been a paradigm developmental system. The question of how HSC can give rise to all mature blood cells of the organism highlights the complexity of this system. Gene specific programs at every differentiation stage are key to ensure proper cell development, therefore conferring to each cellular transition a particular and characteristic cell identity. To ensure the acquisition and maintenance of proper B cell identity and differentiation, several TFs interconnect in complex networks. In addition to positively promoting gene-specific programs, TFs also induce the repression of inappropriate genes of alternative lineages. How TFs exert their gene repressive function and the identity of specific transcriptional repressors during B cell development has remained elusive. Importantly, the deregulation of TFs and gene transcriptional programs may lead to the development of B cell malignancies such as leukemia and lymphoma.

Around sixty years ago, Vincent Allfrey and colleagues discovered that the acetylation of lysine residues in histones is associated with gene expression (Allfrey, Faulkner, and Mirsky 1964). Lysine acetylation neutralizes the positive charge of the histone residues, relaxing the chromatin conformation and enabling greater accessibility of the transcription machinery, being therefore, generally associated with gene activation. Contrarily, the removal of acetyl groups from histones induces chromatin compaction and gene transcriptional repression (Allfrey, Faulkner, and Mirsky 1964). This addition and removal of acetyl groups also occurs in a considerable number of non-histone proteins (Peng and Seto 2011). Lysine acetylation is highly dynamic and is regulated by the opposing role of HATs and HDACs (Morgan and Shilatifard 2020). HDACs have emerged as key transcriptional repressors in several physiological and pathological systems.

In this PhD thesis we show that the transcriptional repressor HDAC7 is strictly required to ensure proper B cell development. First, we unveil the molecular mechanisms by which HDAC7 modulates early B cell development in the bone marrow. Through *Tet2* direct control, HDAC7 maintains the silenced state of some lineage-inappropriate genes. The finding that HDAC7 is essential

for the proper acquisition of B cell progenitors' identity led us to the hypothesis that it may be deregulated in B-ALL. We demonstrate that HDAC7 is a *bona fide* biomarker and prognosis factor in pro-B-ALL, specifically, in infant t(4;11) subtype. Finally, we asked the question of whether HDAC7 could also play an important role in terminal B cell development. We found that HDAC7 is required for the GC formation and is underexpressed in DLBCL.

### **1. HDAC7 preserves pro-B cell chromatin conformation**

A correct gene expression pattern is crucial for the acquisition of cell identity during development. HDAC7 has been previously reported in our laboratory to be a transcriptional repressor of lineage-inappropriate genes during early B lymphocyte differentiation (Azagra et al. 2016). However, the HDAC7-mediated molecular mechanisms remained to be addressed. Gene transcription is strongly influenced by the chromatin state, allowing TFs binding to DNA in open regions and preventing their recruitment in compacted zones (van Schoonhoven et al. 2020). The transition from pro-B to pre-B cells requires massive changes in gene transcription since it represents the first stage at which pre-BCR expression serves as a checkpoint that monitors for functional IgH, directing B cell development (Hendriks and Middendorp 2004). Here, we have reported that HDAC7 deficiency disrupts IgH production, which may drastically affect the immune response. Hence, HDAC7 is essential for the transition of pro-B to pre-B cells in a process that demands a tight regulated gene transcriptional program, accompany by changes in chromatin conformation.

Highly accessible regions in chromatin are marked by histone modifications associated with transcriptional activity, such as H3K27ac, whereas regions of low accessibility are enriched in repressive histone marks such as H3K27me3 (Simonis et al. 2006). Here we have observed that HDAC7 deficiency in pro-B cells resulted in a global chromatin decompaction, correlating with a global increase of H3K27ac enrichment. In line with this finding, HDAC7 deficiency also caused a significant decrease in H3K9me3 enrichment. H3K9me3 is a hallmark of heterochromatin state, which is involved in maintaining lineage stability and preventing cell reprogramming (Becker, Nicetto, and Zaret 2016).

Alterations in the chromatin state upon HDAC7 loss in pro-B cells mainly increased accessibility in distal intergenic regions, and compacted promoter sites. Distal regions normally contain regulatory elements called enhancers, functionally described as DNA sequences with the potential to drive transcription of a gene located nearby (Andersson and Sandelin 2020). Active enhancers can be identified when they contain the deposition of H3K27ac (Creyghton et al. 2010), a histone mark found increased also in distal regions upon HDAC7 loss. Thus, the significant increase of open regions and H3K27ac enrichment in distal regions, probably enhancers, upon HDAC7 deficiency, may indicate a high recruitment of basal transcription machinery in genes that normally are not expressed in pro-B cells. We can conclude that HDAC7 preserves the identity of pro-B cells by maintaining a compact chromatin conformation in regulatory regions of lineage inappropriate genes.

## **2. HDAC7 maintains DNA 5-hmC status through *Tet2* silencing**

DNA methylation provides an additional layer of gene regulation during early B cell development (Benner, Isoda, and Murre 2015). Interestingly, we observed that the absence of HDAC7 from pro-B cells resulted in the upregulation of TET2.

TET proteins are mainly recruited to open chromatin regions, therefore euchromatin is enriched in DNA 5-hmC epigenetic mark (Kubiura et al. 2012). HSCs and lymphocytes present low 5-hmC levels (~0,2% and ~0,1%, respectively) compared to other cell types, such as Purkinje cells or embryonic stem cells (~5%) (Ficz et al. 2011; Kriaucionis and Heintz 2009; Tsagaratou et al. 2017). We observed a significant increase in DNA 5-hmC upon HDAC7 deficiency in pro-B cells. We found a high percentage of 5-hmC peaks located at intergenic and distal promoter regions. These results may imply, as mentioned above, that distal regulatory regions with enhancer features are targets of TET2-mediated DNA demethylation and may correlate with the presence of additional mechanisms that control DNA methylation status at promoter-associated regions (Kasper D. Rasmussen et al. 2019; Kasper Dindler Rasmussen and Helin 2016).

Within the hematopoietic system HDAC7 shows a lymphoid specific expression pattern, whereas TET2 is broadly expressed in the hematopoietic system, having its highest levels of expression in myeloid cells (Azagra et al. 2016; Barneda-Zahonero et al. 2013; Kallin et al. 2012; Ko et al. 2010). It has been reported that TET2 loss in HSCs produced an aberrant increased number of myelomonocytic cells and decreased expression of macrophage markers such as *Mac-1* in myeloid cells (Ko et al. 2011; Moran-Crusio et al. 2011). Within the B cell lineage, TET2 conditional deficiency at pro-B cell stage did not cause any phenotype during development and differentiation. However, conditional deletion of both TET2 and TET3 lead to defective B cell development (Lio et al. 2016). Even though there is no phenotype observed by TET2 deficiency *in vivo* in mice, TET2 has been reported to play a critical role in mediating the hydroxymethylation of cytosine residues from myeloid genes in a reprogramming system that allows the transdifferentiation from pre-B cells into macrophages (Bussmann et al. 2009; Kallin et al. 2012). Despite loss of TET2 and TET3 leads to aberrant lymphocyte development and related disorders (Lio et al. 2016), and loss of TET2 enzymatic activity appears to mainly affect myelopoiesis (Ito et al. 2019; Ko et al. 2011), our results strongly suggest that HDAC7 is a critical factor that preserves B cell identity and correct DNA 5-hmC state via *Tet2* gene silencing.

Using both our conditional knock out mouse model and an *in vitro* reprogramming system (Azagra et al. 2016; Bussmann et al. 2009), we demonstrated the requirement of the HDAC7-TET2 axis in early B cell development. First, we observed that *Tet2* was upregulated in HDAC7-deficient pro-B cells and during the conversion of pre-B cells to macrophages. HDAC7 exogenous expression blocked the upregulation of *Tet2* during cellular conversion. Chromatin immunoprecipitation experiments proved that HDAC7 is recruited to the promoter and enhancer of the *Tet2* gene. Overall, these results demonstrated that HDAC7 directly represses *Tet2* in pro-B and pre-B cells. Deeping into the mechanism, it was previously demonstrated to that HDAC7 requires interaction with MEF2C to ensure its repressive action (Azagra et al. 2016). Therefore, we speculate that MEF2C may recruit HDAC7 to the promoter and enhancer of *Tet2* gene leading to its transcriptional silencing.



TET2 localizes to regions of open chromatin in cell-type-specific enhancers (Kasper D. Rasmussen et al. 2019). We found *Jun* and *Fosl2* among the lineage-inappropriate genes with increased 5-hmC levels in HDAC7-deficient pro-B cells. *Fosl2* has been reported to be a TET2-activated gene during the transdifferentiation of pre-B cells to macrophages (Kallin et al. 2012). In addition, *Jun* gene undergoes enhancer demethylation during the reprogramming of B cells into induced pluripotent stem cells (iPSC) (Sardina et al. 2018). The finding that lineage-inappropriate genes are already marked with 5-hmC in pro-B cells supports the notion that they may be epigenetically poised in early stages of development.

Altogether, our findings further demonstrate the repressive role of HDAC7 of lineage-inappropriate genes and make it an essential regulator of additional epigenetic players such as TET2. Our study not only demonstrates that HDAC7 induces gene silencing by direct recruitment to target genes, but also uncovers its unexpected ability to maintain chromatin architecture by modulating DNA 5-hmC levels. We also speculate that HDAC7 could be directly or indirectly impeding H3K27ac epigenetic mark deposition to avoid chromatin decompaction of the enhancers and promoters of lineage-inappropriate genes.

### **3. HDAC7 role in pro-B-ALL**

According to a broad number of studies reported, if a TF or other type of epigenetic or transcriptional regulator is essential for the correct generation of a cell type, its deregulation may lead to the development of associated malignancies. Given the essential role of HDAC7 at the pro-B cell developmental stage, we asked the question of whether it could be deregulated in pro-B-ALL patients.

RNA-seq data mining of pro-B-ALL (with MLL rearrangement) infants and healthy fetal liver B cell progenitors unveiled a dramatic underexpression of HDAC7 in the t(4;11) pro-B-ALL subtype. The low HDAC7 expression was also associated to poorer outcome of the patients. Therefore, HDAC7 deregulation may play a role in the pathogenesis of t(4;11) pro-B-ALL. We also observed that

the expression pattern of HDAC7 correlated to *MME*, a gene associated to B lymphocyte differentiation, consistent with its repressive role of lineage-inappropriate genes in pro-B cells (Azagra et al. 2016). In consonance, the induction of HDAC7 expression might represent a novel approach to improve the prognosis of infant t(4;11) pro-B-ALL. Accordingly, exogenous expression of HDAC7 in a t(4;11) pro-B-ALL leukemia cell line (SEM-K2) compromised cell viability with increased cell death and decreased proliferation. Concomitantly, gene ontology analysis of RNA-seq data from SEM-K2 cells engineered to express HDAC7 revealed an enrichment of key hallmarks of cancer such as proliferation, migration and apoptosis, indicating that HDAC7 exerts a leukemia-suppressing phenotype. To gain insight into the contribution of HDAC7, we integrated RNA-seq data from healthy B cell progenitors, t(4;11) pro-B-ALL and SEM-K2 transformed cell line. Bioinformatic analysis unveiled that the transcriptional expression profile upon HDAC7 induction in SEM-K2 cell line was shifted towards to that of healthy B cell progenitors. Therefore, HDAC7 expression might be partially restoring the transcriptome towards the healthy condition, in concordance with the described requirement of HDAC7 to preserve pro-B cells identity (Azagra et al. 2016) .

Forced induction of HDAC7 impedes the uncontrolled proliferation of leukemic cells. Therefore, we hypothesize that the presence of HDAC7 may confer higher sensitivity to conventional chemotherapy of t(4;11) pro-B-ALL to conventional therapy, along with a better outcome for patients. To achieve this goal, the elucidation of the mechanisms underlying HDAC7 repression needs to be investigated.

HDAC7 re-expression could be achieved through several ways and distinct hypothesis can be considered. We speculate that changes in HDAC7 driving to its underexpression in pro-B-ALL may be caused by epigenetic mechanisms (Deaton and Bird 2011). Generally, ALL displays a highly methylated genome (Hetzl et al. 2022). However, non-rearranged and MLL-AF4 rearranged ALL present differences in their methylomes (Tejedor et al. 2021). Due to the low HDAC7 expression we observe in MLL-AF4 pro-B-ALL patients, we speculate that HDAC7 might be one of these differentially methylated genes resulting in its

transcriptional silencing. Therefore, it might be plausible that HDAC7 promoter or enhancer regions could be hypermethylated in MLL-AF4 pro-B-ALL. The hypermethylation of HDAC7 regulatory regions would prevent the recruitment of TFs or other transcriptional regulators impeding its expression. Beyond DNA methylation, alterations in histones can also interfere expression. H3K27 is a crucial residue for epigenetic regulation. Its strict modulation at enhancer regions or promoters may determine the expression of associated genes. Trimethylation of H3K27 induces a close chromatin conformation, which is mediated by EZH2, a member of the polycomb repressive complex PRC2 (Wiles and Selker 2017). Although normally, EZH2 displays loss-of-function mutations in ALL (Jaffe et al. 2013), Tejedor and colleagues reported that infant MLL-AF4 pro-B-ALL patients present an increased activity of EZH2 (Tejedor et al. 2021). Therefore, we can hypothesise that the increased EZH2 activity in MLL-AF4 pro-B-ALL, could result in HDAC7 silencing through the deposition of H3K27me3 epigenetic mark in nearby regions.

We believe that the elucidation of the molecular mechanisms involved in HDAC7 repression will open new therapeutic avenues for MLL-AF4 pro-B-ALL patients.

#### **4. HDAC7 is required for the entry into the germinal center**

For the last three decades the GC reaction has been extensively studied and considered the unique anatomical structure where activated B cells undergo massive proliferation, SHM and CSR. Through several selection cycles between the DZ and LZ GC B cells give rise to either PC or MBC.

Recent works from several laboratories have led the immunology community to re-evaluate this classical model of the humoral response. These studies have unambiguously concluded that CSR occurs before the GC has coalesced, and the generation of MBC and PC can also occur early after B cell activation and in a GC-independent manner (Roco et al. 2019; Taylor, Pape, and Jenkins 2012; Weisel et al. 2016). Actually, upon B cell activation, a novel MBC population that has switched its isotype to IgM or IgG arises (Dogan et al. 2009;

Viant et al. 2021; Zuccarino-Catania et al. 2014). The role of several TFs and epigenetic regulators such as BCL6, MEF2B, FOXO1, CREBBP and KMT2D during the GC reaction is well established (Basso and Dalla-Favera 2015). However, the identity of potential regulators of the pre-GC remains unknown. In this work we have unveiled that HDAC7 is required for the GC formation and dynamics. HDAC7 deficiency results in a reduced number of GC B cells, diminished CSR and PC generation. The remaining GC B cells in the absence of HDAC7 are highly aberrant and express cell surface markers characteristic of naïve and pre-GC B cells. In addition, proper polarization of GC is disrupted in the absence of HDAC7.

We speculate that this premature block of differentiation prior GC entrance may also impact into the GC-independent populations. HDAC7-loss upon B cell activation may decrease IgM<sup>+</sup> and IgG<sup>+</sup> MBCs and PCs or evoke into its aberrancy. Consequently, and at the time of second antigen encounter, IgG<sup>+</sup> MBCs will not be able to differentiate into antibody secreting PC whereas IgM<sup>+</sup> MBCs will be incapable of recirculating and initiating a novel GC reaction. Additionally, as long-lived MBCs originate in the pre-GC compartment (Weisel et al. 2016), we also anticipate their diminishment or malfunction. Overall, the allegedly defects in pre-GC cell types will have a repercussion in the humoral immunity, resulting in immunodeficiency consequences.

## **5. Potential HDAC7 intracellular localization upon B cell activation**

A peculiarity of HDAC7, as well as its sister family members HDAC4, 5 and 9, is its phosphorylation-dependent regulation, which mediates its nucleocytoplasmic distribution (Dequiedt et al. 2003, 2005; Kasler et al. 2011; Kasler and Verdin 2007; Navarro et al. 2011; Parra et al. 2005). Previous reports showed that, in resting thymocytes, HDAC7 is localized in the nucleus, where it represses the expression of a large number of genes involved in both positive (survival) and negative (apoptosis) selection of the cells. However, in response to TCR signalling, HDAC7 becomes phosphorylated and translocates to the cytoplasm where it can no longer exert its gene repressive functions (Dequiedt et al. 2003, 2005; Kasler and Verdin 2007; Parra et al. 2005).

We speculate that in naïve B cells that have encountered the antigen, HDAC7 becomes rapidly phosphorylated through BCR or MHC signalling and exported to the cytoplasm. Under this scenario HDAC7 potential target genes, crucial for early pre-GC events, may be derepressed allowing the entrance and initiation of the GC reaction (Figure 10). HDAC7 deficiency mimics the constitutive phosphorylation and cytoplasmic localization resulting in the establishment of aberrant gene signatures. This event of driven phosphorylation is currently under study in our laboratory.

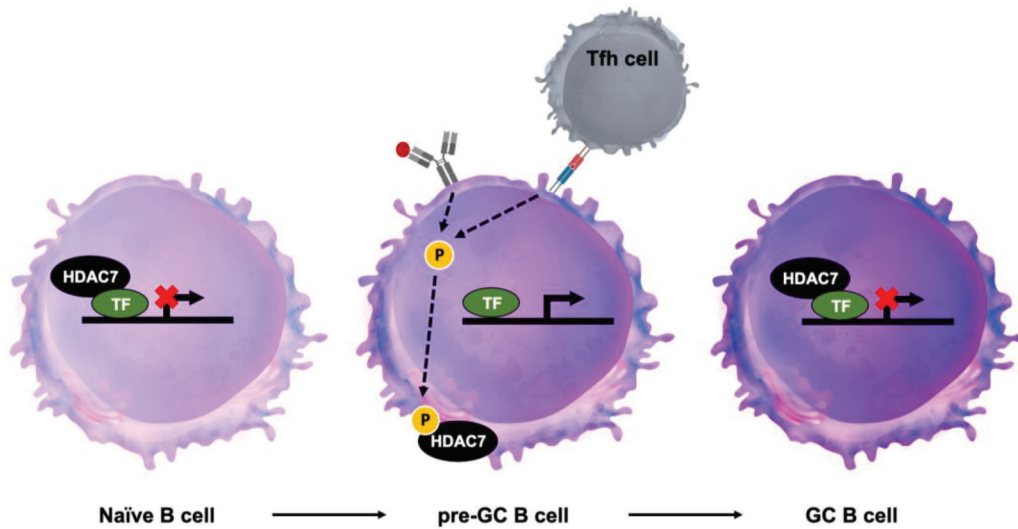


**Figure 10. Schematic representation of HDAC7 silencing hypothesis in the GC entrance.** In the naïve B cell HDAC7 acts as transcriptional repressor. Upon Tfh cell activation, signaling through the BCR or MHC drives to the phosphorylation (P) of HDAC7 in the nucleus, shuttling to the cytoplasm, inactivating it in the pre-GC B cell. The mature GC B cell has recovered HDAC7 repressive function.

In addition, it is highly probable that HDAC7 confers repressive capacity to B cell TFs such as BCL6 and MEF2B within the pre-GC and GC. In fact, it has been reported that BCL6 recruits a co-repressor complex that contain SMRT/N-CoR, HDAC3 and members of the class IIa HDACs sub-family that includes HDAC4, 5, 7 and 9 (Dhordain et al. 1998). The MEF2 family of TFs, also involved in B cell development, are considered classical partners of class IIa HDACs (Park and Kim 2020). In a previous study from our laboratory, it was demonstrated that HDAC7 deletion dramatically blocks early B cell development and gives rise to a severe lymphopenia in peripheral organs, while also leading to pro-B cell lineage promiscuity. Our group found that HDAC7 represses myeloid and T lymphocyte

genes in pro-B cells through interaction with MEF2C (Azagra et al. 2016). MEF2B, another member of the MEF2 family of TFs, has been described as an additional regulator of the GC reaction (Brescia et al. 2018). Brescia *et al.* depict a scenario where MEF2B induces the expression of crucial genes for the GC reaction whereas at the same time, when interacting with HDACs, MEF2B action becomes repressive. MEF2B mutations lead to lymphomagenesis. Preliminary and unpublished data from our laboratory closely links HDAC7 to MEF2B repressive role. Comparison between the transcriptional profiles of HDAC7-deficient GC B cells and GC B cells expressing a MEF2B mutant variant unable to interact with HDACs, unveil several common target genes. HDAC7-loss and MEF2B mutant seem to have a similar effect. In fact, MEF2B deletion, alike HDAC7 deficiency, reduces GC formation in mice, affects proliferation, differentiation, and GC confinement, but is also related to lymphomagenesis.

Overall, this work identifies first, HDAC7 as a crucial regulator of pre-GC events essential for the entrance and formation of a proper GC; and second, points us to speculate that HDAC7 is a cofactor for the transcriptional repressive action of MEF2B in the GC. We hypothesize that during terminal B cell development HDAC7 may be responsible for the repressive function of many other crucial TFs.

## **6. Role of HDAC7 in the germinal center dynamics**

The classical model of cyclic re-entry within the GC requires iterative cycles of SHM in the DZ followed by selection in the LZ, to achieve a high degree of affinity maturation (Kepler and Perelson 1993; Oprea and Perelson 1997). We observed a disturbed polarization of GC B cells within the DZ and LZ in the absence of HDAC7. In particular, HDAC7 deficiency leads to a decrease and an increase in the numbers of B cells within the DZ and LZ, respectively. Intriguingly, the defective GC polarization and the transcriptomic profile of HDAC7-deficient GC B cells appear to be contradictory. In this regard, although a smaller number of DZ cells are found, HDAC7-deficient GC B cells present a genetic signature almost elusive of LZ signatures, that we hypothesize may be provoked by non-mutually exclusive events: i) a continued suppression of the LZ state by other

TFs such as FOXO1 (Dominguez-Sola et al. 2015), and/or ii) lack of DZ essential genes repression required for cycling to the LZ, forced by HDAC7 loss.

Recently, it has been proposed that GC B cells might best be thought of as a single population oscillating through a cycle between two extremes corresponding to the LZ and the DZ, rather than two different populations (Victoria and Nussenzweig 2022). In this study we noticed, within the classically gated DZ, a highly proliferative CXCR4<sup>mid/high</sup> and a significantly present non-proliferative CXCR4<sup>low</sup> subpopulations upon HDAC7 loss. As supported by single-cell transcriptomic studies (Holmes et al. 2020; Kennedy et al. 2020), the subclusters of a single GC B cell population tend to represent the cell cycle phases or transitional states, therefore, HDAC7 seems to be governing the transition between the GC extremes. We speculate that loss of HDAC7 leads to the generation of aberrant GC B cells. In the absence of HDAC7, a significant higher number of GC B cells are able to acquire the expression of the LZ surface marker CD86 but retain the transcriptome of DZ resident GC B cells generating “pseudo-DZ” and “pseudo-LZ” cells.

## **7. HDAC7 role in DLBCL**

DLBCL originates at GCs and is the most aggressive and common type of non-Hodgkin lymphoma worldwide. Due to complex mechanisms such as SHM, GC B cells from which DLBCLs arise are prone to instability and to acquire off target mutations. In fact, a hallmark of DLBCL is the deregulation (mutations, underexpression, overexpression) of many epigenetic regulators and TFs, such as CREBP, p300, KMT2D, BCL6 and MEF2B among others (Brescia et al. 2018; Meyer et al. 2019; Zhang et al. 2015). This epigenetic heterogeneity is also linked to resistance to therapy and poor clinical outcome. We have identified HDAC7 as a potential novel biomarker and prognostic factor in DLBCL patients. In particular, we have found that patients diagnosed with DLBCL harboring normal levels of HDAC7, show a better prognosis, indicating that HDAC7 may exert tumor suppressing effects. Our findings are consistent with previous evidence reported by two laboratories. Morin et al. explored potential new targets of recurrent somatic point mutations and genes targeted by focal somatic deletions in DLBCL

patients, finding HDAC7 as a susceptible mutated gene with significant evidence for positive selection (Morin et al. 2013). Furthermore, Reddy and colleagues performed whole-exome sequencing and RNA-seq in a cohort of 1001 DLBCL patients to comprehensively define the landscape of 150 genetic drivers of the disease, finding HDAC7 among them (Reddy et al. 2017). Accordingly, we show that HDAC7 exogenous expression in DLBCL cells prone malignant cells to proliferation blockade and to induce apoptosis, both *in vitro* and *in vivo*. As previously described in infant pro-B ALL with t(4;11) translocation (de Barrios et al. 2021), we conclude that HDAC7 presence also confers favourable prognosis in DLBCL.

Overall, this study may lead to classify B cell cancers in HDAC7<sup>+</sup> and HDAC7<sup>-</sup>, serving to define patients' outcome and the basis for novel precision medicines. In the near future, the identification of the mechanisms involved in the underexpression of HDAC7 may lead to the design and implementation of novel specific therapeutic strategies.

Altogether, the findings reported in this thesis aim to report HDAC7 essentiality in B lymphocyte development (Figure 11). From a physiological point of view, in the pro-B cell stage, HDAC7 maintains the B cell identity and chromatin conformation through *Tet2* gene silencing. In the GC, HDAC7 is a crucial regulator of the events required for a proper entrance and initiation of the GC reaction. From a pathological point of view, HDAC7 underexpression in infant pro-B-ALL and in DLBCL correlates with a poor prognosis of the patients. Low levels of HDAC7 increase the proliferative capacity of the cells and therefore confers a pro-survival phenotype to the malignant cells. Despite the reported facts, further studies are needed to decipher HDAC7 implication and mechanisms of action it has along B cell differentiation, and this way find novel therapeutic strategies for its re-expression in B cell derived malignancies.



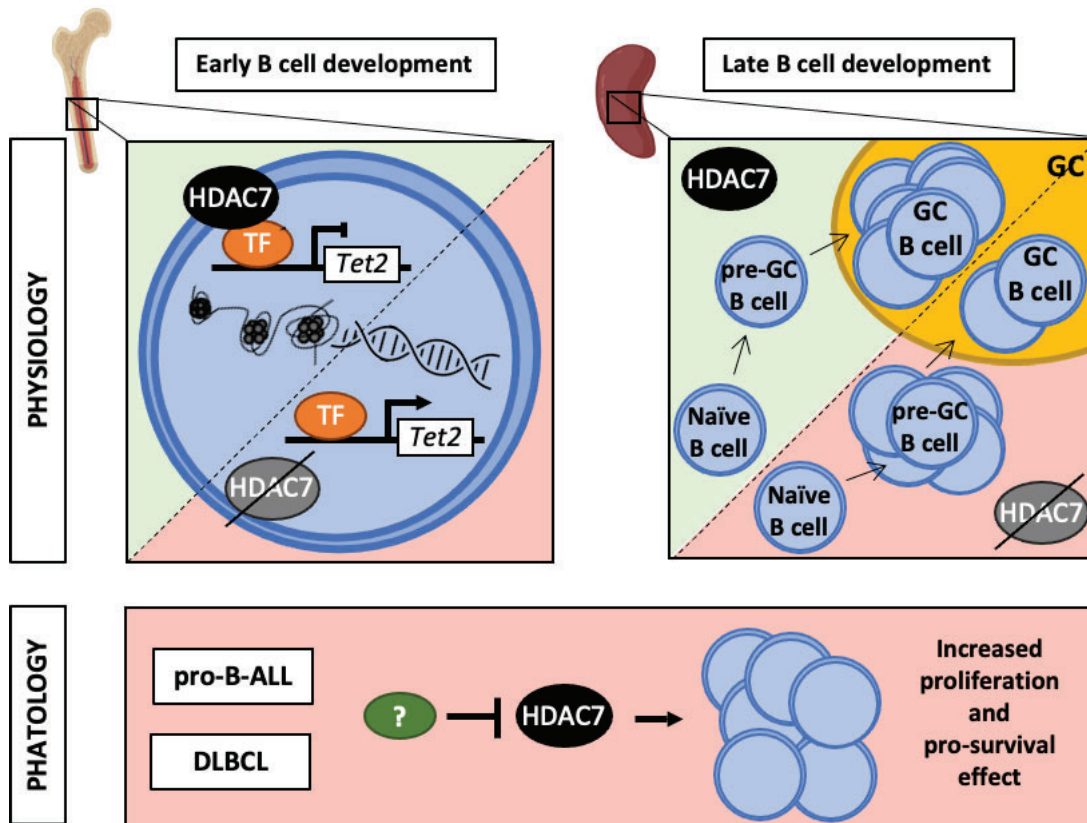


**Figure 11. Graphical summary of HDAC7 role in early and late B cell development, and in derived malignancies.** First, HDAC7 has a physiological role in early and late B cell development. HDAC7 maintains the pro-B cell identity and chromatin conformation through *Tet2* repression. In the GC, HDAC7 is necessary for the entrance and initiation of the GC reaction. Second, HDAC7 deficiency correlates with pathogenesis. In pro-B-ALL and in DLBCL we have observed its re-expression has an anti-oncogenic role.



## **CONCLUSIONS**



## CONCLUSIONS

The results described in this Thesis can be summarized as follows:

1. HDAC7 maintains correct chromatin conformation and histone mark deposition to repress lineage-inappropriate genes in pro-B cells
2. HDAC7 preserves pro-B cell identity by controlling *Tet2* expression levels
3. HDAC7 is underexpressed in infant t(4;11) pro-B-ALL and its re-expression exerts a leukemia-suppressing phenotype
4. HDAC7 ectopic expression in t(4;11) pro-B-ALL cell lines confers a transcriptional profile closer to healthy pro-B cells
5. HDAC7 is required in the early pre-GC events and for the entrance to the GC
6. HDAC7 is essential for the GC reaction and the generation of a proper humoral immune response
7. HDAC7 is underexpressed in DLBCL patients representing a novel biomarker and prognostic factor
8. HDAC7 exogenous expression in DLBCL cell lines limits its lymphomagenic capacity, *in vitro* and *in vivo*



## **BIBLIOGRAPHY**





## BIBLIOGRAPHY

- Alizadeh, A. A., Elsen, M. B., Davis, R. E., Ma, C. L., Lossos, I. S., Rosenwald, A., ... Staudt, L. M. (2000). Distinct types of diffuse large B-cell lymphoma identified by gene expression profiling. *Nature*, *403*(6769), 503–511. <https://doi.org/10.1038/35000501>
- Allen, C. D. C., & Cyster, J. G. (2008). Follicular dendritic cell networks of primary follicles and germinal centers: Phenotype and function. *Seminars in Immunology*, *20*(1), 14–25. <https://doi.org/10.1016/j.smim.2007.12.001>
- Allen, C. D., Okada, T., & Cyster, J. G. (2008). Germinal Center Organization and Cellular Dynamics Role of the GC in Antibody Responses. *Immunity*, *27*(2), 190–202.
- Allfrey, V. G., Faulkner, R., & Mirsky, A. E. (1964). ACETYLATION AND METHYLATION OF HISTONES AND THEIR POSSIBLE ROLE IN THE REGULATION OF RNA SYNTHESIS. *Proceedings of the National Academy of Sciences*, *51*(5), 786–794. <https://doi.org/10.1073/pnas.51.5.786>
- Andersson, R., & Sandelin, A. (2020). Determinants of enhancer and promoter activities of regulatory elements. *Nature Reviews Genetics*, *21*(2), 71–87. <https://doi.org/10.1038/s41576-019-0173-8>
- Asmar, F., Punj, V., Christensen, J., Pedersen, M. T., Pedersen, A., Nielsen, A. B., ... Gronbaek, K. (2013). Genome-wide profiling identifies a DNA methylation signature that associates with TET2 mutations in diffuse large B-cell lymphoma. *Haematologica*, *98*(12), 1912–1920. <https://doi.org/10.3324/haematol.2013.088740>
- Azagra, A., Román-González, L., Collazo, O., Rodríguez-Ubreva, J., de Yébenes, V. G., Barneda-Zahonero, B., ... Parra, M. (2016). In vivo conditional deletion of HDAC7 reveals its requirement to establish proper B lymphocyte identity and development. *Journal of Experimental Medicine*, *213*(12), 2591–2601. <https://doi.org/10.1084/jem.20150821>
- Bannister, A. J., & Kouzarides, T. (2011). Regulation of chromatin by histone modifications. *Cell Research*, *21*(3), 381–395.

<https://doi.org/10.1038/cr.2011.22>

Barneda-Zahonero, B., & Parra, M. (2012). Histone deacetylases and cancer. *Molecular Oncology*, 6(6), 579–589. <https://doi.org/10.1016/j.molonc.2012.07.003>

Barneda-Zahonero, B., Román-González, L., Collazo, O., Rafati, H., Islam, A. B. M. M. K., Bussmann, L. H., ... Parra, M. (2013). HDAC7 Is a Repressor of Myeloid Genes Whose Downregulation Is Required for Transdifferentiation of Pre-B Cells into Macrophages. *PLoS Genetics*, 9(5). <https://doi.org/10.1371/journal.pgen.1003503>

Basso, K., & Dalla-Favera, R. (2015). Germinal centres and B cell lymphomagenesis. *Nature Reviews Immunology*, 15(3), 172–184. <https://doi.org/10.1038/nri3814>

Becker, J. S., Nicetto, D., & Zaret, K. S. (2016). H3K9me3-Dependent Heterochromatin: Barrier to Cell Fate Changes. *Trends in Genetics*, 32(1), 29–41. <https://doi.org/10.1016/j.tig.2015.11.001>

Benner, C., Isoda, T., & Murre, C. (2015). New roles for DNA cytosine modification, eRNA, anchors, and superanchors in developing B cell progenitors. *Proceedings of the National Academy of Sciences of the United States of America*, 112(41), 12776–12781. <https://doi.org/10.1073/pnas.1512995112>

Bhojwani, D., Yang, J. J., & Pui, C.-H. (2015). Biology of Childhood Acute Lymphoblastic Leukemia. *Pediatric Clinics of North America*, 62(1), 47–60. <https://doi.org/10.1016/j.pcl.2014.09.004>

Borriello, F., Sethna, M. P., Boyd, S. D., Schweitzer, A. N., Tivol, E. A., Jacoby, D., ... Sharpe, A. H. (1997). B7-1 and B7-2 have overlapping, critical roles in immunoglobulin class switching and germinal center formation. *Immunity*, 6(3), 303–313. [https://doi.org/10.1016/S1074-7613\(00\)80333-7](https://doi.org/10.1016/S1074-7613(00)80333-7)

Brach, D., Johnston-Blackwell, D., Drew, A., Lingaraj, T., Motwani, V., Warholic, N. M., ... Thomenius, M. J. (2017). EZH2 Inhibition by Tazemetostat Results in Altered Dependency on B-cell Activation Signaling in DLBCL. *Molecular Cancer Therapeutics*, 16(11), 2586–2597. <https://doi.org/10.1158/1535->

7163.MCT-16-0840

- Brescia, P., Schneider, C., Holmes, A. B., Shen, Q., Hussein, S., Pasqualucci, L., ... Dalla-Favera, R. (2018). MEF2B Instructs Germinal Center Development and Acts as an Oncogene in B Cell Lymphomagenesis. *Cancer Cell*, *34*(3), 453-465.e9. <https://doi.org/10.1016/j.ccell.2018.08.006>
- Bueno, C., Montes, R., Catalina, P., Rodríguez, R., & Menendez, P. (2011). Insights into the cellular origin and etiology of the infant pro-B acute lymphoblastic leukemia with MLL-AF4 rearrangement. *Leukemia*, *25*(3), 400–410. <https://doi.org/10.1038/leu.2010.284>
- Bueno, Clara, Ayllón, V., Montes, R., Navarro-Montero, O., Ramos-Mejia, V., Real, P. J., ... Menendez, P. (2013). FLT3 activation cooperates with MLL-AF4 fusion protein to abrogate the hematopoietic specification of human ESCs. *Blood*, *121*(19), 3867–3878. <https://doi.org/10.1182/blood-2012-11-470146>
- Bussmann, L. H., Schubert, A., Vu Manh, T. P., De Andres, L., Desbordes, S. C., Parra, M., ... Graf, T. (2009a). A Robust and Highly Efficient Immune Cell Reprogramming System. *Cell Stem Cell*, *5*(5), 554–566. <https://doi.org/10.1016/j.stem.2009.10.004>
- Bussmann, L. H., Schubert, A., Vu Manh, T. P., De Andres, L., Desbordes, S. C., Parra, M., ... Graf, T. (2009b). A Robust and Highly Efficient Immune Cell Reprogramming System. *Cell Stem Cell*, *5*(5), 554–566. <https://doi.org/10.1016/j.stem.2009.10.004>
- Carotta, S., Willis, S. N., Hasbold, J., Inouye, M., Pang, S. H. M., Emslie, D., ... Nutt, S. L. (2014). The transcription factors IRF8 and PU.1 negatively regulate plasma cell differentiation. *Journal of Experimental Medicine*, *211*(11), 2169–2181. <https://doi.org/10.1084/jem.20140425>
- Cattoretti, G., Shaknovich, R., Smith, P. M., Jäck, H.-M., Murty, V. V., & Alobeid, B. (2006). Stages of Germinal Center Transit Are Defined by B Cell Transcription Factor Coexpression and Relative Abundance. *The Journal of Immunology*, *177*(10), 6930–6939. <https://doi.org/10.4049/jimmunol.177.10.6930>

- Chang, S., Young, B. D., Li, S., Qi, X., Richardson, J. A., & Olson, E. N. (2006). Histone Deacetylase 7 Maintains Vascular Integrity by Repressing Matrix Metalloproteinase 10. *Cell*, 126(2), 321–334. <https://doi.org/10.1016/j.cell.2006.05.040>
- Chávez-Galán, L., Olleros, M. L., Vesin, D., & Garcia, I. (2015). Much More than M1 and M2 Macrophages, There are also CD169(+) and TCR(+) Macrophages. *Frontiers in Immunology*, 6, 263. <https://doi.org/10.3389/fimmu.2015.00263>
- Chen, C.-W., & Armstrong, S. A. (2015). Targeting DOT1L and HOX gene expression in MLL-rearranged leukemia and beyond. *Experimental Hematology*, 43(8), 673–684. <https://doi.org/10.1016/j.exphem.2015.05.012>
- Chiu, Y.-K., Lin, I.-Y., Su, S.-T., Wang, K.-H., Yang, S.-Y., Tsai, D.-Y., ... Lin, K.-I. (2014). Transcription Factor ABF-1 Suppresses Plasma Cell Differentiation but Facilitates Memory B Cell Formation. *The Journal of Immunology*, 193(5), 2207–2217. <https://doi.org/10.4049/jimmunol.1400411>
- Cobaleda, C., Schebesta, A., Delogu, A., & Busslinger, M. (2007). Pax5: The guardian of B cell identity and function. *Nature Immunology*, 8(5), 463–470. <https://doi.org/10.1038/ni1454>
- Cordoba, S., Onuoha, S., Thomas, S., Pignataro, D. S., Hough, R., Ghorashian, S., ... Amrolia, P. J. (2021). CAR T cells with dual targeting of CD19 and CD22 in pediatric and young adult patients with relapsed or refractory B cell acute lymphoblastic leukemia: a phase 1 trial. *Nature Medicine*, 27(10), 1797–1805. <https://doi.org/10.1038/s41591-021-01497-1>
- Creyghton, M. P., Cheng, A. W., Welstead, G. G., Kooistra, T., Carey, B. W., Steine, E. J., ... Jaenisch, R. (2010). Histone H3K27ac separates active from poised enhancers and predicts developmental state. *Proceedings of the National Academy of Sciences*, 107(50), 21931–21936. <https://doi.org/10.1073/pnas.1016071107>
- Crump, M., Neelapu, S. S., Farooq, U., Van Den Neste, E., Kuruvilla, J., Westin, J., ... Gisselbrecht, C. (2017). Outcomes in refractory diffuse large B-cell lymphoma: results from the international SCHOLAR-1 study. *Blood*, 130(16),

1800–1808. <https://doi.org/10.1182/blood-2017-03-769620>

de Barrios, O., Galaras, A., Trincado, J. L., Azagra, A., Collazo, O., Meler, A., ... Parra, M. (2021). HDAC7 is a major contributor in the pathogenesis of infant t(4;11) proB acute lymphoblastic leukemia. *Leukemia*. <https://doi.org/10.1038/s41375-020-01097-x>

De Silva, N. S., & Klein, U. (2015). Dynamics of B cells in germinal centres. *Nature Reviews Immunology*, 15(3), 137–148. <https://doi.org/10.1038/nri3804>

Deaton, A. M., & Bird, A. (2011). CpG islands and the regulation of transcription. *Genes and Development*, 25(10), 1010–1022. <https://doi.org/10.1101/gad.2037511>

Delcuve, G. P., Khan, D. H., & Davie, J. R. (2012). Roles of histone deacetylases in epigenetic regulation: Emerging paradigms from studies with inhibitors. *Clinical Epigenetics*, 4(1), 5. <https://doi.org/10.1186/1868-7083-4-5>

Delogu, A., Schebesta, A., Sun, Q., Aschenbrenner, K., Perlot, T., & Busslinger, M. (2006). Gene Repression by Pax5 in B Cells Is Essential for Blood Cell Homeostasis and Is Reversed in Plasma Cells. *Immunity*, 24(3), 269–281. <https://doi.org/10.1016/j.immuni.2006.01.012>

Dent, A. L., Shaffer, A. L., Yu, X., Allman, D., & Staudt, L. M. (1997). Control of Inflammation, Cytokine Expression, and Germinal Center Formation by BCL-6. *Science*, 276(5312), 589–592. <https://doi.org/10.1126/science.276.5312.589>

Dequiedt, F., Kasler, H., Fischle, W., Kiermer, V., Weinstein, M., Herndier, B. G., & Verdin, E. (2003). HDAC7, a Thymus-Specific Class II Histone Deacetylase, Regulates Nur77 Transcription and TCR-Mediated Apoptosis. *Immunity*, 18(5), 687–698. [https://doi.org/10.1016/S1074-7613\(03\)00109-2](https://doi.org/10.1016/S1074-7613(03)00109-2)

Dequiedt, F., Van Lint, J., Lecomte, E., Van Duppen, V., Seufferlein, T., Vandenhede, J. R., ... Kettmann, R. (2005a). Phosphorylation of histone deacetylase 7 by protein kinase D mediates T cell receptor-induced Nur77 expression and apoptosis. *Journal of Experimental Medicine*, 201(5), 793–804. <https://doi.org/10.1084/jem.20042034>

- Dequiedt, F., Van Lint, J., Lecomte, E., Van Duppen, V., Seufferlein, T., Vandenheede, J. R., ... Kettmann, R. (2005b). Phosphorylation of histone deacetylase 7 by protein kinase D mediates T cell receptor-induced Nur77 expression and apoptosis. *Journal of Experimental Medicine*, 201(5), 793–804. <https://doi.org/10.1084/jem.20042034>
- Dhordain, P., Quief, S., Lantoine, D., Kerckaert, J.-P., Albagli, O., Lin, R. J., & Evans, R. M. (1998). The LAZ3(BCL-6) oncoprotein recruits a SMRT/mSIN3A/histone deacetylase containing complex to mediate transcriptional repression. *Nucleic Acids Research*, 26(20), 4645–4651. <https://doi.org/10.1093/nar/26.20.4645>
- Di Giorgio, E., & Brancolini, C. (2016). Regulation of class IIa HDAC activities: It is not only matter of subcellular localization. *Epigenomics*, 8(2), 251–269. <https://doi.org/10.2217/epi.15.106>
- Di Noia, J. M., & Neuberger, M. S. (2007). Molecular mechanisms of antibody somatic hypermutation. *Annual Review of Biochemistry*, 76, 1–22. <https://doi.org/10.1146/annurev.biochem.76.061705.090740>
- Doblas, A. A., Bueno, C., Rogers, R. B., Roy, A., Schneider, P., Bardini, M., ... Stam, R. W. (2019). Unraveling the cellular origin and clinical prognostic markers of infant B-cell acute lymphoblastic leukemia using genome-wide analysis. *Haematologica*, 104(6), 1176–1188. <https://doi.org/10.3324/haematol.2018.206375>
- Dogan, I., Bertocci, B., Vilmont, V., Delbos, F., Mégret, J., Storck, S., ... Weill, J.-C. (2009). Multiple layers of B cell memory with different effector functions. *Nature Immunology*, 10(12), 1292–1299. <https://doi.org/10.1038/ni.1814>
- Dominguez-Sola, D., Kung, J., Holmes, A. B., Wells, V. A., Mo, T., Basso, K., & Dalla-Favera, R. (2015a). The FOXO1 Transcription Factor Instructs the Germinal Center Dark Zone Program. *Immunity*, 43(6), 1064–1074. <https://doi.org/10.1016/j.immuni.2015.10.015>
- Dominguez-Sola, D., Kung, J., Holmes, A. B., Wells, V. A., Mo, T., Basso, K., & Dalla-Favera, R. (2015b). The FOXO1 Transcription Factor Instructs the Germinal Center Dark Zone Program. *Immunity*, 43(6), 1064–1074.

<https://doi.org/10.1016/j.immuni.2015.10.015>

- Dominguez, P. M., Ghamlouch, H., Rosikiewicz, W., Kumar, P., Béguelin, W., Fontán, L., ... Melnick, A. M. (2018). TET2 Deficiency Causes Germinal Center Hyperplasia, Impairs Plasma Cell Differentiation, and Promotes B-cell Lymphomagenesis. *Cancer Discovery*, 8(12), 1632–1653. <https://doi.org/10.1158/2159-8290.CD-18-0657>
- Dou, Y., Milne, T. A., Tackett, A. J., Smith, E. R., Fukuda, A., Wysocka, J., ... Roeder, R. G. (2005). Physical Association and Coordinate Function of the H3 K4 Methyltransferase MLL1 and the H4 K16 Acetyltransferase MOF. *Cell*, 121(6), 873–885. <https://doi.org/10.1016/j.cell.2005.04.031>
- Dressel, U., Bailey, P. J., Wang, S. C. M., Downes, M., Evans, R. M., & Muscat, G. E. O. (2001). A Dynamic Role for HDAC7 in MEF2-mediated Muscle Differentiation. *Journal of Biological Chemistry*, 276(20), 17007–17013. <https://doi.org/10.1074/jbc.M101508200>
- Du, J., Zhou, Y., Su, X., Yu, J. J., Khan, S., Jiang, H., ... Lin, H. (2011). Sirt5 Is a NAD-Dependent Protein Lysine Demalonylase and Desuccinylase. *Science*, 334(6057), 806–809. <https://doi.org/10.1126/science.1207861>
- Ennishi, D., Mottok, A., Ben-Neriah, S., Shulha, H. P., Farinha, P., Chan, F. C., ... Scott, D. W. (2017). Genetic profiling of MYC and BCL2 in diffuse large B-cell lymphoma determines cell-of-origin–specific clinical impact. *Blood*, 129(20), 2760–2770. <https://doi.org/10.1182/blood-2016-11-747022>
- Ferlay, J., Colombet, M., Soerjomataram, I., Mathers, C., Parkin, D. M., Piñeros, M., ... Bray, F. (2018). Estimating the global cancer incidence and mortality in 2018: GLOBOCAN sources and methods. *International Journal of Cancer*, 144(8), 1941–1953. <https://doi.org/10.1002/ijc.31937>
- Ficz, G., Branco, M. R., Seisenberger, S., Santos, F., Krueger, F., Hore, T. A., ... Reik, W. (2011). Dynamic regulation of 5-hydroxymethylcytosine in mouse ES cells and during differentiation. *Nature*, 473(7347), 398–402. <https://doi.org/10.1038/nature10008>
- Fischle, W., Dequiedt, F., Hendzel, M. J., Guenther, M. G., Lazar, M. A., Voelter, W., & Verdin, E. (2002). Enzymatic activity associated with class II HDACs

is dependent on a multiprotein complex containing HDAC3 and SMRT/N-CoR. *Molecular Cell*, 9(1), 45–57. [https://doi.org/10.1016/S1097-2765\(01\)00429-4](https://doi.org/10.1016/S1097-2765(01)00429-4)

Fisher, R. I., Gaynor, E. R., Dahlborg, S., Oken, M. M., Grogan, T. M., Mize, E. M., ... Miller, T. P. (1993). Comparison of a Standard Regimen (CHOP) with Three Intensive Chemotherapy Regimens for Advanced Non-Hodgkin's Lymphoma. *New England Journal of Medicine*, 328(14), 1002–1006. <https://doi.org/10.1056/NEJM199304083281404>

Friedberg, J. W. (2011). Relapsed/Refractory Diffuse Large B-Cell Lymphoma. *Hematology*, 2011(1), 498–505. <https://doi.org/10.1182/asheducation-2011.1.498>

Gao, L., Cueto, M. A., Asselbergs, F., & Atadja, P. (2002). Cloning and functional characterization of HDAC11, a novel member of the human histone deacetylase family. *Journal of Biological Chemistry*, 277(28), 25748–25755. <https://doi.org/10.1074/jbc.M111871200>

Garside, P., Ingulli, E., Merica, R. R., Johnson, J. G., Noelle, R. J., & Jenkins, M. K. (1998). Visualization of specific B and T lymphocyte interactions in the lymph node. *Science*, 281(5373), 96–99. <https://doi.org/10.1126/science.281.5373.96>

Gatto, D., Paus, D., Basten, A., Mackay, C. R., & Brink, R. (2009). Guidance of B Cells by the Orphan G Protein-Coupled Receptor EBI2 Shapes Humoral Immune Responses. *Immunity*, 31(2), 259–269. <https://doi.org/10.1016/j.immuni.2009.06.016>

Ghorashian, S., Jacoby, E., De Moerloose, B., Rives, S., Bonney, D., Shenton, G., ... Baruchel, A. (2022). Tisagenlecleucel therapy for relapsed or refractory B-cell acute lymphoblastic leukaemia in infants and children younger than 3 years of age at screening: an international, multicentre, retrospective cohort study. *The Lancet Haematology*, 9(10), e766–e775. [https://doi.org/10.1016/S2352-3026\(22\)00225-3](https://doi.org/10.1016/S2352-3026(22)00225-3)

Green, J. A., Suzuki, K., Cho, B., Willison, L. D., Palmer, D., Allen, C. D. C., ... Cyster, J. G. (2011). The sphingosine 1-phosphate receptor S1P2 maintains



- the homeostasis of germinal center B cells and promotes niche confinement. *Nature Immunology*, 12(7), 672–680. <https://doi.org/10.1038/ni.2047>
- Grozinger, C. M., Hassig, C. A., & Schreiber, S. L. (1999). Three proteins define a class of human histone deacetylases related to yeast Hda1p. *Proceedings of the National Academy of Sciences*, 96(9), 4868–4873. <https://doi.org/10.1073/pnas.96.9.4868>
- Guikema, J. E. J., Linehan, E. K., Tsuchimoto, D., Nakabeppu, Y., Strauss, P. R., Stavnezer, J., & Schrader, C. E. (2007). APE1- And APE2-dependent DNA breaks in immunoglobulin class switch recombination. *Journal of Experimental Medicine*, 204(12), 3017–3026. <https://doi.org/10.1084/jem.20071289>
- Guo, K., Ma, Z., Zhang, Y., Han, L., Shao, C., Feng, Y., ... Yan, X. (2022). HDAC7 promotes NSCLC proliferation and metastasis via stabilization by deubiquitinase USP10 and activation of  $\beta$ -catenin-FGF18 pathway. *Journal of Experimental & Clinical Cancer Research*, 41(1), 91. <https://doi.org/10.1186/s13046-022-02266-9>
- Haberland, M., Montgomery, R. L., & Olson, E. N. (2009). The many roles of histone deacetylases in development and physiology: Implications for disease and therapy. *Nature Reviews Genetics*, 10(1), 32–42. <https://doi.org/10.1038/nrg2485>
- Hashimoto, H., Liu, Y., Upadhyay, A. K., Chang, Y., Howerton, S. B., Vertino, P. M., ... Cheng, X. (2012). Recognition and potential mechanisms for replication and erasure of cytosine hydroxymethylation. *Nucleic Acids Research*, 40(11), 4841–4849. <https://doi.org/10.1093/nar/gks155>
- Hatzi, K., Jiang, Y., Huang, C., Garrett-Bakelman, F., Gearhart, M. D., Giannopoulou, E. G., ... Melnick, A. (2013). A Hybrid Mechanism of Action for BCL6 in B Cells Defined by Formation of Functionally Distinct Complexes at Enhancers and Promoters. *Cell Reports*, 4(3), 578–588. <https://doi.org/10.1016/j.celrep.2013.06.016>
- Hatzi, K., & Melnick, A. (2014). Breaking bad in the germinal center: how deregulation of BCL6 contributes to lymphomagenesis. *Trends in Molecular*

- Medicine*, 20(6), 343–352. <https://doi.org/10.1016/j.molmed.2014.03.001>
- He, J.-S., Subramaniam, S., Narang, V., Srinivasan, K., Saunders, S. P., Carbajo, D., ... Curotto de Lafaille, M. A. (2017). IgG1 memory B cells keep the memory of IgE responses. *Nature Communications*, 8(1), 641. <https://doi.org/10.1038/s41467-017-00723-0>
- Heesters, B. A., Myers, R. C., & Carroll, M. C. (2014). Follicular dendritic cells: Dynamic antigen libraries. *Nature Reviews Immunology*, 14(7), 495–504. <https://doi.org/10.1038/nri3689>
- Heizmann, B., Kastner, P., & Chan, S. (2013). Ikaros is absolutely required for pre-B cell differentiation by attenuating IL-7 signals. *Journal of Experimental Medicine*, 210(13), 2823–2832. <https://doi.org/10.1084/jem.20131735>
- Hendriks, R. W., & Middendorp, S. (2004). The pre-BCR checkpoint as a cell-autonomous proliferation switch. *Trends in Immunology*, 25(5), 249–256. <https://doi.org/10.1016/j.it.2004.02.011>
- Herglotz, J., Unrau, L., Hauschildt, F., Fischer, M., Kriebitzsch, N., Alawi, M., ... Stocking, C. (2016). Essential control of early B-cell development by Mef2 transcription factors. *Blood*, 127(5), 572–581. <https://doi.org/10.1182/blood-2015-04-643270>
- Herrera, A. F., Mei, M., Low, L., Kim, H. T., Griffin, G. K., Song, J. Y., ... Armand, P. (2017). Relapsed or Refractory Double-Expressor and Double-Hit Lymphomas Have Inferior Progression-Free Survival After Autologous Stem-Cell Transplantation. *Journal of Clinical Oncology*, 35(1), 24–31. <https://doi.org/10.1200/JCO.2016.68.2740>
- Herzog, S., Reth, M., & Jumaa, H. (2009). Regulation of B-cell proliferation and differentiation by pre-B-cell receptor signalling. *Nature Reviews Immunology*, 9(3), 195–205. <https://doi.org/10.1038/nri2491>
- Hetzel, S., Mattei, A. L., Kretzmer, H., Qu, C., Chen, X., Fan, Y., ... Meissner, A. (2022). Acute lymphoblastic leukemia displays a distinct highly methylated genome. *Nature Cancer*, 3(6), 768–782. <https://doi.org/10.1038/s43018-022-00370-5>

- Holmes, A. B., Corinaldesi, C., Shen, Q., Kumar, R., Compagno, N., Wang, Z., ... Basso, K. (2020). Single-cell analysis of germinal-center B cells informs on lymphoma cell of origin and outcome. *Journal of Experimental Medicine*, 217(10). <https://doi.org/10.1084/jem.20200483>
- Holstein, S. A., & Lunning, M. A. (2020). CAR T-Cell Therapy in Hematologic Malignancies: A Voyage in Progress. *Clinical Pharmacology & Therapeutics*, 107(1), 112–122. <https://doi.org/10.1002/cpt.1674>
- Hu, L., Li, Z., Cheng, J., Rao, Q., Gong, W., Liu, M., ... Xu, Y. (2013). Crystal Structure of TET2-DNA Complex: Insight into TET-Mediated 5mC Oxidation. *Cell*, 155(7), 1545–1555. <https://doi.org/10.1016/j.cell.2013.11.020>
- Hu, L., Lu, J., Cheng, J., Rao, Q., Li, Z., Hou, H., ... Xu, Y. (2015). Structural insight into substrate preference for TET-mediated oxidation. *Nature*, 527(7576), 118–122. <https://doi.org/10.1038/nature15713>
- Hyun, K., Jeon, J., Park, K., & Kim, J. (2017). Writing, erasing and reading histone lysine methylations. *Experimental and Molecular Medicine*, 49(4), e324-22. <https://doi.org/10.1038/emm.2017.11>
- Inaba, H., Greaves, M., & Mullighan, C. G. (2013). Acute lymphoblastic leukaemia. *The Lancet*, 381(9881), 1943–1955. [https://doi.org/10.1016/S0140-6736\(12\)62187-4](https://doi.org/10.1016/S0140-6736(12)62187-4)
- Inamine, A., Takahashi, Y., Baba, N., Miyake, K., Tokuhisa, T., Takemori, T., & Abe, R. (2005). Two waves of memory B-cell generation in the primary immune response. *International Immunology*, 17(5), 581–589. <https://doi.org/10.1093/intimm/dxh241>
- Inoue, T., Shinnakasu, R., Ise, W., Kawai, C., Egawa, T., & Kurosaki, T. (2017). The transcription factor Foxo1 controls germinal center B cell proliferation in response to T cell help. *Journal of Experimental Medicine*, 214(4), 1181–1198. <https://doi.org/10.1084/jem.20161263>
- Ito, K., Lee, J., Chrysanthou, S., Zhao, Y., Josephs, K., Sato, H., ... Ito, K. (2019). Non-catalytic Roles of Tet2 Are Essential to Regulate Hematopoietic Stem and Progenitor Cell Homeostasis. *Cell Reports*, 28(10), 2480-2490.e4. <https://doi.org/10.1016/j.celrep.2019.07.094>

- Ito, S., Shen, L., Dai, Q., Wu, S. C., Collins, L. B., Swenberg, J. A., ... Zhang, Y. (2011). Tet proteins can convert 5-methylcytosine to 5-formylcytosine and 5-carboxylcytosine. *Science*, 333(6047), 1300–1303. <https://doi.org/10.1126/science.1210597>
- Izzo, F., Lee, S. C., Poran, A., Chaligne, R., Gaiti, F., Gross, B., ... Landau, D. A. (2020). DNA methylation disruption reshapes the hematopoietic differentiation landscape. *Nature Genetics*, 52(4), 378–387. <https://doi.org/10.1038/s41588-020-0595-4>
- Jaffe, J. D., Wang, Y., Chan, H. M., Zhang, J., Huether, R., Kryukov, G. V., ... Stegmeier, F. (2013). Global chromatin profiling reveals NSD2 mutations in pediatric acute lymphoblastic leukemia. *Nature Genetics*, 45(11), 1386–1391. <https://doi.org/10.1038/ng.2777>
- Jensen, E. D., Gopalakrishnan, R., & Westendorf, J. J. (2009). Bone morphogenic protein 2 activates protein kinase D to regulate histone deacetylase 7 localization and repression of Runx2. *Journal of Biological Chemistry*, 284(4), 2225–2233. <https://doi.org/10.1074/jbc.M800586200>
- Jensen, E. D., Schroeder, T. M., Bailey, J., Gopalakrishnan, R., & Westendorf, J. J. (2008). Histone deacetylase 7 associates with Runx2 and represses its activity during osteoblast maturation in a deacetylation-independent manner. *Journal of Bone and Mineral Research*, 23(3), 361–372. <https://doi.org/10.1359/jbmr.071104>
- Jiang, Y., Ortega-Molina, A., Geng, H., Ying, H.-Y., Hatzi, K., Parsa, S., ... Melnick, A. M. (2017). CREBBP Inactivation Promotes the Development of HDAC3-Dependent Lymphomas. *Cancer Discovery*, 7(1), 38–53. <https://doi.org/10.1158/2159-8290.CD-16-0975>
- Jin, B., Li, Y., & Robertson, K. D. (2011). DNA Methylation: Superior or Subordinate in the Epigenetic Hierarchy? *Genes & Cancer*, 2(6), 607–617. <https://doi.org/10.1177/1947601910393957>
- Kaji, T., Ishige, A., Hikida, M., Taka, J., Hijikata, A., Kubo, M., ... Takemori, T. (2012). Distinct cellular pathways select germline-encoded and somatically mutated antibodies into immunological memory. *Journal of Experimental*

*Medicine*, 209(11), 2079–2097. <https://doi.org/10.1084/jem.20120127>

Kallin, E. M., Rodríguez-Ubreva, J., Christensen, J., Cimmino, L., Aifantis, I., Helin, K., ... Graf, T. (2012). Tet2 Facilitates the Derepression of Myeloid Target Genes during CEBP $\alpha$ -Induced Transdifferentiation of Pre-B Cells. *Molecular Cell*, 48(2), 266–276. <https://doi.org/10.1016/j.molcel.2012.08.007>

Kao, H. Y., Downes, M., Ordentlich, P., & Evans, R. M. (2000). Isolation of a novel histone deacetylase reveals that class I and class II deacetylases promote SMRT-mediated repression. *Genes and Development*, 14(1), 55–66. <https://doi.org/10.1101/gad.14.1.55>

Kasler, H. G., Lee, I. S., Lim, H. W., & Verdin, E. (2018). Histone Deacetylase 7 mediates tissue-specific autoimmunity via control of innate effector function in invariant Natural Killer T cells. *eLife*, 7, 1–29. <https://doi.org/10.7554/eLife.32109>

Kasler, H. G., Lim, H. W., Mottet, D., Collins, A. M., Lee, I. S., & Verdin, E. (2012). Nuclear export of histone deacetylase 7 during thymic selection is required for immune self-tolerance. *EMBO Journal*, 31(23), 4453–4465. <https://doi.org/10.1038/emboj.2012.295>

Kasler, H. G., & Verdin, E. (2007). Histone Deacetylase 7 Functions as a Key Regulator of Genes Involved in both Positive and Negative Selection of Thymocytes. *Molecular and Cellular Biology*, 27(14), 5184–5200. <https://doi.org/10.1128/MCB.02091-06>

Kasler, H. G., Young, B. D., Mottet, D., Lim, H. W., Collins, A. M., Olson, E. N., & Verdin, E. (2011a). Histone Deacetylase 7 Regulates Cell Survival and TCR Signaling in CD4/CD8 Double-Positive Thymocytes. *The Journal of Immunology*, 186(8), 4782–4793. <https://doi.org/10.4049/jimmunol.1001179>

Kasler, H. G., Young, B. D., Mottet, D., Lim, H. W., Collins, A. M., Olson, E. N., & Verdin, E. (2011b). Histone Deacetylase 7 Regulates Cell Survival and TCR Signaling in CD4/CD8 Double-Positive Thymocytes. *The Journal of Immunology*, 186(8), 4782–4793. <https://doi.org/10.4049/jimmunol.1001179>

Keir, M. E., Butte, M. J., Freeman, G. J., & Sharpe, A. H. (2008). PD-1 and its

- ligands in tolerance and immunity. *Annual Review of Immunology*, 26, 677–704. <https://doi.org/10.1146/annurev.immunol.26.021607.090331>
- Kennedy, D. E., Okoreeh, M. K., Maienschein-Cline, M., Ai, J., Veselits, M., McLean, K. C., ... Clark, M. R. (2020). Novel specialized cell state and spatial compartments within the germinal center. *Nature Immunology*, 21(6), 660–670. <https://doi.org/10.1038/s41590-020-0660-2>
- Kepler, T. B., & Perelson, A. S. (1993). Cyclic re-entry of germinal center B cells and the efficiency of affinity maturation. *Immunology Today*, 14(8), 412–415. [https://doi.org/10.1016/0167-5699\(93\)90145-B](https://doi.org/10.1016/0167-5699(93)90145-B)
- Khiem, D., Cyster, J. G., Schwarz, J. J., & Black, B. L. (2008). A p38 MAPK-MEF2C pathway regulates B-cell proliferation. *Proceedings of the National Academy of Sciences*, 105(44), 17067–17072. <https://doi.org/10.1073/pnas.0804868105>
- Khorasanizadeh, S. (2004). The Nucleosome. *Cell*, 116(2), 259–272. [https://doi.org/10.1016/S0092-8674\(04\)00044-3](https://doi.org/10.1016/S0092-8674(04)00044-3)
- Klein, U., Casola, S., Cattoretti, G., Shen, Q., Lia, M., Mo, T., ... Dalla-Favera, R. (2006). Transcription factor IRF4 controls plasma cell differentiation and class-switch recombination. *Nature Immunology*, 7(7), 773–782. <https://doi.org/10.1038/ni1357>
- Ko, M., An, J., Bandukwala, H. S., Chavez, L., Äijö, T., Pastor, W. A., ... Rao, A. (2013). Modulation of TET2 expression and 5-methylcytosine oxidation by the CXXC domain protein IDAX. *Nature*, 497(7447), 122–126. <https://doi.org/10.1038/nature12052>
- Ko, M., Bandukwala, H. S., An, J., Lamperti, E. D., Thompson, E. C., Hastie, R., ... Rao, A. (2011). Ten-Eleven-Translocation 2 (TET2) negatively regulates homeostasis and differentiation of hematopoietic stem cells in mice. *Proceedings of the National Academy of Sciences of the United States of America*, 108(35), 14566–14571. <https://doi.org/10.1073/pnas.1112317108>
- Ko, M., Huang, Y., Jankowska, A. M., Pape, U. J., Tahiliani, M., Bandukwala, H. S., ... Rao, A. (2010). Impaired hydroxylation of 5-methylcytosine in myeloid cancers with mutant TET2. *Nature*, 468(7325), 839–843.

<https://doi.org/10.1038/nature09586>

- Kochenderfer, J. N., Somerville, R. P. T., Lu, T., Yang, J. C., Sherry, R. M., Feldman, S. A., ... Rosenberg, S. A. (2017). Long-Duration Complete Remissions of Diffuse Large B Cell Lymphoma after Anti-CD19 Chimeric Antigen Receptor T Cell Therapy. *Molecular Therapy*, 25(10), 2245–2253. <https://doi.org/10.1016/j.ymthe.2017.07.004>
- Kong, N. R., Davis, M., Chai, L., Winoto, A., & Tjian, R. (2016). MEF2C and EBF1 Co-regulate B Cell-Specific Transcription. *PLoS Genetics*, 12(2). <https://doi.org/10.1371/journal.pgen.1005845>
- Koyama, M., & Kurumizaka, H. (2018). Structural diversity of the nucleosome. *Journal of Biochemistry*, 163(2), 85–95. <https://doi.org/10.1093/jb/mvx081>
- Kriaucionis, S., & Heintz, N. (2009). The nuclear DNA base 5-hydroxymethylcytosine is present in Purkinje neurons and the brain. *Science (New York, N.Y.)*, 324(5929), 929–930. <https://doi.org/10.1126/science.1169786>
- Kubiura, M., Okano, M., Kimura, H., Kawamura, F., & Tada, M. (2012). Chromosome-wide regulation of euchromatin-specific 5mC to 5hmC conversion in mouse ES cells and female human somatic cells. *Chromosome Research: An International Journal on the Molecular, Supramolecular and Evolutionary Aspects of Chromosome Biology*, 20(7), 837–848. <https://doi.org/10.1007/s10577-012-9317-9>
- Kwon, K., Hutter, C., Sun, Q., Bilic, I., Cobaleda, C., Malin, S., & Busslinger, M. (2008). Instructive Role of the Transcription Factor E2A in Early B Lymphopoiesis and Germinal Center B Cell Development. *Immunity*, 28(6), 751–762. <https://doi.org/10.1016/j.immuni.2008.04.014>
- Laidlaw, B. J., Schmidt, T. H., Green, J. A., Allen, C. D. C., Okada, T., & Cyster, J. G. (2017). The Eph-related tyrosine kinase ligand Ephrin-B1 marks germinal center and memory precursor B cells. *The Journal of Experimental Medicine*, 214(3), 639–649. <https://doi.org/10.1084/jem.20161461>
- Lau, A. W., & Brink, R. (2020). Selection in the germinal center. *Current Opinion in Immunology*, 63, 29–34. <https://doi.org/10.1016/j.coi.2019.11.001>

- Lemercier, C., Verdel, A., Galloo, B., Curtet, S., Brocard, M. P., & Khochbin, S. (2000). mHDA1/HDAC5 histone deacetylase interacts with and represses MEF2A transcriptional activity. *Journal of Biological Chemistry*, *275*(20), 15594–15599. <https://doi.org/10.1074/jbc.M908437199>
- Lin, H., & Grosschedl, R. (1995). Failure of B-cell differentiation in mice lacking the transcription factor EBF. *Nature*, *376*(6537), 263–267. <https://doi.org/10.1038/376263a0>
- Lin, K.-I., Angelin-Duclos, C., Kuo, T. C., & Calame, K. (2002a). Blimp-1-Dependent Repression of Pax-5 Is Required for Differentiation of B Cells to Immunoglobulin M-Secreting Plasma Cells. *Molecular and Cellular Biology*, *22*(13), 4771–4780. <https://doi.org/10.1128/mcb.22.13.4771-4780.2002>
- Lin, K.-I., Angelin-Duclos, C., Kuo, T. C., & Calame, K. (2002b). Blimp-1-Dependent Repression of Pax-5 Is Required for Differentiation of B Cells to Immunoglobulin M-Secreting Plasma Cells. *Molecular and Cellular Biology*, *22*(13), 4771–4780. <https://doi.org/10.1128/MCB.22.13.4771-4780.2002>
- Lin, Y., Wong, K., & Calame, K. (1997). Repression of c- myc Transcription by Blimp-1, an Inducer of Terminal B Cell Differentiation. *Science*, *276*(5312), 596–599. <https://doi.org/10.1126/science.276.5312.596>
- Lio, C.-W., Zhang, J., González-Avalos, E., Hogan, P. G., Chang, X., & Rao, A. (2016). Tet2 and Tet3 cooperate with B-lineage transcription factors to regulate DNA modification and chromatin accessibility. *ELife*, *5*. <https://doi.org/10.7554/eLife.18290>
- Lio, C. W., Zhang, J., González-Avalos, E., Hogan, P. G., Chang, X., & Rao, A. (2016). Tet2 and Tet3 cooperate with B-lineage transcription factors to regulate DNA modification and chromatin accessibility. *ELife*, *5*(NOVEMBER2016), 1–26. <https://doi.org/10.7554/eLife.18290>
- Lo Coco, F., Ye, B. H., Lista, F., Corradini, P., Offit, K., Knowles, D. M., ... Dalla-Favera, R. (1994). Rearrangements of the BCL6 gene in diffuse large cell non-Hodgkin's lymphoma. *Blood*, *83*(7), 1757–1759. Retrieved from <http://www.ncbi.nlm.nih.gov/pubmed/8142643>
- Lohr, J. G., Stojanov, P., Lawrence, M. S., Auclair, D., Chapuy, B., Sougnez, C.,



- ... Golub, T. R. (2012). Discovery and prioritization of somatic mutations in diffuse large B-cell lymphoma (DLBCL) by whole-exome sequencing. *Proceedings of the National Academy of Sciences*, *109*(10), 3879–3884. <https://doi.org/10.1073/pnas.1121343109>
- Lu, E., Wolfreys, F. D., Muppidi, J. R., Xu, Y., & Cyster, J. G. (2019). S-Geranylgeranyl-l-glutathione is a ligand for human B cell-confinement receptor P2RY8. *Nature*, *567*(7747), 244–248. <https://doi.org/10.1038/s41586-019-1003-z>
- Martin-Subero, J. I., & Oakes, C. C. (2018). Charting the dynamic epigenome during B-cell development. *Seminars in Cancer Biology*, *51*(June 2017), 139–148. <https://doi.org/10.1016/j.semcancer.2017.08.008>
- Mayer, C. T., Gazumyan, A., Kara, E. E., Gitlin, A. D., Golijanin, J., Viant, C., ... Nussenzweig, M. C. (2017). The microanatomic segregation of selection by apoptosis in the germinal center. *Science*, *358*(6360). <https://doi.org/10.1126/science.aao2602>
- Mccluskey, R. T., & Schlossman, S. F. (1981). Stages of B Cell Differentiation. *Journal of Experimental Medicine*, *154*(September), 737–749.
- Menendez, P., Catalina, P., Rodríguez, R., Melen, G. J., Bueno, C., Arriero, M., ... García-Castro, J. (2009). Bone marrow mesenchymal stem cells from infants with MLL-AF4+ acute leukemia harbor and express the MLL-AF4 fusion gene. *Journal of Experimental Medicine*, *206*(13), 3131–3141. <https://doi.org/10.1084/jem.20091050>
- Meyer, C., Burmeister, T., Gröger, D., Tsaur, G., Fehina, L., Renneville, A., ... Marschalek, R. (2018). The MLL recombinome of acute leukemias in 2017. *Leukemia*, *32*(2), 273–284. <https://doi.org/10.1038/leu.2017.213>
- Meyer, C., Kowarz, E., Hofmann, J., Renneville, A., Zuna, J., Trka, J., ... Marschalek, R. (2009). New insights to the MLL recombinome of acute leukemias. *Leukemia*, *23*(8), 1490–1499. <https://doi.org/10.1038/leu.2009.33>
- Meyer, S. N., Scuoppo, C., Vlasevska, S., Bal, E., Holmes, A. B., Holloman, M., ... Pasqualucci, L. (2019). Unique and Shared Epigenetic Programs of the

- CREBBP and EP300 Acetyltransferases in Germinal Center B Cells Reveal Targetable Dependencies in Lymphoma. *Immunity*, 51(3), 535-547.e9. <https://doi.org/10.1016/j.immuni.2019.08.006>
- Minnich, M., Tagoh, H., Bönelt, P., Axelsson, E., Fischer, M., Cebolla, B., ... Buslinger, M. (2016a). Multifunctional role of the transcription factor Blimp-1 in coordinating plasma cell differentiation. *Nature Immunology*, 17(3), 331–343. <https://doi.org/10.1038/ni.3349>
- Minnich, M., Tagoh, H., Bönelt, P., Axelsson, E., Fischer, M., Cebolla, B., ... Buslinger, M. (2016b). Multifunctional role of the transcription factor Blimp-1 in coordinating plasma cell differentiation. *Nature Immunology*, 17(3), 331–343. <https://doi.org/10.1038/ni.3349>
- Miska, E. A., Karlsson, C., Langley, E., Nielsen, S. J., Pines, J., & Kouzarides, T. (1999). HDAC4 deacetylase associates with and represses the MEF2 transcription factor. *EMBO Journal*, 18(18), 5099–5107. <https://doi.org/10.1093/emboj/18.18.5099>
- Moran-Crusio, K., Reavie, L., Shih, A., Abdel-Wahab, O., Ndiaye-Lobry, D., Lobry, C., ... Levine, R. L. (2011). Tet2 loss leads to increased hematopoietic stem cell self-renewal and myeloid transformation. *Cancer Cell*, 20(1), 11–24. <https://doi.org/10.1016/j.ccr.2011.06.001>
- Morgan, M. A. J., & Shilatifard, A. (2020). Reevaluating the roles of histone-modifying enzymes and their associated chromatin modifications in transcriptional regulation. *Nature Genetics*, 52(12), 1271–1281. <https://doi.org/10.1038/s41588-020-00736-4>
- Morin, R. D., Mungall, K., Pleasance, E., Mungall, A. J., Goya, R., Huff, R. D., ... Marra, M. A. (2013). Mutational and structural analysis of diffuse large B-cell lymphoma using whole-genome sequencing. *Blood*, 122(7), 1256–1265. <https://doi.org/10.1182/blood-2013-02-483727>
- Muppidi, J. R., Lu, E., & Cyster, J. G. (2015). The G protein-Coupled receptor P2RY8 and follicular dendritic cells promote germinal center confinement of B cells, whereas S1PR3 can contribute to their dissemination. *Journal of Experimental Medicine*, 212(13), 2213–2222.

<https://doi.org/10.1084/jem.20151250>

- Muramatsu, M., Kazuo, K., Sidonia, F., Shuichi, Y., Yoichi, S., & Tasuku, H. (2000). Class Switch Recombination and Hypermutation Require Activation-Induced Cytidine Deaminase (AID), a Potential RNA Editing Enzyme. *Cell*, *102*(5), 553–563.
- Myers, D. R., Lau, T., Markegard, E., Lim, H. W., Kasler, H., Zhu, M., ... Roose, J. P. (2017). Tonic LAT-HDAC7 Signals Sustain Nur77 and Irf4 Expression to Tune Naive CD4 T Cells. *Cell Reports*, *19*(8), 1558–1571. <https://doi.org/10.1016/j.celrep.2017.04.076>
- Nam, H., Kundu, A., Karki, S., Brinkley, G. J., Chandrashekar, D. S., Kirkman, R. L., ... Sudarshan, S. (2021). The TGF- $\beta$ /HDAC7 axis suppresses TCA cycle metabolism in renal cancer. *JCI Insight*, *6*(22). <https://doi.org/10.1172/jci.insight.148438>
- Navarro, M. N., Goebel, J., Feijoo-Carnero, C., Morrice, N., & Cantrell, D. A. (2011a). Phosphoproteomic analysis reveals an intrinsic pathway for the regulation of histone deacetylase 7 that controls the function of cytotoxic T lymphocytes. *Nature Immunology*, *12*(4), 352–362. <https://doi.org/10.1038/ni.2008>
- Navarro, M. N., Goebel, J., Feijoo-Carnero, C., Morrice, N., & Cantrell, D. A. (2011b). Phosphoproteomic analysis reveals an intrinsic pathway for the regulation of histone deacetylase 7 that controls the function of cytotoxic T lymphocytes. *Nature Immunology*, *12*(4), 352–361. <https://doi.org/10.1038/ni.2008>
- Nera, K.-P., Kohonen, P., Narvi, E., Peippo, A., Mustonen, L., Terho, P., ... Lassila, O. (2006). Loss of Pax5 Promotes Plasma Cell Differentiation. *Immunity*, *24*(3), 283–293. <https://doi.org/10.1016/j.immuni.2006.02.003>
- Neuberger, M. S., & Milstein, C. (1995). Somatic hypermutation. *Current Opinion in Immunology*, *7*(2), 248–254. [https://doi.org/10.1016/0952-7915\(95\)80010-7](https://doi.org/10.1016/0952-7915(95)80010-7)
- Nie, Y., Waite, J., Brewer, F., Sunshine, M. J., Littman, D. R., & Zou, Y. R. (2004). The role of CXCR4 in maintaining peripheral B cell compartments and

- humoral immunity. *Journal of Experimental Medicine*, 200(9), 1145–1156. <https://doi.org/10.1084/jem.20041185>
- Niu, H., Cattoretti, G., & Dalla-Favera, R. (2003). BCL6 controls the expression of the B7-1/CD80 costimulatory receptor in germinal center B cells. *Journal of Experimental Medicine*, 198(2), 211–221. <https://doi.org/10.1084/jem.20021395>
- Núñez-Álvarez, Y., & Suelves, M. (2021). HDAC11: a multifaceted histone deacetylase with proficient fatty deacylase activity and its roles in physiological processes. *The FEBS Journal*, 289(10), 2771–2792. <https://doi.org/10.1111/febs.15895>
- Nutt, S. L., & Kee, B. L. (2007). The Transcriptional Regulation of B Cell Lineage Commitment. *Immunity*, 26(6), 715–725. <https://doi.org/10.1016/j.immuni.2007.05.010>
- Ochiai, K., Maienschein-Cline, M., Simonetti, G., Chen, J., Rosenthal, R., Brink, R., ... Sciammas, R. (2013). Transcriptional Regulation of Germinal Center B and Plasma Cell Fates by Dynamical Control of IRF4. *Immunity*, 38(5), 918–929. <https://doi.org/10.1016/j.immuni.2013.04.009>
- Okada, T., Miller, M. J., Parker, I., Krummel, M. F., Neighbors, M., Hartley, S. B., ... Cyster, J. G. (2005). Antigen-engaged B cells undergo chemotaxis toward the T zone and form motile conjugates with helper T cells. *PLoS Biology*, 3(6), 1047–1061. <https://doi.org/10.1371/journal.pbio.0030150>
- Okano, M., Bell, D. W., Haber, D. A., & Li, E. (1999). DNA methyltransferases Dnmt3a and Dnmt3b are essential for de novo methylation and mammalian development. *Cell*, 99(3), 247–257. [https://doi.org/10.1016/S0092-8674\(00\)81656-6](https://doi.org/10.1016/S0092-8674(00)81656-6)
- Oliver, A. M., Martin, F., & Kearney, J. F. (1997). Mouse CD38 is down-regulated on germinal center B cells and mature plasma cells. *Journal of Immunology (Baltimore, Md. : 1950)*, 158(3), 1108–1115. Retrieved from <http://www.ncbi.nlm.nih.gov/pubmed/9013949>
- Oprea, M., & Perelson, A. S. (1997). Somatic mutation leads to efficient affinity maturation when centrocytes recycle back to centroblasts. *Journal of*

*Immunology (Baltimore, Md. : 1950)*, 158(11), 5155–5162. Retrieved from <http://www.ncbi.nlm.nih.gov/pubmed/9164931>

Orlanski, S., Labi, V., Reizel, Y., Spiro, A., Lichtenstein, M., Levin-Klein, R., ... Bergman, Y. (2016). Tissue-specific DNA demethylation is required for proper B-cell differentiation and function. *Proceedings of the National Academy of Sciences of the United States of America*, 113(18), 5018–5023. <https://doi.org/10.1073/pnas.1604365113>

Ouaïssi, M., Sielezneff, I., Silvestre, R., Sastre, B., Bernard, J.-P., Lafontaine, J. S., ... Ouaïssi, A. (2008). High Histone Deacetylase 7 (HDAC7) Expression Is Significantly Associated with Adenocarcinomas of the Pancreas. *Annals of Surgical Oncology*, 15(8), 2318–2328. <https://doi.org/10.1245/s10434-008-9940-z>

Park, S.-Y., & Kim, J.-S. (2020). A short guide to histone deacetylases including recent progress on class II enzymes. *Experimental & Molecular Medicine*, 52(2), 204–212. <https://doi.org/10.1038/s12276-020-0382-4>

Parra, M. (2015). Class IIa HDACs - New insights into their functions in physiology and pathology. *FEBS Journal*, 282(9), 1736–1744. <https://doi.org/10.1111/febs.13061>

Parra, M., Kasler, H., McKinsey, T. A., Olson, E. N., & Verdin, E. (2005a). Protein Kinase D1 Phosphorylates HDAC7 and Induces Its Nuclear Export after T-cell Receptor Activation. *Journal of Biological Chemistry*, 280(14), 13762–13770. <https://doi.org/10.1074/jbc.M413396200>

Parra, M., Kasler, H., McKinsey, T. A., Olson, E. N., & Verdin, E. (2005b). Protein Kinase D1 Phosphorylates HDAC7 and Induces Its Nuclear Export after T-cell Receptor Activation. *Journal of Biological Chemistry*, 280(14), 13762–13770. <https://doi.org/10.1074/jbc.M413396200>

Parra, M., & Verdin, E. (2010). Regulatory signal transduction pathways for class IIa histone deacetylases. *Current Opinion in Pharmacology*, 10(4), 454–460. <https://doi.org/10.1016/j.coph.2010.04.004>

Pasqualucci, L., Migliazza, A., Basso, K., Houldsworth, J., Chaganti, R. S. K., & Dalla-Favera, R. (2003). Mutations of the BCL6 proto-oncogene disrupt its

- negative autoregulation in diffuse large B-cell lymphoma. *Blood*, 101(8), 2914–2923. <https://doi.org/10.1182/blood-2002-11-3387>
- Peng, L., & Seto, E. (2011). *Deacetylation of Nonhistone Proteins by HDACs and the Implications in Cancer*. [https://doi.org/10.1007/978-3-642-21631-2\\_3](https://doi.org/10.1007/978-3-642-21631-2_3)
- Pereira, J. P., Kelly, L. M., Xu, Y., & Cyster, J. G. (2009). EB12 mediates B cell segregation between the outer and centre follicle. *Nature*, 460(7259), 1122–1126. <https://doi.org/10.1038/nature08226>
- Phan, R. T., & Dalla-Favera, R. (2004). The BCL6 proto-oncogene suppresses p53 expression in germinal-centre B cells. *Nature*, 432(7017), 635–639. <https://doi.org/10.1038/nature03147>
- Phan, R. T., Saito, M., Basso, K., Niu, H., & Dalla-Favera, R. (2005). BCL6 interacts with the transcription factor Miz-1 to suppress the cyclin-dependent kinase inhibitor p21 and cell cycle arrest in germinal center B cells. *Nature Immunology*, 6(10), 1054–1060. <https://doi.org/10.1038/ni1245>
- Pieters, R., Schrappe, M., De Lorenzo, P., Hann, I., De Rossi, G., Felice, M., ... Valsecchi, M. G. (2007). A treatment protocol for infants younger than 1 year with acute lymphoblastic leukaemia (Interfant-99): an observational study and a multicentre randomised trial. *The Lancet*, 370(9583), 240–250. [https://doi.org/10.1016/S0140-6736\(07\)61126-X](https://doi.org/10.1016/S0140-6736(07)61126-X)
- Piskurich, J. F., Lin, K., Lin, Y., Wang, Y., Ting, J. P., Calame, K., & Li, C. (2000). BLIMP-1 mediates extinction of major histocompatibility class II transactivator expression in plasma cells. *Nature Immunology*, 1(6).
- Pui, C.-H., & Evans, W. E. (2013). A 50-Year Journey to Cure Childhood Acute Lymphoblastic Leukemia. *Seminars in Hematology*, 50(3), 185–196. <https://doi.org/10.1053/j.seminhematol.2013.06.007>
- Rad, R., Rad, L., Wang, W., Cadinanos, J., Vassiliou, G., Rice, S., ... Bradley, A. (2010). PiggyBac transposon mutagenesis: A tool for cancer gene discovery in mice. *Science*, 330(6007), 1104–1107. <https://doi.org/10.1126/science.1193004>
- Rada, C., Williams, G. T., Nilsen, H., Barnes, D. E., Lindahl, T., & Neuberger, M.

- S. (2002). Immunoglobulin Isotype Switching Is Inhibited and Somatic Hypermutation Perturbed in UNG-Deficient Mice. *Current Biology*, 12(20), 1748–1755. [https://doi.org/10.1016/S0960-9822\(02\)01215-0](https://doi.org/10.1016/S0960-9822(02)01215-0)
- Ramírez, J., Lukin, K., & Hagman, J. (2010). From hematopoietic progenitors to B cells: mechanisms of lineage restriction and commitment. *Current Opinion in Immunology*, 22(2), 177–184. <https://doi.org/10.1016/j.coi.2010.02.003>
- Ramírez, J., Lukin, K., & Hagman, J. (2011). Lineage Restriction and Commitment. *Health (San Francisco)*, 22(2), 177–184. <https://doi.org/10.1016/j.coi.2010.02.003>.From
- Rasmussen, Kasper D., Berest, I., Keßler, S., Nishimura, K., Simón-Carrasco, L., Vassiliou, G. S., ... Helin, K. (2019). TET2 binding to enhancers facilitates transcription factor recruitment in hematopoietic cells. *Genome Research*, 29(4), 564–575. <https://doi.org/10.1101/gr.239277.118>
- Rasmussen, Kasper Dindler, & Helin, K. (2016). Role of TET enzymes in DNA methylation, development, and cancer. *Genes & Development*, 30(7), 733–750. <https://doi.org/10.1101/gad.276568.115>
- Reddy, A., Zhang, J., Davis, N. S., Moffitt, A. B., Love, C. L., Waldrop, A., ... Dave, S. S. (2017a). Genetic and Functional Drivers of Diffuse Large B Cell Lymphoma. *Cell*, 171(2), 481-494.e15. <https://doi.org/10.1016/j.cell.2017.09.027>
- Reddy, A., Zhang, J., Davis, N. S., Moffitt, A. B., Love, C. L., Waldrop, A., ... Dave, S. S. (2017b). Genetic and Functional Drivers of Diffuse Large B Cell Lymphoma. *Cell*, 171(2), 481-494.e15. <https://doi.org/10.1016/j.cell.2017.09.027>
- Reimold, A. M., Iwakoshi, N. N., Manis, J., Vallabhajosyula, P., Szomolanyi-Tsuda, E., Gravallesse, E. M., ... Glimcher, L. H. (2001). Plasma cell differentiation requires the transcription factor XBP-1. *Nature*, 412(6844), 300–307. <https://doi.org/10.1038/35085509>
- Roco, J. A., Mesin, L., Binder, S. C., Nefzger, C., Gonzalez-Figueroa, P., Canete, P. F., ... Vinuesa, C. G. (2019a). Class-Switch Recombination Occurs Infrequently in Germinal Centers. *Immunity*, 51(2), 337-350.e7.

<https://doi.org/10.1016/j.immuni.2019.07.001>

Roco, J. A., Mesin, L., Binder, S. C., Nefzger, C., Gonzalez-Figueroa, P., Canete, P. F., ... Vinuesa, C. G. (2019b). Class-Switch Recombination Occurs Infrequently in Germinal Centers. *Immunity*, *51*(2), 337-350.e7. <https://doi.org/10.1016/j.immuni.2019.07.001>

Roschewski, M., Staudt, L. M., & Wilson, W. H. (2014). Diffuse large B-cell lymphoma—treatment approaches in the molecular era. *Nature Reviews Clinical Oncology*, *11*(1), 12–23. <https://doi.org/10.1038/nrclinonc.2013.197>

Rose, M. L., Birbeck, M. S. C., Wallis, V. J., Forrester, J. A., & Davies, A. J. S. (1980). Peanut lectin binding properties of germinal centers of mouse lymphoid tissue. *Nature*, *284*(5754), 364–366. <https://doi.org/10.1038/284364a0>

Rosikiewicz, W., Chen, X., Dominguez, P. M., Ghamlouch, H., Aoufouchi, S., Bernard, O. A., ... Li, S. (2020). TET2 deficiency reprograms the germinal center B cell epigenome and silences genes linked to lymphomagenesis. *Science Advances*, *6*(25). <https://doi.org/10.1126/sciadv.aay5872>

Ryan, R. J. H., Drier, Y., Whitton, H., Cotton, M. J., Kaur, J., Issner, R., ... Bernstein, B. E. (2015). Detection of Enhancer-Associated Rearrangements Reveals Mechanisms of Oncogene Dysregulation in B-cell Lymphoma. *Cancer Discovery*, *5*(10), 1058–1071. <https://doi.org/10.1158/2159-8290.CD-15-0370>

Sagardoy, A., Martinez-Ferrandis, J. I., Roa, S., Bunting, K. L., Aznar, M. A., Elemento, O., ... Martinez-Climent, J. A. (2013). Downregulation of FOXP1 is required during germinal center B-cell function. *Blood*, *121*(21), 4311–4320. <https://doi.org/10.1182/blood-2012-10-462846>

Saito, M., Novak, U., Piovan, E., Basso, K., Sumazin, P., Schneider, C., ... Dalla-Favera, R. (2009). BCL6 suppression of BCL2 via Miz1 and its disruption in diffuse large B cell lymphoma. *Proceedings of the National Academy of Sciences of the United States of America*, *106*(27), 11294–11299. <https://doi.org/10.1073/pnas.0903854106>

Sander, S., Chu, V. T., Yasuda, T., Franklin, A., Graf, R., Calado, D. P., ...



- Rajewsky, K. (2015). PI3 Kinase and FOXO1 Transcription Factor Activity Differentially Control B Cells in the Germinal Center Light and Dark Zones. *Immunity*, *43*(6), 1075–1086. <https://doi.org/10.1016/j.immuni.2015.10.021>
- Sanjuan-Pla, A., Bueno, C., Prieto, C., Acha, P., Stam, R. W., Marschalek, R., & Menéndez, P. (2015). Revisiting the biology of infant t(4;11)/MLL-AF4+ B-cell acute lymphoblastic leukemia. *Blood*, *126*(25), 2676–2685. <https://doi.org/10.1182/blood-2015-09-667378>
- Sant, M., Allemani, C., & Tereanu, C. (2011). Incidence of hematologic malignancies in Europe by morphologic subtype: Results of the HAEMACARE project (Blood (2010) 116, 19 (3724-3734)). *Blood*, *117*(12), 3477. <https://doi.org/10.1182/blood-2011-02-335794>
- Sardina, J. L., Collombet, S., Tian, T. V., Gómez, A., Di Stefano, B., Berenguer, C., ... Graf, T. (2018). Transcription Factors Drive Tet2-Mediated Enhancer Demethylation to Reprogram Cell Fate. *Cell Stem Cell*, *23*(5), 727-741.e9. <https://doi.org/10.1016/j.stem.2018.08.016>
- Schmitz, R., Wright, G. W., Huang, D. W., Johnson, C. A., Phelan, J. D., Wang, J. Q., ... Staudt, L. M. (2018). Genetics and Pathogenesis of Diffuse Large B-Cell Lymphoma. *New England Journal of Medicine*, *378*(15), 1396–1407. <https://doi.org/10.1056/nejmoa1801445>
- Scott, D. W., Mottok, A., Ennishi, D., Wright, G. W., Farinha, P., Ben-Neriah, S., ... Gascoyne, R. D. (2015). Prognostic significance of diffuse large B-cell lymphoma cell of origin determined by digital gene expression in formalin-fixed paraffin-embedded tissue biopsies. *Journal of Clinical Oncology*, *33*(26), 2848–2856. <https://doi.org/10.1200/JCO.2014.60.2383>
- Scott, E. W., Simon, M. C., Anastasi, J., & Singh, H. (1994). Requirement of Transcription Factor PU.1 in the Development of Multiple Hematopoietic Lineages. *Science*, *265*(5178), 1573–1577. <https://doi.org/10.1126/science.8079170>
- Seto, E., & Yoshida, M. (2014). Erasers of Histone Acetylation: The Histone Deacetylase Enzymes. *Cold Spring Harbor Perspectives in Biology*, *6*(4), a018713–a018713. <https://doi.org/10.1101/cshperspect.a018713>

- Shaffer, A. ., Shapiro-Shelef, M., Iwakoshi, N. N., Lee, A.-H., Qian, S.-B., Zhao, H., ... Staudt, L. M. (2004). XBP1, Downstream of Blimp-1, Expands the Secretory Apparatus and Other Organelles, and Increases Protein Synthesis in Plasma Cell Differentiation. *Immunity*, 21(1), 81–93. <https://doi.org/10.1016/j.immuni.2004.06.010>
- Shalabi, H., & Shah, N. N. (2022). CD19 CAR T cells for infants and young children. *The Lancet Haematology*, 9(10), e712–e714. [https://doi.org/10.1016/S2352-3026\(22\)00258-7](https://doi.org/10.1016/S2352-3026(22)00258-7)
- Shinnakasu, R., Inoue, T., Kometani, K., Moriyama, S., Adachi, Y., Nakayama, M., ... Kurosaki, T. (2016). Regulated selection of germinal-center cells into the memory B cell compartment. *Nature Immunology*, 17(7), 861–869. <https://doi.org/10.1038/ni.3460>
- Simonis, M., Klous, P., Splinter, E., Moshkin, Y., Willemsen, R., de Wit, E., ... de Laat, W. (2006). Nuclear organization of active and inactive chromatin domains uncovered by chromosome conformation capture–on-chip (4C). *Nature Genetics*, 38(11), 1348–1354. <https://doi.org/10.1038/ng1896>
- Skov, V., Larsen, T. S., Thomassen, M., Riley, C. H., Jensen, M. K., Bjerrum, O. W., ... Hasselbalch, H. C. (2012). Increased gene expression of histone deacetylases in patients with Philadelphia-negative chronic myeloproliferative neoplasms. *Leukemia & Lymphoma*, 53(1), 123–129. <https://doi.org/10.3109/10428194.2011.597905>
- Song, J., Rechkoblit, O., Bestor, T. H., & Patel, D. J. (2011). Structure of DNMT1-DNA Complex Reveals a Role for Autoinhibition in Maintenance DNA Methylation. *Science*, 331(6020), 1036–1040. <https://doi.org/10.1126/science.1195380>
- Song, J., Teplova, M., Ishibe-Murakami, S., & Patel, D. J. (2012). Structure-Based Mechanistic Insights into DNMT1-Mediated Maintenance DNA Methylation. *Science*, 335(6069), 709–712. <https://doi.org/10.1126/science.1214453>
- Srivastava, S., & Riddell, S. R. (2015). Engineering CAR-T cells: Design concepts. *Trends in Immunology*, 36(8), 494–502.

<https://doi.org/10.1016/j.it.2015.06.004>

- Stavnezer, J., Guikema, J. E. J., & Schrader, C. E. (2008). Mechanism and regulation of class switch recombination. *Annual Review of Immunology*, *26*, 261–292. <https://doi.org/10.1146/annurev.immunol.26.021607.090248>
- Stehling-Sun, S., Dade, J., Nutt, S. L., DeKoter, R. P., & Camargo, F. D. (2009). Regulation of lymphoid versus myeloid fate “choice” by the transcription factor Mef2c. *Nature Immunology*, *10*(3), 289–296. <https://doi.org/10.1038/ni.1694>
- Su, I., Basavaraj, A., Krutchinsky, A. N., Hobert, O., Ullrich, A., Chait, B. T., & Tarakhovsky, A. (2003). Ezh2 controls B cell development through histone H3 methylation and Igh rearrangement. *Nature Immunology*, *4*(2), 124–131. <https://doi.org/10.1038/ni876>
- Taunton, J., Hassig, C. A., & Schreiber, S. L. (1996). A Mammalian Histone Deacetylase Related to the Yeast Transcriptional Regulator Rpd3p. *Science*, *272*(5260), 408–411. <https://doi.org/10.1126/science.272.5260.408>
- Taylor, J. J., Pape, K. A., & Jenkins, M. K. (2012). A germinal center-independent pathway generates unswitched memory B cells early in the primary response. *Journal of Experimental Medicine*, *209*(3), 597–606. <https://doi.org/10.1084/jem.20111696>
- Tejedor, J. R., Bueno, C., Vinyoles, M., Petazzi, P., Agraz-Doblas, A., Cobo, I., ... Menéndez, P. (2021). Integrative methylome-transcriptome analysis unravels cancer cell vulnerabilities in infant MLL-rearranged B cell acute lymphoblastic leukemia. *Journal of Clinical Investigation*, *131*(13). <https://doi.org/10.1172/JCI138833>
- Tsagaratou, A., Lio, C.-W. J., Yue, X., & Rao, A. (2017a). TET Methylcytosine Oxidases in T Cell and B Cell Development and Function. *Frontiers in Immunology*, *8*. <https://doi.org/10.3389/fimmu.2017.00220>
- Tsagaratou, A., Lio, C. W. J., Yue, X., & Rao, A. (2017b). TET methylcytosine oxidases in T cell and B cell development and function. *Frontiers in Immunology*, *8*(MAR), 1–15. <https://doi.org/10.3389/fimmu.2017.00220>

- Tunyaplin, C., Shaffer, A. L., Angelin-Duclos, C. D., Yu, X., Staudt, L. M., & Calame, K. L. (2004). Direct Repression of *prdm1* by Bcl-6 Inhibits Plasmacytic Differentiation. *The Journal of Immunology*, *173*(2), 1158–1165. <https://doi.org/10.4049/jimmunol.173.2.1158>
- Turner, C. A., Mack, D. H., & Davis, M. M. (1994). Blimp-1, a novel zinc finger-containing protein that can drive the maturation of B lymphocytes into immunoglobulin-secreting cells. *Cell*, *77*(2), 297–306. [https://doi.org/10.1016/0092-8674\(94\)90321-2](https://doi.org/10.1016/0092-8674(94)90321-2)
- van der Linden, M. H., Valsecchi, M. G., De Lorenzo, P., Möricke, A., Janka, G., Leblanc, T. M., ... Pieters, R. (2009). Outcome of congenital acute lymphoblastic leukemia treated on the Interfant-99 protocol. *Blood*, *114*(18), 3764–3768. <https://doi.org/10.1182/blood-2009-02-204214>
- Van der Velden, V. H. J., Corral, L., Valsecchi, M. G., Jansen, M. W. J. C., De Lorenzo, P., Cazzaniga, G., ... Van Dongen, J. J. M. (2009). Prognostic significance of minimal residual disease in infants with acute lymphoblastic leukemia treated within the Interfant-99 protocol. *Leukemia*, *23*(6), 1073–1079. <https://doi.org/10.1038/leu.2009.17>
- van Schoonhoven, A., Huylebroeck, D., Hendriks, R. W., & Stadhouders, R. (2020). 3D genome organization during lymphocyte development and activation. *Briefings in Functional Genomics*, *19*(2), 71–82. <https://doi.org/10.1093/bfpg/elz030>
- Velichutina, I., Shaknovich, R., Geng, H., Johnson, N. A., Gascoyne, R. D., Melnick, A. M., & Elemento, O. (2010). EZH2-mediated epigenetic silencing in germinal center B cells contributes to proliferation and lymphomagenesis. *Blood*, *116*(24), 5247–5255. <https://doi.org/10.1182/blood-2010-04-280149>
- Verdone, L., Caserta, M., & Mauro, E. Di. (2005). Role of histone acetylation in the control of gene expression. *Biochemistry and Cell Biology*, *83*(3), 344–353. <https://doi.org/10.1139/o05-041>
- Viant, C., Wirthmiller, T., ElTanbouly, M. A., Chen, S. T., Cipolla, M., Ramos, V., ... Nussenzweig, M. C. (2021). Germinal center–dependent and –independent memory B cells produced throughout the immune response.

*Journal of Experimental Medicine*, 218(8).  
<https://doi.org/10.1084/jem.20202489>

Victoria, G. D., Dominguez-Sola, D., Holmes, A. B., Deroubaix, S., Dalla-Favera, R., & Nussenzweig, M. C. (2012). Identification of human germinal center light and dark zone cells and their relationship to human B-cell lymphomas. *Blood*, 120(11), 2240–2248. <https://doi.org/10.1182/blood-2012-03-415380>

Victoria, G. D., & Nussenzweig, M. C. (2022a). Germinal Centers. *Annual Review of Immunology*, 40, 413–442. <https://doi.org/10.1146/annurev-immunol-120419-022408>

Victoria, G. D., & Nussenzweig, M. C. (2022b). Germinal Centers. *Annual Review of Immunology*, 40(1), 413–442. <https://doi.org/10.1146/annurev-immunol-120419-022408>

Victoria, G. D., Schwickert, T. A., Fooksman, D. R., Kamphorst, A. O., Meyer-Hermann, M., Dustin, M. L., & Nussenzweig, M. C. (2010). Germinal Center Dynamics Revealed by Multiphoton Microscopy with a Photoactivatable Fluorescent Reporter. *Cell*, 143(4), 592–605. <https://doi.org/10.1016/j.cell.2010.10.032>

Wang, Q., Wu, G., Mi, S., He, F., Wu, J., Dong, J., ... Thirman, M. J. (2011). MLL fusion proteins preferentially regulate a subset of wild-type MLL target genes in the leukemic genome. *Blood*, 117(25), 6895–6905. <https://doi.org/10.1182/blood-2010-12-324699>

Weber, M., & Schübeler, D. (2007). Genomic patterns of DNA methylation: targets and function of an epigenetic mark. *Current Opinion in Cell Biology*, 19(3), 273–280. <https://doi.org/10.1016/j.ceb.2007.04.011>

Weisel, F. J., Zuccarino-Catania, G. V., Chikina, M., & Shlomchik, M. J. (2016). A Temporal Switch in the Germinal Center Determines Differential Output of Memory B and Plasma Cells. *Immunity*, 44(1), 116–130. <https://doi.org/10.1016/j.immuni.2015.12.004>

Wiles, E. T., & Selker, E. U. (2017). H3K27 methylation: a promiscuous repressive chromatin mark. *Current Opinion in Genetics & Development*, 43, 31–37. <https://doi.org/10.1016/j.gde.2016.11.001>

- Wilker, P. R., Kohyama, M., Sandau, M. M., Albring, J. C., Nakagawa, O., Schwarz, J. J., & Murphy, K. M. (2008). Transcription factor Mef2c is required for B cell proliferation and survival after antigen receptor stimulation. *Nature Immunology*, *9*(6), 603–612. <https://doi.org/10.1038/ni.1609>
- Wright, G. W., Huang, D. W., Phelan, J. D., Coulibaly, Z. A., Roulland, S., Young, R. M., ... Staudt, L. M. (2020). A Probabilistic Classification Tool for Genetic Subtypes of Diffuse Large B Cell Lymphoma with Therapeutic Implications. *Cancer Cell*, *37*(4), 551-568.e14. <https://doi.org/10.1016/j.ccell.2020.03.015>
- Wu, X., & Zhang, Y. (2017). TET-mediated active DNA demethylation: Mechanism, function and beyond. *Nature Reviews Genetics*, *18*(9), 517–534. <https://doi.org/10.1038/nrg.2017.33>
- Xia, Z.-B., Anderson, M., Diaz, M. O., & Zeleznik-Le, N. J. (2003). MLL repression domain interacts with histone deacetylases, the polycomb group proteins HPC2 and BMI-1, and the corepressor C-terminal-binding protein. *Proceedings of the National Academy of Sciences*, *100*(14), 8342–8347. <https://doi.org/10.1073/pnas.1436338100>
- Ye, B H, Lista, F., Lo Coco, F., Knowles, D. M., Offit, K., Chaganti, R. S., & Dalla-Favera, R. (1993). Alterations of a zinc finger-encoding gene, BCL-6, in diffuse large-cell lymphoma. *Science (New York, N. Y.)*, *262*(5134), 747–750. <https://doi.org/10.1126/science.8235596>
- Ye, Bihui H., Cattoretti, G., Shen, Q., Zhang, J., Hawe, N., Waard, R. de, ... Dalla-Favera, R. (1997). The BCL-6 proto-oncogene controls germinal-centre formation and Th2-type inflammation. *Nature Genetics*, *16*(2), 161–170. <https://doi.org/10.1038/ng0697-161>
- Ying, C. Y., Dominguez-Sola, D., Fabi, M., Lorenz, I. C., Hussein, S., Bansal, M., ... Dalla-Favera, R. (2013). MEF2B mutations lead to deregulated expression of the oncogene BCL6 in diffuse large B cell lymphoma. *Nature Immunology*, *14*(10), 1084–1092. <https://doi.org/10.1038/ni.2688>
- Yokoyama, A., Wang, Z., Wysocka, J., Sanyal, M., Aufiero, D. J., Kitabayashi, I., ... Cleary, M. L. (2004). Leukemia Proto-Oncoprotein MLL Forms a SET1-Like Histone Methyltransferase Complex with Menin To Regulate Hox Gene

- Expression. *Molecular and Cellular Biology*, 24(13), 5639–5649.  
<https://doi.org/10.1128/MCB.24.13.5639-5649.2004>
- Yoshida, T., Ng, Y. S., C., Z.-P. J., & K., G. (2009). Early hemopoietic lineage restrictions directed by Ikaros Toshimi. *Nature Immunology*, 49(18), 1841–1850. <https://doi.org/10.1038/ni1314>.Early
- Yoshino, T., Kondo, E., Cao, L., Takahashi, K., Hayashi, K., Nomura, S., & Akagi, T. (1994). Inverse expression of bcl-2 protein and Fas antigen in lymphoblasts in peripheral lymph nodes and activated peripheral blood T and B lymphocytes. *Blood*, 83(7), 1856–1861.  
<https://doi.org/10.1182/blood.v83.7.1856.1856>
- Zeng, Y., & Chen, T. (2019). DNA methylation reprogramming during mammalian development. *Genes*, 10(4). <https://doi.org/10.3390/genes10040257>
- Zhang, J., Dominguez-Sola, D., Hussein, S., Lee, J.-E., Holmes, A. B., Bansal, M., ... Pasqualucci, L. (2015). Disruption of KMT2D perturbs germinal center B cell development and promotes lymphomagenesis. *Nature Medicine*, 21(10), 1190–1198. <https://doi.org/10.1038/nm.3940>
- Zhang, J., Vlasevska, S., Wells, V. A., Nataraj, S., Holmes, A. B., Duval, R., ... Pasqualucci, L. (2017). The CREBBP Acetyltransferase Is a Haploinsufficient Tumor Suppressor in B-cell Lymphoma. *Cancer Discovery*, 7(3), 322–337. <https://doi.org/10.1158/2159-8290.CD-16-1417>
- Zuccarino-Catania, G. V, Sadanand, S., Weisel, F. J., Tomayko, M. M., Meng, H., Kleinstein, S. H., ... Shlomchik, M. J. (2014). CD80 and PD-L2 define functionally distinct memory B cell subsets that are independent of antibody isotype. *Nature Immunology*, 15(7), 631–637.  
<https://doi.org/10.1038/ni.2914>

## **ANNEX**

### **Review Article**

*“MYC's Fine Line Between B Cell Development and Malignancy”*





Review

# MYC's Fine Line Between B Cell Development and Malignancy

Oriol de Barrios <sup>†</sup>, Ainara Meler <sup>†</sup> and Maribel Parra <sup>\*</sup>

Lymphocyte Development and Disease Group, Josep Carreras Leukaemia Research Institute, IJC Building, Campus ICO-Germans Trias i Pujol, Ctra de Can Ruti, 08916 Barcelona, Spain; odebarrios@carrerasresearch.org (O.d.B.); ameler@carrerasresearch.org (A.M.)

<sup>\*</sup> Correspondence: mparra@carrerasresearch.org

<sup>†</sup> These authors contributed equally to this work.

Received: 31 January 2020; Accepted: 21 February 2020; Published: 24 February 2020



**Abstract:** The transcription factor MYC is transiently expressed during B lymphocyte development, and its correct modulation is essential in defined developmental transitions. Although temporary downregulation of MYC is essential at specific points, basal levels of expression are maintained, and its protein levels are not completely silenced until the B cell becomes fully differentiated into a plasma cell or a memory B cell. MYC has been described as a proto-oncogene that is closely involved in many cancers, including leukemia and lymphoma. Aberrant expression of MYC protein in these hematological malignancies results in an uncontrolled rate of proliferation and, thereby, a blockade of the differentiation process. MYC is not activated by mutations in the coding sequence, and, as reviewed here, its overexpression in leukemia and lymphoma is mainly caused by gene amplification, chromosomal translocations, and aberrant regulation of its transcription. This review provides a thorough overview of the role of MYC in the developmental steps of B cells, and of how it performs its essential function in an oncogenic context, highlighting the importance of appropriate MYC regulation circuitry.

**Keywords:** MYC; B cell development; leukemia; lymphoma

## 1. The Role of MYC in B Cell Differentiation

Hematopoietic stem cells (HSCs) give rise to mature B cells through the sequential differentiation of lymphoid progenitors. Long-term HSCs (LT-HSCs) have the ability to self-renew and reconstitute the entire immune system by differentiating into short-term HSCs (ST-HSCs). ST-HSCs differentiate into multipotent progenitors (MPPs) that branch later into common myeloid progenitors (CMPs) and lymphoid-primed multipotent progenitors (LMPPs) [1]. LMPPs become common lymphoid progenitors (CLPs) [2], which have the potential to differentiate into B and T lymphocytes, as well as natural killer (NK) cells [2]. Once committed to the lymphoid lineage, additional differentiation steps lead to the formation of pro-B and pre-B cells, which are the early B cell precursors for immature and germinal center (GC) B cells. Bone marrow-escaping mature naïve B cells receiving T cell-dependent signals become activated and localize to the GCs. At this point, they undergo massive proliferation and programmed Ig mutation coupled to antibody affinity-based selection, a process triggered by somatic hypermutation (SHM) and class switch recombination (CSR). Finally, they differentiate into memory B cells or plasma cells (PCs) [3,4] (Figure 1).

The inhibition of erythroid differentiation was the first evidence of MYC activity *in vitro*, leading to the suggestion that it could have a role in hematopoietic cell development [5,6]. Moreover, the findings that some type of retroviruses expressing MYC provoke the formation of hematopoietic tumors, such as myeloid leukemia [7], and that its expression is deregulated in Burkitt lymphoma [8], reinforced the

idea of the potential involvement of MYC in hematopoiesis. In the specific case of B lymphocytes, the use of transgenic mice overexpressing MYC revealed a developmental blockade at the B cell stage, before the onset of lymphoma [9].

Given the importance of MYC deregulation in human leukemia and lymphoma, it is not surprising that its correct modulation is essential throughout the whole B lymphocyte development [10]. At the LT-HSC stage, there is a combined expression of c-MYC and N-MYC isoforms, but there is a complete absence of L-MYC family members [11]. Interestingly, MYC expression allows LT-HSCs and MPPs to be distinguished [10]. On the one hand, LT-HSCs display low levels of MYC to maintain a tight equilibrium between cell self-renewal capacity and differentiation. On the other hand, the activation of MYC expression promotes the differentiation of LT-HSCs into MPPs, which present increased proliferating activity [10,12].

Despite its role in maintaining the self-renewal capacity of LT-HSCs, MYC is also essential for controlling proper hematopoiesis. In fact, *Myc*-deficient murine embryos exhibit impaired hematopoiesis and die before mid-gestation [13]. At this developmental stage, the role of MYC proteins is hierarchical. N-MYC and L-MYC cannot be expressed alone and require the concomitant expression of c-MYC. For instance, the single deletion of N-MYC does not affect the quiescent state of HSCs or hematopoiesis, whereas the deletion of c-MYC in HSCs alters proliferation and survival [11]. In summary, c-MYC is essential for balancing self-renewal and differentiation at the HSC stage. Sustained expression of MYC encompasses the transition from HSCs to lymphoid-committed cells since its extensive ability to bind to promoter and enhancer regions endows it with an extensive gene transcription role in both developmental stages [10,14].

N-MYC and c-MYC are both expressed in lymphocyte progenitors, meanwhile only the expression of c-MYC is maintained during the rest of the differentiation process, despite being reduced in precursor and mature B cell stages [15]. MYC expression is induced in pre-B cells in response to B-cell receptor (BCR) stimulation [16,17]. MYC expression peaks coincide with the stages of higher proliferative rates in B lymphocyte generation [18]. In consequence, MYC has an essential role in the expansion of pro-B cells and differentiation to the pre-B stage [10]. Conditional knockout of c-MYC or N-MYC using the *Cd19-Cre* transgenic mouse model blocks the transition from pro-B to pre-B cells, confirming its role at this stage of lineage development [19].

In connection with these data, aberrant expression of MYC in transgenic mice results in a reduction of mature B lymphocyte numbers relative to those of pre-B cells [9]. In a similar way, the regulation of MYC expression may be altered by the presence of the antiapoptotic factor BCL2 [20], or the stimulation with cytokines, such as interleukin 7 (IL-7) [21], resulting in a tumorigenic outcome, given the ability of these two proteins to enhance cell survival. Conversely, *Myc*-null B lymphocytes have an impaired proliferation capacity when treated with stimulatory cytokines, such as the B-cell surface antigen CD40 and IL-4 [22].

During the complex program that naïve B cells undergo in the GC before they differentiate to memory B cells or PCs, the expression of MYC is maintained, though being depleted when the B cell exits de GC reaction [15,21]. In this context, MYC is basically restricted to specific phases of the GC reaction development and is mainly expressed during naïve B cell expansion and at stages preceding the light zone (LZ) to dark zone (DZ) transition [23,24].

B-cell lymphoma 6 (BCL6) is a direct repressor of MYC during the GC reaction [23]. BCL6 binds to the promoter region of *MYC* in pre-B and differentiated B cells [25–27]. Therefore, the expression pattern of both factors is mutually exclusive in most GC B cells, with 91% of those cells expressing either BCL6 or MYC, and only 8% showing co-expression of both proteins [23]. In GCs, when B cells interact with antigens and access T-helper (Th) cells, they transiently express MYC due to the transcriptional inhibition of *BCL6* by the repressive machinery comprising BCR, IL-2, and interferon regulatory factor 4 (IRF4), the latter being induced upon CD40 activation [24,28,29]. In the LZ, the BCR also synergizes with CD40 to activate MYC and induce p-S6, allowing cell-cycle entry [30,31].

In these early stages of GC formation, MYC-expressing B cells express cyclin D2 (CCND2) [32,33] and D3 (CCND3) [34,35], which possibly contributes to their hyperproliferative phenotype during the

initial rounds of cell division that give rise to the bulk of the GC B cells [36]. As described by Victora et al., B cell clonal expansion is restricted to the DZ, and cells move to the LZ in a bi-directional process controlled by T cells. Based on the amount of Ag captured, Th cells at the LZ determine whether MYC<sup>+</sup> B cells re-enter the DZ for additional rounds of positive selection, or if they remain in the LZ [37].

MYC<sup>+</sup> B cells at the LZ subsequently undergo transcription, whereby BCL6 binds the transcription factor (TF) MYC-interacting zing-finger protein 1 (MIZ1) [38], an MYC partner that acts to suppress CDK inhibitor p21 and thereby induce cell-cycle entry. At this stage, BCL6 and MYC are co-expressed in the LZ [23]. BCL6 also inhibits CCND2 expression [32,33], which is an MYC target. CCND3, which is not controlled by MYC [34,35], is expressed alone in these LZ GC B cells. The TF TCF3 (also called E2A) is intrinsically regulated by the induction of its own inhibitor ID3 (inhibitor of DNA binding 3), is expressed in the GC B cells, and activates CCND3 and E2F2, replacing CCND2-dependent proliferation in the LZ MYC<sup>+</sup> B cells [27,39].

Logically, MYC expression must be tightly controlled in the DZ to limit cell divisions before each round of antigen affinity-based selection, as MYC controls the transcriptional pause release of RNA polymerase II, which is essential for activation-induced cytidine deaminase (AID)-induced somatic hypermutation (SHM) [40,41]. After several rounds of positive selection, the MYC<sup>-</sup> B cells finally exit the GC and become either B memory cells or plasmablasts. B-lymphocyte-induced maturation protein 1 (BLIMP1) suppresses MYC expression in plasmablasts and induces PC differentiation [42]. This dependency effect between MYC and B cell proliferation is known as “cyclic re-entry” [23]. A schematic summary of the role of MYC in B lymphocyte differentiation is shown in Figure 1.

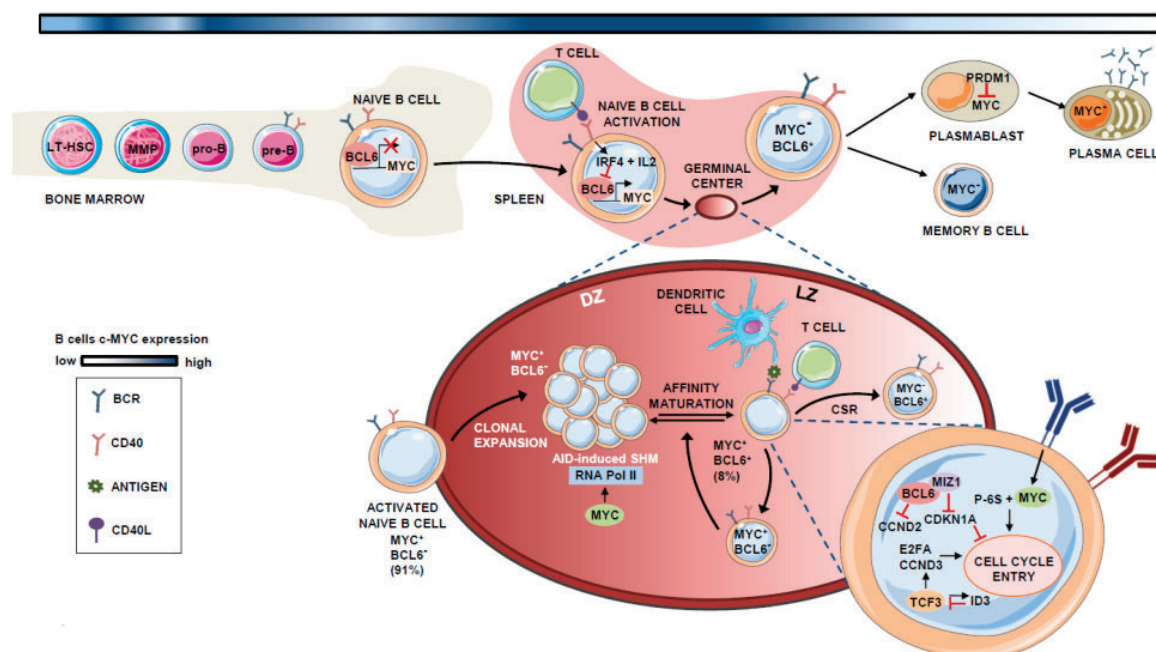


**Figure 1.** Expression and role of MYC in B lymphocyte differentiation. Schematic representation of the participation of the MYC protein throughout B-cell differentiation in the bone marrow and germinal center (GC). The percentages shown refer to the population of MYC<sup>+</sup>, BCL6<sup>+/-</sup> cells in the total number of B cells present in the GC. The blue-colored line at the top of the Figure indicates the evolution of MYC expression, where darker blue indicates steps that require higher MYC levels.

## 2. MYC Role in Leukemogenesis

Unlike other proto-oncogenes, MYC is not activated by oncogenic mutations in the coding sequence. MYC transforms cells via aberrant overexpression of intact MYC protein by three main mechanisms: gene amplification, chromosomal translocation, and aberrant regulation of its expression. In the following sections, we describe the role of MYC in several types of leukemia.

### 2.1. B lymphoblastic Leukemia with t(9;22) BCR-ABL1 Rearrangement

The B-cell receptor – ABL proto-oncogene 1 (BCR-ABL1) fusion (a translocation widely known as the Philadelphia chromosome, Ph) protein product can activate *Myc* in bone marrow-derived murine pre-B cells [43]. The activation of *MYC*, combined with other oncoproteins, such as RAS, c-RAF, and c-JUN, promotes the activation of signaling pathways, leading to malignant cell transformation [44]. Remarkably, the repression of *MYC* impairs BCR-ABL1-mediated transformation, indicating that *MYC* not only has a complementary function but also is essential for ensuring leukemic transformation [43,45].

Whereas the activation of *MYC* in lymphomas is partially caused by an elevated mutation frequency in several cases, B-cell precursor leukemia has an almost negligible mutation rate [46]. However, BCR-ABL rearranged pre-B-acute lymphoblastic leukemia (ALL) is driven by an aberrant expression of AID [47], which is expressed at such an early stage of B lymphocyte development [48], as a consequence of the enhanced kinase activity of BCR-ABL1 fusion protein (i.e., tyrosine kinase P210) [47,49]. Nevertheless, the proportion of patients harboring mutations at the *MYC* gene itself among Ph<sup>+</sup> ALL cases remains low and stable compared with that of Ph<sup>-</sup> patients [47].

In line with these data, *MYC-IGH* translocation, which is a common alteration in B-cell lymphomas [50], is not frequently present in the B-cell precursor ALL. However, when analyzing the genetic deletion of *CDKN2*, a common B-ALL feature, it was found that patients with the wild-type *CDKN2* experienced a higher rate of *MYC-IGH* translocation [51], suggesting that the two genetic alterations may be mutually exclusive.

*MYC* is induced through different pathways triggered by the BCR-ABL1 fusion protein. For instance, the *MYC* gene is one of the pre-BCR downstream effectors whose signaling is transduced through spleen tyrosine kinase (SYK) [52,53]. The inhibition of SYK impairs cell viability via the repressed transcription of *MYC* oncogene [53]. In parallel, the pro-inflammatory marker sphingosine kinase 2 (SK2) promotes the activation of *MYC* in murine models of B-ALL by increasing its acetylation profile. The inhibition of SK2 provokes a drastic reduction in ALL cell proliferation through concomitant repression of *MYC* target genes [54]. Recently, the use of purinostat mesylate (a first-in-class histone deacetylase (HDAC) inhibitor with reported antitumor activity [55]) has also been shown to downregulate the BCR-ABL1 fusion protein targeting of *MYC* through the alteration of global histone 3 (H3) and histone 4 (H4) acetylation [56]. These studies reveal chromatin remodeling to be a promising therapeutic strategy in BCR-ABL1<sup>+</sup> ALL. For instance, as described in greater detail below, the combination of HDAC and PI3K inhibition impairs *MYC*-dependent growth in hematological malignancies [57].

The Wnt signaling cascade is a well-characterized oncogenic pathway that can drive *MYC* oncogene activation. The BCR-ABL1 protein phosphorylates specific tyrosine residues of  $\gamma$ -catenin, thereby enhancing the direct binding of this effector to the *MYC* promoter [58]. The role of this kinase activity differs from that in HSCs, where BCR-ABL1 phosphorylates  $\beta$ -catenin, giving rise to initial forms of chronic myeloid leukemia (CML), without requiring *MYC* induction [58,59]. Instead, BCR-ABL1-driven activation of the JAK/STAT pathway through the phosphorylation of JAK2 has similar effects on both chronic myeloid leukemia (CML) and ALL, whereby pJAK2 and pSTAT5 cooperate to maintain elevated levels of *MYC* by protecting it from ubiquitin-dependent degradation [60,61].

*MYC* is also regulated at several post-transcriptional levels in Ph<sup>+</sup> B-ALL. Since the highly structured 5'-UTR of *MYC* determines its translation rate, eIFs are key translation factors that enable *MYC* mRNA translation [62]. IgM signaling, which is active in chronic lymphoid leukemia (CLL) cells, promotes increased translation of *MYC* mRNA, together with the induction of eIF4 and eIF4GI [63,64]. eIF4 and *MYC* participate in a feedforward loop that enhances both activities [65]. This is not the only mechanism through which *MYC* reinforces its own expression. For instance, *MYC*, in cooperation with its TF partner MAX, binds to the promoter of *BCR-ABL1*, activating its transcription [66].

The aberrantly activated function of *MYC* in ALL also depends on protein stabilization. Some of the first evidence demonstrated that the induction of the Ras pathway prevents proteasomal-mediated degradation of *MYC* [67,68]. Moreover, most leukemia cell lines harbor an altered *MYC* form with a

prolonged half-life, without possessing genetic mutations or chromosomal alterations [47,69]. The increased stability of MYC is explained by an excess of phosphorylation at Ser62, combined with low levels of pThr58, which promote glycogen synthase kinase 3 beta GSK3β-mediated ubiquitylation and proteasomal degradation [69,70].

Apart from its main function in driving tumor progression, MYC also induces apoptosis, since it targets some genes involved in the BCL2 network [71,72]. As part of this network, the apoptosis-inducer protein BIM acts as a major antagonist of BCL2. In fact, the *Eμ-myc* murine leukemia model has demonstrated that the deletion of *Bim* counteracts the potential induction of cell death by MYC, worsening the B-cell leukemia-associated prognosis of these mice [73]. The regulation of BIM is partially mediated by the miR-17-92 cluster (also known as MIR17HG), in MYC-driven leukemia [74,75] and the inhibition of this specific microRNA endows leukemic cells with a pro-apoptotic phenotype [75], making microRNA networks an alternative entry point for interfering with MYC function in the B-cell precursor ALL. The regulation of MYC in BCR-ABL1-rearranged leukemia is depicted in Figure 2.

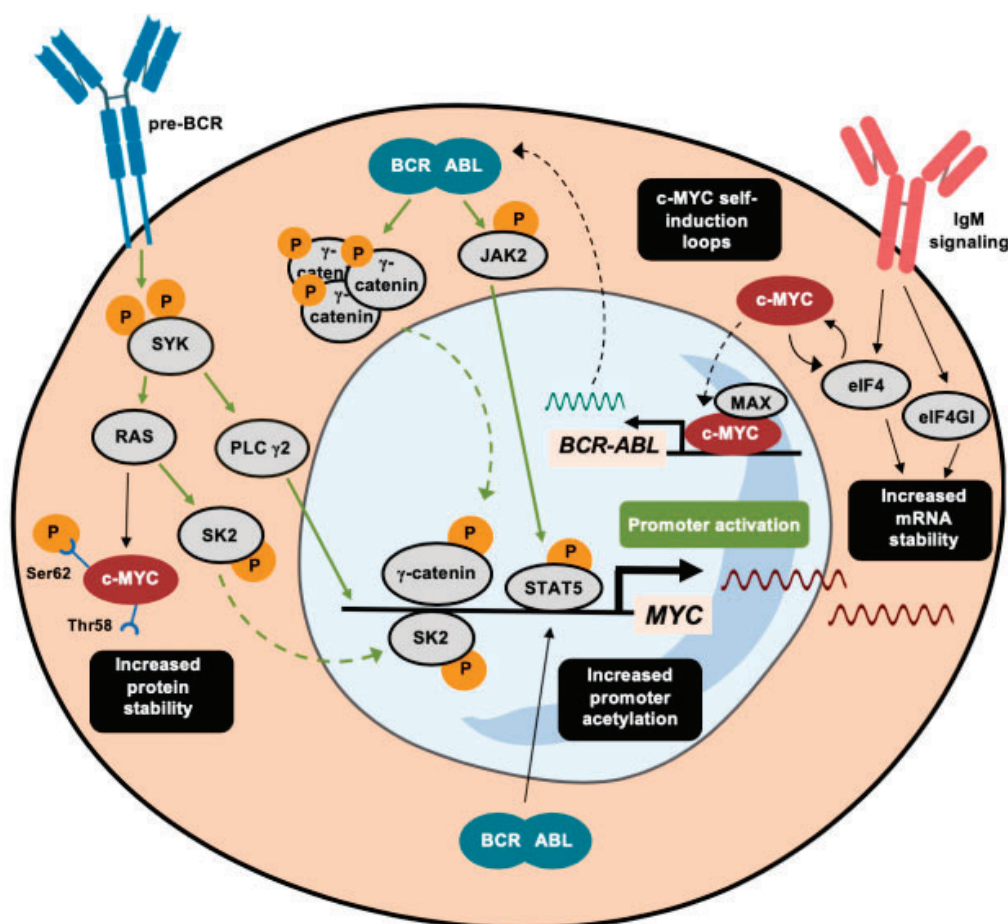


**Figure 2.** Activating mechanisms of c-MYC in leukemia with the BCR-ABL1 rearrangement. A summary of the different transduction signaling pathways that trigger the activation of MYC promoter in BCR-ABL1-rearranged leukemia. Apart from direct transcriptional activation pathways, marked in green, alternative mechanisms that induce c-MYC are depicted in black and highlighted in black squares. Dashed arrows indicate the translocation of proteins between the nucleus and the cytoplasm.

### 2.2. B lymphoblastic Leukemia with the *t(v;11)* MLL Rearrangement

Translocations in the histone methyltransferase MLL gene are the most common chromosomal alteration in infant leukemia and, in general, exhibit a very poor prognosis, such that the disease is an extremely lethal malignancy in infants [76–78]. As in other types of B-cell leukemia, the MYC

gene is not commonly involved in chromosomal translocations, although rare individual cases with t(8;22) have been reported [77]. Recently, a revised characterization of the RS4;11 leukemic cell line has demonstrated the presence of i(8q), resulting in *MYC* duplication, which confers a selective growth advantage in vitro [79]. In B-ALL, this alteration is considered a secondary hit that contributes to disease progression. Patients with the MLL-AF4 fusion protein have a strongly enriched *MYC* gene signature compared with AML patients [80,81].

Consequently, MLL-fusion proteins activate the expression of the *MYC* oncogene in pre-B and pro-B-cell leukemia [82,83]. For instance, MLL protein can prompt additional activity by fusing to USP2 deubiquitinating protein, leading to the enrichment of USP2 activity on MDM2, ending with the enhanced degradation of p53, which, in turn, activates *MYC* expression [84,85].

The binding of MLL-rearranged proteins to the regulatory regions of target genes depends on the presence of chromatin adaptors that comprise the super-elongation complex (SEC). The bromodomain and extra-terminal domain (BET) family of proteins (BRD2/3/4) are part of this complex and contribute to the induction of *MYC* [86–88]. Initial evidence showed that suppression of BRD4 induces potent cell growth arrest and cell senescence, combined with *MYC* downregulation, meaning that the BET family is a promising therapeutic target [86–89].

For instance, a small molecule inhibitor of BET (iBET-151) prevents the recruitment of BET proteins to chromatin by inhibiting the transcription of key targets, such as *BCL2* and *MYC* [87]. In parallel, JQ1 (a potent inhibitor of BRD4) greatly reduces *MYC* expression and activity, jointly with a large set of its target genes [88]. Moreover, JQ1 has also been tested in patient-derived xenograft from ALL patients, confirming its ability to inhibit *MYC* expression [90]. BET proteins are involved in maintaining aberrantly altered chromatin states in ALL. At this point, BRD4 cooperates with *MYC* in recruiting TEFb complexes to initiate transcriptional elongation at active promoters, while the transcriptional regulator HEXIM1 counteracts BRD4 and *MYC* role by inactivating the complex. Therefore, tight regulation of BRD4, *MYC*, and HEXIM1 is required for proper elongation [40,91,92]. A novel oral BRD2/3/4 inhibitor (OTX015) has been shown to reduce *MYC* expression and to increase HEXIM1 levels in MLL-rearranged leukemia [89]. Apart from OTX015, the specific BRD4 inhibitor CPI-0610 has been selected for phase I clinical trials in ALL patients [93].

Histone deacetylases (HDACs) have a differential expression pattern in ALL patients with MLL rearrangement and are commonly overexpressed. For instance, HDAC9 is associated with an adverse prognosis, whereas SIRT1 is involved in drug resistance through its regulation of the acetylation of the *TP53*, *MYC*, and *NF- $\kappa$ B* genes. Consequently, HDAC inhibitors (HDACis) have emerged as potential therapeutic options in treating hematological malignancies [94,95]. However, conceptualizing the role of HDACs in leukemia as inducers of malignant transformation would be a too simplistic view, given that some histone deacetylases, such as HDAC7, carry out an opposite function. As reported by Barneda-Zahonero et al., HDAC7 is involved in the repressive transcriptional machinery of *MYC* and, therefore, it is often reduced in different types of leukemia and lymphoma, including MLL-rearranged malignancies [96].

In this sense, newly developed compounds that selectively inhibit specific HDAC subtypes are gaining relevance in the treatment of hematological malignancies [97]. For instance, class I/IIb-selective HDACi purinostat has demonstrated a direct effect on *MYC* downregulation [56], while other selective drugs (mocetinostat, entinostat) are already undergoing clinical trials for diverse hematological malignancies [97]. The use of combinatorial therapies merging selective HDACi and classical treatments emerges as a promising therapeutic option, and it is tempting to speculate that its ability to induce apoptosis resides, at least partially, in *MYC* negative regulation [97].

The relevance of the *MYC* oncogene in hematopoiesis is restricted to its functions in aberrantly proliferating B-cell precursors and in the normal hematopoietic stem cell hierarchy. The expression of *MYC* throughout this process is controlled by a super-enhancer region located 1.7 Mb downstream of the gene [98]. This super-enhancer, known as the “blood enhancer cluster” (BENC), is comprised of several selectively active modules that recruit a wide range of transcription factors due to the

increased chromatin accessibility. This differential access to regulatory regions has also been reported in murine models of MLL-AF9-driven leukemia, indicating that *MYC* hyperactivation during leukemia can be driven by BENC-unbalanced modulation [99,100]. BENC deletion entails a drastic depletion of B lymphocytes during normal development, as well as an improved prognosis in MLL-AF9<sup>+</sup> leukemia [100]. Regarding the regulation of *MYC* at the promoter level, we strongly consider that recently developed techniques for 3D chromatin architecture analysis will improve our knowledge about the coordination of transcriptional machinery, chromatin accessibility, and 3D structure. Not in vain, this novel methodology has already conferred a new dimension to the study of B cell development at different stages [101].

### 2.3. B Lymphoblastic Leukemia with the t(12;21) ETV6/RUNX1 Rearrangement

The t(12;21) translocation, which involves the *ETV6* and *RUNX1* (also known as AML1) genes, is the most frequent lesion in childhood B-ALL (20–30% of cases), at early diagnosis and remission [102,103]. The N-terminal region of *ETV6* displays weak homology with the bHLH region of *MYC* protein [104]. This homology enables the induction of the targets of these factors through protein-protein interaction, enhancing *MYC* oncogenic function [103]. Apart from its characteristic fusion to *RUNX1* protein, *ETV6* also forms fusion proteins with *PAX5*, which is a key inducer of B-cell-specific genes (such as *CD19* and *CD79A*) [104,105]. The combination of *PAX5* activity with *ETV6*-mediated *MYC* targets induction establishes the *ETV6/PAX5* fusion protein as a powerful mediator of ALL progression.

Alterations affecting the *MYC* gene itself should be highlighted as examples of chromosomal aberrations. For instance, a double *MYC* gene translocation t(8;14)t(8;9) was reported in a B-ALL patient with *ETV6* amplification [106]. Copy number variation (CNV) was reported in a substantial 65% of relapsing *ETV6/RUNX1*-positive ALL patients, including *MYC* expression gain at chromosome 8 (q23.1-24.1) in 10% of cases [107].

An indirect pathway of *MYC* activation in *ETV6/RUNX1*-rearranged leukemia is mediated by the GTP-binding protein *RAC1*, a pivotal modulator of hematopoiesis [108], that increases the phosphorylation levels of *STAT3* [109]. *ETV6/RUNX1* protein enhances the activity of *RAC1*, increasing *MYC* expression, induced by the phosphorylation of *STAT3* [110]. Specific *STAT3* inhibitors revert *MYC* induction by blocking cell proliferation and promoting apoptosis in pro-B-ALL cells [110].

Additionally, the *ETV6/RUNX1* fusion gene can be stabilized at the mRNA level by the RNA-binding protein *IGF2BP1*, which is overexpressed in this type of leukemia [111]. *IGF2BP1* leads to an eventual increase of *MYC*, linked to aberrant leukemogenesis in *ETV6/RUNX1*-mediated ALL [111,112]. Finally, and similarly to the mechanism reported for *BCR-ABL1*-rearranged leukemia, *MYC* is also stabilized at the protein level through aberrantly altered phosphorylation at the Thr58 and Ser62 residues [69].

### 2.4. B Lymphoblastic Leukemia with other Chromosomal Rearrangements

Expression of B220 and CD43 determines the transition of pro-B into pre-B lymphocytes [113]. Leukemia derived from this developmental stage usually displays *TCF3/PBX1* chromosomal rearrangement, which is commonly found in leukemia derived from pre-B lymphocytes (in more than 90% of cases) [114]. Survival of *TCF3/PBX1*<sup>+</sup> cells critically depends on the activity of the pre-BCR [52,53]. Immunoglobulin  $\mu$  (Ig $\mu$ ) heavy-chain knockdown impairs the proper assembly of pre-BCR and blocks signal transduction through the Ig $\alpha$ -Ig $\beta$  heterodimer [115]. Ig $\mu$  downregulation in *TCF3/PBX1*-rearranged cell lines significantly suppresses *MYC* expression at the mRNA and protein levels. *MYC* is regulated by the pre-BCR in a *FOXO*-dependent manner since the forced expression of a constitutive form of *FOXO1* reverts the blockade of pre-BCR signaling, and partially restores *MYC* expression [53].

Under physiological conditions, *MYC* mRNA is modulated by miR-24, which is able to bind at its 3'-UTR region to reduce *MYC* levels, thereby controlling cell-cycle progression [116]. miR-24 is frequently downregulated in *TCF3/PBX1*<sup>+</sup> pre-B-ALL, concomitantly with other miRNAs involved in proliferation and apoptosis modulation in various cancers (e.g., miR-126 and miR-365) [117].



Surprisingly, the restoration of miR-24 expression in *TCF3*-rearranged leukemic cell lines neither affects the expression of some of its targets nor alters the frequency of apoptotic cells, suggesting that *MYC* is regulated by a combination of mechanisms in this type of leukemia [117].

Despite not being the most frequent alteration, the *IGH* gene (located at chromosome 5) can also be translocated to chromosomes 14 or 12, as is the case for the NALM-6 cell line, which harbors the t(5;12) translocation. This cell line was recently used to identify the transcriptional cofactor apoptosis antagonizing transcription factor (AATF) as being a direct target of *MYC* since it features canonical binding motifs at the promoter region [118]. AATF promotes cell-cycle progression by inhibiting TP53 expression and mediating the response to DNA damage [119]. It is of particular note that, when inhibiting the expression of *MYC*, there is a drastic downregulation of *MLL* gene expression, a previously described key mediator of pediatric leukemia. This downregulation can be counteracted by the exogenous induction of AATF. Therefore, AATF mediates a positive feedback loop between *MYC* and *MLL* gene in pro-B-ALL [118].

### 3. *MYC* Role in Lymphomagenesis

In hematopoietic malignancies, genomic abnormalities involving the *MYC* gene are almost always found in B cell lymphomas, but rarely in T cell lymphomas. 30% of all lymphoid neoplasms are B cell non-Hodgkin lymphomas. These can be classified further as Burkitt lymphoma (BL), diffuse large B cell lymphoma (DLBCL), follicular lymphoma (FL), mantle cell lymphoma (MCL), and plasmablastic lymphoma (PBL), among others.

#### 3.1. *MYC* in Burkitt Lymphomas

BL arises mostly in children and young adults and has an extremely high proliferation rate. Endemic, sporadic, and immunodeficiency-associated BLs are distinguished as clinical variants in the World Health Organization (WHO) classification. BL has a mature B cell phenotype with expression of GC/post-GC markers such as immunoglobulin M (IgM), CD10, and is typically negative for *BCL2* [120].

The genetic hallmark that characterizes BL is the rearrangement of *MYC* with one of the *IG* gene loci. Translocation triggers constitutive *MYC* hypermutation of the translocated gene in germinal centers [121], subjected to AID-dependent SHM [41], which is susceptible to generating *MYC* variants and increasing its oncogenic potential [122]. Specifically, an *MYC* translocation to the *IG* heavy chain gene locus 14q32 (80% of the cases), or to the *IGκ* or *IGλ* light chain genes at 2p12 or 22q11 (10%) are the main rearrangement sites [123,124]. Most mutations of the rearranged *MYC* gene are point SNPs or deletions in the 3' border of the first exon and the first intron [125,126], altering the coding sequence but permitting its transcription from the translocated chromosome. In consequence, there is an *MYC* expression that terminates inhibiting cell differentiation and inducing proliferation, probably keeping the cells in a hyperproliferative state.

In a gene expression profile study of human samples of BL (and DLBCL), three main cytogenetic groups within the mature aggressive B cell lymphomas were distinguished: *MYC*-simple, with *IG-MYC* fusions and a low chromosomal complexity score, no *IGH-BCL2* fusions, and no *BCL6* breakpoints, and with a favorable prognosis; *MYC*-complex, including *IG/MYC*-rearranged BLs with highly complex karyotypes, non-*IG/MYC*-rearranged cases, and all *IGH/BCL2* fusions and/or *BCL6* breakpoints, or any combination of these; and *MYC*-negative, comprising lymphomas with unaltered *MYC* [127].

Inhibitor of DNA binding (ID) proteins, such as *ID3*, bind E-proteins such as *TCF3* via HLH common motifs, preventing the binding of the latter to DNA. Schmitz et al. shed light on some oncogenic pathways, suggesting that *MYC* translocation is insufficient to induce BL [128]. The next-generation sequencing (NGS) study performed by Love et al. identified *MYC* and *ID3* as the genes most frequently mutated in BL [128,129].

In the setting of deregulated *MYC*, samples with *ID3* mutations show a higher level of expression of known *MYC* target genes, and give rise to increased G1-to-S-phase cell-cycle progression in BL, suggesting a role for *ID3* as a tumor suppressor in this type of lymphoma [129]. The high level of

ID3 expression in BL might be because the *ID3* locus itself is a direct target of MYC [130] and due to BCR triggering, as described using an *Id3*<sup>-/-</sup> mouse model [131]. Functional analyses suggested that *ID3*-inactivating mutations and *TCF3*-activating mutations (by blocking ID3 binding sites) lead to the activation of a TCF3-dependent transcriptional program that consequently promotes tonic BCR signaling [132]. TCF3 would repress *PTPN6*, which encodes SHP-1, a BCR-attenuating factor that acts by dephosphorylating the ITAM motifs of the CD79A and CD79B signaling subunits of the BCR [39]. In addition, BCR can activate both MYC and ID3 by a sequential process in which MYC rapidly upregulates its expression. Later, upon MYC downregulation, levels of ID3 increase [131]. This effect may be produced by direct BCR activation, or through an indirect effect of MYC, highlighting the existence of a positive feedback loop between BCR, ID3, and MYC regulation.

Tonic BCR activation requires PI3K signaling in mature B cells to maintain its continuity [132], and the pro-survival pathway cooperates with MYC in BL [133]. MYC deregulation induces the expression of the MIR17HG, a microRNA host gene amplified in ~10% of BL cases [134]. Particularly, miR-19 is the key oncogenic component of the cluster, which antagonizes PTEN and, consequently, activates the AKT-mTOR pathway, the consequence of which is exacerbated cell survival in MYC-driven lymphomagenesis [128,135,136]. See [137] for an extensive review of the involvement of MYC and miRNAs in lymphomagenesis.

BCR-induced PI3K pathway activation in BL contrasts with the absence of NF- $\kappa$ B survival pathway signaling in these tumors [138]. Reinforcing this, the study by Klapproth et al. in *Myc* transgenic mice showed that constitutive NF- $\kappa$ B activity is incompatible with the development of the MYC-induced lymphomas [139]. The resting state of the NF- $\kappa$ B apoptotic pathway confers a selective advantage on MYC-driven oncogenic cells.

### 3.2. MYC in Diffuse Large B Cell Lymphoma

DLBCL accounts for approximately 40% of all non-Hodgkin lymphomas [120]. Two major subtypes can be identified: germinal center B-cell-like (GCB), which has a gene expression profile similar to that of the GC B cell; and activated B cell-like (ABC), which has a worse outcome because it expresses genes present in activated peripheral B cells [120]. The principal translocated sites in DLBCL are a rearrangement of *BCL6* (30% of cases) and t(14;18)(q32;q21) with *BCL2* rearrangement to the *IGH* gene locus (20–30% of cases) [140,141]. Globally *BCL2* is rearranged in 30% of cases in the GCB-DLBCL subgroup and in <5% of ABC-DLBCL cases [140,142,143].

Considering MYC specifically, its protein expression is detected in ~40% of diagnoses, but its rearrangement is found in only around 10% of them, suggesting that alternative mechanisms may be associated with MYC deregulation [143–146]. With regard to translocations, similar to what is observed in BLs, the *IG* genes are the most frequent MYC partners, the latter being most commonly fused to *IGH* or to non-*IG* genes such as *BCL6*, *BCL2*, *PAX5*, or *IKAROS*, which appear as translocation partners in 35–50% of MYC-rearranged DLBCLs [145–147]. In addition to MYC translocations, DLBCLs are characterized by the presence of MYC amplification and gains, and increased copy numbers of MYC are associated with higher levels of mRNA and protein, resulting in a very poor prognosis [148,149]. However, careful examination of Cosmic, a public catalog of somatic mutations in cancer, revealed that SNPs in MYC sequence could be detected in a significant fraction of DLBCLs, as reported in BL. According to this data and as described before, polymorphisms in MYC sequence do not impair its transcription, permitting in consequence, a dysregulated gene expression that could maintain the cell in a hyperproliferative state that, in the end, will endow cells with increased aggressiveness.

MYC rearrangements are often involved in complex karyotypes and are frequently associated with other oncogenic abnormalities. Lymphomas that carry MYC and either a *BCL2* or a *BCL6* translocation (a double-hit lymphoma, DHL) or all three rearrangements (a triple-hit lymphoma, THL) are included in the current WHO classification as a new entity termed “High-grade B cell lymphomas with MYC and *BCL2* and *BCL6* rearrangements” [150]. Molecularly, DHL with MYC and *BCL2* rearrangements present a *TP53* mutation, inhibiting TP53-mediated apoptosis at a higher frequency than DHL, including

*MYC* and *BCL6* alterations, which account for 35% and 6% of cases, respectively [151,152]. Therefore, in the first group, upregulated *MYC* expression promotes proliferation and disables the capacity to induce apoptosis, while *BCL2* expression fosters cell survival. Together their co-expression confers an aggressive proliferating phenotype on these DHLs.

*MYC* overexpression is a reliable biomarker for predicting therapeutic response, since its expression is a poor prognostic factor in DLBCL [153] but, beyond the aforementioned rearrangements, the mechanisms underlying its overexpression are still unknown. The stability of *MYC* is regulated by GSK-3 $\beta$ , which phosphorylates *MYC* at Thr58 and induces its degradation via the ubiquitin-proteasome pathway [154]. Wang et al. demonstrated that BCR stimulation could activate downstream PI3K signaling, phosphorylating GSK-3 $\beta$  at Ser9, and abolishing its ability to induce *MYC* degradation in DLBCL [155]. Moreover, the PI3K pathway inhibitory elements such as PTEN are frequently lost in GCB-DLBCL [156], while BCR mutations also result in its constitutive activation [157], leading to *MYC* dysregulation in DLBCL.

Finally, the upregulation of *MYC* expression in DLBCL promotes BCR signaling by inducing the MIR17HG cluster, employing a mechanism similar to that described above in the section on BL [158,159]. Taken together, these data suggest that a positive feedback loop operates in the BCR-PI3K-*MYC* signaling axis in DLBCL.

### 3.3. *MYC* In Plasmablastic Lymphoma

PBL is an aggressive, high-grade lymphoma that is most commonly diagnosed in patients with HIV infection or an immunocompromised phenotype [120]. The cell of origin in PBL is thought to be the plasmablast, an activated B cell that has undergone SHM and CSR, and that expresses cell surface markers such as CD138, CD38, MUM1, and Ig, similar to a plasma cell [120]. Signaling pathways leading to plasma cell differentiation involve gene silencing of *PAX5* and *BCL6* through BLIMP1 [160,161], which also represses *MYC* expression through promoter binding [42]. Recurrent somatic mutations in *PRDM1* (the gene encoding BLIMP1) occur in 50% of cases, where they affect the regulation of diverse targets, such as *MYC* [162]. Moreover, *MYC* and BLIMP1 proteins were found to be co-expressed in 80% of diagnoses [162]. These findings are firm evidence that *PRDM1* contributes to the oncogenicity of dysregulated *MYC*.

Although *MYC* rearrangement is the genetic hallmark of BL and is characteristic of an aggressive subset of DLBCL, it is also a common finding in PBL, along with *MYC* gains [163,164]. In PBL, *MYC* rearrangements have been found in ~50% of cases, and the *IG* genes are the most frequent partners (~85%), with t(8;14) *MYC/IGH* being the commonest fusion product [163]. Gene expression analysis of PBL revealed *MYC* overexpression at mRNA and protein levels [165]. *MYC* overexpression facilitates PBL cell apoptosis escape through cell-cycle dysregulation, and jointly with loss of TP53 [166]. Together, these two processes enhance the aggressiveness of PBL.

In the absence of translocations, the mechanisms of *MYC* dysregulation are poorly understood, suggesting that *MYC* may be activated by other mutated genes. Rearrangements of *BCL2*, *BCL6*, *MALT1*, and *PAX5*, which are common in BL and DLBCL, are not detected in PBL. Conversely, gains of these loci are frequent in PBL, where 30% of cases display amplification of three or more of them [163]. Paradoxically, Ouansafi et al. demonstrated in a single case report the concomitant presence of *BCL2* and *MYC* translocation in a rare case of FL-to-PBL transformation [167].

### 3.4. *MYC* in Other Non-Hodgkin B Cell Lymphomas

FL is an indolent non-Hodgkin lymphoma that transforms into a high-grade lymphoma, mostly DLBCL, in about one-third of patients. The genetic hallmark of FL is t(14;18)(q32;q21), which brings about *BCL2/IGH* fusion protein [168]. Low-grade lymphomas containing a *BCL2* rearrangement need subsequent secondary genetic hits for the disease to evolve. The genetic alteration of *MYC* may suffice as this secondary alteration, leading to the transformation into a high-grade B cell lymphoma [169]. Actually, the majority of FLs express *MYC*, but only in a small fraction of the cells (<25%) [146].

Pasqualucci et al. investigated the genetic drivers of transformed follicular lymphoma (t-FL) and determined that there is a common mutated precursor that experiences distinct genetic events that are specifically associated with alterations deregulating cell-cycle progression and DNA damage [46], evidence that matches perfectly with *MYC* oncogene among others. t-FL to DLBCL progression occurs in 30% of the cases, mainly among GCB-DLBCL patients [170,171]. t-FL oncogenic mechanisms are characterized by the presence of a proliferation signature, together with recurrent oncogenic transformations such as *TP53* mutation, *CDKN2A* loss, and *c-REL* amplification [171], giving rise to a proliferative phenotype in which *MYC* could be involved. In fact, genetic lesions deregulating *MYC* are the second most common tFL-specific lesion (including translocations, point mutations, and CNVs) [46]. Alternative pathways involving *MYC* and its targets could help distinguish between two types of morphologically similar lymphomas, such as tFL-derived DLBCL and de novo DLBCL, this signature being more enriched in de novo cases than in transformed ones [172].

As reported by Martinez-Climent et al., when examining gene expression changes in t-FL, a considerable number of *MYC* target genes are differentially expressed, although the *MYC* gene locus remains unaltered in terms of copy number [173]. Consequently, *MYC* genetic abnormalities are not the driving mutations of FL transformation and may only serve as a surrogate for the entire proliferation signature.

MCL is generally an aggressive malignancy, but it is thought in some cases to remain latently quarrelsome in an indolent phase. It is characterized by t(11;14)(q13;q32), juxtaposing *IGH*, and *CCND1*, resulting in *CCND1* overexpression, which drives the cells through the G1/S transition [174]. Interestingly, a partnership between *CCND1* and *MYC* has been reported in the oncogenic transformation of B cells to MCL [175]. The coexistence of *MYC* and *CCND1/IGH* rearrangements [176] is commonly found in double-hit (DH)-MCL [177], which is associated with a high-risk prognostic index. As reported for FL, most of the MCL cases display an intense *MYC* expression, but the percentage of positive cells is frequently low (<25%) [146].

Aggressive MCL subset variants can be divided between the blastoid variants (resembling lymphoblast cells) and pleomorphic variants (DLBCL-like cells). MCL is also characterized by large numbers of secondary gains and losses of genes that are mainly involved in cell-cycle regulation, response to DNA damage, and survival [178]. Regarding the blastoid variant, *MYC* alterations such as the rearrangement involving *IGH* in t(8;14), disruption of the *MYC* locus in t(2;8), and gains in add(8)(q24) have been described [179,180]. These aberrations, along with a high level of *TP53* expression, are features associated with MCL aggressiveness [181].

*CDK4* and *CDK6* are catalytic subunits of the cyclin D family that govern G1-to-S-phase progression; p16<sup>INK4a</sup> and all members of the *INK4* family act as their negative regulators by specifically binding to them [182]. *CDK4* mutations abolish the binding motif of the *INK4* family, thereby functioning as an oncogene capable of directing proliferation [183]. Surprisingly, cyclin D1/*CDK4* and p16<sup>INK4a</sup> complexes are known to be upstream regulators of *MYC* [184], while *CDK4* has been identified as a target of *MYC* [185]. In the context of *MYC* dysregulation, *CDK4-INK4* imbalance plays a role in lymphomagenesis [183].

The *MYC*-driven gene expression network is maintained through the stability of the *MYC* protein, which itself is sustained in MCL by *MALT1* [186]. Constitutively activated *MALT1* expression, together with *BCL10*, is orchestrated by the activation of the BCR, which recruits *CARD11* scaffold protein and ultimately results in a BCR-driven *CARD11-BCL10-MALT1* (CBM) complex. CBM subsequently activates the NF- $\kappa$ B pathway [187] and, combined with *MYC* stabilization by *MALT1*, drives lymphomagenesis progression.

Table 1 summarizes the essential information about the aberrant activation of *MYC* in leukemia and lymphoma disorders (Chapters 2 and 3).

**Table 1.** MYC alterations in leukemia and lymphoma. Summary of the gene alterations, chromosomal translocations, regulatory pathways, and post-transcriptional modifications involved in MYC activation that are included in this review, assigned to their corresponding subtype of leukemia and lymphoma.

	Gene Alterations (Mutations, CNV)	Involvement of Translocations	Activating Pathways	MyC Stabilization at Post-Transcriptional Level	
LEUKEMIA	t(9;22) BCR/ABL1 rearrangement	Almost negligible mutation rate [46]	Induced by aberrant AID [47], pre-BCR/SYK signaling [53], Wnt [58] and JAK/STAT [60,61] pathways	Translation rate controlled by EIFs [62–65], prevention of proteasomal degradation [67–69], induction mediated by MIR17HG cluster [74,75]	
	t(v;11) KMT2A rearrangement	i(8q) MYC duplication in RS4;11 cell line [79]	Indirect activation through TP53 inhibition [84,85], direct binding of MLL-fusion proteins and BET adaptors [86–88], regulation by BENC super-enhancer region [99,100]		
	t(12;21) ETV6/RUNX1 rearrangement	MYC gene expression gain 8(q23.1-24.1). CNVs reported in 65% of cases [107]	Double MYC gene translocation reported [106]	ETV6 also fuses to PAX5 and induces MYC expression [104]. Also triggered by RAC1-STAT3 [110]	Stabilized at mRNA level by IGF2BP1 [111] and at the protein level by prevention of proteasomal degradation [69]
LYMPHOMA	Burkitt lymphoma	Point SNPs and deletions in the 3'border [125,126]	MYC/IGH t(8;14q32) in 80% of the cases and MYC/IGk or Igλ t(8;2p12) or t(8;22q11) in 10% of the diagnoses [123,124]	BCR-induced PI3K pathway in cooperation with TCF3, ID3 and SHP-1 [129–134]	
	Diffuse large B cell Lymphoma	Point SNPs, amplifications, gains and increased copy numbers of MYC [148,149]	Found in 10% of the cases, being MYC/IGL the most common [144], but also to BCL6, BCL2, PAX5, IKAROS [145–147]. Often participate in complex karyotypes and associated to a second hit such as MYC/BCL2 and MYC/BCL6 [151,152]	Mutations in the BCR or PI3K pathway inhibitory elements [156,157]	GSK-3β phosphorylation abolishing MYC degradation [155] MYC upregulation promotes BCR signaling by induction of MIR17HG cluster [158,159]
	Plasmablastic lymphoma	Gains [163,164] and somatic mutations in MYC inhibitor PRDM1 [42,162]	Observed in 50% of the cases, being MYC/IGH the most common [163]		

Table 1. Cont.

	Gene Alterations (Mutations, CNV)	Involvement of Translocations	Activating Pathways	Myc Stabilization at Post-Transcriptional Level
Follicular lymphoma	Remains unaltered in terms of copy number [173]	Second most common tFL-specific lesion [46]	Proliferation signature with oncogenic transformations such as <i>TP53</i> mutations, <i>CDKN2A</i> loss and <i>c-REL</i> amplification [171]	
Mantle cell lymphoma	Disruption of <i>MYC</i> locus in t(2;8) and <i>MYC</i> gains at (8)(q24) [179,180]	Coexistence of <i>CCND1/IGH</i> and <i>MYC</i> rearrangements [176,177], and also <i>MYC/IGH</i> t(8;14) [179,180]	<i>CCND1/CDK4</i> and <i>p16<sup>INK4a</sup></i> imbalance [183–185]	BCR-driven <i>CARD11-BCL10-MALT1</i> complex together with <i>Nf-κβ</i> pathway orchestrates <i>MYC</i> stability [186,187]

#### 4. Concluding Remarks

The appropriate path that lymphoid progenitors should ideally follow on their way towards fully differentiated B cells is constantly under threat of being wrecked by the alteration of regulatory mechanisms. Beyond its widely known function as an oncogene, MYC also plays an essential role at different steps of B-cell differentiation, and its deregulation is one of the main hazards that can disrupt the process. As described in this review and in a physiological context, MYC is strongly expressed on the way to producing mature B lymphocytes, whereas its transient downregulation is required at some specific points. However, MYC basal levels are maintained and are not completely switched off at any point before the late memory and plasmatic B cell stages, demonstrating that only tight regulation of MYC levels ensures that the B lymphocytes achieve their correct fate.

When the expression of MYC protein is aberrantly altered, the risk of developing a hematological malignancy, such as leukemia or lymphoma, increases substantially through the acquisition of an uncontrolled proliferative rate and a blockade of differentiation. Remarkably, the alterations that trigger MYC overexpression differ between leukemia and lymphoma cells. In fact, leukemic cells have low rates of MYC mutations and a low frequency of chromosomal translocations involving the MYC gene, whereas the aforementioned genetic alterations are a hallmark in some types of non-Hodgkin B cell lymphoma. Nevertheless, and even when not altered at the genetic level, the expression of MYC is usually disrupted in the commonest types of leukemia, where it is activated by several pathways, as well as at the post-transcriptional level. Most types of lymphoma present high levels of MYC expression that are not always correlated with a mutated MYC gene, opening the door to speculation that, as in leukemia, multiple pathways may act to facilitate its dysregulation.

In terms of therapeutic perspectives, the possibilities for interfering with MYC activity are still to be adequately explored. However, the identification of regulatory cascades and other mechanisms that trigger its induction opens a wide range of possibilities for indirectly impairing MYC function. As reported here, we believe that the disruption of altered epigenetic regulation with HDAC inhibitors, the blockade of microRNAs function, or the use of BET inhibitors that obstruct scaffold transcriptional activating machinery, are but a few examples of the promising therapeutic strategies that will lead to an improved prognosis of hematological disorders, mostly mediated by the maintenance of MYC at physiological levels.

**Author Contributions:** O.d.B. and A.M. did the bibliographic research and wrote the manuscript. M.P. conceived the manuscript, supervised the work, and provided critical comments on the review. All authors have read and agreed to the published version of the manuscript.

**Funding:** This manuscript was funded by grants to M.P. by the Spanish Ministry of Science, Innovation, and Universities (SAF2017-87990-R and EUR2019-103835) and elaborated at the Josep Carreras Leukaemia Research Institute (IJC, Badalona, Barcelona). O.d.B. is funded by a Juan de la Cierva - Formación fellowship from the Spanish Ministry of Science, Innovation, and Universities (FJCI-2017-32430). A.M. is funded by the Spanish Ministry of Science, Innovation and Universities, which is part of the Agencia Estatal de Investigación (AEI), through grant PRE2018-083183 (co-funded by the European Social Fund.). We thank the CERCA Programme/Generalitat de Catalunya and the Josep Carreras Foundation for institutional support.

**Conflicts of Interest:** The authors declare no conflict of interest.

#### References

1. Adolfsson, J.; Månsson, R.; Buza-Vidas, N.; Hultquist, A.; Liuba, K.; Jensen, C.T.; Bryder, D.; Yang, L.; Borge, O.-J.; Thoren, L.A.M.; et al. Identification of Flt3+ lympho-myeloid stem cells lacking erythro-megakaryocytic potential. *Cell* **2005**, *121*, 295–306. [[CrossRef](#)]
2. Kondo, M.; Weissman, I.L.; Akashi, K. Identification of clonogenic common lymphoid progenitors in mouse bone marrow. *Cell* **1997**, *91*, 661–672. [[CrossRef](#)]
3. Victora, G.D.; Nussenzweig, M.C. Germinal centers. *Annu. Rev. Immunol.* **2012**, *30*, 429–457. [[CrossRef](#)] [[PubMed](#)]
4. Huang, C.; Melnick, A. Mechanisms of action of BCL6 during germinal center B cell development. *Sci. China Life Sci.* **2015**, *58*, 1226–1232. [[CrossRef](#)] [[PubMed](#)]

5. Coppola, F.; Cole, M. Constitutive c-myc oncogene expression blocks mouse erythroleukaemia cell differentiation but not commitment. *Nature* **1986**, *320*, 760–763. [[CrossRef](#)] [[PubMed](#)]
6. Leon, J.; Ferrandiz, N.; Acosta, J.C.; Delgado, M.D. Inhibition of cell differentiation: A critical mechanism for MYC-mediated carcinogenesis? *Cell Cycle* **2009**, *8*, 1148–1157. [[CrossRef](#)] [[PubMed](#)]
7. Sheiness, D.; Bishop, J.M. DNA and RNA from uninfected vertebrate cells contain nucleotide sequences related to the putative transforming gene of avian myelocytomatosis virus. *J. Virol.* **1979**, *31*, 514–521. [[CrossRef](#)]
8. Varmus, H. The molecular genetics of cellular oncogenes. *Annu. Rev. Genet.* **1984**, *18*, 553–612. [[CrossRef](#)]
9. Langdon, W.Y.; Harris, A.W.; Cory, S.; Adams, J.M. The c-myc oncogene perturbs B lymphocyte development in E $\mu$ -myc transgenic mice. *Cell* **1986**, *47*, 11–18. [[CrossRef](#)]
10. Delgado, M.D.; León, J. Myc roles in hematopoiesis and leukemia. *Genes Cancer* **2010**, *1*, 605–616. [[CrossRef](#)]
11. Laurenti, E.; Varnum-Finney, B.; Wilson, A.; Ferrero, I.; Blanco-Bose, W.E.; Ehninger, A.; Knoepfler, P.S.; Cheng, P.F.; MacDonald, H.R.; Eisenman, R.N.; et al. Hematopoietic stem cell function and survival depend on c-Myc and N-Myc activity. *Cell Stem Cell* **2008**, *3*, 611–624. [[CrossRef](#)] [[PubMed](#)]
12. Reavie, L.; Della Gatta, G.; Crusio, K.; Aranda-Orgilles, B.; Buckley, S.M.; Thompson, B.; Lee, E.; Gao, J.; Bredemeyer, A.L.; Helmink, B.A.; et al. Regulation of hematopoietic stem cell differentiation by a single ubiquitin ligase-substrate complex. *Nat. Immunol.* **2010**, *11*, 207–215. [[CrossRef](#)] [[PubMed](#)]
13. He, C.; Hu, H.; Braren, R.; Fong, S.Y.; Trumpp, A.; Carlson, T.R.; Wang, R.A. C-Myc in the hematopoietic lineage is crucial for its angiogenic function in the mouse embryo. *Development* **2008**, *135*, 2467–2477. [[CrossRef](#)] [[PubMed](#)]
14. Nie, Z.; Hu, G.; Wei, G.; Cui, K.; Yamane, A.; Resch, W.; Wang, R.; Green, D.R.; Tessarollo, L.; Casellas, R.; et al. c-Myc Is a universal amplifier of expressed genes in lymphocytes and embryonic stem cells. *Cell* **2012**, *151*, 68–79. [[CrossRef](#)]
15. Smith, R.K.; Zimmerman, K.; Yancopoulos, G.D. Transcriptional down-regulation of N-myc expression during B-cell development. *Mol. Cell Biol.* **1992**, *12*, 1578–1584. [[CrossRef](#)]
16. Klemsz, M.J.; Justement, L.B.; Palmer, E.; Cambier, J. Induction of c-fos and c-myc expression during B cell activation by IL-4 and immunoglobulin binding ligands. *J. Immunol.* **1989**, *143*, 1032–1039.
17. Larsson, L.G.; Schena, M.; Carlsson, M.; Sallstrom, J.; Nilsson, K. Expression of the c-myc protein is down-regulated at the terminal stages during in vitro differentiation of B-type chronic lymphocytic leukemia cells. *Blood* **1991**, *77*, 1025–1032. [[CrossRef](#)]
18. Huang, C.Y.; Bredemeyer, A.L.; Walker, L.M.; Bassing, C.H.; Sleckman, B.P. Dynamic regulation of c-Myc proto-oncogene expression during lymphocyte development revealed by a GFP-c-Myc knock-in mouse. *Eur. J. Immunol.* **2008**, *38*, 342–349. [[CrossRef](#)]
19. Habib, T.; Park, H.; Tsang, M.; De Alborán, I.M.; Nicks, A.; Wilson, L.; Knoepfler, P.S.; Andrews, S.; Rawlings, D.J.; Eisenman, R.N.; et al. Myc stimulates B lymphocyte differentiation and amplifies calcium signaling. *J. Cell Biol.* **2007**, *179*, 717–731. [[CrossRef](#)]
20. Vaux, D.L.; Cory, S.; Adams, J.M. Bcl-2 gene promotes haematopoietic cell survival and cooperates with c-myc to immortalize pre-B cells. *Nature* **1988**, *335*, 440–442. [[CrossRef](#)]
21. Morrow, M.A.; Lee, G.; Gillis, S.; Yancopoulos, G.D.; Alt, F.W. Interleukin-7 induces N-myc and c-myc expression in normal precursor B lymphocytes. *Genes Dev.* **1992**, *6*, 61–70. [[CrossRef](#)] [[PubMed](#)]
22. De Alboran, I.M.; O'Hagan, R.C.; Gärtner, F.; Malynn, B.; Davidson, L.; Rickert, R.; Rajewsky, K.; DePinho, R.A.; Alt, F.W. Analysis of c-Myc function in normal cells via conditional gene-targeted mutation. *Immunity* **2001**, *14*, 45–55. [[CrossRef](#)]
23. Dominguez-Sola, D.; Vitorica, G.D.; Ying, C.Y.; Phan, R.T.; Saito, M.; Dalla-Favera, R.; Nussenzweig, M.C. c-MYC is required for germinal center selection and cyclic re-entry. *Nat. Immunol.* **2012**, *13*, 1083–1091. [[CrossRef](#)]
24. De Silva, N.S.; Klein, U. Dynamics of B cells in germinal centres. *Nat. Rev. Immunol.* **2015**, *15*, 137–148. [[CrossRef](#)]
25. Ci, W.; Polo, J.M.; Cerchietti, L.; Shaknovich, R.; Wang, L.; Shao, N.Y.; Ye, K.; Farinha, P.; Horsman, D.E.; Gascoyne, R.D.; et al. The BCL6 transcriptional program features repression of multiple oncogenes in primary B cells and is deregulated in DLBCL. *Blood* **2009**, *113*, 5536–5548. [[CrossRef](#)]



26. Basso, K.; Saito, M.; Sumazin, P.; Margolin, A.A.; Wang, K.; Lim, W.K.; Kitagawa, Y.; Schneider, C.; Alvarez, M.J.; Califano, A.; et al. Integrated biochemical and computational approach identifies BCL6 direct target genes controlling multiple pathways in normal germinal center B cells. *Blood* **2010**, *115*, 975–984. [[CrossRef](#)]
27. Nahar, R.; Ramezani-Rad, P.; Mossner, M.; Duy, C.; Cerchietti, L.; Geng, H.; Dovat, S.; Jumaa, H.; Ye, B.H.; Melnick, A.; et al. Pre-B cell receptor-mediated activation of BCL6 induces pre-B cell quiescence through transcriptional repression of MYC. *Blood* **2011**, *118*, 4174–4178. [[CrossRef](#)]
28. Oestreich, K.J.; Mohn, S.E.; Weinmann, A.S. Molecular mechanisms that control the expression and activity of Bcl-6 in TH1 cells to regulate flexibility with a TFH-like gene profile. *Nat. Immunol.* **2013**, *13*, 405–411. [[CrossRef](#)]
29. Saito, M.; Gao, J.; Basso, K.; Kitagawa, Y.; Smith, P.M.; Bhagat, G.; Pernis, A.; Pasqualucci, L.; Dalla-Favera, R. A signaling pathway mediating downregulation of BCL6 in germinal center B cells is blocked by BCL6 gene alterations in B cell lymphoma. *Cancer Cell* **2007**, *12*, 280–292. [[CrossRef](#)]
30. Luo, W.; Weisel, F.; Shlomchik, M.J. B cell receptor and CD40 signaling are rewired for synergistic induction of the c-Myc transcription factor in germinal center B cells. *Immunity* **2018**, *25*, 1032–1057. [[CrossRef](#)]
31. Ersching, J.; Efeyan, A.; Mesin, L.; Jacobsen, J.T.; Pasqual, G.; Grabiner, B.C.; Dominguez-Sola, D.; Sabatini, D.M.; Victora, G.D. Germinal center selection and affinity maturation require dynamic regulation of mTORC1 kinase. *Immunity* **2017**, *46*, 1045–1058.e6. [[CrossRef](#)] [[PubMed](#)]
32. Perez-Roger, I.; Kim, S.H.; Griffiths, B.; Sewing, A.; Land, H. Cyclins D1 and D2 mediate Myc-induced proliferation via sequestration of p27(Kip1) and p21(Cip1). *EMBO J.* **1999**, *18*, 5310–5320. [[CrossRef](#)] [[PubMed](#)]
33. Bouchard, C.; Thieke, K.; Maier, A.; Saffrich, R.; Hanley-Hyde, J.; Ansorge, W.; Reed, S.; Sicinski, P.; Bartek, J.; Eilers, M. Direct induction of cyclin D2 by Myc contributes to cell cycle progression and sequestration of p27. *EMBO J.* **1999**, *18*, 5321–5333. [[CrossRef](#)] [[PubMed](#)]
34. Cato, M.H.; Chintalapati, S.K.; Yau, I.W.; Omori, S.A.; Rickert, R.C. Cyclin D3 is selectively required for proliferative expansion of germinal center B cells. *Mol. Cell. Biol.* **2011**, *31*, 127–137. [[CrossRef](#)]
35. Peled, J.U.; Yu, J.J.; Venkatesh, J.; Bi, E.; Ding, B.B.; Krupski-Downs, M.; Shakhovich, R.; Sicinski, P.; Diamond, B.; Scharff, M.D.; et al. Requirement for cyclin D3 in germinal center formation and function. *Cell Res.* **2010**, *20*, 631–646. [[CrossRef](#)]
36. Calado, D.P.; Sasaki, Y.; Godinho, S.A.; Pellerin, A.; Sleckman, B.P.; Alborán, I.M.D.; Janz, M.; Rodig, S.; Rajewsky, K. MYC is essential for the formation and maintenance of germinal centers. *Nat. Immunol.* **2012**, *13*, 1092–1100. [[CrossRef](#)]
37. Victora, G.D.; Schwickert, T.A.; Fooksman, D.R.; Kamphorst, A.O.; Meyer-Hermann, M.; Dustin, M.L.; Nussenzweig, M.C. Germinal center dynamics revealed by multiphoton microscopy with a photoactivatable fluorescent reporter. *Cell* **2010**, *143*, 592–605. [[CrossRef](#)]
38. Phan, R.T.; Saito, M.; Basso, K.; Niu, H.; Dalla-Favera, R. BCL6 interacts with the transcription factor Miz-1 to suppress the cyclin-dependent kinase inhibitor p21 and cell cycle arrest in germinal center B cells. *Nat. Immunol.* **2005**, *6*, 1054–1060. [[CrossRef](#)] [[PubMed](#)]
39. Schmitz, R.; Ceribelli, M.; Pittaluga, S.; Wright, G.; Staudt, L.M. Oncogenic mechanisms in burkitt lymphoma. *Cold Spring Harb. Perspect. Med.* **2014**, *4*, a014282. [[CrossRef](#)]
40. Rahl, P.B.; Lin, C.Y.; Seila, A.C.; Flynn, R.A.; McCuine, S.; Burge, C.B.; Sharp, P.A.; Young, R.A. C-Myc regulates transcriptional pause release. *Cell* **2010**, *141*, 432–445. [[CrossRef](#)]
41. Ramiro, A.R.; Jankovic, M.; Eisenreich, T.; Difilippantonio, S.; Chen-Kiang, S.; Muramatsu, M.; Honjo, T.; Nussenzweig, A.; Nussenzweig, M.C. AID is required for c-myc/IgH chromosome translocations in vivo. *Cell* **2004**, *118*, 431–438. [[CrossRef](#)] [[PubMed](#)]
42. Lin, Y.; Wong, K.K.; Calame, K. Repression of c-myc transcription by Blimp-1, an inducer of terminal B cell differentiation. *Science* **1997**, *276*, 596–599. [[CrossRef](#)] [[PubMed](#)]
43. Sawyers, C.L.; Callahan, W.; Witte, O.N. Dominant negative MYC blocks transformation by ABL oncogenes. *Cell* **1992**, *70*, 901–910. [[CrossRef](#)]
44. Advani, A.S.; Pendergast, A.M. Bcr-Abl variants: Biological and clinical aspects. *Leuk. Res.* **2002**, *26*, 713–720. [[CrossRef](#)]
45. Afar, D.E.H.; Goga, A.; McLaughlin, J.; Witte, O.N.; Sawyers, C.L. Differential complementation of Bcr-Abl point mutants with c-Myc. *Science* **1994**, *264*, 424–426. [[CrossRef](#)] [[PubMed](#)]

46. Pasqualucci, L.; Khiabani, H.; Fangazio, M.; Vasishtha, M.; Messina, M.; Holmes, A.B.; Ouillette, P.; Trifonov, V.; Rossi, D.; Tabbò, F.; et al. Genetics of follicular lymphoma transformation. *Cell Rep.* **2014**, *6*, 130–140. [[CrossRef](#)]
47. Feldhahn, N.; Henke, N.; Melchior, K.; Duy, C.; Soh, B.N.; Klein, F.; Von Levetzow, G.; Giebel, B.; Li, A.; Hofmann, W.K.; et al. Activation-induced cytidine deaminase acts as a mutator in BCR-ABL1-transformed acute lymphoblastic leukemia cells. *J. Exp. Med.* **2007**, *204*, 1157–1166. [[CrossRef](#)]
48. Dorsett, Y.; Robbiani, D.F.; Jankovic, M.; Reina-San-Martin, B.; Eisenreich, T.R.; Nussenzweig, M.C. A role for AID in chromosome translocations between c-myc and the IgH variable region. *J. Exp. Med.* **2007**, *204*, 2225–2232. [[CrossRef](#)]
49. Liu, Z.J.; Wu, X.; Duan, Y.; Wang, Y.M.; Shan, B.; Kong, J.X.; Ma, X.B.; Bao, Y.X. AID expression is correlated with Bcr-Abl expression in CML-LBC and can be down-regulated by As2O3 and/or imatinib. *Leuk. Res.* **2011**, *35*, 1355–1359. [[CrossRef](#)]
50. Tomita, N.; Tokunaka, M.; Nakamura, N.; Takeuchi, K.; Koike, J.; Motomura, S.; Miyamoto, K.; Kikuchi, A.; Hyo, R.; Yakushijin, Y.; et al. Clinicopathological features of lymphoma/leukemia patients carrying both BCL2 and MYC translocations. *Haematologica* **2009**, *94*, 935–943. [[CrossRef](#)]
51. Xu, N.; Li, Y.L.; Zhou, X.; Cao, R.; Li, H.; Lu, Q.S.; Li, L.; Lu, Z.Y.; Huang, J.X.; Sun, J.; et al. CDKN2 gene deletion as poor prognosis predictor involved in the progression of adult B-lineage acute lymphoblastic leukemia patients. *J. Cancer* **2015**, *6*, 1114–1120. [[CrossRef](#)]
52. Eswaran, J.; Sinclair, P.; Heidenreich, O.; Irving, J.; Russell, L.J.; Hall, A.; Calado, D.P.; Harrison, C.J.; Vormoor, J. The pre-B-cell receptor checkpoint in acute lymphoblastic leukaemia. *Leukemia* **2015**, *29*, 1623–1631. [[CrossRef](#)] [[PubMed](#)]
53. Köhrer, S.; Havranek, O.; Seyfried, F.; Hurtz, C.; Coffey, G.P.; Kim, E.; Ten Hacken, E.; Jäger, U.; Vanura, K.; O'Brien, S.; et al. Pre-BCR signaling in precursor B-cell acute lymphoblastic leukemia regulates PI3K/AKT, FOXO1 and MYC, and can be targeted by SYK inhibition. *Leukemia* **2016**, *30*, 1246–1254. [[CrossRef](#)] [[PubMed](#)]
54. Wallington-Beddoe, C.T.; Powell, J.A.; Tong, D.; Pitson, S.M.; Bradstock, K.F.; Bendall, L.J. Sphingosine kinase 2 promotes acute lymphoblastic leukemia by enhancing myc expression. *Cancer Res.* **2014**, *74*, 2803–2815. [[CrossRef](#)] [[PubMed](#)]
55. Chen, Y.; Wang, X.; Xiang, W.; He, L.; Tang, M.; Wang, F.; Wang, T.; Yang, Z.; Yi, Y.; Wang, H.; et al. Development of purine-based hydroxamic acid derivatives: Potent histone deacetylase inhibitors with marked in vitro and in vivo antitumor activities. *J. Med. Chem.* **2016**, *59*, 5488–5504. [[CrossRef](#)]
56. Yang, L.; Qiu, Q.; Tang, M.; Wang, F.; Yi, Y.; Yi, D.; Yang, Z.; Zhu, Z.; Zheng, S.; Yang, J.; et al. Purinostat mesylate is a uniquely potent and selective inhibitor of HDACs for the treatment of BCR-ABL1-induced B-cell acute lymphoblastic leukemia. *Clin. Cancer Res.* **2019**, *25*, 7527–7539. [[CrossRef](#)]
57. Sun, K.; Atoyian, R.; Borek, M.A.; Dellarocca, S.; Samson, M.E.S.; Ma, A.W.; Xu, G.X.; Patterson, T.; Tuck, D.P.; Viner, J.L.; et al. Dual HDAC and PI3K inhibitor CUDC-907 down regulates MYC and suppresses growth of MYC-dependent cancers. *Mol. Cancer Ther.* **2017**, *16*, 285–299. [[CrossRef](#)]
58. Luong-Gardioli, N.; Siddiqui, I.; Pizzitola, I.; Jeevan-Raj, B.; Charmoy, M.; Huang, Y.; Irmisch, A.; Curtet, S.; Angelov, G.S.; Danilo, M.; et al.  $\gamma$ -catenin-dependent signals maintain BCR-ABL1 + B cell acute lymphoblastic leukemia. *Cancer Cell* **2019**, *35*, 649–663.e10. [[CrossRef](#)] [[PubMed](#)]
59. O'Hare, T.; Zabriskie, M.S.; Eiring, A.M.; Deininger, M.W. Pushing the limits of targeted therapy in chronic myeloid leukaemia. *Nat. Rev. Cancer* **2012**, *12*, 513–526. [[CrossRef](#)]
60. Xie, S.; Lin, H.; Sun, T.; Arlinghaus, R.B. Jak2 is involved in c-Myc induction by Bcr-Abl. *Oncogene* **2002**, *21*, 7137–7146. [[CrossRef](#)]
61. Wu, S.C.; Li, L.S.; Kopp, N.; Montero, J.; Chapuy, B.; Yoda, A.; Christie, A.L.; Liu, H.; Christodoulou, A.; van Bodegom, D.; et al. Activity of the type II JAK2 inhibitor CHZ868 in B cell acute lymphoblastic leukemia. *Cancer Cell* **2015**, *28*, 29–41. [[CrossRef](#)] [[PubMed](#)]
62. Pelletier, J.; Graff, J.; Ruggero, D.; Sonenberg, N. Targeting the eIF4F translation initiation complex: A critical nexus for cancer development. *Cancer Res.* **2015**, *75*, 250–263. [[CrossRef](#)]
63. Krysov, S.; Dias, S.; Paterson, A.; Mockridge, C.I.; Potter, K.N.; Smith, K.A.; Ashton-Key, M.; Stevenson, F.K.; Packham, G. Surface IgM stimulation induces MEK1/2-dependent MYC expression in chronic lymphocytic leukemia cells. *Blood* **2012**, *119*, 170–179. [[CrossRef](#)] [[PubMed](#)]

64. Yeomans, A.; Thirdborough, S.M.; Valle-Argos, B.; Linley, A.; Krysov, S.; Hidalgo, M.S.; Leonard, E.; Ishfaq, M.; Wagner, S.D.; Willis, A.E.; et al. Engagement of the B-cell receptor of chronic lymphocytic leukemia cells drives global and MYC-specific mRNA translation. *Blood* **2016**, *127*, 449–457. [[CrossRef](#)] [[PubMed](#)]
65. Lin, C.J.; Cencic, R.; Mills, J.R.; Robert, F.; Pelletier, J. c-Myc and eIF4F are components of a feedforward loop that links transcription and translation. *Cancer Res.* **2008**, *68*, 5326–5334. [[CrossRef](#)]
66. Shinohara, H.; Taniguchi, K.; Kumazaki, M.; Yamada, N.; Ito, Y.; Otsuki, Y.; Uno, B.; Hayakawa, F.; Minami, Y.; Naoe, T.; et al. Anti-cancer fatty-acid derivative induces autophagic cell death through modulation of PKM isoform expression profile mediated by bcr-abl in chronic myeloid leukemia. *Cancer Lett.* **2015**, *360*, 28–38. [[CrossRef](#)]
67. Sears, R.; Leone, G.; DeGregori, J.; Nevins, J.R. Ras enhances Myc protein stability. *Mol. Cell* **1999**, *3*, 169–179. [[CrossRef](#)]
68. Sears, R.; Nuckolls, F.; Haura, E.; Taya, Y.; Tamai, K.; Nevins, J.R. Multiple Ras-dependent phosphorylation pathways regulate Myc protein stability. *Genes Dev.* **2000**, *14*, 2501–2514. [[CrossRef](#)]
69. Malempati, S.; Tibbitts, D.; Cunningham, M.; Akkari, Y.; Olson, S.; Fan, G.; Sears, R.C. Aberrant stabilization of c-Myc protein in some lymphoblastic leukemias. *Leukemia* **2006**, *20*, 1572–1581. [[CrossRef](#)]
70. Welcker, M.; Orian, A.; Jin, J.; Grim, J.A.; Harper, J.W.; Eisenman, R.N.; Clurman, B.E. The Fbw7 tumor suppressor regulates glycogen synthase kinase 3 phosphorylation-dependent c-Myc protein degradation. *Proc. Natl. Acad. Sci. USA* **2004**, *101*, 9085–9090. [[CrossRef](#)]
71. Nilsson, J.A.; Cleveland, J.L. Myc pathways provoking cell suicide and cancer. *Oncogene* **2003**, *22*, 9007–9021. [[CrossRef](#)]
72. Pelengaris, S.; Khan, M.; Evan, G. c-MYC: More than just a matter of life and death. *Nat. Rev. Cancer* **2002**, *2*, 764–776. [[CrossRef](#)] [[PubMed](#)]
73. Egle, A.; Harris, A.W.; Bouillet, P.; Cory, S. Bim is a suppressor of Myc-induced mouse B cell leukemia. *Proc. Natl. Acad. Sci. USA* **2004**, *101*, 6164–6169. [[CrossRef](#)] [[PubMed](#)]
74. Mraz, M.; Kipps, T.J. MicroRNAs and B cell receptor signaling in chronic lymphocytic leukemia. *Leuk. Lymphoma* **2013**, *54*, 1836–1839. [[CrossRef](#)] [[PubMed](#)]
75. Li, Y.; Deutzmann, A.; Choi, P.S.; Fan, A.C.; Felsner, D.W. BIM mediates oncogene inactivation-induced apoptosis in multiple transgenic mouse models of acute lymphoblastic leukemia. *Oncotarget* **2016**, *7*, 26926–26934. [[CrossRef](#)]
76. Chowdhury, T.; Brady, H.J.M. Insights from clinical studies into the role of the MLL gene in infant and childhood leukemia. *Blood Cells Mol. Dis.* **2008**, *40*, 192–199. [[CrossRef](#)]
77. Meeker, N.D.; Cherry, A.M.; Bangs, C.D.; Frazer, J.K. A pediatric B lineage leukemia with coincident MYC and MLL translocations. *J. Pediatr. Hematol. Oncol.* **2011**, *33*, 158–160. [[CrossRef](#)]
78. Sanjuan-Pla, A.; Bueno, C.; Prieto, C.; Acha, P.; Stam, R.W.; Marschalek, R.; Menéndez, P. Revisiting the biology of infant t(4;11)/MLL-AF4+ B-cell acute lymphoblastic leukemia. *Blood* **2015**, *126*, 2676–2685. [[CrossRef](#)]
79. Ragusa, D.; Makarov, E.M.; Britten, O.; Moralli, D.; Green, C.M.; Tosi, S. The RS4;11 cell line as a model for leukaemia with t(4;11)(q21;q23): Revised characterisation of cytogenetic features. *Cancer Rep.* **2019**, *1–11*, e1207. [[CrossRef](#)]
80. Hyrenius-Wittsten, A.; Pilheden, M.; Stureson, H.; Hansson, J.; Walsh, M.P.; Song, G.; Kazi, J.U.; Liu, J.; Ramakrishan, R.; Garcia-Ruiz, C.; et al. De novo activating mutations drive clonal evolution and enhance clonal fitness in KMT2A-rearranged leukemia. *Nat. Commun.* **2018**, *9*, 1–13. [[CrossRef](#)]
81. Neff, T.; Sinha, A.U.; Kluk, M.J.; Zhu, N.; Khattab, M.H.; Stein, L.; Xie, H.; Orkin, S.H.; Armstrong, S.A. Polycomb repressive complex 2 is required for MLL-AF9 leukemia. *Proc. Natl. Acad. Sci. USA* **2012**, *109*, 5028–5033. [[CrossRef](#)] [[PubMed](#)]
82. Schreiner, S.; Birke, M.; García-Cuellar, M.P.; Zilles, O.; Greil, J.; Slany, R.K. MLL-ENL causes a reversible and myc-dependent block of myelomonocytic cell differentiation. *Cancer Res.* **2001**, *61*, 6480–6486. [[PubMed](#)]
83. Jiang, X.; Huang, H.; Li, Z.; Li, Y.; Wang, X.; Gurbuxani, S.; Chen, P.; He, C.; You, D.; Zhang, S.; et al. Blockade of miR-150 maturation by MLL-fusion/MYC/LIN-28 is required for MLL-associated leukemia. *Cancer Cell* **2012**, *22*, 524–535. [[CrossRef](#)] [[PubMed](#)]
84. Sacco, J.J.; Coulson, J.M.; Clague, M.J.; Urbé, S. Emerging roles of deubiquitinases in cancer-associated pathways. *IUBMB Life* **2010**, *62*, 140–157. [[CrossRef](#)]

85. Meyer, C.; Lopes, B.A.; Caye-Eude, A.; Cavé, H.; Arfeuille, C.; Cucuini, W.; Sutton, R.; Venn, N.C.; Oh, S.H.; Tsaour, G.; et al. Human MLL/KMT2A gene exhibits a second breakpoint cluster region for recurrent MLL–USP2 fusions. *Leukemia* **2019**, *33*, 2306–2340. [[CrossRef](#)]
86. Delmore, J.E.; Issa, G.C.; Lemieux, M.E.; Rahl, P.B.; Shi, J.; Jacobs, H.M.; Kastritis, E.; Gilpatrick, T.; Paranal, R.M.; Qi, J.; et al. BET bromodomain inhibition as a therapeutic strategy to target c-Myc. *Cell* **2011**, *146*, 904–917. [[CrossRef](#)]
87. Dawson, M.A.; Prinjha, R.K.; Dittmann, A.; Giotopoulos, G.; Bantscheff, M.; Chan, W.I.; Robson, S.C.; Chung, C.W.; Hopf, C.; Savitski, M.M.; et al. Inhibition of BET recruitment to chromatin as an effective treatment for MLL–fusion leukaemia. *Nature* **2011**, *478*, 529–533. [[CrossRef](#)]
88. Ott, C.J.; Kopp, N.; Bird, L.; Paranal, R.M.; Qi, J.; Bowman, T.; Rodig, S.J.; Kung, A.L.; Bradner, J.E.; Weinstock, D.M. BET bromodomain inhibition targets both c-Myc and IL7R in high-risk acute lymphoblastic leukemia. *Blood* **2012**, *120*, 2843–2852. [[CrossRef](#)]
89. Coudé, M.M.; Braun, T.; Berrou, J.; Dupont, M.; Bertrand, S.; Masse, A.; Raffoux, E.; Itzykson, R.; Delord, M.; Riveiro, M.E.; et al. BET inhibitor OTX015 targets BRD2 and BRD4 and decreases c-MYC in acute leukemia cells. *Oncotarget* **2015**, *6*, 17698–17712. [[CrossRef](#)]
90. McCalmont, H.; Li, K.L.; Jones, L.; Toubia, J.; Bray, S.C.; Casolari, D.A.; Mayoh, C.; Samaraweera, S.E.; Lewis, I.D.; Prinjha, R.K.; et al. Efficacy of combined CDK9/BET inhibition in preclinical models of MLL-rearranged acute leukemia. *Blood Adv.* **2020**, *4*, 296–300. [[CrossRef](#)]
91. Bisgrove, D.A.; Mahmoudi, T.; Henklein, P.; Verdin, E. Conserved P-TEFb-interacting domain of BRD4 inhibits HIV transcription. *Proc. Natl. Acad. Sci. USA* **2007**, *104*, 13690–13695. [[CrossRef](#)] [[PubMed](#)]
92. Dey, A.; Chao, S.H.; Lane, D.P. HEXIM1 and the control of transcription elongation: From cancer and inflammation to AIDS and cardiac hypertrophy. *Cell Cycle* **2007**, *6*, 1856–1863. [[CrossRef](#)] [[PubMed](#)]
93. Alqahtani, A.; Choucair, K.; Ashraf, M.; Hammouda, D.M.; Alloghbi, A.; Khan, T.; Senzer, N.; Nemunaitis, J. Bromodomain and extra-terminal motif inhibitors: A review of preclinical and clinical advances in cancer therapy. *Future Sci. OA* **2019**, *5*, 372. [[CrossRef](#)] [[PubMed](#)]
94. Li, L.; Osdal, T.; Ho, Y.; Chun, S.; McDonald, T.; Agarwal, P.; Lin, A.; Chu, S.; Qi, J.; Li, L.; et al. SIRT1 activation by a c-MYC oncogenic network promotes the maintenance and drug resistance of human FLT3-ITD acute myeloid leukemia stem cells. *Cell Stem Cell* **2014**, *15*, 431–446. [[CrossRef](#)] [[PubMed](#)]
95. Vega-García, N.; Malatesta, R.; Estella, C.; Pérez-Jaume, S.; Esperanza-Cebollada, E.; Torreadell, M.; Català, A.; Gassiot, S.; Berruero, R.; Ruiz-Llobet, A.; et al. Paediatric patients with acute leukaemia and KMT2A (MLL) rearrangement show a distinctive expression pattern of histone deacetylases. *Br. J. Haematol.* **2018**, *182*, 542–553. [[CrossRef](#)] [[PubMed](#)]
96. Barneda-Zahonero, B.; Collazo, O.; Azagra, A.; Fernández-Duran, I.; Serra-Musach, J.; Islam, A.B.M.M.K.; Vega-García, N.; Malatesta, R.; Camós, M.; Gómez, A.; et al. The transcriptional repressor HDAC7 promotes apoptosis and c-Myc downregulation in particular types of leukemia and lymphoma. *Cell Death Dis.* **2015**, *6*, e1635. [[CrossRef](#)]
97. Haery, L.; Thompson, R.C.; Gilmore, T.D. Histone acetyltransferases and histone deacetylases in B- and T-cell development, physiology and malignancy. *Genes Cancer* **2015**, *6*, 184–213.
98. Shi, J.; Whyte, W.A.; Zepeda-Mendoza, C.J.; Milazzo, J.P.; Shen, C.; Roe, J.S.; Minder, J.L.; Mercan, F.; Wang, E.; Eckersley-Maslin, M.A.; et al. Role of SWI/SNF in acute leukemia maintenance and enhancer-mediated Myc regulation. *Genes Dev.* **2013**, *27*, 2648–2662. [[CrossRef](#)]
99. Rathert, P.; Roth, M.; Neumann, T.; Muerdter, F.; Roe, J.S.; Muhar, M.; Deswal, S.; Cerny-Reiterer, S.; Peter, B.; Jude, J.; et al. Transcriptional plasticity promotes primary and acquired resistance to BET inhibition. *Nature* **2015**, *525*, 543–547. [[CrossRef](#)]
100. Bahr, C.; Von Paleske, L.; Uslu, V.V.; Remeseiro, S.; Takayama, N.; Ng, S.W.; Murison, A.; Langenfeld, K.; Petretich, M.; Scognamiglio, R.; et al. A Myc enhancer cluster regulates normal and leukaemic haematopoietic stem cell hierarchies. *Nature* **2018**, *553*, 515–520. [[CrossRef](#)]
101. Azagra, A.; Marina-Zárate, E.; Ramiro, A.R.; Javierre, B.M.; Parra, M. From loops to looks: Transcription factors and chromatin organization shaping terminal B cell differentiation. *Trends Immunol.* **2020**, *41*, 46–60. [[CrossRef](#)] [[PubMed](#)]

102. Borkhardt, A.; Cazzaniga, G.; Viehmann, S.; Valsecchi, M.G.; Ludwig, W.D.; Burci, L.; Mangioni, S.; Schrappe, M.; Riehm, H.; Lampert, F.; et al. Incidence and clinical relevance of TEL/AML1 fusion genes in children with acute lymphoblastic leukemia enrolled in the German and Italian Multicenter Therapy Trials. *Blood* **1997**, *90*, 571–577. [[CrossRef](#)] [[PubMed](#)]
103. Biondi, A.; Masera, G. Molecular pathogenesis of childhood acute lymphoblastic leukemia. *Haematologica* **1998**, *83*, 651–659. [[PubMed](#)]
104. Cazzaniga, G.; Daniotti, M.; Tosi, S.; Giudici, G.; Aloisi, A.; Pogliani, E.; Kearney, L.; Biondi, A. The paired box domain gene PAX5 is fused to ETV6/TEL in an acute lymphoblastic leukemia case. *Cancer Res.* **2001**, *61*, 4666–4670.
105. Nutt, S.L.; Heavey, B.; Rolink, A.G.; Busslinger, M. Commitment to the B-lymphoid lineage depends on the transcription factor Pax5. *J. Immunol.* **1999**, *401*, 556–562.
106. Chae, H.; Kim, M.; Lim, J.; Kim, Y.; Han, K.; Lee, S. B lymphoblastic leukemia with ETV6 amplification. *Cancer Genet. Cytogenet.* **2010**, *203*, 284–287. [[CrossRef](#)]
107. Bokemeyer, A.; Eckert, C.; Meyr, F.; Koerner, G.; von Stackelberg, A.; Ullmann, R.; Türkmen, S.; Henze, G.; Seeger, K. Copy number genome alterations are associated with treatment response and outcome in relapsed childhood ETV6/RUNX1-positive acute lymphoblastic leukemia. *Haematologica* **2014**, *99*, 706–714. [[CrossRef](#)]
108. Cancelas, J.A.; Williams, D.A. Rho GTPases in hematopoietic stem cell functions. *Curr. Opin. Hematol.* **2009**, *16*, 249–254. [[CrossRef](#)]
109. Raptis, L.; Arulanandam, R.; Geletu, M.; Turkson, J. The R(h)oads to Stat3: Stat3 activation by the Rho GTPases. *Exp. Cell Res.* **2011**, *317*, 1787–1795. [[CrossRef](#)] [[PubMed](#)]
110. Mangolini, M.; De Boer, J.; Walf-Vorderwülbecke, V.; Pieters, R.; Den Boer, M.L.; Williams, O. STAT3 mediates oncogenic addiction to TEL-AML1 in t(12;21) acute lymphoblastic leukemia. *Blood* **2013**, *122*, 542–549. [[CrossRef](#)]
111. Stoskus, M.; Vaitkeviciene, G.; Eidukaite, A.; Griskevicius, L. ETV6/RUNX1 transcript is a target of RNA-binding protein IGF2BP1 in t(12;21)(p13;q22)-positive acute lymphoblastic leukemia. *Blood Cells Mol. Dis.* **2016**, *57*, 30–34. [[CrossRef](#)] [[PubMed](#)]
112. Stöhr, N.; Hüttelmaier, S. IGF2BP1: A post-transcriptional “driver” of tumor cell migration. *Cell Adhes. Migr.* **2012**, *6*, 312–318. [[CrossRef](#)] [[PubMed](#)]
113. Hardy, R.R. B-cell commitment: deciding on the players. *Curr. Opin. Immunol.* **2003**, *15*, 158–165. [[CrossRef](#)]
114. Geng, H.; Hurtz, C.; Lenz, K.B.; Chen, Z.; Baumjohann, D.; Thompson, S.; Goloviznina, N.A.; Chen, W.-Y.; Huan, J.; LaTocha, D.; et al. Self-enforcing feedback activation between BCL6 and Pre-B cell receptor signaling defines a distinct subtype of acute lymphoblastic leukemia. *Cancer Cell* **2015**, *27*, 409–425. [[CrossRef](#)] [[PubMed](#)]
115. Bankovich, A.J.; Raunser, S.; Juo, Z.S.; Walz, T.; Davis, M.M.; Garcia, K.C. Structural insight into pre-B cell receptor function. *Science* **2007**, *316*, 291–294. [[CrossRef](#)]
116. Lal, A.; Navarro, F.; Maher, C.A.; Maliszewski, L.E.; Yan, N.; O’Day, E.; Chowdhury, D.; Dykxhoorn, D.M.; Tsai, P.; Hofmann, O.; et al. miR-24 inhibits cell proliferation by targeting E2F2, MYC, and other cell-cycle genes via binding to “seedless” 3’UTR microrna recognition elements. *Mol. Cell* **2009**, *35*, 610–625. [[CrossRef](#)]
117. Akbari Moqadam, F.; Boer, J.M.; Lange-Turenhout, E.A.M.; Pieters, R.; Den Boer, M.L. Altered expression of miR-24, miR-126 and miR-365 does not affect viability of childhood TCF3-rearranged leukemia cells. *Leukemia* **2014**, *28*, 1008–1014. [[CrossRef](#)]
118. Folgiero, V.; Sorino, C.; Pallocca, M.; De Nicola, F.; Goeman, F.; Bertaina, V.; Strocchio, L.; Romania, P.; Pitisci, A.; Iezzi, S.; et al. Che-1 is targeted by c-Myc to sustain proliferation in pre-B-cell acute lymphoblastic leukemia. *EMBO Rep.* **2018**, *19*, 1–14. [[CrossRef](#)]
119. Bruno, T.; De Nicola, F.; Iezzi, S.; Lecis, D.; D’Angelo, C.; Di Padova, M.; Corbi, N.; Dimiziani, L.; Zannini, L.; Jekimovs, C.; et al. Che-1 phosphorylation by ATM/ATR and Chk2 kinases activates p53 transcription and the G2/M checkpoint. *Cancer Cell* **2006**, *10*, 473–486. [[CrossRef](#)]
120. Swerdlow, S.H.; Campo, E.; Pileri, S.A.; Harris, N.L.; Stein, H.; Siebert, R.; Advani, R.; Ghielmini, M.; Salles, G.A.; Zelenetz, A.D.; et al. The 2016 revision of the World Health Organization classification of lymphoid neoplasms. *Blood* **2016**, *127*, 2375–2390. [[CrossRef](#)]
121. Bemark, M.; Neuberger, M.S. The c-MYC allele that is translocated into the IgH locus undergoes constitutive hypermutation in a Burkitt’s lymphoma line. *Oncogene* **2000**, *19*, 3404–3410. [[CrossRef](#)] [[PubMed](#)]

122. Hemann, M.T.; Bric, A.; Teruya-Feldstein, J.; Herbst, A.; Nilsson, J.A.; Cordon-Cardo, C.; Cleveland, J.L.; Tansey, W.P.; Lowe, S.W. Evasion of the p53 tumour surveillance network by tumour-derived MYC mutants. *Nature* **2005**, *436*, 807–811. [[CrossRef](#)] [[PubMed](#)]
123. Seegmiller, A.C.; Garcia, R.; Huang, R.; Maleki, A.; Karandikar, N.J.; Chen, W. Simple karyotype and bcl-6 expression predict a diagnosis of Burkitt lymphoma and better survival in IG-MYC rearranged high-grade B-cell lymphomas. *Mod. Pathol.* **2010**, *23*, 909–920. [[CrossRef](#)]
124. Cory, S. Activation of cellular oncogenes in hemopoietic cells by chromosome translocation. *Adv. Cancer Res.* **1986**, *47*, 189–234.
125. Cesarman, E.; Dalla-Favera, R.; Bentley, D.; Groudine, M. Mutations in the first exon are associated with altered transcription of c-myc in Burkitt lymphoma. *Science* **1987**, *238*, 1272–1275. [[CrossRef](#)]
126. Rabbits, T.H.; Forster, A.; Hamlyn, P.; Baer, R. Effect of somatic mutation within translocated c-myc genes in Burkitt's lymphoma. *Nature* **1984**, *309*, 592–597. [[CrossRef](#)]
127. Hummel, M.; Bentink, S.; Berger, H.; Klapper, W.; Wessendorf, S.; Barth, T.F.E.; Bernd, H.; Cogliatti, S.B.; Dierlamm, J.; Feller, A.C.; et al. A biologic definition of burkitt's lymphoma from transcriptional and genomic profiling michael. *N. Engl. J. Med.* **2006**, *354*, 2419–2430. [[CrossRef](#)]
128. Schmitz, R.; Young, R.M.; Ceribelli, M.; Jhavar, S.; Xiao, W.; Zhang, M.; Wright, G.; Shaffer, A.L.; Hodson, D.J.; Buras, E.; et al. Burkitt lymphoma pathogenesis and therapeutic targets from structural and functional genomics. *Nature* **2012**, *490*, 116–120. [[CrossRef](#)]
129. Love, C.; Sun, Z.; Jima, D.; Li, G.; Zhang, J.; Miles, R.; Richards, K.L.; Dunphy, C.H.; Choi, W.W.L.; Srivastava, G.; et al. The genetic landscape of mutations in Burkitt lymphoma. *Nat. Genet.* **2012**, *44*, 1321–1325. [[CrossRef](#)]
130. Seitz, V.; Butzhammer, P.; Hirsch, B.; Hecht, J.; Gütgemann, I.; Ehlers, A.; Lenze, D.; Oker, E.; Sommerfeld, A.; von der Wall, E.; et al. Deep sequencing of MYC DNA-Binding sites in Burkitt lymphoma. *PLoS ONE* **2011**, *6*, e26837. [[CrossRef](#)]
131. Pan, L.; Sato, S.; Frederick, J.P.; Sun, X.-H.; Zhuang, Y. Impaired immune responses and B-cell proliferation in mice lacking the Id3 gene. *Mol. Cell. Biol.* **1999**, *19*, 5969–5980. [[CrossRef](#)] [[PubMed](#)]
132. Srinivasan, L.; Sasaki, Y.; Calado, D.P.; Zhang, B.; Paik, J.H.; DePinho, R.A.; Kutok, J.L.; Kearney, J.F.; Otipoby, K.L.; Rajewsky, K. PI3 kinase signals BCR-dependent mature B cell survival. *Cell* **2009**, *139*, 573–586. [[CrossRef](#)] [[PubMed](#)]
133. Sander, S.; Calado, D.P.; Srinivasan, L.; Köchert, K.; Zhang, B.; Rosolowski, M.; Rodig, S.J.; Holzmann, K.; Stilgenbauer, S.; Siebert, R.; et al. Synergy between PI3K signaling and MYC in burkitt lymphomagenesis. *Cancer Cell* **2012**, *22*, 167–179. [[CrossRef](#)] [[PubMed](#)]
134. Schiffman, J.D.; Lorimer, P.D.; Rodic, V.; Jahromi, M.S.; Downie, J.M.; Bayerl, M.G.; Sanmann, J.N.; Althof, P.A.; Sanger, W.G.; Barnette, P.; et al. Genome wide copy number analysis of paediatric Burkitt lymphoma using formalin-fixed tissues reveals a subset with gain of chromosome 13q and corresponding miRNA over expression. *Br. J. Haematol.* **2011**, *155*, 477–486. [[CrossRef](#)] [[PubMed](#)]
135. Olive, V.; Bennett, M.J.; Walker, J.C.; Ma, C.; Jiang, I.; Cordon-Cardo, C.; Li, Q.J.; Lowe, S.W.; Hannon, G.J.; He, L. miR-19 is a key oncogenic component of mir-17-92. *Genes Dev.* **2009**, *23*, 2839–2849. [[CrossRef](#)] [[PubMed](#)]
136. Xiao, C.; Srinivasan, L.; Calado, D.P.; Patterson, H.C.; Zhang, B.; Wang, J.; Henderson, J.M.; Kutok, J.L.; Rajewsky, K. Lymphoproliferative disease and autoimmunity in mice with increased miR-17-92 expression in lymphocytes. *Nat. Immunol.* **2008**, *9*, 405–414. [[CrossRef](#)]
137. Robaina, M.C.; Mazzocchi, L.; Klumb, C.E. Germinal centre B cell functions and lymphomagenesis: Circuits involving MYC and MicroRNAs. *Cells* **2019**, *8*, 1365. [[CrossRef](#)]
138. Dave, S.S.; Fu, K.; Wright, G.W.; Lam, L.T.; Kluin, P.; Boerma, E.; Greiner, T.C.; Weisenburger, D.D.; Rosenwald, A.; Ott, G.; et al. Molecular diagnosis of burkitt's lymphoma. *N. Engl. J. Med.* **2006**, *354*, 2431–2442. [[CrossRef](#)]
139. Klapproth, K.; Sander, S.; Marinkovic, D.; Baumann, B.; Wirth, T.; Dc, W.; Klapproth, K.; Sander, S.; Marinkovic, D.; Baumann, B.; et al. The IKK2/NF- $\kappa$  B pathway suppresses MYC-induced lymphomagenesis. *Blood* **2011**, *114*, 2448–2458. [[CrossRef](#)]
140. Ngan, B.Y.; Chen-Levy, Z.; Weiss, L.M.; Warnke, R.A.; Cleart, M.L. Expression in non-hodgkin's lymphoma of the bcl-2 protein associated with the t(14;18) chromosomal translocation. *N. Engl. J. Med.* **1988**, *318*, 1638–1644. [[CrossRef](#)]

141. Lo Coco, F.; Ye, B.H.; Lista, F.; Corradini, P.; Offit, K.; Knowles, D.M.; Chaganti, R.S.K.; Dalla-Favera, R. Rearrangements of the BCL6 gene in diffuse large cell non-Hodgkin's lymphoma. *Blood* **1994**, *83*, 1757–1759. [[CrossRef](#)]
142. Gascoyne, R.D. Pathologic prognostic factors in diffuse aggressive non-Hodgkin's lymphoma. *Hematol. Oncol. Clin. N. Am.* **1997**, *11*, 847–862. [[CrossRef](#)]
143. Kramer, M.H.H.; Hermans, J.; Wijburg, E.; Philippo, K.; Geelen, E.; van Krieken, J.H.J.M.; de Jong, D.; Maartense, E.; Schuurin, E.; Kluin, P.M. Clinical relevance of BCL2, BCL6, and MYC rearrangements in diffuse large B-cell lymphoma. *Blood* **1998**, *92*, 3152–3162. [[CrossRef](#)] [[PubMed](#)]
144. Akasaka, T.; Akasaka, H.; Ueda, C.; Yonetani, N.; Maesako, Y.; Shimizu, A.; Yamabe, H.; Fukuhara, S.; Uchiyama, T.; Ohno, H. Molecular and clinical features of non-burkitt's, diffuse large-cell lymphoma of B-cell type associated with the c-MYC/immunoglobulin heavy-chain fusion gene. *J. Clin. Oncol.* **2000**, *18*, 510–518. [[CrossRef](#)] [[PubMed](#)]
145. Kawasaki, C.; Ohshima, K.; Suzumiya, J.; Kanda, M.; Tsuchiya, T.; Tamura, K.; Kikuchi, M. Rearrangements of bcl-1, bcl-2, bcl-6, and c-myc in diffuse large B-cell lymphomas. *Leuk. Lymphoma* **2001**, *42*, 1099–1106. [[CrossRef](#)] [[PubMed](#)]
146. Chisholm, K.M.; Bangs, C.D.; Bacchi, C.E.; Molina-Kirsch, H.; Cherry, A.; Natkunam, Y. Expression profiles of MYC protein and MYC gene rearrangement in lymphomas. *Am. J. Surg. Pathol.* **2015**, *39*, 294–303. [[CrossRef](#)] [[PubMed](#)]
147. Bertrand, P.; Bastard, C.; Maingonnat, C.; Jardin, F.; Maisonneuve, C.; Courel, M.-N.; Ruminy, P.; Picquenot, J.M.; Tilly, H. Mapping of MYC breakpoints in 8q24 rearrangements involving non-immunoglobulin partners in B-cell lymphomas. *Leukemia* **2007**, *21*, 515–523. [[CrossRef](#)] [[PubMed](#)]
148. Stasik, C.J.; Nitta, H.; Zhang, W.; Mosher, C.H.; Cook, J.R.; Tubbs, R.R.; Unger, J.M.; Brooks, T.A.; Persky, D.O.; Wilkinson, S.T.; et al. Increased MYC gene copy number correlates with increased mRNA levels in diffuse large B-cell lymphoma. *Haematologica* **2010**, *95*, 597–603. [[CrossRef](#)]
149. Valera, A.; Lopez-Guillermo, A.; Cardesa-Salzmann, T.; Climent, F.; Gonzalez-Barca, E.; Mercadal, S.; Espinosa, I.; Novelli, S.; Briones, J.; Mate, J.L.; et al. MYC protein expression and genetic alterations have prognostic impact in patients with diffuse large B-cell lymphoma treated with immunochemotherapy. *Haematologica* **2013**, *98*, 1554–1562. [[CrossRef](#)]
150. Grimm, K.E.; O'Malley, D.P. Aggressive B cell lymphomas in the 2017 revised WHO classification of tumors of hematopoietic and lymphoid tissues. *Ann. Diagn. Pathol.* **2019**, *38*, 6–10. [[CrossRef](#)]
151. Gebauer, N.; Bernard, V.; Gebauer, W.; Thorns, C.; Feller, A.C.; Merz, H. TP53 mutations are frequent events in double-hit B-cell lymphomas with MYC and BCL2 but not MYC and BCL6 translocations. *Leuk. Lymphoma* **2015**, *56*, 179–185. [[CrossRef](#)]
152. Aukema, S.M.; Kreuz, M.; Kohler, C.W.; Rosolowski, M.; Hasenclever, D.; Hummel, M.; Küppers, R.; Lenze, D.; Ott, G.; Pott, C.; et al. Biological characterization of adult MYC-translocation-positive mature B-cell lymphomas other than molecular Burkitt lymphoma. *Haematologica* **2014**, *99*, 726–735. [[CrossRef](#)]
153. Cook, J.R.; Goldman, B.; Tubbs, R.R.; Rimsza, L.; Leblanc, M.; Stiff, P.; Fisher, R. Clinical significance of MYC expression and/or "High-grade" morphology in non-burkitt, diffuse aggressive B-cell lymphomas: A SWOG s9704 correlative study. *Am. J. Surg. Pathol.* **2014**, *38*, 494–501. [[CrossRef](#)]
154. Huang, M.; Kamasani, U.; Prendergast, G.C. RhoB facilitates c-Myc turnover by supporting efficient nuclear accumulation of GSK-3. *Oncogene* **2006**, *25*, 1281–1289. [[CrossRef](#)]
155. Wang, W.G.; Liu, Z.B.; Jiang, X.N.; Lee, J.; Zhou, X.Y.; Li, X.Q. MYC protein dysregulation is driven by BCR-PI3K signalling in diffuse large B-cell lymphoma. *Histopathology* **2017**, *71*, 778–785. [[CrossRef](#)]
156. Pfeifer, M.; Grau, M.; Lenze, D.; Wenzel, S.S.; Wolf, A.; Wollert-Wulf, B.; Dietze, K.; Nogai, H.; Storek, B.; Madle, H.; et al. PTEN loss defines a PI3K/AKT pathway-dependent germinal center subtype of diffuse large B-cell lymphoma. *Proc. Natl. Acad. Sci. USA* **2013**, *110*, 12420–12425. [[CrossRef](#)]
157. Kim, Y.; Ju, H.; Kim, D.H.; Yoo, H.Y.; Kim, S.J.; Kim, W.S.; Ko, Y.H. CD79B and MYD88 mutations in diffuse large B-cell lymphoma. *Hum. Pathol.* **2014**, *45*, 556–564. [[CrossRef](#)]
158. Tagawa, H.; Karube, K.; Tsuzuki, S.; Ohshima, K.; Seto, M. Synergistic action of the microRNA-17 polycistron and Myc in aggressive cancer development. *Cancer Sci.* **2007**, *98*, 1482–1490. [[CrossRef](#)]
159. Psathas, J.N.; Doonan, P.J.; Raman, P.; Freedman, B.D.; Minn, A.J.; Thomas-Tikhonenko, A. Lymphoid neoplasia: The Myc-miR-17-92 axis amplifies B-cell receptor signaling via inhibition of ITIM proteins: A novel lymphomagenic feed-forward loop. *Blood* **2013**, *122*, 4220–4229. [[CrossRef](#)]

160. Shapiro-Shelef, M.; Lin, K.I.; McHeyzer-Williams, L.J.; Liao, J.; McHeyzer-Williams, M.G.; Calame, K. Blimp-1 is required for the formation of immunoglobulin secreting plasma cells and pre-plasma memory B cells. *Immunity* **2003**, *19*, 607–620. [[CrossRef](#)]
161. Shaffer, A.L.; Lin, K.I.; Kuo, T.C.; Yu, X.; Hurt, E.M.; Rosenwald, A.; Giltnane, J.M.; Yang, L.; Zhao, H.; Calame, K.; et al. Blimp-1 orchestrates plasma cell differentiation by extinguishing the mature B cell gene expression program. *Immunity* **2002**, *17*, 51–62. [[CrossRef](#)]
162. Montes-Moreno, S.; Martinez-Magunacelaya, N.; Zecchini-Barrese, T.; De Villambrosía, S.G.; Linares, E.; Ranchal, T.; Rodriguez-Pinilla, M.; Batlle, A.; Cereceda-Company, L.; Revert-Arce, J.B.; et al. Plasmablastic lymphoma phenotype is determined by genetic alterations in MYC and PRDM1. *Mod. Pathol.* **2017**, *30*, 85–94. [[CrossRef](#)]
163. Valera, A.; Balagué, O.; Colomo, L.; Martínez, A.; Delabie, J.; Taddesse-Heath, L.; Jaffe, E.S.; Campo, E. IG/MYC rearrangements are the main cytogenetic alteration in plasmablastic lymphomas. *Am. J. Surg. Pathol.* **2010**, *34*, 1686–1694. [[CrossRef](#)]
164. Taddesse-Heath, L.; Meloni-Ehrig, A.; Scheerle, J.; Kelly, J.C.; Jaffe, E.S. Plasmablastic lymphoma with MYC translocation: evidence for a common pathway in the generation of plasmablastic features. *Mod. Pathol.* **2010**, *23*, 991–999. [[CrossRef](#)]
165. Chapman, J.; Gentles, A.J.; Sujoy, V.; Vega, F.; Dumur, C.I.; Blevins, T.L.; Bernal-Mizrachi, L.; Mosunjac, M.; Pimentel, A.; Zhu, D.; et al. Gene expression analysis of plasmablastic lymphoma identifies downregulation of B-cell receptor signaling and additional unique transcriptional programs. *Leukemia* **2015**, *29*, 2270–2273. [[CrossRef](#)]
166. Simonitsch-Klupp, I.; Hauser, I.; Ott, G.; Drach, J.; Ackermann, J.; Kaufmann, J.; Weltermann, A.; Greinix, H.T.; Skrabbs, C.; Dittrich, C.; et al. Diffuse large B-cell lymphomas with plasmablastic/plasmacytoid features are associated with TP53 deletions and poor clinical outcome. *Leukemia* **2004**, *18*, 146–155. [[CrossRef](#)]
167. Ouansafi, I.; He, B.; Fraser, C.; Nie, K.; Mathew, S.; Bhanji, R.; Hoda, R.; Arabadjief, M.; Knowles, D.; Cerutti, A.; et al. Transformation of follicular lymphoma to plasmablastic lymphoma with c-myc gene rearrangement. *Am. J. Clin. Pathol.* **2010**, *134*, 972–981. [[CrossRef](#)]
168. Li, S.; Lin, P.; Fayad, L.E.; Lennon, P.A.; Miranda, R.N.; Yin, C.C.; Lin, E.; Medeiros, L.J. B-cell lymphomas with MYC/8q24 rearrangements and IGH@BCL2/t(14;18) (q32;q21): An aggressive disease with heterogeneous histology, germinal center B-cell immunophenotype and poor outcome. *Mod. Pathol.* **2012**, *25*, 145–156. [[CrossRef](#)]
169. Yano, T.; Jaffe, E.S.; Longo, D.L.; Raffeld, M. MYC rearrangements in histologically progressed follicular lymphomas. *Blood* **1992**, *80*, 758–767. [[CrossRef](#)]
170. Al-Tourah, A.J.; Gill, K.K.; Chhanabhai, M.; Hoskins, P.J.; Klasa, R.J.; Savage, K.J.; Sehn, L.H.; Shenkier, T.N.; Gascoyne, R.D.; Connors, J.M. Population-based analysis of incidence and outcome of transformed non-hodgkin's lymphoma. *J. Clin. Oncol.* **2008**, *26*, 5165–5169. [[CrossRef](#)]
171. Davies, A.J.; Rosenwald, A.; Wright, G.; Lee, A.; Last, K.W.; Weisenburger, D.D.; Chan, W.C.; Delabie, J.; Braziel, R.M.; Campo, E.; et al. Transformation of follicular lymphoma to diffuse large B-cell lymphoma proceeds by distinct oncogenic mechanisms. *Br. J. Haematol.* **2007**, *136*, 286–293. [[CrossRef](#)]
172. Lossos, I.S.; Alizadeh, A.A.; Diehn, M.; Warnke, R.; Thorstenson, Y.; Oefner, P.J.; Brown, P.O.; Botstein, D.; Levy, R. Transformation of follicular lymphoma to diffuse large-cell lymphoma: Alternative patterns with increased or decreased expression of c-myc and its regulated genes. *Proc. Natl. Acad. Sci. USA* **2002**, *99*, 8886–8891. [[CrossRef](#)]
173. Martinez-Climent, J.A.; Alizadeh, A.A.; Segraves, R.; Blesa, D.; Rubio-Moscardo, F.; Albertson, D.G.; Garcia-Conde, J.; Dyer, M.J.S.; Levy, R.; Pinkel, D.; et al. Transformation of follicular lymphoma to diffuse large cell lymphoma is associated with a heterogeneous set of DNA copy number and gene expression alterations. *Blood* **2003**, *101*, 3109–3117. [[CrossRef](#)]
174. Lukas, J.; Jadayel, D.; Bartkova, J.; Nacheva, E.; Dyer, M.J.; Strauss, M.; Bartek, J. BCL-1/cyclin D1 oncoprotein oscillates and subverts the G1 phase control in B-cell neoplasms carrying the t(11;14) translocation. *Oncogene* **1994**, *9*, 2159–2167.
175. Lovec, H.; Grzeschiczek, A.; Kowalski, M.B.; Möröy, T. Cyclin D1/bcl-1 cooperates with myc genes in the generation of B-cell lymphoma in transgenic mice. *EMBO J.* **1994**, *13*, 3487–3495. [[CrossRef](#)]



176. Sander, S.; Bullinger, L.; Leupolt, E.; Benner, A.; Kienle, D.; Katzenberger, T.; Kalla, J.; Ott, G.; Müller-Hermelink, H.K.; Barth, T.F.E.; et al. Genomic aberrations in mantle cell lymphoma detected by interphase fluorescence in situ hybridization. Incidence and clinicopathological correlations. *Haematologica* **2008**, *93*, 680–687. [[CrossRef](#)]
177. Aukema, S.M.; Siebert, R.; Schuurin, E.; Van Imhoff, G.W.; Kluin-nelemans, H.C.; Boerma, E.; Kluin, P.M. Review article Double-hit B-cell lymphomas. *Hematology* **2011**, *117*, 2319–2331.
178. Royo, C.; Salaverria, I.; Hartmann, E.M.; Rosenwald, A.; Campo, E.; Beà, S. The complex landscape of genetic alterations in mantle cell lymphoma. *Semin. Cancer Biol.* **2011**, *21*, 322–334. [[CrossRef](#)]
179. Hao, S.; Sanger, W.; Onciu, M.; Lai, R.; Schlette, E.J.; Medeiros, L.J. Mantle cell lymphoma with 8q24 chromosomal abnormalities: A report of 5 cases with blastoid features. *Mod. Pathol.* **2002**, *15*, 1266–1272. [[CrossRef](#)]
180. Hu, Z.; Medeiros, L.J.; Chen, Z.; Chen, W.; Li, S.; Konoplev, S.N.; Lu, X.; Pham, L.V.; Young, K.H.; Wang, W.; et al. Mantle cell lymphoma with MYC rearrangement: A report of 17 patients. *Am. J. Surg. Pathol.* **2017**, *41*, 216–224. [[CrossRef](#)]
181. Sander, B.; Quintanilla-Martinez, L.; Ott, G.; Xerri, L.; Kuzu, I.; Chan, J.K.C.; Swerdlow, S.H.; Campo, E. Mantle cell lymphoma—A spectrum from indolent to aggressive disease. *Virchows Arch.* **2016**, *468*, 245–257. [[CrossRef](#)] [[PubMed](#)]
182. Ruas, M.; Peters, G. The p16INK4a/CDKN2A tumor suppressor and its relatives. *Biochim. Biophys. Acta Rev. Cancer* **1998**, *1378*, F115–F177. [[CrossRef](#)]
183. Vincent-Fabert, C.; Fiancette, R.; Rouaud, P.; Baudet, C.; Truffinet, V.; Magnone, V.; Guillaudeau, A.; Cogné, M.; Dubus, P.; Denizot, Y. A defect of the INK4-Cdk4 checkpoint and Myc collaborate in blastoid mantle cell lymphomalike lymphoma formation in mice. *Am. J. Pathol.* **2012**, *180*, 1688–1701. [[CrossRef](#)]
184. Haas, K.; Staller, P.; Geisen, C.; Bartek, J.; Eilers, M.; Möröy, T. Mutual requirement of CDK4 and Myc in malignant transformation: Evidence for cyclin D1/CDK4 and p16(INK4A) as upstream regulators of Myc. *Oncogene* **1997**, *15*, 179–192. [[CrossRef](#)]
185. Hermeking, H.; Rago, C.; Schuhmacher, M.; Li, Q.; Barrett, J.F.; Obaya, A.J.; O’Connell, B.C.; Mateyak, M.K.; Tam, W.; Kohlhuber, F.; et al. Identification of CDK4 as a target of c-MYC. *Proc. Natl. Acad. Sci. USA* **2000**, *97*, 2229–2234. [[CrossRef](#)]
186. Dai, B.; Grau, M.; Juilland, M.; Klener, P.; Höring, E.; Molinsky, J.; Schimmack, G.; Aukema, S.M.; Hoster, E.; Vogt, N.; et al. B-cell receptor-driven MALT1 activity regulates MYC signaling in mantle cell lymphoma. *Blood* **2017**, *129*, 333–346. [[CrossRef](#)]
187. Saba, N.S.; Liu, D.; Herman, S.E.M.; Underbayev, C.; Tian, X.; Behrend, D.; Weniger, M.A.; Skarzynski, M.; Gyamfi, J.; Fontan, L.; et al. Pathogenic role of B-cell receptor signaling and canonical NF-κB activation in mantle cell lymphoma. *Blood* **2016**, *128*, 82–92. [[CrossRef](#)]



© 2020 by the authors. Licensee MDPI, Basel, Switzerland. This article is an open access article distributed under the terms and conditions of the Creative Commons Attribution (CC BY) license (<http://creativecommons.org/licenses/by/4.0/>).

